

X chromosome inactivation:

Activation of Silencing

Iris Jonkers

The work presented in this thesis was performed at the department of Cell Biology and the department of Reproduction and Development, at the ErasmusMC in Rotterdam.

The studies described in this thesis were supported by a VIDI grant from NWO, and a grant from the BSIK Innovation programme “Stem Cells in Development and Disease” (SCDD, BSIK 03038).

Financial support by the ErasmusMC, SCDD, and J.E. Jurriaanse Stichting for the publication of this thesis is gratefully acknowledged.

This thesis was printed by CPI-Wöhrmann Print Service and designed by Iris.

Cover picture: Enlargement of a tetraploid XXXX_{MS2} cell after 4 days of differentiation. RNA-FISH is performed with an *Xist* RNA probe in green and a MS2-repeat probe in red. The nucleus is stained with DAPI in blue.

Back cover picture: Female XX mouse ES cells targeted with a BAC containing an *Xist* gene after 3 days of differentiation. RNA-FISH was performed as described above.

**X chromosome inactivation:
Activation of Silencing**

**X chromosoom inactivatie:
activering van het stilleggen**

Proefschrift

Ter verkrijging van de graad van doctor aan de Erasmus Universiteit
van Rotterdam op gezag van Rector Magnificus

Professor dr. S.W.J. Lamberts

en volgens besluit van het College voor Promoties.

De openbare verdediging zal plaatsvinden op
Woensdag 13 mei 2009 om 13.45 uur.

door

Iris Hélène Jonkers
geboren te Eindhoven



Promotie commissie

Promotors:

Prof. dr. J.A. Grootegoed

Prof. dr. F. Grosveld

Overige leden:

Prof. dr. B. Oostra

Dr. D. Meijer

Dr. N.J. Galjart

Co-promotor:

Dr. J. Gribnau

Content

Abbreviations	6
Scope of the thesis	8
Chapter 1	9
<i>Introduction</i>	
Chapter 2	61
<i>X inactivation counting and choice is a stochastic process: evidence for involvement of an X-linked activator</i>	
Chapter 3	85
<i>The probability to initiate X chromosome inactivation is determined by the X to autosomal ratio and X chromosome specific allelic properties</i>	
Chapter 4	115
<i>RNF12 is an X-encoded activator of X chromosome inactivation</i>	
Chapter 5	133
<i>Xist RNA is confined to the nuclear territory of the silenced X chromosome throughout the cell cycle</i>	
Chapter 6	161
<i>General discussion</i>	
Summary/Samenvatting	189
Curriculum Vitae	194
PhD Portpholio	196
Dankwoord	198

List of abbreviations

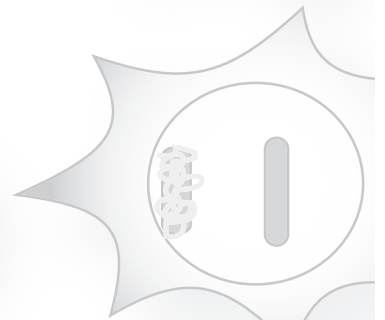
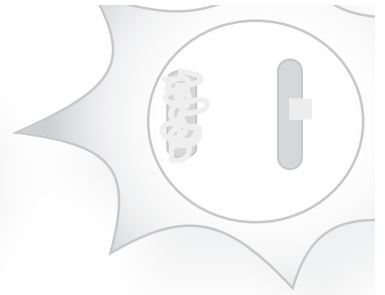
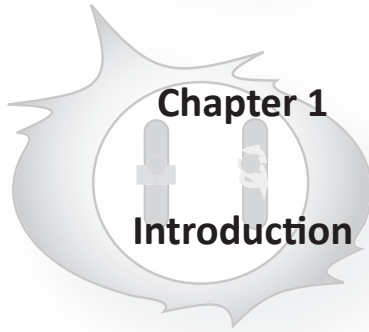
ATRX	alpha thalassemia/mental retardation syndrome X-linked
BAC	bacterial artificial chromosome
bp	base pairs
CBX	chromobox homolog
cDNA	complementary DNA
CF	competence factor
CpG	cytosine-guanine
CTCF	CCCTC-binding factor
DCC	dosage compensation complex
dpc	days post coitum
DNA	deoxyribonucleic acid
DNMT	DNA methyltransferase
DPY	dumpy
E	embryonic
EED	embryonic ectoderm development
ES	embryonic stem
EzH2	enhancer of zeste homolog 2
FACS	fluorescence activated cell sorting
FISH	fluorescence in situ hybridization
Fox1	feminizing gene on X 1
HDAC	histone deacetylase
hESC	human embryonic stem cell
HMTase	histone methyltransferase
ICM	inner cell mass
Kb	kilo base
LDB1	LIM domain binding protein 1
LIM	Lin11/ISL1/MEC3
LINE	long interspersed nuclear element
Mb	mega base
MCB	macro chromatin body
MEFS	mouse embryonic fibroblasts
MHM	male hypermethylated
MLE	maleless
MOF	males absent on the first
MRE	MSL complex recognition sites
mRNA	messenger RNA
MSCI	meiotic sex chromosome silencing
MSL	male sex lethal
ncRNA	non-coding RNA
NEO	neomycin
ORF	open reading frame
PolII	RNA polymerase II
PRC	polycomb-group repressive complex

rex	recognition elements on X
RLIM	RING finger LIM domain-binding protein
RING	really interesting new gene
RNA	ribonucleic acid
RNAi	RNA interference
RNF12	RING finger protein 12
roX	RNA on the X
SAF-A	scaffold attachment factor A
SDC	sex determination and dosage compensation defect
Sex1	signal element on X 1
siRNA	small interfering RNA
SmcHD1	SMC hinge domain containing 1
SNP	single nucleotide polymorphism
SRY	sex determining region Y
SUZ12	suppressor of zeste 12
Sxl	sex lethal
TBP	TATA binding protein
TF	transcription factor
Tsix	X inactive specific transcript, antisense
TSS	transcription start site
WT	wild type
Xa	active X chromosome
Xce	X chromosome choosing element
XCI	X chromosome inactivation
Xi	inactive X chromosome
XIC	X chromosome inactivation center
Xist	X inactive specific transcript
Xite	X-inactivation intergenic transcription element
Xm	maternal X chromosome
xol1	XO lethal 1
Xp	paternal X chromosome
YAC	yeast artificial chromosome
YY1	yin yang 1

Scope of the thesis

X chromosome inactivation is a process that ensures equal expression of the X chromosomes between males, which have one X and one Y chromosome, and females, which have two X chromosomes, in mammals. Females initiate inactivation of one of their two X chromosomes early during embryogenesis, by expressing an untranslated RNA from the X-encoded *Xist* gene. *Xist* RNA coats and silences the X chromosome in *cis*, after which the silenced state of the inactive X chromosome is propagated through many cell divisions.

Three major research questions dominate the field of XCI. How is a cell able to count the number of X chromosomes present? How is it possible that only one of the two X chromosomes in female diploid cells is inactivated? And how is the X chromosome silenced in *cis*? Although many researchers have attempted to explain the initiation and regulation of the XCI process with a wide array of models, none of the proposed models is able to explain all observations made with deletion and overexpression studies in mouse ES cell lines and embryos. Therefore, the aim of this thesis is to obtain additional data, and to postulate a comprehensive model for the initiation of XCI in the mouse. This model will encompass how the cell is able to detect the number of X chromosomes and how it can inactivate only one of them without inactivating all X chromosomes present in a cell. The discovery of an important activator of XCI initiation strengthens this model. Furthermore, the mechanism of spreading of *Xist* RNA, and thus the silencing of the X chromosome in *cis*, will be addressed. A hypothesis regarding the spreading of *Xist* RNA over the inactive X, and how *Xist* RNA is restricted to the Xi, will be formulated. Overall, the most important conundrums in XCI will be addressed in this thesis, and we present a more logical and complete model explaining the regulation of XCI.



1. Introduction

1.1 Evolution of sex chromosomes in mammals

Many living organisms have separate sexes, and the determination of sex within one species can be achieved in many ways. For instance, many reptiles use environmental cues, like the incubation temperature of their eggs, to determine the sex of their offspring. Other species have genetic based sex determination, but no distinguishable sex chromosomes. Finally, many species, for example most birds, mammals, and insects, have sex chromosomes and employ sex chromosome linked genetic cues to achieve sex determination. Two forms of sex chromosome systems exist (based on heterogametic sex), the ZW system present in birds and the XY system employed by mammals [1].

In mammals, males have an X and a Y chromosome and females two X chromosomes. The X chromosome is large, comprising approximately a thousand genes in human and mouse. In contrast, the Y chromosome, the smallest mammalian chromosome, encodes less than thirty different proteins in human. One of these proteins is SRY, which has been characterized as the master regulator in male development. SRY is the testis-determining factor and initiates a cascade of molecular events that turns the indifferent gonads into testis, thereby driving male development. Without SRY, the gonads will develop into ovaries, resulting in female development. Female development is therefore often considered the default state of mammals [2].

What is the origin of sex chromosomes? It has been proposed that sex chromosomes originate from a set of autosomal chromosomes, of which one acquired a sex determining locus in mammals, probably the SRY gene, and then became a male-limited proto-Y chromosome (Fig. 1). This event was quickly followed by accumulation of genes advantageous to males around the sex determining locus due to positive selection. Because this sex determining region on the proto-Y became more and more divergent from the proto-X, recombination events were omitted from this region. This resulted in an increased rate of mutations, inversions, deletions and translocations on the proto-Y, and consequent degradation of the chromosome (Fig. 1).

This evolutionary theory is supported by the classification of different evolutionary chromosome layers on the Y chromosome, of which layer 1, containing the SRY gene, shows most divergence from the homologous X chromosomal region and most likely represents the earliest stage of sex chromosome divergence. The different layers probably arose subsequently during evolution after inversions on the Y and expansion of the pseudoautosomal region on the X and Y chromosomes

[3,4]. Ultimately, layer 5 is most conserved between the X and Y chromosomes, and this region represents the pseudo-autosomal region, which is still able to pair during meiosis between the X and Y. Furthermore, the ongoing degradation of the Y chromosome becomes visible when Y chromosomes of various species are compared. Some show extensive degradation, whereas others still have high homology with the X chromosome, indicating that divergence of the sex chromosomes is an ongoing process, and might result in the loss of the Y chromosome in some species altogether [1].

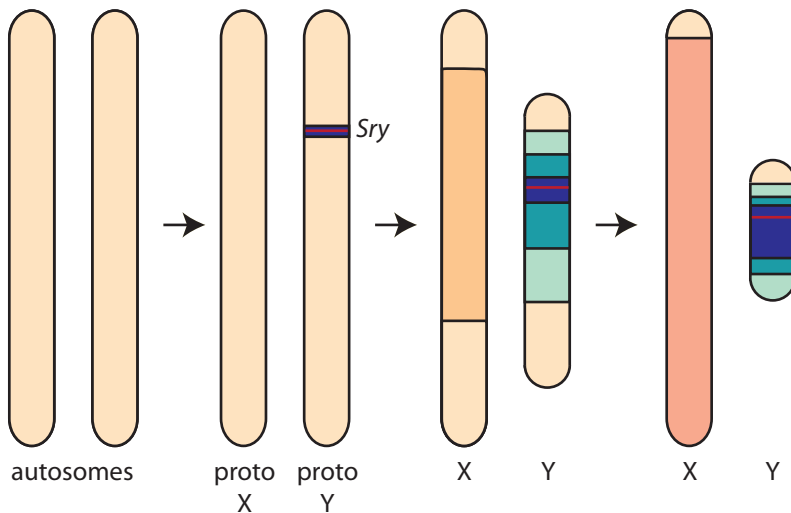


Figure 1. Evolution of mammalian sex chromosomes

After a mutation resulted to the *Sry* gene (in red), which drives male development, on one of a pair of autosomes in an early mammalian ancestor (in yellow), a gradual transition of the autosomal pair of chromosomes towards sex chromosomes has taken place. The Y chromosome gradually accumulated mutations and deletions, starting in the region around the *Sry* gene and spreading from there, as indicated by the spreading of the light and dark blue coloring. Recombination between X and Y is becoming impossible, apart from the pseudo-autosomal region. The pseudo-autosomal region is depicted in yellow. The X chromosome becomes more active to compensate for the loss of genes on the Y chromosome, as indicated by the increasing intensity of the color of the chromosome.

1.2 Dosage compensation in mammals

The X chromosome in mammals is protected from degradation because it has the ability to recombine in the female germline, whereas the Y chromosome has gradually degraded due to lack of recombination. As a consequence, the present Y chromosome carries relatively few functional genes, generating an unequal dosage of X chromosomal genes that have no or a non-functional Y chromosomal partner. To equalize the dose of X-linked genes, mammals almost completely inactivate one of the two female X chromosomes in a process named X chromosome inactivation (XCI). XCI is a gene-by-gene adaptation to the degradation of the Y chromosome,

which is supported by the finding that X-linked genes that still have a functional Y chromosomal homologue and even some X-linked genes of which the homologue is lost, are not yet subject to dosage compensation [5]. This is confirmed by the observation that of the 15% of human X-linked genes that escape XCI, nearly all are located in the layers of the X chromosome that only recently diverged from the Y chromosome (X-Y conserved region) [6]. Also, another 20% of the genes on the human X chromosome are heterogeneously expressed, that is, different individual cells display a large variation in expression of these genes [6].

Expression of only one X chromosomal gene copy in both males and females would result in a difference in expression between the X and autosomes. Interestingly, in both males and females, the single active X is two-fold upregulated to compensate for the difference in expression between the X and autosomes [7,8]. Thus, dosage compensation in mammals does not only encompass XCI in females, but also upregulation of the active X to equalize the expression of autosomal and sex chromosomal genes in both sexes.

Is upregulation of the genes located on the active X a result of XCI evolution or did this process evolve independently, thereby initiating XCI evolution? Jegalian et al. [5] state that, before XCI evolved, X-linked genes would compensate for the loss of their Y chromosomal homologues by upregulation of gene expression. As degradation of the Y chromosome progressed, more X-linked genes needed to be upregulated subsequently, resulting in overexpression of the two X chromosomal gene copies in females [5]. Therefore, XCI evolved to counteract the overexpression of X-linked genes in females. Ultimately, XCI was sufficient to ensure equal expression between the sex chromosomal genes in males and females, while the initial upregulation of the X-linked genes also ensured equal expression between sex chromosomes and autosomes. Nevertheless, in haploid cells like secondary spermatocytes, oocytes, and spermatids, the genes on the single X chromosome are not overexpressed compared to autosomal genes, indicating that overexpression of the single X chromosome is not an intrinsic characteristic of the X, but can be regulated depending on the ploidy of the cell. This implies that an active mechanism ensures equalized X:autosome gene expression ratios, and indicates that the upregulation of the active X chromosome evolved as a response to XCI evolution and Y chromosome degradation, to equalize the difference in gene expression of the active X chromosome and autosomes in females and in males [7].

1.3 Mouse X chromosome inactivation in a nutshell

XCI occurs early in the development of the female embryo, in mice already after the 4-cell stage [9,10,11]. Cells in the early embryo always inactivate the paternally

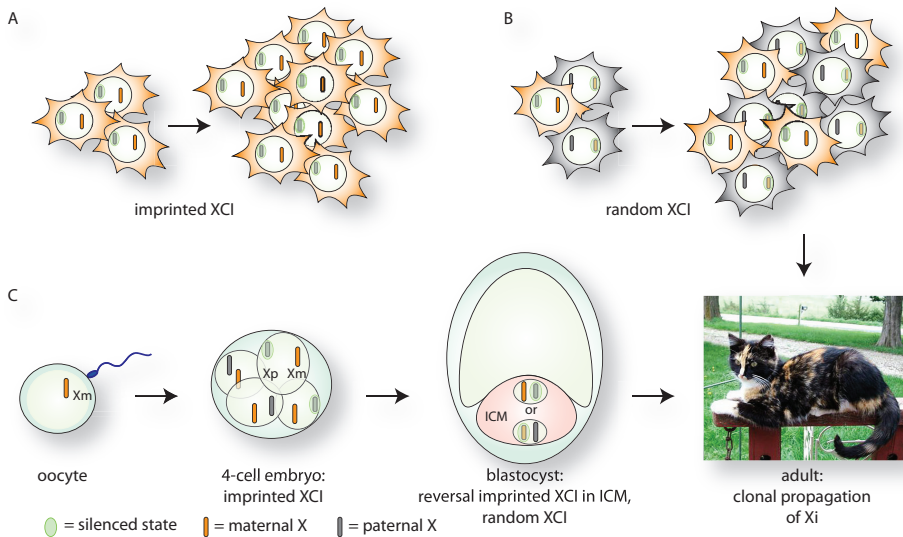


Figure 2. Imprinted and random XCI

A. Schematic representation of imprinted XCI: The paternal X (in grey) is always inactivated, leading to a cell population in which only the Xm is active (in red).

B. Schematic representation of random XCI: Both Xp and Xm have an equal chance to be inactivated, after which the decision to be inactivated is memorized and clonally propagated, leading to a mosaic cell population. A nice example of a clearly visible mosaic cell population due to random XCI is the tortoiseshell cat, which is always female. The Xp encodes one fur color, whereas the Xm encodes the other fur color.

C. During mouse embryogenesis, imprinted XCI is initiated at the 4-cell stage. At blastocyst stage, imprinted XCI is reversed in the inner cell mass (ICM), and random XCI takes place. Random XCI is clonally propagated, resulting in a mosaic adult.

inherited X chromosome (Xp), and leave the maternally inherited X chromosome (Xm) active, which is referred to as imprinted XCI (Fig. 2A and C)[12,13].

The embryo develops into a blastocyst after 3.5 days post coitum (dpc) in mouse and after 5.5 dpc in human, in which the inner cell mass (ICM) will develop into the embryo proper. In the ICM of gastrulation stage embryos, imprinted XCI is reversed, resulting in reactivation of the Xp and subsequent initiation of random XCI, whereas imprinted XCI is maintained in the extraembryonic tissue (Fig. 2B and C) [9,11,14]. Unlike imprinted XCI, random XCI ensures that both X chromosomes have an equal chance to be inactivated, causing ~50% of the cells to have an active Xp and ~50% of the cells to have an active Xm [15]. Only one of the two X chromosomes should be inactivated, because inactivation of all X's, or even leaving both X's active, is lethal to the cell [16,17]. Therefore, the number of X chromosomes in the cell must be determined in the developing embryo. When a female cell has established that two X chromosomes are present, XCI is initiated on one of the two X chromosomes.

Once random XCI is completed, the process is irreversible, and after each cell division the inactivated X (Xi) will be clonally propagated, meaning that the same X remains inactivated in all daughter cells [18]. Silencing of X-linked genes spreads in *cis* soon after initiation of XCI, repressing transcription of nearly all genes on the Xi [18]. In mice, only a few genes escape XCI and remain transcribed on both X chromosomes [19]. XCI can only take place during an early developmental window of embryogenesis up to 12.5 dpc in mice, after which it can no longer be induced [20].

Obviously, using embryos as a model system is not ideal. Many test animals have to be sacrificed in order to obtain enough embryos for significant results, and studying XCI in embryos is laborious and time consuming. Therefore, much research relating to XCI has used mouse embryonic stem cells (ES cells) as a model system. Female undifferentiated XX ES cells have two active X chromosomes, but upon differentiation of ES cells, random XCI is initiated and one of the X chromosomes is inactivated [21,22]. In contrast, male XY ES cells do not initiate XCI upon differentiation. The developmental window in which XCI can be initiated in ES cells appears to be much shorter compared to the embryo [23]. Nevertheless, comparison of different aspects of XCI in the embryo proper with ES cells has shown that ES cells encompass nearly all aspects of random XCI [24].

1.4 Random XCI in mice

1.4.1 Counting

The first essential step in the initiation phase of XCI is counting. The counting process involves determination of the number of X chromosomes present in the cell. Based on the X:autosome ratio, the cell establishes how many X chromosomes will be turned off to ensure the optimal dosage of X-linked gene expression. Genetic studies have indicated that the counting process is controlled by factors located in the X chromosome inactivation center (XIC). Analysis of two diploid mouse cell lines, the Searle's translocation cell line and the HD truncation cell line, indicated that the XIC is located within a 10 megabase (Mb) region of the X chromosome. The Searle's translocation cell line has a wild type X chromosome and an X;16 translocation, that has a substantial part of the telomeric region of the second X chromosome attached to chromosome 16 [25]. The HD truncation cell line is a cell line that has a deletion of the telomeric part of one of the X chromosomes [26]. The HD truncation cell line is able to initiate XCI in all cells, whereas the unbalanced Searle's translocation cell line is not. Therefore, the 10 Mb region of the X chromosome that is present in the HD truncation cell line, but not in the unbalanced Searle's translocation cell line can be defined as the XIC. In human, the XIC has been narrowed down to a 2.6 Mb contig

on the X chromosome, and the mouse homologue of this contig maps within the 10 Mb mouse XIC [27].

Studies on human and mouse aneuploid and tetraploid embryos and adults, and cell lines derived from these, reveal that one X chromosome per diploid autosome background remains active (Fig. 3). For instance, tetraploid XXXX mouse embryos preferentially inactivate two out of four X chromosomes [28], whereas tetraploid XXYY mouse embryos only rarely inactivate an X [29]. Interestingly, in triploid cells the ratio of one active X per diploid autosomal set cannot be obtained, and as a consequence the inactivation pattern in mouse triploid cell cultures and embryos is variable. In triploid XXY mouse embryos one or no X chromosome is inactivated, while in triploid XXX mouse embryos one or two X chromosomes are inactivated. However, the preference seems to be one Xi for XXY embryos and two Xi's for XXX embryos [30]. The same inactivation pattern is observed in human triploid embryos [31] and human triploid cell cultures [32], but here the preference is shifted towards two active X chromosomes instead of one. The difference between human and mouse triploid cells can be explained by secondary selection process in human cells with two active X chromosomes, as has been shown by a study following human triploid cell lines for ten passages or more [32].

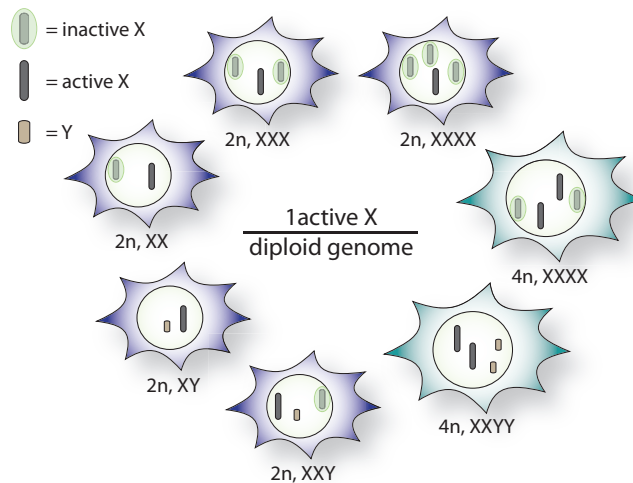


Figure 3. Counting

Cells count the number of X chromosomes by comparing the X to autosome ratio and leaving one X chromosome per diploid genome active. The ploidy of a cell is n .

1.4.2 Choice?

Once female XX cells have established that one X chromosome has to be silenced to obtain the optimal X:autosome ratio, XCI is initiated on one X chromosome, whereas the other X chromosome remains active. Normally, both X chromosomes have an

equal opportunity to become inactivated, so that ~50% of the cells inactivate one X chromosome, and the residual ~50% of the cells inactivate the other X. Until recently, inactivation of either X chromosome was thought to be a result of an active choice process that is mutually exclusive. In this view, either the future active X or the future inactive X is chosen. Both scenarios will have the same result, but are principally different and subject to heavy debate.

Choice of the future active or inactive X chromosome can be influenced by the genetically determined X chromosome controlling element (Xce), and combinations of different Xce's result in skewed, non-random XCI [33]. In mice, the Xce has been mapped to the XIC and has different strengths, ranging from very strong, Xce^a, to very weak, Xce^c [34,35]. A female XX ES cell containing an X chromosome with a strong Xce, Xce^a for instance, in combination with a weak Xce, like Xce^c, will preferentially chose the X chromosome with the strong Xce to be the future Xa, resulting in inactivation of the X chromosome with Xce^c in ~70% of the cells, and inactivation of the X chromosome with Xce^a in ~30% of the cells [35].

Although a mutually exclusive choice process is theoretically a reasonable hypothesis, it is not always supported by experimental data. Therefore, we propose a stochastic model for XCI, in this thesis. In this model, the inactivation of an X chromosome is not the result of an active and mutually exclusive choice process, but is dependent on the intrinsic chance of the X chromosome to initiate XCI, in combination with selection (Chapters 2 and 3).

1.4.3 Factors involved in XCI

To better understand the counting and choice process, more detailed knowledge about the molecular mechanism underlying XCI is required. The two main regulatory factors involved in XCI are *Xist* and *Tsix* [17,36,37], both located in the XIC on the X chromosome (Fig. 4). *Xist* and *Tsix* are genes coding for functional non-coding-RNAs (ncRNAs). *Xist* expression and spreading of RNA is necessary for XCI to occur on an X chromosome while *Tsix* represses expression of *Xist* in *cis*. *Tsix* is positioned at the 3' end of the *Xist* gene and is transcribed in an antisense direction through the entire *Xist* locus. Together the two genes determine whether XCI occurs in *cis* on the X chromosome. Other elements, proteins or genes that are involved in regulation of XCI are *DXPas34*, *Xite*, CTCF and YY1, which seem to regulate *Xist* or *Tsix* expression and function, directly or indirectly, as described below.

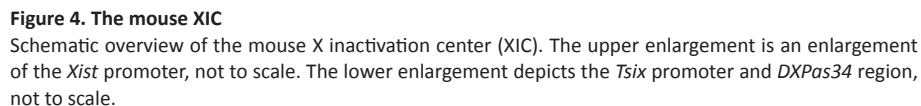
1.4.3.1 *Xist*

The *Xist* gene, as mentioned, is located on the X chromosome and is required for XCI to occur in *cis* [17,36]. It is expressed at low levels in undifferentiated XX ES cells,

and upregulated at the onset of XCI on the future inactive X chromosome and finally expressed exclusively from the Xi after XCI has been completed (Fig. 5) [28,37,38,39]. *Xist* RNA coats the entire Xi, attracting many histone modifiers directly or indirectly, which ultimately results in silencing of the Xi [40,41]. Many experiments have proven the importance of *Xist* in the XCI process. For instance, deletion of *Xist* from one X chromosome in XX female ES cells causes complete skewing of XCI towards the wild type X chromosome, while XY male ES cells are not affected [36]. This is not a consequence of secondary selection in benefit of the cells inactivating the wild type X chromosome when XCI has been completed, but the wild type X chromosome is always inactivated when *Xist* is deleted on one allele in female XX embryos (primary non-random XCI) [17,42]. Furthermore, ectopic expression and spreading of *Xist* is enough to initiate chromosome inactivation, even on an autosome [43,44,45]. Silencing, at least partially, of a chromosome from which *Xist* is transcribed is irreversible after three days of differentiation in ES cells, as has been shown using an inducible *Xist* transgene. However, when *Xist* RNA is removed beforehand, the silenced state of genes is reversed [23]. Importantly, the expression level of *Xist* is one of the factors that determines skewing of XCI, as has been shown by changing the *Xist* transcription level on one of two alleles by introducing a mutation or deletion in the *Xist* promoter [46,47].

Xist consists of 7 exons and *Xist* RNA is spliced and polyadenylated, does not contain an ORF and is restricted to the nucleus [40,48,49]. Furthermore, *Xist* is conserved between mouse and human, with an overall homology of more than 70%, but a few repeat regions have a much higher homology of approximately 90%. Indeed, these repeat sequences appear to be functional in the XCI process, as shown by analysis of ectopic XCI with mutated *Xist* cDNA transgenes [50]. The A-repeat in exon1 is solely necessary for silencing, whereas the tandem repeats downstream of the A-repeat are redundant and needed to localize *Xist* to the X chromosome in *cis* [50]. Also, after deletion of the endogenous A-repeat, *Xist* is not upregulated in ES cells or the embryo, probably because the mutated *Xist* can no longer silence *Tsix* and overcome *Tsix* repression [51].

The primary promoter of *Xist* (P1) is directly upstream of the gene and contains 7 footprints and 2 DNase I hypersensitive sites (HS sites) (Fig. 4, enlargement of *Xist* promoter) [52,53]. Footprint V contains a single nucleotide polymorphism (SNP) between *Mus musculus* and *Mus spretus* [54]. Footprint II is a putative TATA-box, but does not seem to be a direct TATA-binding-protein (TBP) binding site. Footprint I, which is the transcriptional start site, contains a putative YY1 binding site. Four more footprints have been described further upstream of *Xist*, but the functional relevance of these sites has not been determined [46,47].



Initially, based on non-strand specific analysis of transcription, *Tsix* was identified as unstable *Xist* RNA transcribed from P0 in undifferentiated ES cells [57,58]. However, Lee et al. [37] were the first to recognize that *Tsix* is a gene located 15 kb downstream from *Xist* and is transcribed in antisense direction of *Xist*. *Tsix* encodes a continuous antisense RNA of approximately 40 kb that spans all of *Xist*. Multiple transcription start sites for *Tsix* have been identified and approximately 50% of the *Tsix* transcripts are spliced into various small isoforms of which the 3' ends have an overlap with the 5' part of *Xist* [61,62]. *Tsix* is transcribed in male and female undifferentiated ES cells in 10 to 100 times excess to *Xist*, and during establishment of XCI from the allele that is to remain active in male and female differentiating ES cells. After completion of

XCI, *Tsix* is downregulated (Fig. 5)[37,61].

Tsix is generally regarded as the major inhibitor of *Xist* and therefore as an important factor in XCI regulation. However, careful examination of the literature shows that overall antisense transcription through the *Xist* locus determines inhibition of *Xist*. For example, loss of the major promoter of *Tsix* has no significant effect on counting or initiation processes of XCI [63]. However, deletion of *DXPas34*, a CpG island located downstream of the *Tsix* TSS from which antisense transcription is also initiated (Fig. 4, enlargement *Tsix* major promoter), significantly decreases antisense transcription through the *Xist* locus, and causes primary non-random inactivation of the targeted allele in female XX ES cells [63,64,65] and inappropriate XCI on male XY ES cells [65]. Lee et al. [66] do not observe primary non-random XCI in XY ES cells upon deletion of *DXPas34* and the promoter of *Tsix*. A possible explanation for this latter result could be that the transgenic male cell line in question contained a neomycin (NEO) cassette integrated at the former *DXPas34* locus. A NEO cassette introduced by others at the same location influenced XCI similarly, because the NEO cassette probably influences transcription of *Tsix* [65]. Furthermore, the authors may have missed cells that inactivated the single X chromosome, because these cells might have died before analysis of XCI initiation was performed.

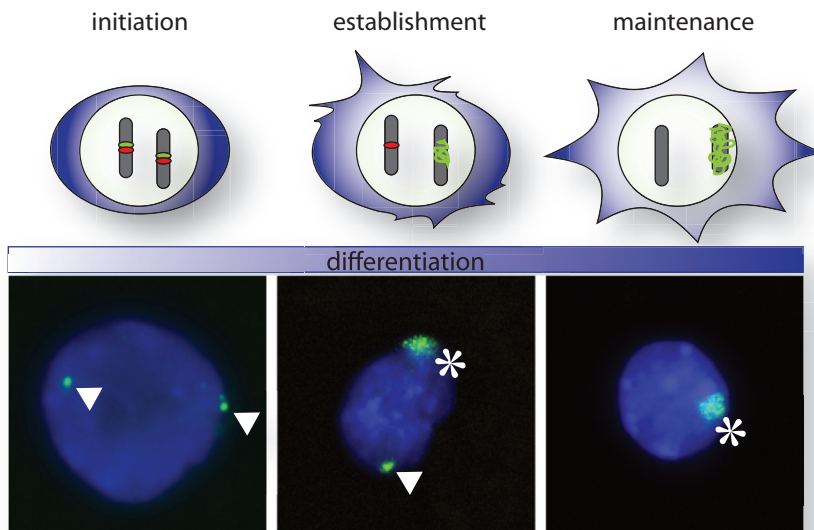


Figure 5. *Xist* and *Tsix* expression during XCI

The upper panels depict a schematic overview of the expression pattern of *Xist* (in green) and *Tsix* (in red) during the initiation, establishment, and maintenance phase of XCI.

The lower panels show *Tsix* and *Xist* pinpoints (arrowhead), and *Xist* clouds (asterix) during the initiation, establishment, and maintenance phase of XCI in differentiating ES cells. *Xist* and *Tsix* are labeled with a double strand cDNA probe in green.

Interestingly, the methylation status of *DXPas34* coincides perfectly with antisense transcription through *Xist*. The CpG island is hypomethylated when actively transcribed and hypermethylated when antisense transcription is downregulated [67,68]. Antisense transcription is also initiated at a region ~10 kb upstream of *Tsix*, called *Xite*. The *Xite* expression and methylation pattern during XCI is similar to the *Tsix* methylation and expression pattern, and deletion of *Xite* results in reduced antisense transcription through the *Xist* locus and skewing of XCI towards inactivation of the targeted allele [68,69,70], implying a similar role for *Xite* in inhibition of *Xist* function as *DXPas34* and *Tsix*. Furthermore, direct inhibition of antisense transcription by insertion of a polyA site between *Xist* and *DXPas34* also causes primary non-random XCI in female ES cells and inappropriate XCI in male ES cells. Even more so, overexpression of antisense transcription on one allele results in primary non-random inactivation of the wild type allele [71]. Finally, a 65 kilobase (kb) deletion encompassing not only *Tsix*, but also *Xite* and *DXPas34*, thus abrogating all antisense transcription, shows not only complete primary non-random XCI of the targeted allele, but also severe cell death in XO and XY cells containing the deletion, invoked by improper XCI [72,73]. Thus, inhibition of *Xist* seems to correlate with an increase in antisense transcription through the *Xist* locus. For simplicity reasons, I will refer to antisense transcription through the *Xist* locus as *Tsix* transcription.

How does *Tsix* inhibit *Xist* expression? Three hypotheses have been proposed. First, *Tsix* may function by forming a double stranded RNA heteroduplex with *Xist* resulting in repressive siRNA, which functionally silences *Xist* in *cis* [74]. However, overexpression of *Tsix* cDNA, which includes the homologous region with *Xist* on an allele with abrogated endogenous *Tsix* transcription by insertion of a polyA signal, does not restore *Xist* inhibition [75], arguing against RNAi based inhibition of *Xist*. Also, Dicer knockout mice that have an impaired RNAi machinery exhibit correct XCI, although *Xist* is indirectly upregulated due to loss of DNA methylation at the *Xist* promoter [76].

Secondly, *Tsix* and *Xite* might form a three-dimensional chromatin structure via DNA looping that enhances *Tsix* and *Xite* antisense transcription, but excludes the *Xist* promoter and thereby inhibits *Xist* expression in *cis*. A chromosome-conformation-capture (3C) study has shown that *Tsix* and *Xite* interact over a long distance, while the *Xist* promoter seems to co-localize with the *Jpx* promoter when *Xist* is transcribed. *DXPas34* is a likely candidate for looping, because deletion of *DXPas34* causes a severely skewed phenotype in female ES cells and XCI in male ES cells [63,64,65], and it is bound by CTCF, a protein that is often implicated in looping of DNA [77]. However, the *DXPas34* deletion does not significantly change the three-dimensional chromatin structure in male ES cells. Furthermore, it is hard to determine

whether a specific three-dimensional chromatin formation in *cis* is the cause or the consequence of the transcription profile of that allele [78].

Finally, not *Tsix* RNA, but antisense transcription through the *Xist* locus may inhibit *Xist* upregulation through a transcription interference mechanism. How antisense transcription based inhibition of *Xist* works mechanistically has not been shown, but one can envision that promoter polymerase initiation complexes (PICs) will have more difficulty forming on a promoter when an elongation complex transcribing in the antisense direction co-exists at the locus. Furthermore, RNA polymerase II complexes of *Xist* and *Tsix* may collide during transcription elongation, causing a premature halt of *Xist* transcription and less *Xist* accumulation. Alternatively, inhibition of *Xist* might be caused by alteration of the chromatin state of the *Xist* locus by antisense transcription. It has been postulated that *Tsix* transcription induces heterochromatin formation at the *Xist* promoter by attracting histone modifiers, and thereby silencing it [79,80]. Recently, EED, a component of the PRC2 Polycomb complex, has been shown to work synergistically with *Tsix* transcription in silencing *Xist* [81]. Furthermore, loss of antisense transcription through the *Xist* promoter causes reduction of CpG methylation and repressive histone modifications, indicating that transcription from the *Xist* promoter is enhanced [82]. However, findings of Sun et al. [60] argue against this hypothesis by showing that activation of *Xist* on the future Xi is characterized by a transient heterochromatic state at the *Xist* promoter, perhaps induced by the silencing capacity of *Xist* itself, and thus contradicting a functional role of chromatin modifications in inhibition of *Xist* by *Tsix*. In conclusion, most evidence points towards transcription mediated repression of *Xist* by *Tsix*, but the exact mechanism has yet to be established.

1.4.3.3 Protein Factors

CTCF is a protein with 11 DNA or protein binding Zinc fingers, which has approximately 14,000 binding sites in the human genome and is implicated in different functions such as transcription regulation, genome organization and insulation of chromatin domains [83,84,85,86]. Furthermore, CTCF has been shown to regulate allele specific expression in imprint controlled regions like the H19/Igf2 region [87], by binding only the allele with the non-methylated CTCF binding sites [84]. Binding of CTCF has been postulated to prevent promoter-enhancer interactions when located in between the two. Like CTCF, YY1 is a multi zinc finger protein that binds DNA and is associated with imprinted control regions like *Peg3* and *Nespas* [87]. Putative CTCF and YY1 binding sites have been found throughout the XIC, especially in the *Xist* promoter and at the *DXPas34* region (Fig. 4) [53,68,77,87,88,89]. Interestingly, YY1 and CTCF seem to form a complex that binds the *DXPas34* region [89].

Although the function of CTCF and YY1 in XCI is not fully understood, several lines of evidence indicate that both are important for expression of *Tsix* and *Xist*. First, point mutations in the CTCF binding site of the *XIST* promoter cause skewed XCI in humans. Point mutations that enhance CTCF binding on one of two X chromosomes result in preferred inactivation of the mutated allele, whereas abrogation of CTCF binding by a point mutation on one allele will keep this allele active [54]. Also, CTCF binds specifically to the inactivated X chromosome in mice [54]. Furthermore, the CTCF binding sites found in the *DXPas34* and *Xite* region show increased de novo methylation during ES cell differentiation [68]. Because CTCF binds methylated sites less efficiently [77], de novo methylation might result in loss of CTCF binding during differentiation, which coincidentally corresponds to *Tsix* downregulation, implicating that CTCF may function as an activator of *Tsix*.

Nonetheless, most reports attribute an insulator function to CTCF and YY1 bound to the Xi, especially at sites positioned on the *DXPas34* locus [54,77,83]. How do the observations described above correlate to an insulator function of CTCF and YY1? Most likely, CTCF forms a boundary between silent and active chromatin [86], as has been shown for CTCF that binds regions adjacent to genes that escape XCI on the Xi [83]. CTCF and YY1 might facilitate an allele-specific 3D chromatin conformation, dependent on the differentiation state of ES cells and thus the methylation status of the alleles. Indeed, *DXPas34* and *Xite* form a DNA loop on the active X that might protect *Tsix* from being silenced, which coincides with the methylation profile of the X chromosome. Similarly, *Xist* interacts with an enhancer 5' of the *Xist* promoter on the Xi [78]. However, deletion of most, but not all, CTCF binding sites in the *DXPas34* region does not interfere with the 3D conformation of the XIC, while the deletion does affect XCI regulation. This argues against a role of CTCF and YY1 in regulation of XCI via looping of DNA [78].

Reduction of CTCF or YY1 levels indicates a functional role of both in XCI. Embryos carrying a homozygous deletion of YY1 die shortly after implantation, and analysis of preimplantation YY1^{-/-} embryos shows aberrant *Xist* expression [89]. Female embryos with reduced YY1 levels are viable, but have a reduced body weight and are born less frequently than their male and female wild type, and transgenic male littermates [89,90]. Some male YY1^{+/-} embryos, as well as male ES cells derived from these embryos have a decreased *Tsix* transcription level and increased *Xist* expression [89], and male live-born YY1 knock-down pups display a slight upregulation of *Xist* [90]. Thus, the reduced body weight and non-mendelian ratios of offspring with decreased YY1 levels may be caused by faulty regulation of XCI, resulting in cell death caused by inappropriate XCI. CTCF knock-down in early mouse embryos reduces litter size, which is caused by embryonic lethality before implantation of the

embryo, but it is unknown if the mendelian ratios of the offspring are affected [91]. In differentiating male ES cells, knock-down of CTCF results in a similar phenotype as found in YY1 knock-down in male ES cells (hence, increased *Xist* transcription) [89]. However, CTCF knock-down in differentiating female XX ES cells gives rise to a reduced number of *Xist* clouds compared to wild type cells, while YY1 knock-down in female ES cells does not [92]. Thus, CTCF knock-down data are conflicting between male and female ES cells, leaving the exact role of CTCF in XCI unknown.

Thus far, CTCF and YY1 are the only *trans*-acting proteins that are thought to be involved in the choice and counting mechanism of XCI. In addition, mutagenesis studies on mice have resulted in two potential autosomal regions that influence skewing of XCI choice [93]. In contrast, a study of human trisomy embryos has excluded all autosomes, except parts of chromosome 1 and 19, to encompass a locus that influences choice and/or counting in XCI [94]. The autosomal regions in mice and humans that are implied to contain factors influencing XCI counting and choice do not encompass the CTCF or YY1 genes.

1.4.4 Models for regulation of random XCI

All data at hand has resulted in heavy speculation about how counting and initiation of XCI is regulated. Many models have been postulated and the most important ones are described below and in Figure 6.

1.4.4.1 Blocking factor

The blocking factor model states that a limiting factor blocks XCI on one of the two X chromosomes in female cells and on the single X chromosomes in male cells [25]. The cell is able to count, because the blocking factor is encoded by an autosomally located gene, and thus the excess of autosomes over X chromosomes determines whether enough blocking factor is present in order to inhibit XCI on one X chromosome in a diploid background. The blocking factor will bind an element in the XIC that prevents *Xist* to accumulate on that X chromosome in *cis*. Therefore, a heterozygous deletion of this element in female cells will cause primary non-random XCI of the targeted X chromosome, whereas a homozygous deletion should result in two inactive X chromosomes or XCI in male cells (Fig. 6).

The phenotype of the *Tsix* or *DXPas34* deletion greatly resembles the hypothetical counting element deletion [16,63,64,66,72] and is therefore the most likely candidate to be the counting element, which would suggest that the blocking factor is the activator of *Tsix*. A potential candidate to be the blocking factor is YY1, because it binds the *DXPas34* region and knock-down of YY1 by ~50% causes a slight upregulation of *Xist* expression and reduced body weight in newborn mouse pups,

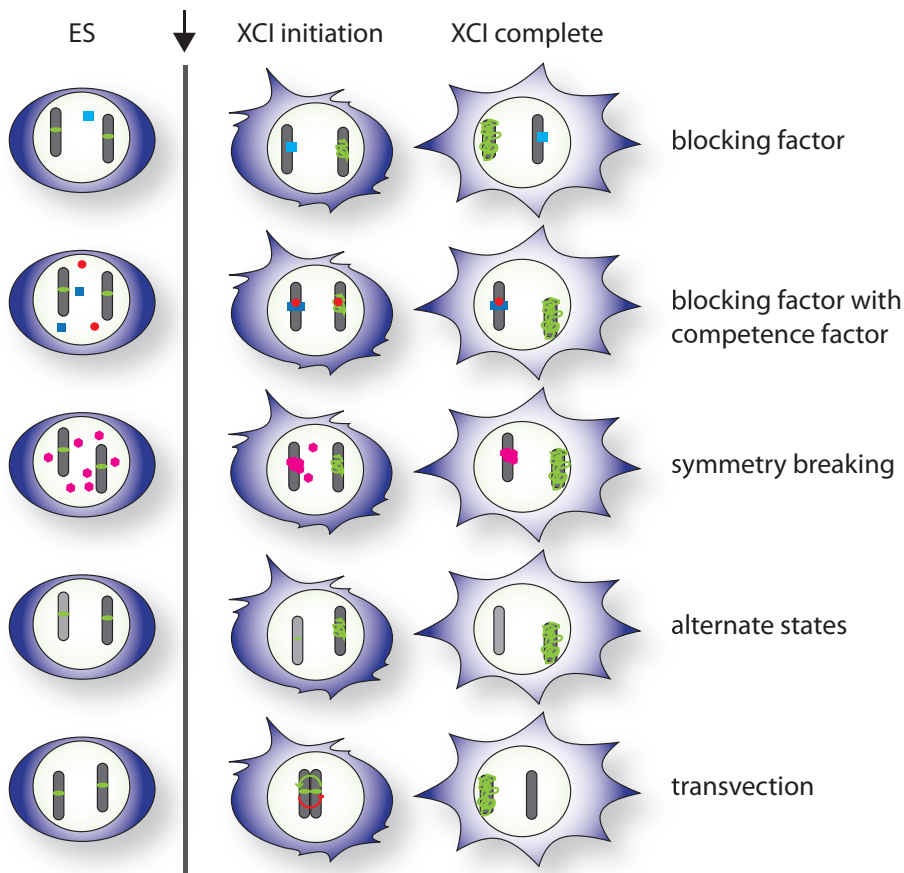


Figure 6. Models for XCI

Five models for the counting and choice mechanism of XCI. The X chromosomes are shown in grey, *Xist* expression is depicted in green, the blocking factor in blue, the competence factor in red, and the symmetry-breaking factors in pink. The arrow indicates the differentiation step.

which could indicate inappropriate XCI in the embryos, resulting in cell death [89,90]. However, YY1 is not located on the autosomal regions that have been defined by mutagenesis and analysis of human trisomy embryos to potentially contain *trans*-acting factors involved in XCI [93,94]. Furthermore, YY1 is abundantly present in cells and will not have a limiting protein concentration, which is hypothesized to be a critical aspect of the blocking factor model. In fact, it is difficult to envision that every cell will have exactly the same extremely low concentration of blocking factor at the onset of XCI, so that only one allele will be protected against XCI. Nevertheless, postulating that the blocking factor is a nuclear entity could circumvent this. Another complication of the model in which the *Tsix* activator would act as the blocking factor, is that *Tsix* should be upregulated at the onset of XCI on one allele, while

in fact *Tsix* is not upregulated, but downregulated on the future Xi [37,61]. Finally, with *Tsix* activator as the blocking factor binding only one of the two alleles, thereby protecting it from XCI, than the other allele should inactivate. If this allele is impaired for XCI, because *Xist* is deleted for example, than the cell should not be able to inactivate, which should result in death of half the cell population. In contrast, cells with a heterozygous *Xist* deletion all make the right choice and initiate XCI on the wild type X chromosome, resulting in primary non-random XCI [42]. Therefore, a positive XCI factor was hypothesized, named the competence factor (CF). One model encompassing the blocking factor and a CF postulates that the abundantly present CF can only bind an X chromosome when the blocking factor does not bind, which results in inactivation of all remaining X chromosomes [42]. Another hypothesis states that the autosomally encoded blocking factor determines how many X chromosomes remain active, because it is present in a low dose so that it can bind only one X chromosome. Also, the blocking factor titrates away one 'copy' of the X-encoded CF, which corresponds to a single X chromosome. When more than one X chromosome is present in a diploid background, the extra copies of CF will not be titrated by the blocking factor and inactivate the remaining unprotected X chromosome(s) (Fig. 6) [66,95].

Overall, conclusive evidence in favor of the blocking factor model, like a proper dosage dependent trans-acting blocking factor, has yet to be found.

1.4.4.2 Symmetry-breaking

The main problem of the blocking factor model is that a single entity or molecule will be present in a diploid cell, and will always bind only one X chromosome present. However, cell-to-cell variegation is likely to make such a system unstable. A model in which not one factor, but many factors bind only one of two X chromosomes in a female diploid cell overcomes this problem (Fig. 6)[96,97]. This model, dubbed the symmetry-breaking model, states that at the onset of XCI a blocking complex will form on one X chromosome, composed of many autosomally encoded molecules that will bind to the DNA and itself through self-assembly. Computational analysis shows that this self-assembly is energetically more favorable if it takes place on only one X chromosome in the cell and not two. Because each X chromosome initially has an equal chance to be bound, while only one X will be ultimately protected by the blocking complex, this model is similar to the blocking factor model, but circumvents the problem of having a single factor present in a cell. Nevertheless, physical evidence of complex formation on the active X at the onset of XCI has never been presented.

1.4.4.3 Alternate states

Unlike the blocking factor models, the alternate state model postulates that the choice for an X chromosome to be inactivated is intrinsically determined by the chromatin state of the X prior to XCI (Fig. 6)[98]. The nature of this chromatin state is unknown, but can be determined by looking at the fraction of alleles that have replicated DNA strands that remain close together after replication versus the ones that are clearly separated. It seems that the X chromosomes with the connected duplicated DNA strands are more prone to XCI than the ones with separated duplicated DNA strands. These different states of sister chromatid cohesion are transient and are locked in at the onset of XCI, thereby ensuring random XCI. However, cell lines that display primary nonrandom XCI because either the *Xist* gene or *Tsix* is deleted on a single X chromosome [36,71] only show a mild shift of bound replicated DNA strands on the allele destined to be inactivated, indicating that not all cells will make the right “choice” to inactivate one X chromosome (see 1.4.2) and will die due to absence of XCI. The fact that both mutated cell lines exhibit primary non-random XCI and that mutated cells are not more likely to die upon XCI than wild type cell lines [17,42,71], argues against this model.

1.4.4.4 Transvection

The final model discussed here is based on the observation that co-localization of the XICs in XX ES cells precedes XCI (Fig. 6). This XIC co-localization or pairing is very transient and can only be observed in a subset of cells, but does occur more frequently than what would be expected from random co-localization [92,99]. Pairing seems to depend on a few locations within the XIC. A *Tsix* or *Xite* deletion in female ES cell lines results in loss of pairing [92,99,100]. However, reconstitution of pairing by restoring the *Tsix* or *Xite* pairing sites does not regain random XCI [99], or induce XCI in male ES cells [100] indicating that another pairing region is crucial for initiation of XCI. Indeed, a BAC sequence located ~400 kb upstream of *Xist* was found to pair with other copies of this region and to induce XCI in male ES cells when randomly integrated [101]. It was suggested that the BAC region is essential for sensing the presence of more than one X chromosomal allele and subsequent initiation of XCI, while pairing of the *Tsix* and *Xite* region provides a feedback loop to prevent that the second X chromosome will inactivate [101].

Pairing of the X chromosomes at the onset of XCI seems to be mediated by CTCF. Knock-down of CTCF, but not of YY1, causes less pairing and reduced initiation of XCI [100]. Another requirement for pairing is transcriptional activity of *Tsix* and *Xist* [100]. When DNA polymerase II transcription is inhibited, pairing of the *Tsix* and *Xist* regions is lost [102]. This result might indicate that the pairing events observed

are not the cause of XCI, but a consequence of transcriptional activation of *Xist* at the onset of XCI, which may result in relocation of the XIC in the nucleus.

1.5 Silencing the X chromosome

1.5.1 Chromatin of the inactive X chromosome

The first step in silencing the X chromosome is the spread of *Xist* RNA in *cis* over the X chromosome. Several redundant repeats of *Xist* are important for the localization of *Xist* RNA to the Xi [50]. Spreading of *Xist* causes depletion of RNA polymerase II and other components of the transcription machinery on the Xi within one day, and abrogates transcription of repeat and intergenic sequences, independently of the A-repeat [103]. However, silencing of genes is mediated by the A-repeat within *Xist* RNA and starts after one to two days, continuing until gene silencing is more or less completed after approximately seven days of differentiation [8,103]. Silencing of genes is hypothesized to be associated with the relocation of active genes at the outer rim of the X chromosome territory towards the silent Xi territory by the A-repeats [103,104].

After depletion of the transcription machinery from the Xi territory, the Xi chromatin is changed drastically (Fig. 7A and B). First, histone 3 lysine 27 trimethylation (H3K27me3) is acquired by transient localization to the Xi of the Polycomb-repressor complex 2 (PRC2), which is comprised of protein subunits EED, EzH2, RbAp47/48 and Suz12, of which EzH2 has histone methyltransferase activity [105,106,107,108,109]. PRC2 binds *Xist* directly, as has been shown by either deletion of EED or conditional deletion of *Xist*, which both cause loss of H3K27me3 [107,108,110]. Recently, PRC2 subunit EzH2 has been identified as the protein that targets the PRC2 complex to the A-repeat of *Xist* RNA [111]. Knock-down of EzH2 or EED caused decreased *Xist* binding to the Xi and H3K27me3 enrichment. Although PRC2 seems to be important for binding *Xist* to the Xi, it is not likely to be the only protein complex doing so, because loss of PRC2 does not seem to affect random XCI in the embryo proper [107,108].

Apart from histone methylation, most cells also show accumulation of H2A lysine 119 ubiquitination (ubH2A) on the Xi after the onset of XCI, which is established by the Ring1A/B subunit of Polycomb repressor complex 1 (PRC1) [110,112,113]. Ring1A and Ring1B have redundant functions in ubiquitination [112,114] and only deletion of both Ring1 proteins results in loss of ubH2A on the Xi [112]. PRC1 recruitment to the Xi follows PRC2 recruitment, but is not solely mediated by H3K27me3, as has been shown in EED deficient ES cells, but also by the 3' end of *Xist* RNA, either directly through interaction with *Xist* or by indirect interaction with

an *Xist* binding protein [110,115]. A potential candidate for targeting of the PRC1 complex to *Xist* RNA is the Polycomb homolog CBX7, which shows a high affinity for H3K27me3 and for RNA [116], and has been shown to interact with the Ring1 protein [117].

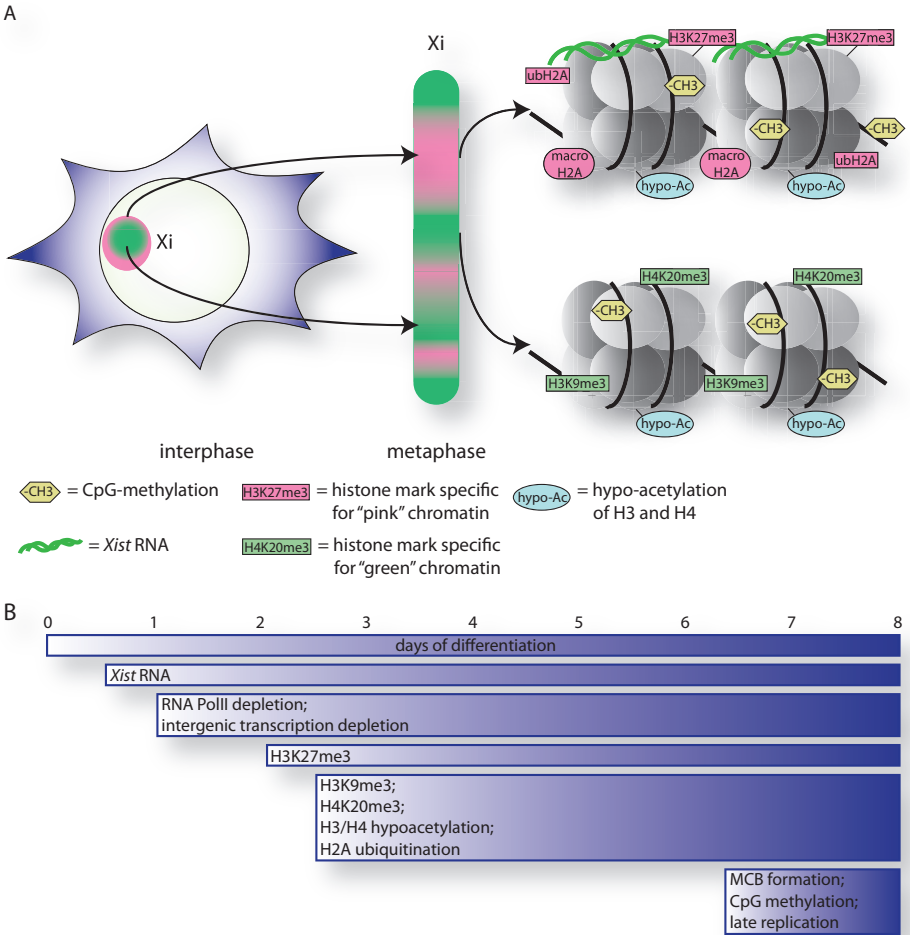


Figure 7. Chromatin of the Xi

A. Chromatin marks of the Xi. On the left, the Xi in interphase is shown and divided into two distinct silent chromatin states, in pink and green. H3K27me3 and ubH2A, amongst others, characterize the pink chromatin state while histone marks such as H3K9me3 characterizes the green chromatin. In the middle, the Xi is depicted in metaphase state, again divided into two distinct pink or green chromatin states that are the same as in interphase. On the right, the histone marks specific for the pink chromatin state are depicted in the upper string of nucleosomes, while the histone marks specific for the green chromatin state are shown in the lower string of nucleosomes.

B. A large number of protein and DNA hallmarks accumulate on the Xi during differentiation. Differentiation is temporally displayed from left to right, at the top bar, while a selection of hallmarks specific for the Xi are added at different time points during differentiation as represented by the bars below the differentiation bar.

Another histone methylation mark associated with silenced chromatin, histone 3 lysine 9 trimethylation (H3K9me3), accumulates on the Xi just after H3K27me3 [118,119,120,121,122]. H3K9me3 is most likely put in place by HMTase Suv39, and maintained by HP1, which is enriched on the Xi [123,124], but other histone methyltransferases (HMTases) might also play a role.

H3K9me3 accumulation appears more or less simultaneous with loss of acetylation of histone H3 and H4 (H3K9Ac and H4K5Ac, H4K8Ac and H4K12Ac, respectively) and trimethylation of histone H3 lysine 4 (H3K4me3) and histone H3 lysine 36 (H3K36me3), which are all hallmarks of euchromatin [21,118,119,124,125,126,127,128]. Probably, a set of histone modifiers, including histone deacetylases (HDACs) and histone demethylases (HDMs), are attracted by H3K27me3 and *Xist* and co-localize with the Xi to direct the chromatin towards a heterochromatic state. Among the late epigenetic changes are macroH2A incorporation [129,130] and CpG island methylation [131,132]. MacroH2A is a H2A variant with a large C-terminal domain [133] that replaces H2A histones on the Xi after approximately 7 days of differentiation [129,130], forming a macro-chromatin body (MCB) in a significant proportion of the cells [129,134]. *Xist* expression is sufficient for initiation of H2A replacement by macroH2A and MCB formation [134], and conditional deletion of *Xist* leads to loss of the MCB [135]. CpG methylation is also a late Xi mark, and is put in place by *de novo* methyltransferase 3A (DNMT3A) [136] and maintained by DNMT1 [137].

Recently, two other factors have been shown to be involved in the maintenance phase of XCI. First, the DNA binding hinge-domain protein SmcHD1 plays a role in DNA methylation of the Xi. Loss of SmcHD1 results in depletion of DNA methylation at the X-linked CpG islands and reactivation of the Xi [138]. It was postulated that SmcHD1 targets DNMT3A to the Xi, although no direct evidence in that direction was presented. Second, ATRX, encoded by an X-linked gene, has been shown to be involved in XCI. ATRX is a chromatin remodeler and member of the SWI/SNF2 helicase family, which is enriched at the Xi, and accumulation of ATRX can be regarded as a late mark of the Xi [139]. Interestingly, ATRX does not only repress X-linked genes on the Xi, but also pseudo-autosomal genes that have translocated to an autosome, implicating that a (former) X chromosomal sequence is required to attract ATRX to a gene [140]. The recent discovery of these factors indicates that silencing of the Xi is more complex than initially thought and involves multiple factors, of which many are probably not yet revealed.

The first established epigenetic hallmark of the Xi is that it replicates very late during the S phase of the cell cycle, whereas the Xa replicates early [141]. This is caused by the heterochromatic state of the Xi [142,143], and replication timing is not

involved in the initiation of XCI [144].

All these features of the Xi are important to lock-in the silenced state of the X chromosome (Fig. 7). Together, they ensure that the Xi is nearly impossible to reactivate and that the cell contains some kind of memory of which X chromosome is inactivated through many cell cycles. The redundancy of the Xi hallmarks is demonstrated by conditional deletion of *Xist* after establishment of XCI, which causes loss of the macroH2A [135], but still only leads to minor reactivation of the Xi, even when it is combined with loss of DNA methylation and inhibition of hypoacetylation [145,146]. Furthermore, loss of H3K27me3 in EED-/- knockout does not appear to influence random XCI [107,108].

1.5.2 *Xist* spreading, Xi organization and nuclear organization

After *Xist* is upregulated on one of the two X chromosomes, it starts to spread in *cis* over the entire chromosome [41,147]. Somehow, *Xist* RNA is restricted to the inactivated X chromosome and does not localize to neighboring autosomes. Furthermore, X;autosome translocations show that endogenously expressed *Xist* preferentially binds the X chromosomal part of the chromosome [148,149,150], whereas spreading into the autosome seems to be correlated with the density of LINE repeats [150]. This observation has led to the LINE repeat hypothesis [151], in which it is stated that spreading of *Xist* is mediated by binding to LINE repeats. Indeed, LINE repeats are twice more abundant on the human X chromosome as on autosomes and the distribution of LINE repeats seems to correlate with the degree of XCI on the X chromosome [152,153,154]. Also, computational studies of the DNA sequence surrounding genes escaping XCI compared to silenced X-chromosomal genes indicate a depletion of LINE repeats around escaping genes [155,156].

Nevertheless, not all computational studies on the DNA sequence of the X chromosome find a clear correlation between LINE repeats and XCI [157,158]. Furthermore, *Xist* RNA does not spread over the X chromosome homogenously, but appears to have a banded pattern when detected on a metaphase Xi and an open circle shape at the periphery of the Xi in interphase cells (Fig. 7A, left)[123,148,159]. Curiously, this *Xist* RNA pattern does not seem to correspond to the density of underlying LINE repeats, but rather with the gene density on the X chromosome [104,159]. The banded pattern on the metaphase Xi of *Xist* RNA and gene rich regions can also be observed with histone markers H3K27me3, macroH2A and ubH2A, while histone markers H4K20me3 and H3K9me3 are enriched on the gene poor regions of the Xi metaphase chromosome (Fig.7)[123,159,160,161].

Together, these data suggest a three dimensional organization of the Xi, in which the gene poor regions enriched by histone marks H4K20me3 and H3K9me3

are more internally located and the gene rich regions, enriched by *Xist* RNA, H3K27me3, macroH2A and ubH2A are present on the outer rim of the Xi territory [103,104,123]. Overall, the Xi becomes more spherical, but retains a similar volume to the Xa [162]. This Xi organization corresponds to DNA-FISH analysis of escaping and silenced X chromosomal genes, that shows that all analyzed genes are localized at the periphery of the Xi territory, but that active genes seem to 'loop-out' of the chromosome territory [103,104,163]. Still, the importance of the DNA sequence in the organization of the Xi remains illusive, as a direct interaction of LINE repeats or another specific DNA motive with histone marks and/or *Xist* RNA has not yet been reported.

The Xi might not only have an intrinsic three-dimensional organization, but is also specifically positioned within the nucleus. After inactivation, the Xi is preferentially located either at the periphery of the nucleus [164,165] or near the perinucleolar region [165,166]. The specific positioning of the Xi could be mediated by components of the nuclear matrix. For instance, nuclear matrix scaffold protein SAF-A co-localizes with the Xi, which seems to be dependent on the RNA binding domain of the protein [167,168]. Furthermore, cells expressing mutated LaminA show depletion of heterochromatic markers H3K27me3 and H3K9me3 at the Xi, and the peripheral localization of the Xi is lost [169]. These results indicate that the localization of the Xi in the nuclear periphery is either a consequence of its heterochromatic state or affects the heterochromatic state of the Xi [169,170]. However, the perinucleolar localization of the Xi is less easy to comprehend, especially because the Xi seems to preferentially co-localize with the perinucleolar region during S phase [166]. The S phase specific localization is dependent on *Xist*, as autosomes containing an *Xist* transgene are also repositioned to the perinucleolar region in S phase, and conditional *Xist* knockout cells lose the preferential perinucleolar localization of the Xi. Interestingly, heterochromatin replication occurs late during S phase, at which point replication can only be observed around nucleoli and at the periphery of the nucleus [143,171]. Thus, perhaps, heterochromatin characterized by H3K27me3 needs a specialized nuclear compartment for replication and/or maintenance of the silenced state after replication.

1.6 Imprinted XCI

While in random XCI in the mouse embryo the maternal X chromosome (Xm) and the paternal X chromosome (Xp) have equal chances to inactivate, it is always the Xp that is inactivated in the extraembryonic tissues of the mouse, due to imprinted XCI [12,13]. Therefore, embryos with XpXp, XpY or Xp0 (androgenetic embryo's) always inactivate both or the single Xp, respectively [172,173,174] whereas XmXm

(parthenogenetic and gynogenetic embryo's display severely delayed XCI, resulting in extensive cell death and embryonic lethality [172,175]. Imprinted XCI initiates in the whole embryo just after fertilization at the 2- to 4-cell stage, but is only maintained in the extraembryonic tissue of the embryo, like the placenta and yolk sac [9,10,11]. Silencing of the X chromosome is acquired in much the same way as in random XCI. *Xist* spreads over the future inactive Xp chromosome and following spreading of *Xist*, RNA polIII is excluded from the Xp [10] and many chromatin modifications are enriched on the Xi, like H3K27me3, H3K9me3, ubH2A, hypoacetylation and macroH2A incorporation [10,107,109,113,176]. A significant difference between silencing of the X chromosome in imprinted and random XCI is that in imprinted XCI the Xp does not become late-replicating in S phase in contrast to the Xi after random XCI [11]. Similarly, undifferentiated female ES cells ectopically expressing *Xist* from an X chromosome, display silencing in *cis*, but no late-replication of the X chromosome, and silencing can be reversed [23]. Also, EED null trophoblast giant cells have the tendency to reactivate the Xi after imprinted XCI [108], in contrast to Xi's that have been subjected to random XCI, which do not reactivate. Together these results suggest that maintenance of the silenced state of the Xp after imprinted XCI is less profound as after random XCI. This could be a consequence of the fact that the Xp has to be reactivated in the embryo proper after 3.5 days of development [177].

The most important questions relating to imprinted XCI are how the imprint is established and where it is located. The most likely locations are the *Tsix* promoter and/or enhancers and the *Xist* promoter (Fig. 4, enlargements). Heterozygous deletions of *Tsix* on the Xm or of *Xist* on the Xp both have a severe phenotype, while deletion of *Tsix* on the Xp or deletion of *Xist* on the Xm does not show aberrant imprinted XCI (Fig. 8A) [16,17,62,63,82,178]. Heterozygous loss of *Tsix* transcription on the Xm (which is inherited from a female chimera with a heterozygous deletion of *Tsix*) causes *Xist* expression and inactivation of the Xm, which leads to two inactivated X chromosomes and embryonic lethality [16,62,63,82,178], while a severe decrease of *Tsix* transcription by deletion of *DXPas34* on the Xm (Δ CpG) reduces the number of viable female offspring severely [63,178]. A cross of heterozygous Δ CpG female mice with hemizygous Δ CpG male mice resulted in less than 5% viable homozygous Δ CpG female offspring, and approximately 10% viable Δ CpG male offspring (Fig. 8A), presumably because too many X chromosomes are inactivated in the embryos with the CpG island deletions [16]. Deletion of *Xist* on the Xp prohibits the Xp from inactivation and results in two active X chromosomes and embryonic lethality, even though the Xm displays some delayed *Xist* upregulation and XCI [17]. Combination of the two heterozygous deletions in a single embryo, resulting in an $Xp\Delta Xist/Xm\Delta Tsix$ embryo, rescues the embryo to some extent resulting in ~20% viable offspring,

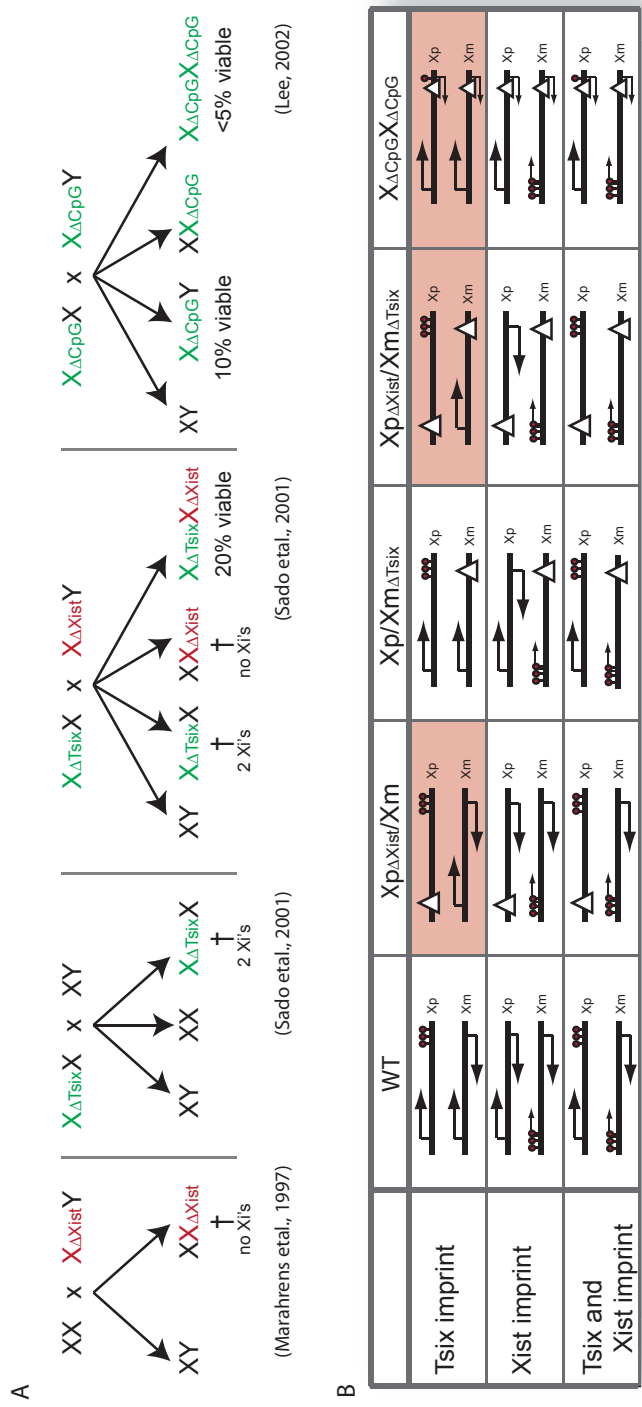


Figure 8. Imprinted XCI

A. Crosses of mice with an *Xist* or a *Tsix* deletion are displayed, followed by the potential genotypes of their offspring and the viability of the offspring. X chromosomes with a *Xist* deletion are depicted in red, and deletions resulting in decreased or loss of *Tsix* transcription are in green. The $X_{\Delta Tsix}/X$ female used in the depicted crosses is a chimera.

B. Table of embryos with various *Xist* and *Tsix* deletion X chromosomes that are explained by a *Tsix* imprint (first line), or an *Xist* imprint (second line), or a combination of both (third line). An arrow to the right represents *Tsix* transcription, while the size of the arrow is indicative of the level of transcription. Δ represents a deletion resulting in decrease or loss of *Xist* or *Tsix* transcription on an X chromosome, and lollipops represent the imprint that results in down regulation or inhibition of expression from the locus. The red highlighted boxes represent potential imprints that cannot explain the observed phenotype depicted in A. Further explanation can be found in the accompanying text.

presumably because a significant number of cells inactivate the X_m (Fig. 8A)[62].

Assuming that the imprint consists of a methylation mark that prevents transcription of the gene, and that the imprint is either located in the *Tsix* or *Xist* promoter regions, we can try to explain the phenotypes of the deletion studies described above with either an *Xist* imprint or a *Tsix* imprint or both (Fig. 8B). First, normal imprinted XCI is considered.

In wild type X_p/X_m embryos, a *Tsix* imprint on the X_p prevents *Xist* repression and subsequent inactivation of the X_p is initiated before *Xist* on the X_m can overcome *Tsix* repression. When *Xist* is imprinted on the X_m, only *Xist* on the X_p is upregulated to an extent sufficient to overcome *Tsix* repression, resulting in inactivation of the X_p. An imprint repressing both *Xist* on X_m and *Tsix* on X_p would also result in correct inactivation of the X_p, so based on a WT XX embryo one cannot conclude if imprinted XCI is caused by an imprint of *Tsix* on the X_p or an imprint of *Xist* on the X_m.

The lethality of the X_pΔ*Xist*/X_m embryo is more difficult to explain with a *Tsix* imprint on the X_p, because one would expect that *Xist* expression on the X_m would eventually overcome *Tsix* repression, which would rescue the phenotype at least partially. However, an *Xist* imprint on the X_m would inhibit *Xist* transcription, so that *Xist* cannot be upregulated enough to overcome *Tsix* repression, which will lead to two active X chromosomes and subsequent embryonic lethality. An imprint repressing both *Xist* on X_m and *Tsix* on X_p would also result in the observed phenotype. Therefore, an *Xist* imprint seems to be necessary to explain the phenotype of the X_pΔ*Xist*/X_m embryo.

The lethality of the X_p/X_mΔ*Tsix* is caused by inactivation of both X chromosomes, which can be explained by a *Tsix* imprint on the X_p, which results in lack of *Tsix* inhibition and expression of *Xist* on both X chromosomes. However, if an *Xist* imprint on the X_m would not completely inhibit *Xist* transcription, the X_m might still be inactivated if *Tsix* is deleted. Thus, full *Xist* expression will be sufficient to overcome *Tsix* repression on the X_p, while impaired *Xist* expression would be enough to initiate XCI on the X_m, because *Tsix* is deleted. If *Xist* and *Tsix* are both imprinted in the X_p/X_mΔ*Tsix* embryo, one would expect initial inactivation of the X_p only, but because *Tsix* is deleted on the X_m, initiation of XCI will not be inhibited and result in two inactive X chromosomes and embryonic lethality.

For the X_pΔ*Xist*/X_mΔ*Tsix* embryo, a *Tsix* imprint alone cannot explain the phenotype, because *Xist* transcription on the X_m will not be repressed by *Tsix*, which should result in inactivation of the X_m and rescue of the phenotype. Inhibition of *Xist* by a mild maternal *Xist* imprint would only result in inactivation of the X_m in a number of cells, resulting in partial rescue of the phenotype, as observed. Nevertheless, only ~20% of the X_pΔ*Xist*/X_mΔ*Tsix* embryos are viable, which indicates that not all *Tsix*

deleted Xm's are able to upregulate *Xist*, and that many cells will have two active X chromosomes. Therefore, one would expect, based on an *Xist* imprint that the Xp/Xm Δ *Tsix* embryos also inactivate one X chromosome instead of two in a number of cells. The Xp/Xm Δ *Tsix* embryo is nevertheless non-viable and a possible explanation for this is that female cells are better capable of withstanding expression of two X chromosomes than having little to no expression from either X chromosome, so that inactivation of both X chromosomes in the early Xm Δ *Tsix*/Xp embryo will lead to immediate cell death and embryonic lethality, while two active X chromosomes in the early Xm Δ *Tsix*/Xp Δ *Xist* embryo will only lead to growth impairment, but not necessarily embryonic lethality.

Finally, the outcome of XCI in the X Δ CpG/X Δ CpG embryo, in which the CpG island in the *Tsix* promoter region is deleted, also implicates that an *Xist* imprint partially inhibits *Xist* expression. If an *Xist* imprint would be absent while the CpG island is deleted on the Xm and the Xp, one would expect that *Xist* would overcome residual *Tsix* repression on both X chromosomes, resulting in two Xi's and 100% cell death. Some X Δ CpG/X Δ CpG embryos are still viable however, suggesting that *Xist* upregulation is partially inhibited on the Xm so that only a proportion of the cells inactivate two X chromosomes, while the others inactivate only the Xm. The X Δ CpG/X Δ CpG embryos are less informative however than the other mutant embryos, because it is difficult to determine how much *Tsix* expression is still present from the Δ CpG X chromosomes, and therefore what the role of *Tsix* transcription in the phenotype is. Overall, it appears that an *Xist* imprint that partially inhibits *Xist* transcription on the Xm is necessary to explain the observations made with the functional deletion studies of *Xist* and *Tsix*. However, a *Tsix* imprint repressing *Tsix* transcription on the Xp cannot be excluded and would enhance exclusive inactivation of the Xp.

Other indications on where the XCI imprint might be located come from observations regarding methylation profiles of the XIC. For instance, one report showed that the CTCF sites at the *DXPas34* and *Xite* region are hypermethylated in sperm, but hypomethylated in oocytes, corresponding to the imprinted XCI pattern in embryo's [68]. However, another report claimed that the methylation profile of the *DXPas34* region does not correlate with the imprinted XCI pattern [67]. *Xist* expression is correlated with the degree of methylation present on the *Xist* promoter [179] and the promoter is methylated in oocytes, but not in sperm [24,180]. Interestingly, a parthenogenic embryo when an immature oocyte is fused with a fully-grown oocyte, appears to be able to inactivate the Xm of the immature oocyte at the blastocyst stage. This indicates that a maternal imprint that prohibits the Xm from becoming inactivated could be installed on the X chromosome during oocyte growth [181].

Finally, if *Tsix* plays a role in early imprinted XCI, than it should be expressed at the 2 to 4-cell stage in embryogenesis. *Tsix* expression has not yet been examined at this stage of development and expression at the 8-cell stage is still debated. Sado et al. [62] could not detect *Tsix* transcription at the 8-cell stage while another group detected antisense transcription at the 8-cell embryonic stage from the Xm and never from the Xp [64].

Overall, neither the deletion studies of *Tsix* or *Xist*, nor the analysis of the methylation profile of the XIC in gametes, provide enough evidence to prove that the imprint represses *Xist* expression on the Xm or *Tsix* expression on the Xp or both, to ensure that the Xp is inactivated during imprinted XCI. A *Tsix* imprint only, however, does not agree with the phenotypes of the $Xp\Delta Xist/Xm$, the $Xm\Delta Tsix/Xp\Delta Xist$, or the $X\Delta CpG/X\Delta CpG$ embryos, which makes a mild *Xist* imprint far more likely. Nevertheless, a *Tsix* imprint together with a mild *Xist* imprint cannot be excluded and would enhance the accuracy of imprinted XCI.

As mentioned, at the blastocyst stage, imprinted XCI is reversed in the ICM, whereas it is maintained in the extraembryonic tissue. The loss of the imprint in the ICM can be a result from the global passive demethylation that takes place in the early mouse embryo. DNA replication without restoration of the DNA methylation mark dilutes the marks in the embryo until they are gone. This would explain why parthenogenetic embryos are capable of initiating XCI in a delayed fashion [175]. At the blastocyst stage, however, the embryo is reprogrammed, and methylation marks are restored, including the autosomal imprints [182,183]. These imprints are probably established because epigenetic marks other than DNA methylation are still present and recognized by the DNA methylase (probably DNMT3a and 3b) that reinstalls the methylation marks. This occurs normally in the extraembryonic tissue, but for an unknown reason, the X chromosomal imprint is not reinstalled in the ICM. It could be that H3K9me3 and H3K27me3, and other epigenetic marks on the Xi, are lost from the Xp in the ICM, but not from the Xp in the extraembryonic tissue during early embryonic development [9,10]. Indeed, Mak et al. show that in the early blastocyst, *Xist* and EED association with the Xi is lost in cells that express Nanog, and thus form the ICM [9]. Also, Navarro et al. have shown that *Xist* is repressed when Nanog is bound to the *Xist* locus [22]. Perhaps, *Xist* expression is repressed exclusively in the ICM by Nanog, which results in loss of the PRC2 complex [111] and other histone modifiers from the Xi, and in the gradual loss of epigenetic marks such as H3K27me3 and H3K9me3 during cell division. As a result, no epigenetic marks are present on the X chromosomes in the ICM that can be recognized by the DNA methylase that installs autosomal and extraembryonic imprints, leaving an empty canvas for random XCI to commence.

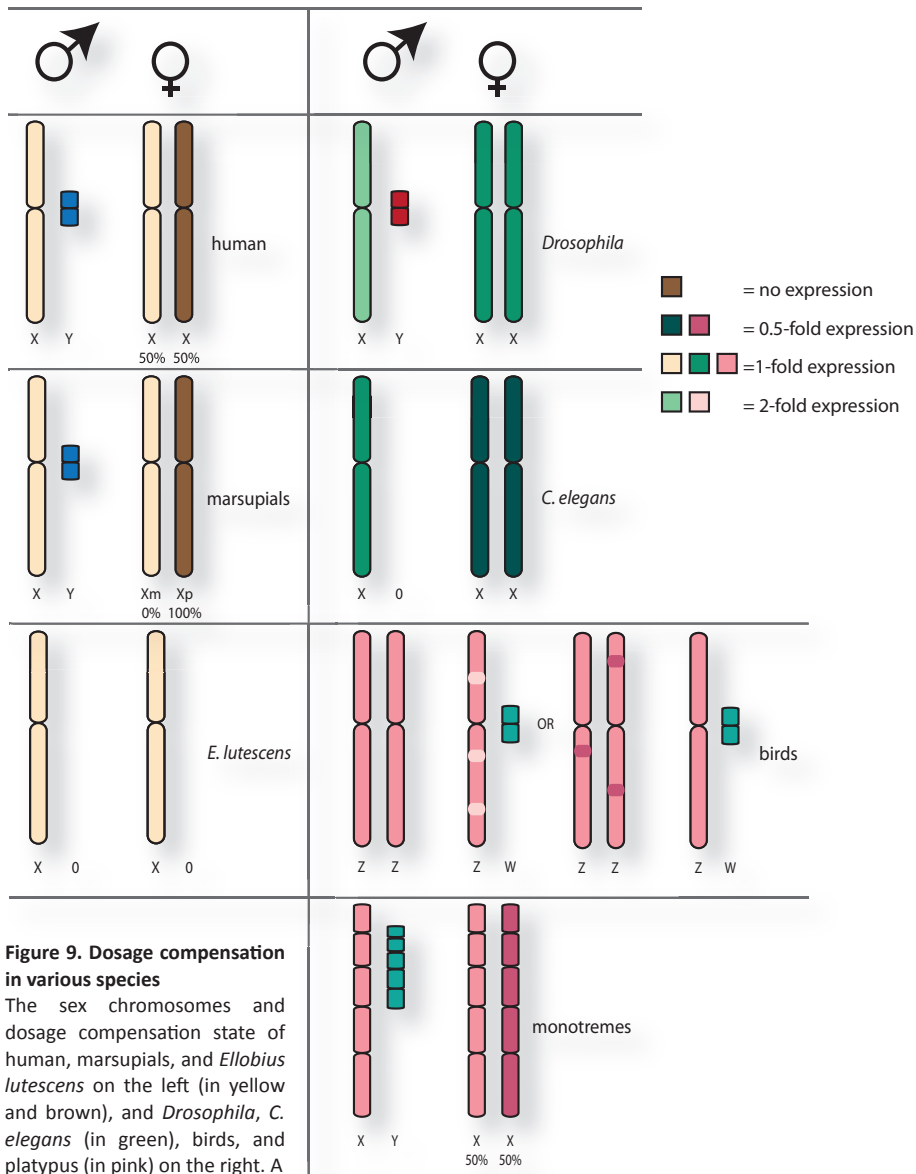
1.7 Dosage compensation in other species

1.7.1 Humans

Research on human XCI has always been performed with differentiated cell lines, including somatic, cancer or placental cell lines, making investigation into the mechanism of human XCI difficult. The emergence of human stem cell lines (hESC) was a promising development for XCI research, but analysis of these cell lines has shown that in nearly all cases XCI has already been initiated before differentiation [184,185,186]. The hESC cell lines could be in a semi-differentiated state, causing XCI to have commenced already. It is also possible that XCI initiation in the human pre-implantation embryo is not reversed in the embryo proper, in contrast to mouse embryos. Therefore, most data reviewed here are from analysis of cancer, placental or other somatic cell lines.

The molecular mechanism of human XCI is largely in accordance with mouse XCI (Fig. 9). Analysis of the human inactive X chromosome has shown that most hallmarks characteristic of the mouse Xi are also present on the human Xi and that an *XIST* cloud is formed. Human *XIST* is approximately 70% homologous to its mouse counterpart *Xist* and appears functionally similar [187]. Antisense *TSIX* transcription has also been identified, but seems to have very different characteristics from mouse *Tsix*. First of all, *TSIX/Tsix* is far less conserved between human and mouse than *XIST/Xist* and does not have a distinct CpG island located near the human *TSIX* promoter [188]. Moreover, human *TSIX* expression does not extend through the entire *XIST* locus, but stops near exon7 of *XIST* [189] and its expression persists well after completion of XCI [190]. Intriguingly, *TSIX* is expressed from the same allele as *XIST*, hence from the inactive X chromosome, and does not seem to repress *XIST* in any way [189,190]. Therefore, the function of human *TSIX* is unknown and it could be a non-functional evolutionary remnant of an ancestral form of *Tsix*.

The well-defined genomic background in mice has made early discovery of imprinted XCI possible [12]. Unfortunately, human XX embryos with distinguishable X chromosomes are not at hand, which is the reason that human imprinted XCI is still a topic of debate. Evidence in early human embryos concerning the presence of imprinted XCI is scarce and inconclusive, because only a few embryos have been tested. Initially, analysis of chorionic villi cell cultures determined that both X chromosomes could be expressed in the placenta [191,192], which would be an argument against imprinted XCI. However, the Xi in extraembryonic tissue can be reactivated [193], which could also explain expression from both X chromosomes. Nevertheless, others have shown that the Xm is preferentially expressed in human extraembryonic tissue [194,195,196], and that *XIST* seems to be expressed from the



Xm in early male embryos [197,198], which argues against imprinted XCI of the Xp.

1.7.2 Marsupials

Unlike mammalian XCI, XCI in marsupials, such as *Monodelphis domestica* is imprinted in all tissues, showing inactivation of the Xp (Fig. 9)[199]. Many genes escape XCI and the Xi is reactivated in patches of cells in the adult marsupial, implying that marsupial XCI is less stringently regulated as in mammals [200]. Although the marsupial Xi is late-replicating and hypoacetylated [201,202], DNA-methylation has not been detected [203]. Overall, imprinted XCI in marsupials seems to be very similar to imprinted XCI in extraembryonic tissue of mouse with respect to maintenance. However, the mechanism by which imprinted XCI is regulated in marsupials is different from its mammalian counterpart, because an *Xist* orthologue has not been found in marsupials [204,205,206]. How the future Xi attracts chromatin modifiers to the chromosome to spread the silenced state is therefore unknown. The LINE repeat density is not elevated on the *Monodelphis* X chromosome, so that a general role in spreading of silencing of these repeats is unlikely [206]. So far, it is unknown how the imprint in marsupials is set up, because marsupials are thought to lack differentially methylated CpG islands [207], but a possible mechanism could be inheritance of a silenced Xp after meiotic sex chromosome inactivation (MSCI) in the male germline. MSCI is caused by the inability of male sex chromosomes to pair during meiosis, which results in a silent sex body of the X and Y chromosomes in the male germline [208]. The silent state of the Xp of marsupials might persist after fertilization and provide a mechanism for inheritance of imprinted XCI in marsupials.

1.7.3 Birds

Sex chromosomes in birds are non-homologous to mammalian sex chromosomes and are most likely derived from a different set of autosomes. Female birds are heterogametic and have ZW sex chromosomes, while males have two Z chromosomes, potentially resulting in a difference of expression level of the sex chromosomes between males and females. Nevertheless, the existence of active dosage compensation to overcome differential gene expression from sex chromosomes in birds is still debated (Fig. 9). A reason for this is that dosage compensation appears incomplete. Expression of Z-linked genes in males is biallelic [209,210], and not always compensated to the female expression level [211,212,213]. Gene expression varies from gene to gene and the level of compensation is dependent on the tissue and developmental stage in which the gene is expressed [211,212]. This could reflect the absence of a general dosage compensation mechanism, while some genes are dosage compensated intrinsically because of tissue or gene specific requirements.

However, gene expression in a specific region located on the Zp arm in male cells seems to be compensated more than the rest of the male Z chromosome [212,213]. Interestingly, this region contains a female specific non-coding RNA called MHM that accumulates at this region [214], and might be induced in dosage compensation in females by upregulation of gene expression two-fold at this locus. Therefore, a dosage compensation mechanism may be employed at the avian sex chromosomes, but has not yet spread over the entire Z chromosome.

1.7.4 Monotremes

The monotreme taxon only contains two living species, the platypus (*Ornithorhynchus anatinus*) and the echidna (*Tachyglossus aculeatus*). Both species lay eggs, like birds, but lactate like mammals. Also, the platypus has webbed feet and males have venom that is highly similar to that of reptiles. Overall, especially the platypus is a bizarre animal, which is reflected by its genome. The diploid platypus genome is small and consists of 52 chromosomes, of which ten are sex chromosomes. During meiosis, the X chromosomes or Y chromosomes line up in a string to segregate together towards gametes. Interestingly, the platypus X chromosomes resemble the bird Z chromosome more than the mammalian X chromosome [215] and have no region homologous to *Xist* or *Tsix* [205]. Dosage compensation of the X chromosome seems to be regulated by X chromosome inactivation, because X-linked genes are mono-allelically expressed per cell, although XCI appears to be incomplete (Fig. 9). Also, XCI does not seem to be imprinted, as both alleles can be expressed within the same platypus fibroblast cell line [216]. Overall, dosage compensation resembles mammalian XCI, but seems to be incomplete as in chickens.

1.7.5 Fruit flies

Like mammals, fruit flies (*Drosophila melanogaster*) are heterogametic with XX chromosomes in females and an X and Y chromosome in males. In contrast to mammals, sex determination is based on the X:autosome ratio. Also, instead of inactivating one of two X chromosomes in females, the single male X chromosome is up-regulated two-fold (Fig. 9)[217]. Although this implicates a radically different process from the XCI mechanism employed by mammals, the molecular mechanism used to overexpress the male X chromosome seems to be remarkably similar to the X chromosome silencing mechanism in female mammals. Like in mammals, non-coding RNAs are essential for dosage compensation. In *Drosophila*, two redundant genes, *roX1* and *roX2*, both encoding a non-translated functional mRNA, are located on the X chromosome and are expressed in male cells only [218]. The *roX* RNA forms a RNA-protein complex with proteins MSL1, MSL2, MSL3, MLE, and MOF, resulting in the male

specific lethal (MSL) complex, which is located mainly on the male X chromosome. The complex has histone acetyltransferase activity and interacts with many histone modifiers to enhance transcription on the X chromosome [219]. Spreading of the MSL complex over the X chromosome is dependent on balancing the concentration of *roX* RNA and MSL protein components. Overexpression of MSL1 and MSL2 causes localization of the MSL complex around the *roX* gene, especially when one of the two *roX* genes is deleted, while overexpression of a *roX* transgene on an autosome in a *roX* null background enhances local spreading of the MSL complex over the autosome [220,221,222,223]. Spreading of the MSL complex seems to be dependent on approximately 150 chromosome entry sites located on the X chromosome, that are defined by a specific binding motif [224]. From there on, the MSL complex spreads preferentially onto the 3' end of transcriptionally active genes [225,226,227]. Overall, the mechanism of spreading by the MSL complex over the male X chromosome in *Drosophila* could also be hypothesized for *Xist* mediated spreading during XCI in mammals. For instance, the chromosome entry sites could consist of LINE repeat sequences [151], while the MSL complex proteins could be replaced by putative *Xist* RNA associating factors like Ezh2, ATRX and others [111,139].

Dosage compensation in *Drosophila* is restricted to male cells by the sex-determining gene sex-lethal (*Sxl*). When in the early embryo the X:autosome ratio is high like in females, *Sxl* is turned on. *SXL* directly inhibits the dosage compensation mechanism by inhibiting translation of *msl2* mRNA and transcriptional repression of *roX1* and *roX2*. In males, *Sxl* is not expressed at the early stages of embryonic development and does not inhibit *msl2* translation and *roX* transcription, thus enabling the DCC to bind the single male X chromosome [228,229].

1.7.6 Worms

Caenorhabditis elegans is a nematode that is commonly used as a model organism to study molecular processes. *C. elegans* hermaphrodites have two X chromosomes, whereas males have only one X chromosome and no Y chromosome. To resolve differences in gene expression levels between the sexes, gene expression from the sex chromosomes in *C. elegans* is equalized between males and hermaphrodites by means of dosage compensation [230]. The two hermaphrodite X chromosomes are both downregulated twice by the dosage compensation complex (DCC), which is hermaphrodite specific and binds both X chromosomes (Fig. 9). The DCC consists of at least nine proteins, of which SDC2, SDC3 and DPY30 attract all other components. SDC2 is the component that targets the DCC to the X chromosomes and is controlled by *xol1*. *Xol1* is the primary sex determination signal and is regulated by the X:autosome ratio. A set of X-linked genes including *Sex1* and *Fox1* are involved in determining

the number of X chromosomes by repressing *xol1* in a dose dependent manner. In males, the X:autosome ratio of 0.5 and single dosage of *Sex1* and *Fox1* leads to *xol1* expression, which in turn causes repression of *Sdc2*, while in hermaphrodites *xol1* is turned off by the double dosage of *Sex1* and *Fox1* and *Sdc2* is expressed, which results in accumulation of the DCC on the X chromosomes and dosage compensation [230]. Spreading of the DCC over the X chromosome is dependent on recruitment-element-on-X (rex) DNA sequences that are not unique to the X chromosome, but occur in condensed repeats at sites on the X [231]. The rex sequences serve as “way-stations” from which DCC spreads onto active genes by binding to the promoter sequences, which suggests that inhibition of transcription is regulated at the initiation phase of transcription [232].

1.7.7 Beyond dosage compensation: *Ellobius lutescens*

What will be the next step in the evolution of sex chromosomes and dosage compensation? As explained at the beginning of this chapter, the Y chromosome has been degrading in time, which might eventually lead to loss of the Y chromosome. If this event takes place, the sex determining gene *Sry*, the pseudo-autosomal region and Y specific genes involved in spermatogenesis have to be relocated to an autosome or replaced by other functionally equivalent genes, in order for a mammalian species to survive this. The autosome pair to which the sex determining gene is relocated to, will replace the X and Y chromosome as the sex determining chromosome pair. After initiation of degradation of the new Y chromosome, a dosage compensation mechanism might evolve for these new sex chromosomes.

Interestingly, two mammalian species have already undergone this drastic alteration, being *Ellobius lutescens* and the Japanese spiny rat or *Tokudaia osimensis*. *Ellobius lutescens* is a rodent that lives in the foothills of the Caucasus mountains, and is unique with regard to its karyotype, which consists of $2n=17,X$ both in males and females (Fig. 9)[233]. Although the direct chain of events leading to this karyotype is a mystery, it is clear that the Y chromosome is lost, and that the *Sry* gene is not located on one of the autosomes. Due to the absence of *Sry*, another unknown gene must have taken over the function as a sex determining gene.

Because both females and males are XO , gametes with and without an X chromosome will be formed, which in theory will result in XX , XO and OO offspring. Naturally, the OO offspring is non-viable because the X chromosome contains many essential genes. However, XX offspring is also not found. The loss of an XCI mechanism is a likely explanation for the absence of XX offspring. Supporting this theory is the observation that *Xist* does not seem to be conserved between mouse and *E. lutescens*, because a full length *Xist* gene could not be isolated from *E. lutescens*. In fact, *Xist*

is already divergent between *Ellobius* species, indicating that *Xist* might not have a function in *E. lutescens*. Nevertheless, no direct evidence for the absence of XCI in *E. lutescens* has been found [233]. Also, the potential absence of XCI in *E. lutescens* is curious from an evolutionary point of view, because proper XCI would result in viability of the offspring with either a karyotype of XX or XO (75%), which seems to be a clear advantage over species with only viable XO offspring (50%). In fact, if a species loses its Y chromosome, it would be best to arrive at XX males and females, giving up XCI. This would guarantee that the X chromosomes turn into a normal pair of autosomes. This is achieved in the species *Ellobius tancrei* and *Ellobius talpinus* ($2n = 32, XX$ and $2n = 54, XX$ in both males and females, respectively) [233].

Overall, *E. lutescens* exemplifies that degradation followed by the loss of the Y chromosome does not have to equal the loss of males and the extinction of the species. *E. lutescens* and other species have shown that many different routes can determine sex and that an organism can cope with potential gene dosage differences as a consequence of the evolution of sex chromosomes.

References

1. Graves JA (2006) Sex chromosome specialization and degeneration in mammals. *Cell* 124: 901-914.
2. Waters PD, Wallis MC, Marshall Graves JA (2007) Mammalian sex--Origin and evolution of the Y chromosome and SRY. *Semin Cell Dev Biol* 18: 389-400.
3. Lahn BT, Page DC (1999) Four evolutionary strata on the human X chromosome. *Science* 286: 964-967.
4. Sandstedt SA, Tucker PK (2004) Evolutionary strata on the mouse X chromosome correspond to strata on the human X chromosome. *Genome Res* 14: 267-272.
5. Jegalian K, Page DC (1998) A proposed path by which genes common to mammalian X and Y chromosomes evolve to become X inactivated. *Nature* 394: 776-780.
6. Carrel L, Willard HF (2005) X-inactivation profile reveals extensive variability in X-linked gene expression in females. *Nature* 434: 400-404.
7. Nguyen DK, Disteché CM (2006) Dosage compensation of the active X chromosome in mammals. *Nat Genet* 38: 47-53.
8. Lin H, Gupta V, Vermilyea MD, Falciani F, Lee JT, et al. (2007) Dosage compensation in the mouse balances up-regulation and silencing of X-linked genes. *PLoS Biol* 5: e326.
9. Mak W, Nesterova TB, de Napoles M, Appanah R, Yamanaka S, et al. (2004) Reactivation of the paternal X chromosome in early mouse embryos. *Science* 303: 666-669.
10. Okamoto I, Otte AP, Allis CD, Reinberg D, Heard E (2004) Epigenetic dynamics of imprinted X inactivation during early mouse development. *Science* 303: 644-649.
11. Okamoto I, Heard E (2006) The dynamics of imprinted X inactivation during preimplantation development in mice. *Cytogenet Genome Res* 113: 318-324.
12. Takagi N, Sasaki M (1975) Preferential inactivation of the paternally derived X chromosome in the extraembryonic membranes of the mouse. *Nature* 256: 640-642.
13. West JD, Frels WI, Chapman VM, Papaioannou VE (1977) Preferential expression of the maternally derived X chromosome in the mouse yolk sac. *Cell* 12: 873-882.
14. Rastan S (1982) Timing of X-chromosome inactivation in postimplantation mouse embryos. *J Embryol Exp Morphol* 71: 11-24.
15. Lyon MF (1961) Gene action in the X-chromosome of the mouse (*Mus musculus*)

- L.). *Nature* 190: 372-373.
16. Lee JT (2002) Homozygous Tsix mutant mice reveal a sex-ratio distortion and revert to random X-inactivation. *Nat Genet* 32: 195-200.
 17. Marahrens Y, Panning B, Dausman J, Strauss W, Jaenisch R (1997) Xist-deficient mice are defective in dosage compensation but not spermatogenesis. *Genes Dev* 11: 156-166.
 18. Plath K, Mlynarczyk-Evans S, Nusinow DA, Panning B (2002) Xist RNA and the mechanism of X chromosome inactivation. *Annu Rev Genet* 36: 233-278.
 19. Disteche CM (1999) Escapees on the X chromosome. *Proc Natl Acad Sci U S A* 96: 14180-14182.
 20. Savarese F, Flahndorfer K, Jaenisch R, Busslinger M, Wutz A (2006) Hematopoietic precursor cells transiently reestablish permissiveness for X inactivation. *Mol Cell Biol* 26: 7167-7177.
 21. Chaumeil J, Okamoto I, Guggiari M, Heard E (2002) Integrated kinetics of X chromosome inactivation in differentiating embryonic stem cells. *Cytogenet Genome Res* 99: 75-84.
 22. Navarro P, Chambers I, Karwacki-Neisius V, Chureau C, Morey C, et al. (2008) Molecular coupling of Xist regulation and pluripotency. *Science* 321: 1693-1695.
 23. Wutz A, Jaenisch R (2000) A shift from reversible to irreversible X inactivation is triggered during ES cell differentiation. *Mol Cell* 5: 695-705.
 24. Norris DP, Patel D, Kay GF, Penny GD, Brockdorff N, et al. (1994) Evidence that random and imprinted Xist expression is controlled by preemptive methylation. *Cell* 77: 41-51.
 25. Rastan S (1983) Non-random X-chromosome inactivation in mouse X-autosome translocation embryos--location of the inactivation centre. *J Embryol Exp Morphol* 78: 1-22.
 26. Rastan S, Robertson EJ (1985) X-chromosome deletions in embryo-derived (EK) cell lines associated with lack of X-chromosome inactivation. *J Embryol Exp Morphol* 90: 379-388.
 27. Lafreniere RG, Brown CJ, Rider S, Chelly J, Taillon-Miller P, et al. (1993) 2.6 Mb YAC contig of the human X inactivation center region in Xq13: physical linkage of the RPS4X, PHKA1, XIST and DXS128E genes. *Hum Mol Genet* 2: 1105-1115.
 28. Brown CJ, Ballabio A, Rupert JL, Lafreniere RG, Grompe M, et al. (1991) A gene from the region of the human X inactivation centre is expressed exclusively from the inactive X chromosome. *Nature* 349: 38-44.
 29. Webb S, de Vries TJ, Kaufman MH (1992) The differential staining pattern

- of the X chromosome in the embryonic and extraembryonic tissues of postimplantation homozygous tetraploid mouse embryos. *Genet Res* 59: 205-214.
30. Speirs S, Cross JM, Kaufman MH (1990) The pattern of X-chromosome inactivation in the embryonic and extra-embryonic tissues of post-implantation digynic triploid LT/Sv strain mouse embryos. *Genet Res* 56: 107-114.
 31. Jacobs PA, Matsuyama AM, Buchanan IM, Wilson C (1979) Late replicating X chromosomes in human triploidy. *Am J Hum Genet* 31: 446-457.
 32. Gartler SM, Varadarajan KR, Luo P, Norwood TH, Canfield TK, et al. (2006) Abnormal X: autosome ratio, but normal X chromosome inactivation in human triploid cultures. *BMC Genet* 7: 41.
 33. Cattanach BM, Williams CE (1972) Evidence of non-random X chromosome activity in the mouse. *Genet Res* 19: 229-240.
 34. Cattanach BM, Papworth D (1981) Controlling elements in the mouse. V. Linkage tests with X-linked genes. *Genet Res* 38: 57-70.
 35. Johnston PG, Cattanach BM (1981) Controlling elements in the mouse. IV. Evidence of non-random X-inactivation. *Genet Res* 37: 151-160.
 36. Penny GD, Kay GF, Sheardown SA, Rastan S, Brockdorff N (1996) Requirement for Xist in X chromosome inactivation. *Nature* 379: 131-137.
 37. Lee JT, Davidow LS, Warshawsky D (1999) Tsix, a gene antisense to Xist at the X-inactivation centre. *Nat Genet* 21: 400-404.
 38. Borsani G, Tonlorenzi R, Simmler MC, Dandolo L, Arnaud D, et al. (1991) Characterization of a murine gene expressed from the inactive X chromosome. *Nature* 351: 325-329.
 39. Brockdorff N, Ashworth A, Kay GF, Cooper P, Smith S, et al. (1991) Conservation of position and exclusive expression of mouse Xist from the inactive X chromosome. *Nature* 351: 329-331.
 40. Brown CJ, Hendrich BD, Rupert JL, Lafreniere RG, Xing Y, et al. (1992) The human XIST gene: analysis of a 17 kb inactive X-specific RNA that contains conserved repeats and is highly localized within the nucleus. *Cell* 71: 527-542.
 41. Clemson CM, McNeil JA, Willard HF, Lawrence JB (1996) XIST RNA paints the inactive X chromosome at interphase: evidence for a novel RNA involved in nuclear/chromosome structure. *J Cell Biol* 132: 259-275.
 42. Marahrens Y, Loring J, Jaenisch R (1998) Role of the Xist gene in X chromosome choosing. *Cell* 92: 657-664.
 43. Lee JT, Jaenisch R (1997) Long-range cis effects of ectopic X-inactivation centres on a mouse autosome. *Nature* 386: 275-279.
 44. Herzing LB, Romer JT, Horn JM, Ashworth A (1997) Xist has properties of the

- X-chromosome inactivation centre. *Nature* 386: 272-275.
45. Lee JT, Strauss WM, Dausman JA, Jaenisch R (1996) A 450 kb transgene displays properties of the mammalian X-inactivation center. *Cell* 86: 83-94.
 46. Nesterova TB, Johnston CM, Appanah R, Newall AE, Godwin J, et al. (2003) Skewing X chromosome choice by modulating sense transcription across the Xist locus. *Genes Dev* 17: 2177-2190.
 47. Newall AE, Duthie S, Formstone E, Nesterova T, Alexiou M, et al. (2001) Primary non-random X inactivation associated with disruption of Xist promoter regulation. *Hum Mol Genet* 10: 581-589.
 48. Brockdorff N, Ashworth A, Kay GF, McCabe VM, Norris DP, et al. (1992) The product of the mouse Xist gene is a 15 kb inactive X-specific transcript containing no conserved ORF and located in the nucleus. *Cell* 71: 515-526.
 49. Cohen HR, Panning B (2007) XIST RNA exhibits nuclear retention and exhibits reduced association with the export factor TAP/NXF1. *Chromosoma* 116: 373-383.
 50. Wutz A, Rasmussen TP, Jaenisch R (2002) Chromosomal silencing and localization are mediated by different domains of Xist RNA. *Nat Genet* 30: 167-174.
 51. Hoki Y, Kimura N, Kanbayashi M, Amakawa Y, Ohhata T, et al. (2009) A proximal conserved repeat in the Xist gene is essential as a genomic element for X-inactivation in mouse. *Development* 136: 139-146.
 52. Pillet N, Bonny C, Schorderet DF (1995) Characterization of the promoter region of the mouse Xist gene. *Proc Natl Acad Sci U S A* 92: 12515-12519.
 53. Sheardown SA, Newall AE, Norris DP, Rastan S, Brockdorff N (1997) Regulatory elements in the minimal promoter region of the mouse Xist gene. *Gene* 203: 159-168.
 54. Pugacheva EM, Tiwari VK, Abdullaev Z, Vostrov AA, Flanagan PT, et al. (2005) Familial cases of point mutations in the XIST promoter reveal a correlation between CTCF binding and pre-emptive choices of X chromosome inactivation. *Hum Mol Genet* 14: 953-965.
 55. Johnston CM, Nesterova TB, Formstone EJ, Newall AE, Duthie SM, et al. (1998) Developmentally regulated Xist promoter switch mediates initiation of X inactivation. *Cell* 94: 809-817.
 56. Navarro P, Pichard S, Ciaudo C, Avner P, Rougeulle C (2005) Tsix transcription across the Xist gene alters chromatin conformation without affecting Xist transcription: implications for X-chromosome inactivation. *Genes Dev* 19: 1474-1484.
 57. Panning B, Dausman J, Jaenisch R (1997) X chromosome inactivation is mediated by Xist RNA stabilization. *Cell* 90: 907-916.

58. Sheardown SA, Duthie SM, Johnston CM, Newall AE, Formstone EJ, et al. (1997) Stabilization of Xist RNA mediates initiation of X chromosome inactivation. *Cell* 91: 99-107.
59. Warshawsky D, Stavropoulos N, Lee JT (1999) Further examination of the Xist promoter-switch hypothesis in X inactivation: evidence against the existence and function of a P(0) promoter. *Proc Natl Acad Sci U S A* 96: 14424-14429.
60. Sun BK, Deaton AM, Lee JT (2006) A transient heterochromatic state in Xist preempts X inactivation choice without RNA stabilization. *Mol Cell* 21: 617-628.
61. Shibata S, Lee JT (2003) Characterization and quantitation of differential Tsix transcripts: implications for Tsix function. *Hum Mol Genet* 12: 125-136.
62. Sado T, Wang Z, Sasaki H, Li E (2001) Regulation of imprinted X-chromosome inactivation in mice by Tsix. *Development* 128: 1275-1286.
63. Cohen DE, Davidow LS, Erwin JA, Xu N, Warshawsky D, et al. (2007) The DXPas34 repeat regulates random and imprinted X inactivation. *Dev Cell* 12: 57-71.
64. Debrand E, Chureau C, Arnaud D, Avner P, Heard E (1999) Functional analysis of the DXPas34 locus, a 3' regulator of Xist expression. *Mol Cell Biol* 19: 8513-8525.
65. Vigneau S, Augui S, Navarro P, Avner P, Clerc P (2006) An essential role for the DXPas34 tandem repeat and Tsix transcription in the counting process of X chromosome inactivation. *Proc Natl Acad Sci U S A* 103: 7390-7395.
66. Lee JT, Lu N (1999) Targeted mutagenesis of Tsix leads to nonrandom X inactivation. *Cell* 99: 47-57.
67. Prissette M, El-Maarri O, Arnaud D, Walter J, Avner P (2001) Methylation profiles of DXPas34 during the onset of X-inactivation. *Hum Mol Genet* 10: 31-38.
68. Boumil RM, Ogawa Y, Sun BK, Huynh KD, Lee JT (2006) Differential methylation of Xite and CTCF sites in Tsix mirrors the pattern of X-inactivation choice in mice. *Mol Cell Biol* 26: 2109-2117.
69. Ogawa Y, Lee JT (2003) Xite, X-inactivation intergenic transcription elements that regulate the probability of choice. *Mol Cell* 11: 731-743.
70. Stavropoulos N, Rowntree RK, Lee JT (2005) Identification of developmentally specific enhancers for Tsix in the regulation of X chromosome inactivation. *Mol Cell Biol* 25: 2757-2769.
71. Luikenhuis S, Wutz A, Jaenisch R (2001) Antisense transcription through the Xist locus mediates Tsix function in embryonic stem cells. *Mol Cell Biol* 21: 8512-8520.
72. Clerc P, Avner P (1998) Role of the region 3' to Xist exon 6 in the counting process of X-chromosome inactivation. *Nat Genet* 19: 249-253.

73. Morey C, Navarro P, Debrand E, Avner P, Rougeulle C, et al. (2004) The region 3' to Xist mediates X chromosome counting and H3 Lys-4 dimethylation within the Xist gene. *Embo J* 23: 594-604.
74. Ogawa Y, Sun BK, Lee JT (2008) Intersection of the RNA interference and X-inactivation pathways. *Science* 320: 1336-1341.
75. Shibata S, Lee JT (2004) Tsix transcription- versus RNA-based mechanisms in Xist repression and epigenetic choice. *Curr Biol* 14: 1747-1754.
76. Nesterova TB, Popova BC, Cobb BS, Norton S, Senner CE, et al. (2008) Dicer regulates Xist promoter methylation in ES cells indirectly through transcriptional control of Dnmt3a. *Epigenetics Chromatin* 1: 2.
77. Chao W, Huynh KD, Spencer RJ, Davidow LS, Lee JT (2002) CTCF, a candidate trans-acting factor for X-inactivation choice. *Science* 295: 345-347.
78. Tsai CL, Rowntree RK, Cohen DE, Lee JT (2008) Higher order chromatin structure at the X-inactivation center via looping DNA. *Dev Biol* 319: 416-425.
79. Sado T, Hoki Y, Sasaki H (2005) Tsix silences Xist through modification of chromatin structure. *Dev Cell* 9: 159-165.
80. Navarro P, Page DR, Avner P, Rougeulle C (2006) Tsix-mediated epigenetic switch of a CTCF-flanked region of the Xist promoter determines the Xist transcription program. *Genes Dev* 20: 2787-2792.
81. Shibata S, Yokota T, Wutz A (2008) Synergy of Eed and Tsix in the repression of Xist gene and X-chromosome inactivation. *Embo J* 27: 1816-1826.
82. Ohhata T, Hoki Y, Sasaki H, Sado T (2008) Crucial role of antisense transcription across the Xist promoter in Tsix-mediated Xist chromatin modification. *Development* 135: 227-235.
83. Filippova GN, Cheng MK, Moore JM, Truong JP, Hu YJ, et al. (2005) Boundaries between chromosomal domains of X inactivation and escape bind CTCF and lack CpG methylation during early development. *Dev Cell* 8: 31-42.
84. Ohlsson R, Renkawitz R, Lobanenkov V (2001) CTCF is a uniquely versatile transcription regulator linked to epigenetics and disease. *Trends Genet* 17: 520-527.
85. Kim TH, Abdullaev ZK, Smith AD, Ching KA, Loukinov DI, et al. (2007) Analysis of the vertebrate insulator protein CTCF-binding sites in the human genome. *Cell* 128: 1231-1245.
86. Guelen L, Pagie L, Brasset E, Meuleman W, Faza MB, et al. (2008) Domain organization of human chromosomes revealed by mapping of nuclear lamina interactions. *Nature* 453: 948-951.
87. Kim J (2008) Multiple YY1 and CTCF binding sites in imprinting control regions. *Epigenetics* 3: 115-118.

88. Kim JD, Hinz AK, Bergmann A, Huang JM, Ovcharenko I, et al. (2006) Identification of clustered YY1 binding sites in imprinting control regions. *Genome Res* 16: 901-911.
89. Donohoe ME, Zhang LF, Xu N, Shi Y, Lee JT (2007) Identification of a Ctfc cofactor, Yy1, for the X chromosome binary switch. *Mol Cell* 25: 43-56.
90. Kim J, Kim JD (2008) In vivo YY1 knockdown effects on genomic imprinting. *Hum Mol Genet* 17: 391-401.
91. Fedoriw AM, Stein P, Svoboda P, Schultz RM, Bartolomei MS (2004) Transgenic RNAi reveals essential function for CTCF in H19 gene imprinting. *Science* 303: 238-240.
92. Xu N, Tsai CL, Lee JT (2006) Transient homologous chromosome pairing marks the onset of X inactivation. *Science* 311: 1149-1152.
93. Percec I, Plenge RM, Nadeau JH, Bartolomei MS, Willard HF (2002) Autosomal dominant mutations affecting X inactivation choice in the mouse. *Science* 296: 1136-1139.
94. Migeon BR, Pappas K, Stetten G, Trunca C, Jacobs PA (2008) X inactivation in triploidy and trisomy: the search for autosomal transactors that choose the active X. *Eur J Hum Genet* 16: 153-162.
95. Lee JT (2005) Regulation of X-chromosome counting by Tsix and Xite sequences. *Science* 309: 768-771.
96. Nicodemi M, Prisco A (2007) Self-assembly and DNA binding of the blocking factor in x chromosome inactivation. *PLoS Comput Biol* 3: e210.
97. Nicodemi M, Prisco A (2007) Symmetry-breaking model for X-chromosome inactivation. *Phys Rev Lett* 98: 108104.
98. Mlynarczyk-Evans S, Royce-Tolland M, Alexander MK, Andersen AA, Kalantry S, et al. (2006) X chromosomes alternate between two states prior to random X-inactivation. *PLoS Biol* 4: e159.
99. Bacher CP, Guggiari M, Brors B, Augui S, Clerc P, et al. (2006) Transient colocalization of X-inactivation centres accompanies the initiation of X inactivation. *Nat Cell Biol* 8: 293-299.
100. Xu N, Donohoe ME, Silva SS, Lee JT (2007) Evidence that homologous X-chromosome pairing requires transcription and Ctfc protein. *Nat Genet* 39: 1390-1396.
101. Augui S, Filion GJ, Huart S, Nora E, Guggiari M, et al. (2007) Sensing X chromosome pairs before X inactivation via a novel X-pairing region of the Xic. *Science* 318: 1632-1636.
102. Xu M, Cook PR (2008) The role of specialized transcription factories in chromosome pairing. *Biochim Biophys Acta* 1783: 2155-2160.

103. Chaumeil J, Le Baccon P, Wutz A, Heard E (2006) A novel role for Xist RNA in the formation of a repressive nuclear compartment into which genes are recruited when silenced. *Genes Dev* 20: 2223-2237.
104. Clemson CM, Hall LL, Byron M, McNeil J, Lawrence JB (2006) The X chromosome is organized into a gene-rich outer rim and an internal core containing silenced nongenic sequences. *Proc Natl Acad Sci U S A* 103: 7688-7693.
105. Cao R, Zhang Y (2004) SUZ12 is required for both the histone methyltransferase activity and the silencing function of the EED-EZH2 complex. *Mol Cell* 15: 57-67.
106. de la Cruz CC, Fang J, Plath K, Worringer KA, Nusinow DA, et al. (2005) Developmental regulation of Suz 12 localization. *Chromosoma* 114: 183-192.
107. Plath K, Fang J, Mlynarczyk-Evans SK, Cao R, Worringer KA, et al. (2003) Role of histone H3 lysine 27 methylation in X inactivation. *Science* 300: 131-135.
108. Wang J, Mager J, Chen Y, Schneider E, Cross JC, et al. (2001) Imprinted X inactivation maintained by a mouse Polycomb group gene. *Nat Genet* 28: 371-375.
109. Silva J, Mak W, Zvetkova I, Appanah R, Nesterova TB, et al. (2003) Establishment of histone h3 methylation on the inactive X chromosome requires transient recruitment of Eed-Enx1 polycomb group complexes. *Dev Cell* 4: 481-495.
110. Plath K, Talbot D, Hamer KM, Otte AP, Yang TP, et al. (2004) Developmentally regulated alterations in Polycomb repressive complex 1 proteins on the inactive X chromosome. *J Cell Biol* 167: 1025-1035.
111. Zhao J, Sun BK, Erwin JA, Song JJ, Lee JT (2008) Polycomb proteins targeted by a short repeat RNA to the mouse X chromosome. *Science* 322: 750-756.
112. de Napoles M, Mermoud JE, Wakao R, Tang YA, Endoh M, et al. (2004) Polycomb group proteins Ring1A/B link ubiquitylation of histone H2A to heritable gene silencing and X inactivation. *Dev Cell* 7: 663-676.
113. Fang J, Chen T, Chadwick B, Li E, Zhang Y (2004) Ring1b-mediated H2A ubiquitination associates with inactive X chromosomes and is involved in initiation of X inactivation. *J Biol Chem* 279: 52812-52815.
114. Leeb M, Wutz A (2007) Ring1B is crucial for the regulation of developmental control genes and PRC1 proteins but not X inactivation in embryonic cells. *J Cell Biol* 178: 219-229.
115. Schoeftner S, Sengupta AK, Kubicek S, Mechtler K, Spahn L, et al. (2006) Recruitment of PRC1 function at the initiation of X inactivation independent of PRC2 and silencing. *Embo J* 25: 3110-3122.
116. Bernstein E, Duncan EM, Masui O, Gil J, Heard E, et al. (2006) Mouse polycomb

- proteins bind differentially to methylated histone H3 and RNA and are enriched in facultative heterochromatin. *Mol Cell Biol* 26: 2560-2569.
117. Gil J, Bernard D, Martinez D, Beach D (2004) Polycomb CBX7 has a unifying role in cellular lifespan. *Nat Cell Biol* 6: 67-72.
 118. Boggs BA, Cheung P, Heard E, Spector DL, Chinault AC, et al. (2002) Differentially methylated forms of histone H3 show unique association patterns with inactive human X chromosomes. *Nat Genet* 30: 73-76.
 119. Heard E, Rougeulle C, Arnaud D, Avner P, Allis CD, et al. (2001) Methylation of histone H3 at Lys-9 is an early mark on the X chromosome during X inactivation. *Cell* 107: 727-738.
 120. Mermoud JE, Popova B, Peters AH, Jenuwein T, Brockdorff N (2002) Histone H3 lysine 9 methylation occurs rapidly at the onset of random X chromosome inactivation. *Curr Biol* 12: 247-251.
 121. Peters AH, Mermoud JE, O'Carroll D, Pagani M, Schweizer D, et al. (2002) Histone H3 lysine 9 methylation is an epigenetic imprint of facultative heterochromatin. *Nat Genet* 30: 77-80.
 122. Rougeulle C, Chaumeil J, Sarma K, Allis CD, Reinberg D, et al. (2004) Differential histone H3 Lys-9 and Lys-27 methylation profiles on the X chromosome. *Mol Cell Biol* 24: 5475-5484.
 123. Chadwick BP, Willard HF (2004) Multiple spatially distinct types of facultative heterochromatin on the human inactive X chromosome. *Proc Natl Acad Sci U S A* 101: 17450-17455.
 124. Chadwick BP, Willard HF (2003) Chromatin of the Barr body: histone and non-histone proteins associated with or excluded from the inactive X chromosome. *Hum Mol Genet* 12: 2167-2178.
 125. Belyaev N, Keohane AM, Turner BM (1996) Differential underacetylation of histones H2A, H3 and H4 on the inactive X chromosome in human female cells. *Hum Genet* 97: 573-578.
 126. Boggs BA, Connors B, Sobel RE, Chinault AC, Allis CD (1996) Reduced levels of histone H3 acetylation on the inactive X chromosome in human females. *Chromosoma* 105: 303-309.
 127. Jeppesen P, Turner BM (1993) The inactive X chromosome in female mammals is distinguished by a lack of histone H4 acetylation, a cytogenetic marker for gene expression. *Cell* 74: 281-289.
 128. Keohane AM, O'Neill LP, Belyaev ND, Lavender JS, Turner BM (1996) X-Inactivation and histone H4 acetylation in embryonic stem cells. *Dev Biol* 180: 618-630.
 129. Costanzi C, Pehrson JR (1998) Histone macroH2A1 is concentrated in the inactive X chromosome of female mammals. *Nature* 393: 599-601.

130. Mermoud JE, Costanzi C, Pehrson JR, Brockdorff N (1999) Histone macroH2A1.2 relocates to the inactive X chromosome after initiation and propagation of X-inactivation. *J Cell Biol* 147: 1399-1408.
131. Norris DP, Brockdorff N, Rastan S (1991) Methylation status of CpG-rich islands on active and inactive mouse X chromosomes. *Mamm Genome* 1: 78-83.
132. Mohandas T, Sparkes RS, Shapiro LJ (1981) Reactivation of an inactive human X chromosome: evidence for X inactivation by DNA methylation. *Science* 211: 393-396.
133. Nusinow DA, Sharp JA, Morris A, Salas S, Plath K, et al. (2007) The histone domain of macroH2A1 contains several dispersed elements that are each sufficient to direct enrichment on the inactive X chromosome. *J Mol Biol* 371: 11-18.
134. Rasmussen TP, Wutz AP, Pehrson JR, Jaenisch RR (2001) Expression of Xist RNA is sufficient to initiate macrochromatin body formation. *Chromosoma* 110: 411-420.
135. Csankovszki G, Panning B, Bates B, Pehrson JR, Jaenisch R (1999) Conditional deletion of Xist disrupts histone macroH2A localization but not maintenance of X inactivation. *Nat Genet* 22: 323-324.
136. Hansen RS (2003) X inactivation-specific methylation of LINE-1 elements by DNMT3B: implications for the Lyon repeat hypothesis. *Hum Mol Genet* 12: 2559-2567.
137. Sado T, Fenner MH, Tan SS, Tam P, Shioda T, et al. (2000) X inactivation in the mouse embryo deficient for Dnmt1: distinct effect of hypomethylation on imprinted and random X inactivation. *Dev Biol* 225: 294-303.
138. Blewitt ME, Gendrel AV, Pang Z, Sparrow DB, Whitelaw N, et al. (2008) SmcHD1, containing a structural-maintenance-of-chromosomes hinge domain, has a critical role in X inactivation. *Nat Genet* 40: 663-669.
139. Baumann C, De La Fuente R (2008) ATRX marks the inactive X chromosome (Xi) in somatic cells and during imprinted X chromosome inactivation in trophoblast stem cells. *Chromosoma*.
140. Levy MA, Fernandes AD, Tremblay DC, Seah C, Berube NG (2008) The SWI/SNF protein ATRX co-regulates pseudoautosomal genes that have translocated to autosomes in the mouse genome. *BMC Genomics* 9: 468.
141. Priest JH, Heady JE, Priest RE (1967) Delayed onset of replication of human X chromosomes. *J Cell Biol* 35: 483-487.
142. Gilbert DM (2002) Replication timing and transcriptional control: beyond cause and effect. *Curr Opin Cell Biol* 14: 377-383.
143. O'Keefe RT, Henderson SC, Spector DL (1992) Dynamic organization of DNA replication in mammalian cell nuclei: spatially and temporally defined

- replication of chromosome-specific alpha-satellite DNA sequences. *J Cell Biol* 116: 1095-1110.
144. Gribnau J, Luikenhuis S, Hochedlinger K, Monkhorst K, Jaenisch R (2005) X chromosome choice occurs independently of asynchronous replication timing. *J Cell Biol* 168: 365-373.
 145. Csankovszki G, Nagy A, Jaenisch R (2001) Synergism of Xist RNA, DNA methylation, and histone hypoacetylation in maintaining X chromosome inactivation. *J Cell Biol* 153: 773-784.
 146. Hernandez-Munoz I, Lund AH, van der Stoop P, Boutsma E, Muijers I, et al. (2005) Stable X chromosome inactivation involves the PRC1 Polycomb complex and requires histone MACROH2A1 and the CULLIN3/SPOP ubiquitin E3 ligase. *Proc Natl Acad Sci U S A* 102: 7635-7640.
 147. Hall LL, Lawrence JB (2003) The cell biology of a novel chromosomal RNA: chromosome painting by XIST/Xist RNA initiates a remodeling cascade. *Semin Cell Dev Biol* 14: 369-378.
 148. Duthie SM, Nesterova TB, Formstone EJ, Keohane AM, Turner BM, et al. (1999) Xist RNA exhibits a banded localization on the inactive X chromosome and is excluded from autosomal material in cis. *Hum Mol Genet* 8: 195-204.
 149. Keohane AM, Barlow AL, Waters J, Bourn D, Turner BM (1999) H4 acetylation, XIST RNA and replication timing are coincident and define X;autosome boundaries in two abnormal X chromosomes. *Hum Mol Genet* 8: 377-383.
 150. Popova BC, Tada T, Takagi N, Brockdorff N, Nesterova TB (2006) Attenuated spread of X-inactivation in an X;autosome translocation. *Proc Natl Acad Sci U S A* 103: 7706-7711.
 151. Lyon MF (1998) X-chromosome inactivation: a repeat hypothesis. *Cytogenet Cell Genet* 80: 133-137.
 152. Boyle AL, Ballard SG, Ward DC (1990) Differential distribution of long and short interspersed element sequences in the mouse genome: chromosome karyotyping by fluorescence in situ hybridization. *Proc Natl Acad Sci U S A* 87: 7757-7761.
 153. Bailey JA, Carrel L, Chakravarti A, Eichler EE (2000) Molecular evidence for a relationship between LINE-1 elements and X chromosome inactivation: the Lyon repeat hypothesis. *Proc Natl Acad Sci U S A* 97: 6634-6639.
 154. Ross MT, Grafham DV, Coffey AJ, Scherer S, McLay K, et al. (2005) The DNA sequence of the human X chromosome. *Nature* 434: 325-337.
 155. Carrel L, Park C, Tyekucheva S, Dunn J, Chiaromonte F, et al. (2006) Genomic environment predicts expression patterns on the human inactive X chromosome. *PLoS Genet* 2: e151.

156. Wang Z, Willard HF, Mukherjee S, Furey TS (2006) Evidence of influence of genomic DNA sequence on human X chromosome inactivation. *PLoS Comput Biol* 2: e113.
157. Chureau C, Prissette M, Bourdet A, Barbe V, Cattolico L, et al. (2002) Comparative sequence analysis of the X-inactivation center region in mouse, human, and bovine. *Genome Res* 12: 894-908.
158. Ke X, Collins A (2003) CpG islands in human X-inactivation. *Ann Hum Genet* 67: 242-249.
159. Smith KP, Byron M, Clemson CM, Lawrence JB (2004) Ubiquitinated proteins including uH2A on the human and mouse inactive X chromosome: enrichment in gene rich bands. *Chromosoma* 113: 324-335.
160. Chadwick BP (2007) Variation in Xi chromatin organization and correlation of the H3K27me3 chromatin territories to transcribed sequences by microarray analysis. *Chromosoma* 116: 147-157.
161. Gilbert SL, Pehrson JR, Sharp PA (2000) XIST RNA associates with specific regions of the inactive X chromatin. *J Biol Chem* 275: 36491-36494.
162. Eils R, Dietzel S, Bertin E, Schrock E, Speicher MR, et al. (1996) Three-dimensional reconstruction of painted human interphase chromosomes: active and inactive X chromosome territories have similar volumes but differ in shape and surface structure. *J Cell Biol* 135: 1427-1440.
163. Dietzel S, Schiebel K, Little G, Edelmann P, Rappold GA, et al. (1999) The 3D positioning of ANT2 and ANT3 genes within female X chromosome territories correlates with gene activity. *Exp Cell Res* 252: 363-375.
164. Belmont AS, Bignone F, Ts'o PO (1986) The relative intranuclear positions of Barr bodies in XXX non-transformed human fibroblasts. *Exp Cell Res* 165: 165-179.
165. Bourgeois CA, Laquerriere F, Hemon D, Hubert J, Bouteille M (1985) New data on the in-situ position of the inactive X chromosome in the interphase nucleus of human fibroblasts. *Hum Genet* 69: 122-129.
166. Zhang LF, Huynh KD, Lee JT (2007) Perinucleolar targeting of the inactive X during S phase: evidence for a role in the maintenance of silencing. *Cell* 129: 693-706.
167. Fackelmayer FO (2005) A stable proteinaceous structure in the territory of inactive X chromosomes. *J Biol Chem* 280: 1720-1723.
168. Helbig R, Fackelmayer FO (2003) Scaffold attachment factor A (SAF-A) is concentrated in inactive X chromosome territories through its RGG domain. *Chromosoma* 112: 173-182.
169. Shumaker DK, Dechat T, Kohlmaier A, Adam SA, Bozovsky MR, et al. (2006)

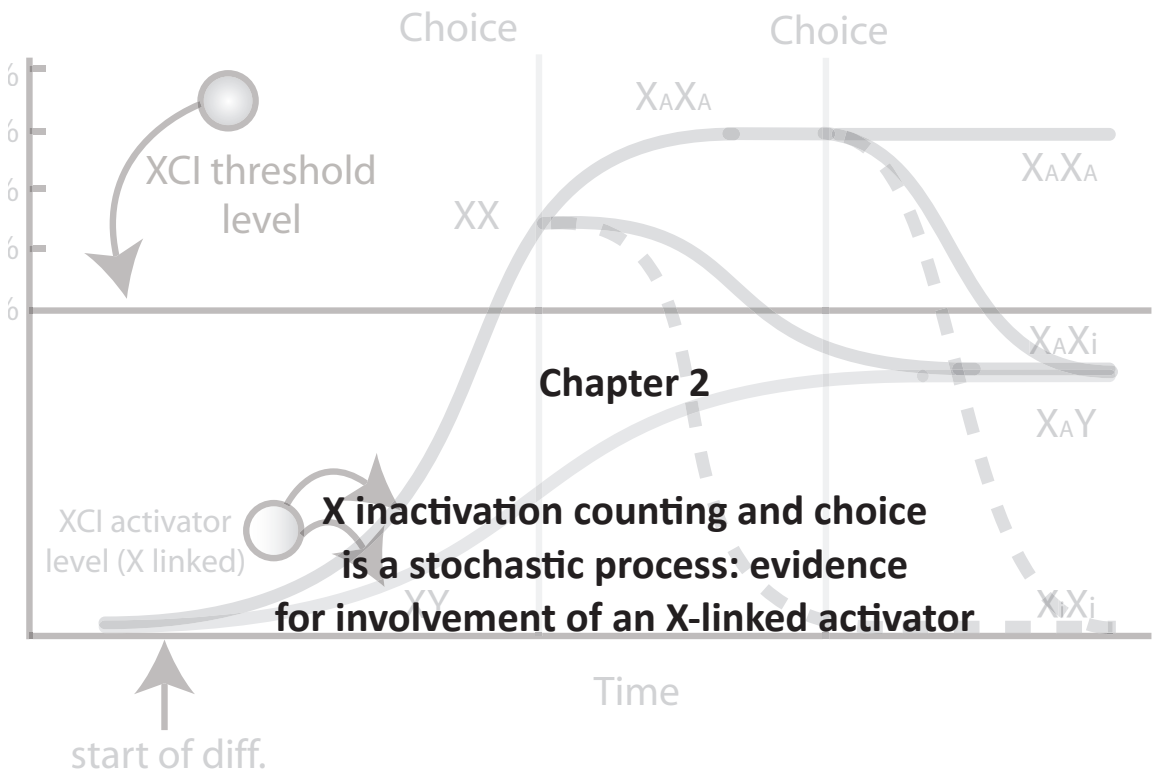
- Mutant nuclear lamin A leads to progressive alterations of epigenetic control in premature aging. *Proc Natl Acad Sci U S A* 103: 8703-8708.
170. Fedorova E, Zink D (2008) Nuclear architecture and gene regulation. *Biochim Biophys Acta* 1783: 2174-2184.
171. Kennedy BK, Barbie DA, Classon M, Dyson N, Harlow E (2000) Nuclear organization of DNA replication in primary mammalian cells. *Genes Dev* 14: 2855-2868.
172. Kay GF, Barton SC, Surani MA, Rastan S (1994) Imprinting and X chromosome counting mechanisms determine Xist expression in early mouse development. *Cell* 77: 639-650.
173. Matsui J, Goto Y, Takagi N (2001) Control of Xist expression for imprinted and random X chromosome inactivation in mice. *Hum Mol Genet* 10: 1393-1401.
174. Okamoto I, Tan S, Takagi N (2000) X-chromosome inactivation in XX androgenetic mouse embryos surviving implantation. *Development* 127: 4137-4145.
175. Nesterova TB, Barton SC, Surani MA, Brockdorff N (2001) Loss of Xist imprinting in diploid parthenogenetic preimplantation embryos. *Dev Biol* 235: 343-350.
176. Costanzi C, Stein P, Worrall DM, Schultz RM, Pehrson JR (2000) Histone macroH2A1 is concentrated in the inactive X chromosome of female preimplantation mouse embryos. *Development* 127: 2283-2289.
177. Hadjantonakis AK, Cox LL, Tam PP, Nagy A (2001) An X-linked GFP transgene reveals unexpected paternal X-chromosome activity in trophoblastic giant cells of the mouse placenta. *Genesis* 29: 133-140.
178. Lee JT (2000) Disruption of imprinted X inactivation by parent-of-origin effects at Tsix. *Cell* 103: 17-27.
179. Goto T, Christians E, Monk M (1998) Expression of an Xist promoter-luciferase construct during spermatogenesis and in preimplantation embryos: regulation by DNA methylation. *Mol Reprod Dev* 49: 356-367.
180. Ariel M, Robinson E, McCarrey JR, Cedar H (1995) Gamete-specific methylation correlates with imprinting of the murine Xist gene. *Nat Genet* 9: 312-315.
181. Tada T, Obata Y, Tada M, Goto Y, Nakatsuji N, et al. (2000) Imprint switching for non-random X-chromosome inactivation during mouse oocyte growth. *Development* 127: 3101-3105.
182. Morgan HD, Santos F, Green K, Dean W, Reik W (2005) Epigenetic reprogramming in mammals. *Hum Mol Genet* 14 Spec No 1: R47-58.
183. Reik W, Dean W, Walter J (2001) Epigenetic reprogramming in mammalian development. *Science* 293: 1089-1093.
184. Hall LL, Byron M, Butler J, Becker KA, Nelson A, et al. (2008) X-inactivation reveals

- epigenetic anomalies in most hESC but identifies sublines that initiate as expected. *J Cell Physiol* 216: 445-452.
185. Shen Y, Matsuno Y, Fouse SD, Rao N, Root S, et al. (2008) X-inactivation in female human embryonic stem cells is in a nonrandom pattern and prone to epigenetic alterations. *Proc Natl Acad Sci U S A* 105: 4709-4714.
 186. Silva SS, Rowntree RK, Mekhoubad S, Lee JT (2008) X-chromosome inactivation and epigenetic fluidity in human embryonic stem cells. *Proc Natl Acad Sci U S A* 105: 4820-4825.
 187. Chow JC, Hall LL, Baldry SE, Thorogood NP, Lawrence JB, et al. (2007) Inducible XIST-dependent X-chromosome inactivation in human somatic cells is reversible. *Proc Natl Acad Sci U S A* 104: 10104-10109.
 188. Migeon BR, Chowdhury AK, Dunston JA, McIntosh I (2001) Identification of TSIX, encoding an RNA antisense to human XIST, reveals differences from its murine counterpart: implications for X inactivation. *Am J Hum Genet* 69: 951-960.
 189. Chow JC, Hall LL, Clemson CM, Lawrence JB, Brown CJ (2003) Characterization of expression at the human XIST locus in somatic, embryonal carcinoma, and transgenic cell lines. *Genomics* 82: 309-322.
 190. Migeon BR, Lee CH, Chowdhury AK, Carpenter H (2002) Species differences in TSIX/Tsix reveal the roles of these genes in X-chromosome inactivation. *Am J Hum Genet* 71: 286-293.
 191. Migeon BR, Wolf SF, Axelman J, Kaslow DC, Schmidt M (1985) Incomplete X chromosome dosage compensation in chorionic villi of human placenta. *Proc Natl Acad Sci U S A* 82: 3390-3394.
 192. Willemsen R, Bontekoe CJ, Severijnen LA, Oostra BA (2002) Timing of the absence of FMR1 expression in full mutation chorionic villi. *Hum Genet* 110: 601-605.
 193. Migeon BR, Axelman J, Jeppesen P (2005) Differential X reactivation in human placental cells: implications for reversal of X inactivation. *Am J Hum Genet* 77: 355-364.
 194. Goto T, Wright E, Monk M (1997) Paternal X-chromosome inactivation in human trophoblastic cells. *Mol Hum Reprod* 3: 77-80.
 195. Harrison KB (1989) X-chromosome inactivation in the human cytotrophoblast. *Cytogenet Cell Genet* 52: 37-41.
 196. Harrison KB, Warburton D (1986) Preferential X-chromosome activity in human female placental tissues. *Cytogenet Cell Genet* 41: 163-168.
 197. Ray PF, Winston RM, Handyside AH (1997) XIST expression from the maternal X chromosome in human male preimplantation embryos at the blastocyst

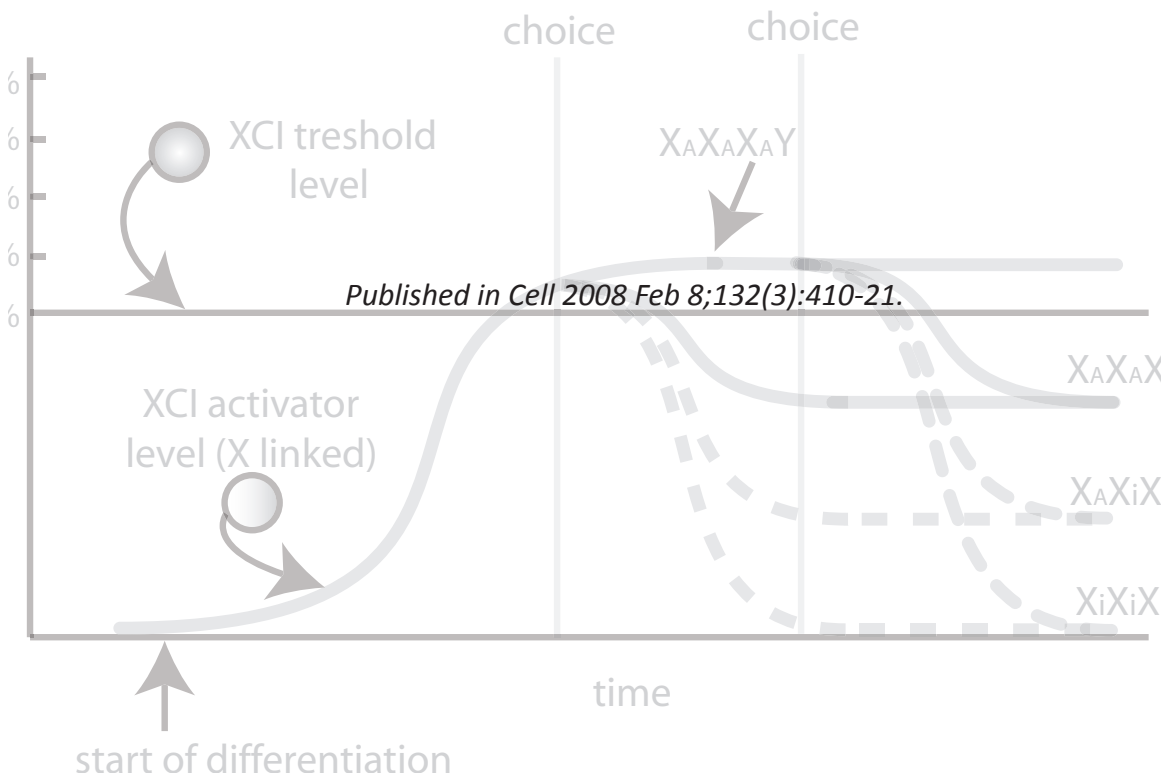
- stage. *Hum Mol Genet* 6: 1323-1327.
198. Daniels R, Zuccotti M, Kinis T, Serhal P, Monk M (1997) XIST expression in human oocytes and preimplantation embryos. *Am J Hum Genet* 61: 33-39.
 199. Richardson BJ, Czuppon AB, Sharman GB (1971) Inheritance of glucose-6-phosphate dehydrogenase variation in kangaroos. *Nat New Biol* 230: 154-155.
 200. VandeBerg JL, Robinson ES, Samollow PB, Johnston PG (1987) X-linked gene expression and X-chromosome inactivation: marsupials, mouse, and man compared. *Isozymes Curr Top Biol Med Res* 15: 225-253.
 201. Sharman GB (1971) Late DNA replication in the paternally derived X chromosome of female kangaroos. *Nature* 230: 231-232.
 202. Wakefield MJ, Keohane AM, Turner BM, Graves JA (1997) Histone underacetylation is an ancient component of mammalian X chromosome inactivation. *Proc Natl Acad Sci U S A* 94: 9665-9668.
 203. Kaslow DC, Migeon BR (1987) DNA methylation stabilizes X chromosome inactivation in eutherians but not in marsupials: evidence for multistep maintenance of mammalian X dosage compensation. *Proc Natl Acad Sci U S A* 84: 6210-6214.
 204. Koina E, Wakefield MJ, Walcher C, Disteché CM, Whitehead S, et al. (2005) Isolation, X location and activity of the marsupial homologue of SLC16A2, an XIST-flanking gene in eutherian mammals. *Chromosome Res* 13: 687-698.
 205. Hore TA, Koina E, Wakefield MJ, Marshall Graves JA (2007) The region homologous to the X-chromosome inactivation centre has been disrupted in marsupial and monotreme mammals. *Chromosome Res* 15: 147-161.
 206. Mikkelsen TS, Wakefield MJ, Aken B, Amemiya CT, Chang JL, et al. (2007) Genome of the marsupial *Monodelphis domestica* reveals innovation in non-coding sequences. *Nature* 447: 167-177.
 207. Hore TA, Rapkins RW, Graves JA (2007) Construction and evolution of imprinted loci in mammals. *Trends Genet* 23: 440-448.
 208. Namekawa SH, VandeBerg JL, McCarrey JR, Lee JT (2007) Sex chromosome silencing in the marsupial male germ line. *Proc Natl Acad Sci U S A* 104: 9730-9735.
 209. Kuroda Y, Arai N, Arita M, Teranishi M, Hori T, et al. (2001) Absence of Z-chromosome inactivation for five genes in male chickens. *Chromosome Res* 9: 457-468.
 210. McQueen HA, McBride D, Miele G, Bird AP, Clinton M (2001) Dosage compensation in birds. *Curr Biol* 11: 253-257.
 211. Itoh Y, Melamed E, Yang X, Kampf K, Wang S, et al. (2007) Dosage compensation

- is less effective in birds than in mammals. *J Biol* 6: 2.
212. Mank JE, Ellegren H (2008) All dosage compensation is local: Gene-by-gene regulation of sex-biased expression on the chicken Z chromosome. *Heredity*.
213. Melamed E, Arnold AP (2007) Regional differences in dosage compensation on the chicken Z chromosome. *Genome Biol* 8: R202.
214. Teranishi M, Shimada Y, Hori T, Nakabayashi O, Kikuchi T, et al. (2001) Transcripts of the MHM region on the chicken Z chromosome accumulate as non-coding RNA in the nucleus of female cells adjacent to the DMRT1 locus. *Chromosome Res* 9: 147-165.
215. Warren WC, Hillier LW, Marshall Graves JA, Birney E, Ponting CP, et al. (2008) Genome analysis of the platypus reveals unique signatures of evolution. *Nature* 453: 175-183.
216. Deakin JE, Hore TA, Koina E, Marshall Graves JA (2008) The status of dosage compensation in the multiple X chromosomes of the platypus. *PLoS Genet* 4: e1000140.
217. Baker BS, Gorman M, Marin I (1994) Dosage compensation in *Drosophila*. *Annu Rev Genet* 28: 491-521.
218. Meller VH, Rattner BP (2002) The roX genes encode redundant male-specific lethal transcripts required for targeting of the MSL complex. *EMBO J* 21: 1084-1091.
219. Mendjan S, Akhtar A (2007) The right dose for every sex. *Chromosoma* 116: 95-106.
220. Kelley RL, Lee OK, Shim YK (2008) Transcription rate of noncoding roX1 RNA controls local spreading of the *Drosophila* MSL chromatin remodeling complex. *Mech Dev* 125: 1009-1019.
221. Oh H, Park Y, Kuroda MI (2003) Local spreading of MSL complexes from roX genes on the *Drosophila* X chromosome. *Genes Dev* 17: 1334-1339.
222. Park Y, Kelley RL, Oh H, Kuroda MI, Meller VH (2002) Extent of chromatin spreading determined by roX RNA recruitment of MSL proteins. *Science* 298: 1620-1623.
223. Kelley RL (2004) Path to equality strewn with roX. *Dev Biol* 269: 18-25.
224. Alekseyenko AA, Peng S, Larschan E, Gorchakov AA, Lee OK, et al. (2008) A sequence motif within chromatin entry sites directs MSL establishment on the *Drosophila* X chromosome. *Cell* 134: 599-609.
225. Alekseyenko AA, Larschan E, Lai WR, Park PJ, Kuroda MI (2006) High-resolution ChIP-chip analysis reveals that the *Drosophila* MSL complex selectively identifies active genes on the male X chromosome. *Genes Dev* 20: 848-

- 857.
226. Gilfillan GD, Straub T, de Wit E, Greil F, Lamm R, et al. (2006) Chromosome-wide gene-specific targeting of the *Drosophila* dosage compensation complex. *Genes Dev* 20: 858-870.
227. Legube G, McWeeney SK, Lercher MJ, Akhtar A (2006) X-chromosome-wide profiling of MSL-1 distribution and dosage compensation in *Drosophila*. *Genes Dev* 20: 871-883.
228. Franke A, Baker BS (2000) Dosage compensation rox! *Curr Opin Cell Biol* 12: 351-354.
229. Penalva LO, Sanchez L (2003) RNA binding protein sex-lethal (Sxl) and control of *Drosophila* sex determination and dosage compensation. *Microbiol Mol Biol Rev* 67: 343-359, table of contents.
230. Meyer BJ (2005) X-Chromosome dosage compensation. *WormBook*: 1-14.
231. McDonel P, Jans J, Peterson BK, Meyer BJ (2006) Clustered DNA motifs mark X chromosomes for repression by a dosage compensation complex. *Nature* 444: 614-618.
232. Ercan S, Giresi PG, Whittle CM, Zhang X, Green RD, et al. (2007) X chromosome repression by localization of the *C. elegans* dosage compensation machinery to sites of transcription initiation. *Nat Genet* 39: 403-408.
233. Just W, Baumstark A, Suss A, Graphodatsky A, Rens W, et al. (2007) *Ellobius lutescens*: sex determination and sex chromosome. *Sex Dev* 1: 211-221.



Kim Monkhorst, Iris Jonkers, Eveline Rentmeester,
Frank Grosveld and Joost Gribnau



Summary

Female mammalian cells achieve dosage compensation of X-encoded genes by X-chromosome inactivation (XCI). This process is thought to involve X chromosome counting and choice. To explore how this process is initiated we analyzed XCI in tetraploid XXXX, XXXY and XXYY embryonic stem cells and find that every X chromosome within a single nucleus has an independent probability to initiate XCI. This finding suggests a stochastic mechanism directing XCI counting and choice. The probability is directly proportional to the X chromosome:ploidy ratio, indicating the presence of an X-encoded activator of XCI, that itself is inactivated by the XCI process. Deletion of a region including *Xist*, *Tsix* and *Xite* still results in XCI on the remaining wild type X chromosome in female cells. This result supports a stochastic model in which each X chromosome in a nucleus initiates XCI independently, and positions a X-encoded trans-acting XCI-activator outside the deleted region.

Introduction

In placental mammals, gene dosage of X chromosomal genes is equalized between sexes by inactivation of one of the two X chromosomes in female cells [1]. In mouse and human embryos, XCI is initiated early in development and is random with respect to the parental origin of the X chromosome. Three X-linked non-coding genes, *Xist*, *Tsix*, and *Xite*, located within the X inactivation center (Xic), play a crucial role in the XCI process [2,3,4,5]. At the start of XCI, the cell determines the number of X chromosomes and elects the future inactive and active X chromosomes. Next, *Xist* RNA accumulates *in cis* on the future inactive X chromosome (Xi), followed by several epigenetic changes that 'lock in' and maintain the inactive state through many cell divisions [6,7]. *Tsix* and *Xite* play an essential role in down-regulation of *Xist* RNA before and during the XCI process

Despite the progress made over the last decades in understanding XCI, the mechanism underlying the counting and choice process remains unclear. X:autosome translocations suggested the presence of a blocking factor that protects one X chromosome from inactivation per diploid nucleus [8]. Different deletions 3' of the *Xist* gene resulted in XCI in male cells thus suggesting the location of the blocking factor binding site [9,10]. Other elements are also involved in the counting and choice process. For example, in female cells with a heterozygous *Xist* mutation (that abolishes *Xist* function), the mutant allele is never chosen to be inactivated [2,11]. In agreement with this, heterozygous mutations that abolish *Tsix* transcription result in preferential inactivation of the mutant X chromosome [5,9,12]. To explain the finding that initiation of XCI is absent in a *Tsix* mutant male cells, an X-linked competence factor was introduced (two copies are required for initiation of XCI) [5].

Interestingly, a homozygous mutation of the *Tsix* promoter revealed a ‘chaotic’ choice mechanism, in which zero, one or two X chromosomes were chosen for inactivation [13]. However, only cells with a single Xi were capable of contributing to a developing embryo [14].

Besides a blocking factor model, other models have been put forward to explain XCI counting and choice. One model predicts that the fate of an X chromosome is determined prior to the start of the XCI process and is based on differences in sister chromatid cohesion in female ES cells [15]. A different model explains counting and choice through transient cross communication between X chromosomes [16]. This is supported by two studies showing that the X chromosomes in female cells transiently move closer during the initiation phase of XCI in a subset of cells [17,18]. However, it is currently unclear how this model can explain observations made in diploid XXXX and tetraploid XXXX cells, that inactivate three and two X chromosomes respectively, and the XX 65kb deletion line that does not show a counting defect despite the absence of transvection [7,19].

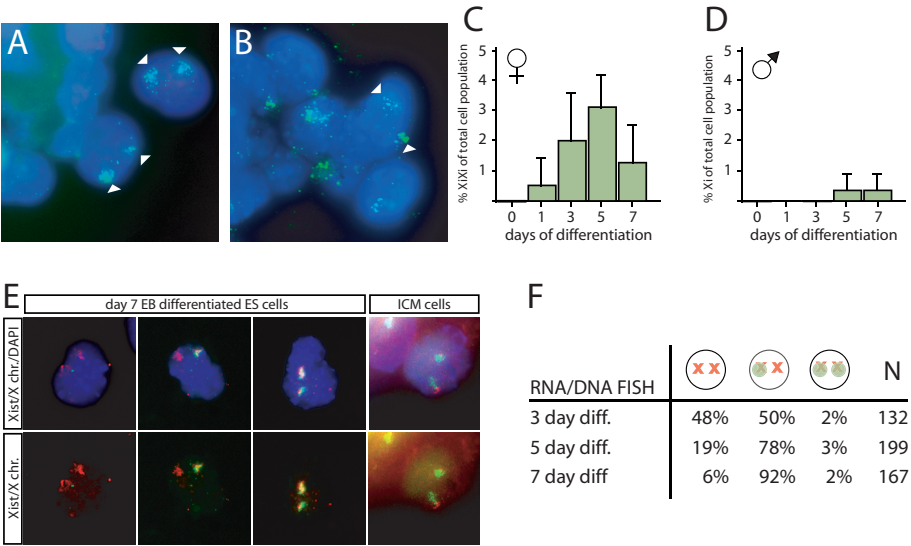


Figure 1. Double *Xist* clouds in diploid female cells
(A,B) *Xist* RNA FISH (FITC) on 3 day differentiated F1 2-1 female diploid ES cells (A) and differentiating ICM cells (B) revealed cells with two *Xist* clouds (indicated with triangles).
(C,D) Three independent experiments with standard deviation of the relative number of double clouds in female F1 2-1 (C) and single clouds in male (J1, V6.5 and E1) (D) diploid ES cells at different time points after differentiation, determined by RNA FISH.
(E) RNA/DNA FISH with an *Xist* probe (FITC) and an X chromosome paint probe (Cy3, DNA is DAPI stained, blue), on day 7 differentiated ES cells and differentiated ICM cells. Left panels: cells with no and one *Xist* cloud, right panels: ES and ICM cells with two *Xist* clouds.
(F) Quantification of *Xist* clouds in day 3, 5 and 7 differentiated female F1 2-1 ES cells by RNA/DNA FISH.

Stochastic model systems have been postulated to explain a variety of cellular choice processes, including lineage specification in the haematopoietic system [20], VDJ recombination [21], olfactory receptor choice [22], and the retinal mosaic for color vision [23]. Here we propose a stochastic model for XCI, in which each X chromosome has a probability to be inactivated within a certain time span. To validate such a model, we have analyzed XCI in differentiating diploid and tetraploid ES cells, the latter providing a much wider spectrum of possible outcomes of the XCI process. In addition, we have analyzed XCI in female ES cells with a deletion encompassing all elements that have previously been shown to be involved in XCI counting, including *Xist*, *Tsix* and *Xite*. Our results support a stochastic model for XCI counting and choice, and indicate the presence of a novel X-encoded factor, XCI-activator, involved in initiation of XCI.

Results

Diploid female ES cells with two *Xist* clouds

In differentiating diploid female ES cell cultures we observed a reproducible proportion of cells with two *Xist* RNA FISH clouds in one nucleus (Figure 1A). In ICM-derived cells that were allowed to differentiate *in vitro* (Figure 1B) we also noticed female cells with two *Xist* clouds. These observations suggest that some of the female cells attempt to inactivate both X chromosomes. Three independent EB differentiation experiments with female ES cells showed that the relative number of cells with two *Xist* clouds, as determined by RNA FISH, is low but consistent throughout differentiation. The proportion of these double cloud cells seemed to increase up to day 5 of differentiation and then decreased subsequently (Figure 1C). The presence of cells with two *Xist* clouds could be attributed to leakiness of the XCI mechanism, resulting in inactivation of the future Xa, and would predict the presence of a comparable percentage of *Xist* clouds in male cells during ES cell differentiation. Analysis of three different male cell lines showed almost no cells initiating XCI on their single X chromosome, indicating that the presence of the female cells with two Xi-s cannot be explained by sporadic leakiness of the XCI mechanism (Figure 1D). To exclude the possibility that cells with two *Xist* clouds were aneuploid, we performed RNA/DNA FISH on day 3, 5 and 7 EB differentiated female cells, and *in vitro* differentiated female ICM cells. The ploidy status of cells with two *Xist* clouds was confirmed to be diploid (Figure 1E and F). Thus, cells with two *Xist* RNA clouds are present in early differentiating female ES and ICM cell populations.

Generation of tetraploid ES cell lines

To investigate this observation in more detail, we generated tetraploid ES cell lines. Different combinations of neomycin and puromycin resistant female and male diploid F1 hybrid ES cell lines were fused to generate tetraploid XXXX, XXXY and XXYY cell

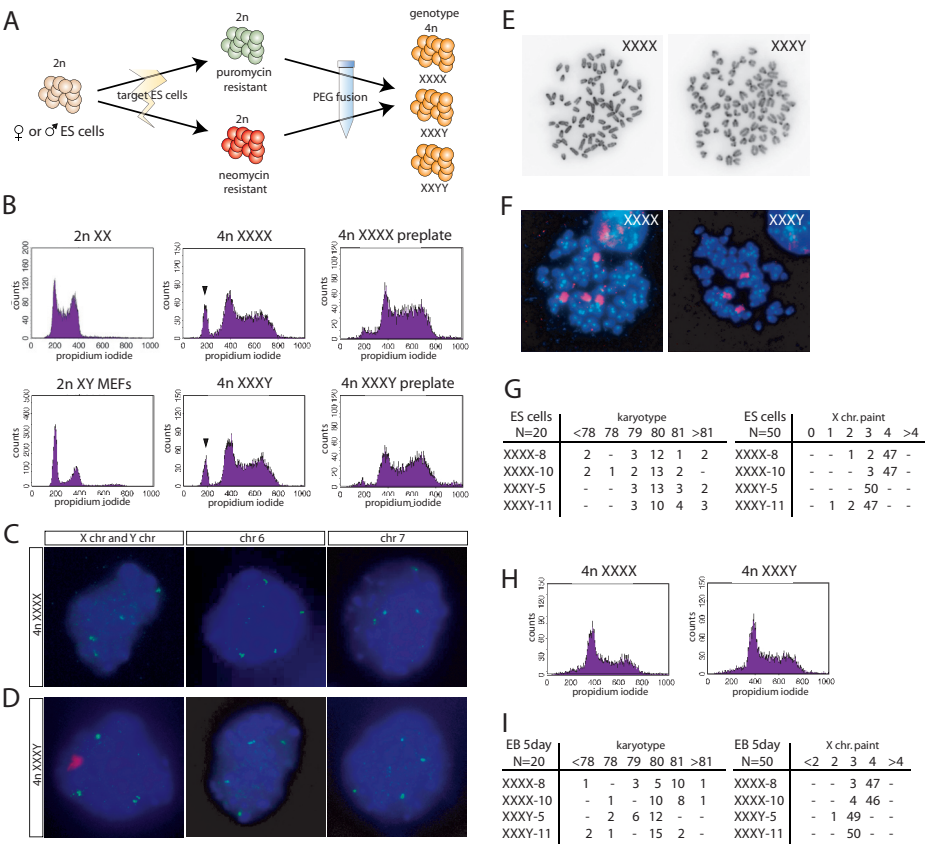


Figure 2. Generation of tetraploid ES cell lines

(A) Neomycin or puromycin resistant male and female diploid ES cells were targeted and fused in different combinations to generate tetraploid ES cells.

(B) FACS analysis of tetraploid XXXX-8 and XXXY-5 lines shows doubling of DNA content compared to diploid XX ES lines and XY MEFs. Note the decrease diploid MEFs after 1 hour preplating (arrowheads).

(C and D) DNA FISH: X chr., chr. 6 and 7 in FITC (green), Y chr. in Rhodamine (red), DNA is DAPI stained, blue, performed on XXXX-1 (C) and XXXY-1 (D) ES cells.

(E) Metaphase spreads of XXXX-8 and XXXY-5 cells (inverted Dapi image).

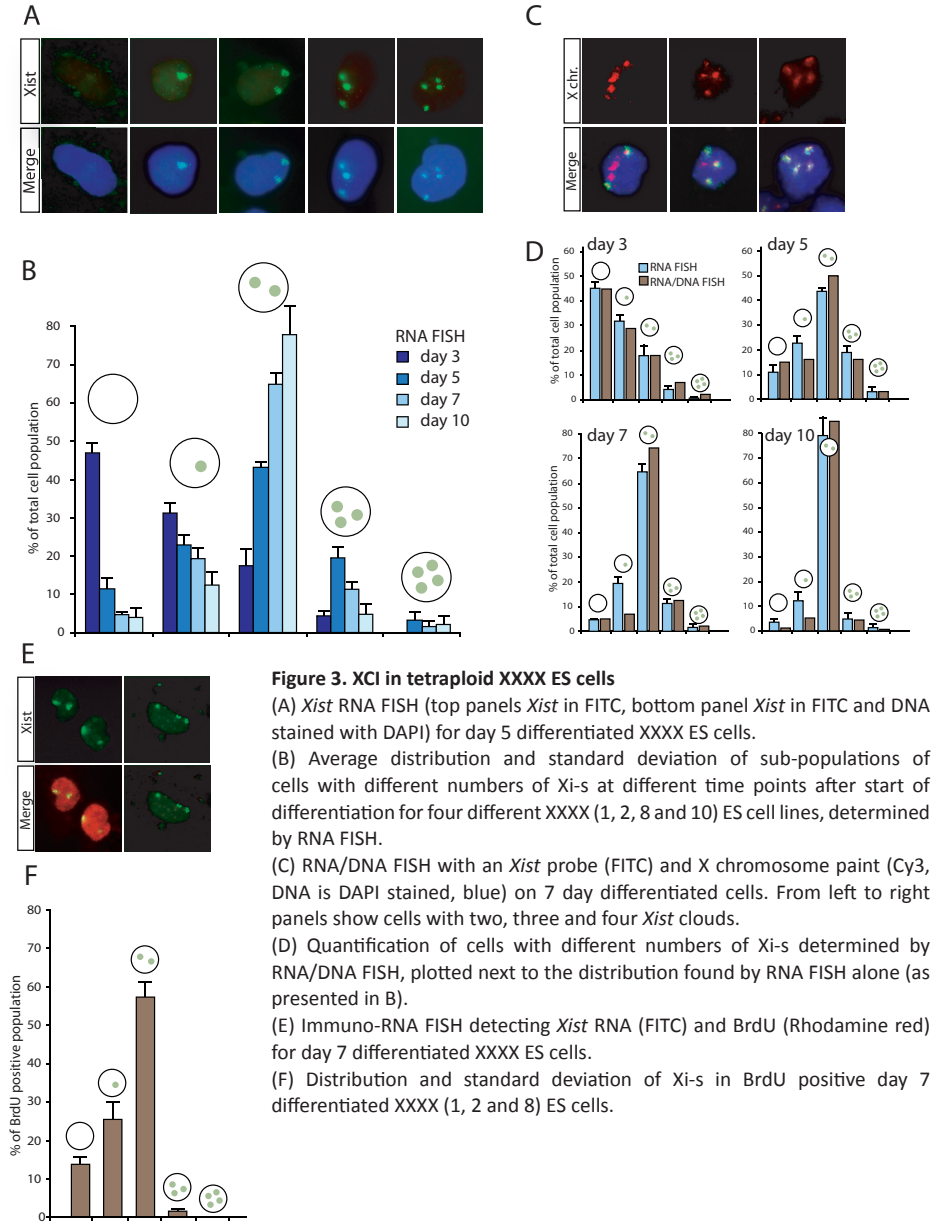
(F) X paint analysis of XXXX-8 and XXXY-5 cells (X paint in Cy3, DNA is DAPI stained).

(G) Left panel, shows the number of chromosomes determined in 20 metaphase spreads of undifferentiated tetraploid cell lines. Right panel, shows the number of X chromosomes of 50 metaphase spreads using X chromosome paint.

(H) FACS analysis of XXXX-8 and XXXY-5 tetraploid ES lines after 5 days of differentiation.

(I) Same as G only in day 5 differentiated cells

lines (Figure 2A). Clones were grown under continuous double selection. Withdrawal of double selection or the use of inbred ES cells resulted in accelerated chromosome loss. FACS analysis of different tetraploid ES cell lines showed a doubling in DNA content compared to diploid XX ES cells and male mouse embryonic fibroblasts



(MEFs, Figure 2B). The 2n peak in our tetraploid samples decreased after one hour of pre-plating on non-gelatinized dishes, indicating that this peak represents male MEFs used for culturing our ES cells. DNA FISH analysis using different autosomal and sex-chromosomal probes confirmed tetraploidy of the cell lines (Figure 2C and D). In addition, extensive karyotyping of two XXXX (8 and 10) lines and two XXXY (5 and 11) lines showed that the chromosome number in all the lines was around 80 chromosomes, with the majority of cells retaining 80 chromosomes (Figure 2E, F and G). With DNA FISH analysis using an X paint probe, we found that around 94% of the XXXX cells retain four X chromosomes, and more than 94% of the XXXY cells retain three X chromosomes (Figure 2E, F and G). We did not find XXXX cells with more than four X chromosomes, or XXXY cells with more than three X chromosomes.

To test whether tetraploid ES cells have a stable karyotype throughout embryoid body (EB) differentiation, we repeated the FACS analysis and karyotyping with day 5 EB differentiated cells from two different XXXX and XXXY ES cell lines. We found that our differentiated ES cells maintain a stable karyotype throughout the differentiation process (Figure 2H and I). More importantly, X-paint DNA FISH analysis indicated that a small gain in chromosome number could not be attributed to an increase in the number of X chromosomes. Taken together, these results show that the generated tetraploid ES cell lines have a stable karyotype throughout EB differentiation.

Analysis of X chromosome inactivation in tetraploid cells

To study the XCI process in different XXXX, XXXY and XXYY tetraploid ES cell lines, we differentiated and fixed the cells at day 3, 5, 7 and 10 of differentiation. Interestingly, RNA FISH analysis with an *Xist* probe on XXXX ES cells indicated the presence of cells with zero to four Xi-s (Figure 3A). The populations of cells with different numbers of Xi-s during EB differentiation changed over time (Figure 3B). At day 3 of differentiation most of the cells had no *Xist* cloud while fewer cells have one, two and three clouds. Later in differentiation (day 5, 7 and 10) cells with two clouds represented the largest population, and this increased over time. Other populations with no, one, or three clouds, declined over time.

In addition to the karyotyping (Figure 2I), we performed RNA/DNA FISH on XXXX line 8 at different time points during differentiation to further exclude the possibility that the analyzed cell lines were aneuploid. We first selected cells with 4 X chromosomes as judged by X chromosome paint signal (day 7 and day 10 samples) or an X chromosome specific BAC signal (day 3 and day 5 samples) and subsequently counted the number of *Xist* RNA clouds in the nucleus (Figure 3C). We compared these results to the RNA FISH data obtained at different time points and

confirmed the presence of cells with 3 and 4 *Xist* clouds (Figure 3D). We also found a relative increase in the percentage of cells with two clouds and a relative decrease in the percentage of cells with one cloud in day 5, 7 and 10 differentiated ES cells. These differences can be explained by the fact that RNA/DNA FISH analysis results in the exclusion of XXXO cells (Figure 2I) that show preferential inactivation of one X chromosome (see below).

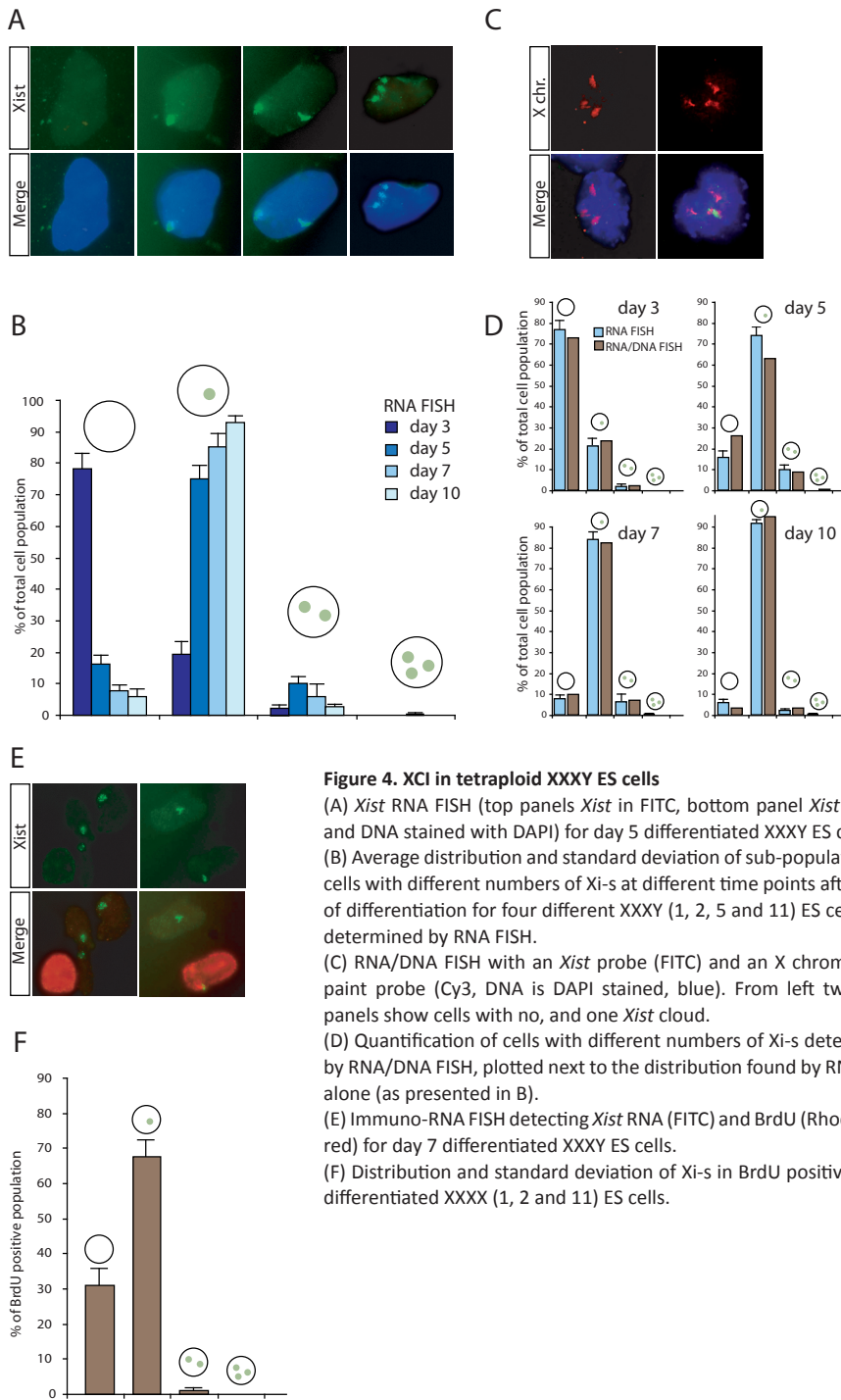
The distribution of cells over time suggests that cells with the correct Xa:ploidy ratio, are selected for during differentiation. Indeed, BrdU analysis of ES cells at day 7 of differentiation showed that BrdU positive cells with three and four Xi-s are severely reduced compared to the total population of cells, indicating that these cells stop dividing (Figure 3E and F). In contrast, the BrdU positive population consists almost entirely of cells with no, one or two Xi-s indicating that this part of the population remains proliferative (Figure 3F). The small number of BrdU positive cells with three Xi-s may indicate that these cells can still divide, albeit at a slower rate when compared to cells with two or less Xi-s, or perhaps more likely, they represent cells that were BrdU labeled prior to XCI. Interestingly, cells with none or one Xi disappeared during the differentiation process, suggesting that these cells initiate XCI on the remaining Xa-s.

XXXY cells preferably inactivate one X chromosome (Figure 4A, and B) Initiation of XCI was delayed as demonstrated by the percentage of cells with no clouds at day 3 of differentiation, as compared to day 3 differentiated XXXX ES cells (Figure 3B, and 4B). RNA/DNA FISH on XXXY ES line 11, at different time points after differentiation revealed a similar distribution when compared to RNA FISH alone (Figure 4C and D). BrdU incorporation analysis of cells at day 7 of differentiation showed that cells with more than one Xi stop dividing. Cells with no Xi are a large proportion of the BrdU positive cells, but disappear over time, again indicating that these cells are still initiating XCI (Figure 4E and F). XXYY cell lines only sporadically initiate XCI at day 3 and day 7 of differentiation similar to diploid XY cells (<0.3%, data not shown).

The above experiments with tetraploid ES cells show that all cell lines preferably keep one Xa per diploid genome. Nevertheless, a significant number of cells do inactivate an aberrant number of X chromosomes during the XCI process. Cells with less than one Xa per diploid genome stop dividing, and are lost in time in the proliferating cell population.

Calculating a probability to initiate XCI

The existence of cells with an unexpected number of *Xist* clouds in differentiated ES cells led us to hypothesize that each X chromosome within a cell has a certain



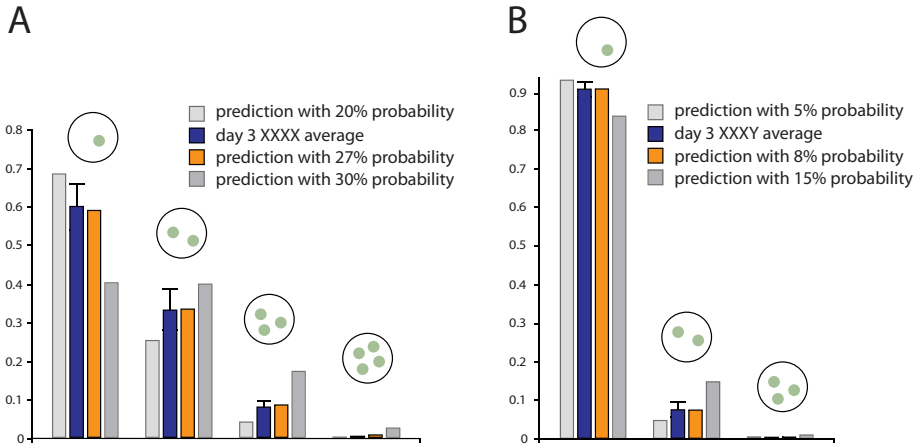


Figure 5. Comparison of the experimental and predicted distributions

(A) Distribution of sub-populations of cells with different numbers of Xi-s at day 3. The average and standard deviation of four XXXX cell lines (blue bars), and predicted distribution after one choice round based on a 20%, and 30% probability (gray bars) and a 27% probability per X chromosome to be inactivated (orange bar).

(B) Similar to (A) but for the four XXXY cell lines (blue bars), and the predicted distributions based on a 5%, and 15% probability (gray bars) and 8% probability per X chromosome to be inactivated (orange bar).

probability to initiate XCI. Indeed, for the XXXX cell lines the distribution of cells with different numbers of Xi-s (day 3 of differentiation) can be explained by assuming a 27% probability for each X chromosome to initiate XCI, after subtraction of cells without an *Xist* cloud (Figure 5A). We excluded this fraction because we cannot distinguish between the cell population that, has not yet initiated XCI and that which has initiated XCI but has not chosen an X chromosome for inactivation. Also, this population is not required to calculate the probability. Day 3 differentiated samples were used to avoid potential influences of cell selection or multiple rounds of inactivation in our calculation. Nonetheless, the calculated probability remains a cumulative probability over the first 3 days of differentiation. For the XXXY cells, a probability of 8% would generate a distribution that matches our experimental observation at day 3 of differentiation (Figure 5B). Based on these calculations, we conclude that the distribution of the different populations could be explained by assuming a probability for each X chromosome in a cell to initiate XCI. In addition, the probability increased with the X:ploidy ratio, indicating the presence of an X linked activator of XCI.

Initiation of XCI in female cells despite deletion of *Xist* *Tsix* and *Xite*

Our results suggest an independent probability for each X chromosome to initiate XCI, followed by selection of cells with the correct number of Xa-s. Therefore,

deletion of the *cis* acting genes (*Xist*, *Tsix* and *Xite*) and all known elements involved in the counting process should have no effect on the probability to initiate inactivation on the remaining wild type X chromosome in a diploid female cell. To test this hypothesis, we integrated a floxed hygroTK cassette between *Tsx* and *Xite* in a previously described (1lox) $\Delta Xist$ ES cell line with a conditional *Xist* deletion [11,24] (Figure 6A). Cre recombinase mediated deletion of the remaining part of *Xist*, and *Tsix* and *Xite*, designated $\Delta Xist$ -*Tsix*-*Xite* (ΔXTX), was confirmed by Southern and PCR analysis (Figure 6B-E). RNA FISH analysis of undifferentiated $XX_{\Delta XTX}$ cell lines with an *Xist* probe detecting *Tsix* transcription showed a single pinpoint signal (N=100), also confirming that the remaining part of *Tsix* has been deleted from the $\Delta Xist$ allele (Figure 6F).

To explore the pattern of XCI in differentiating $XX_{\Delta XTX}$ ES cell lines, we subjected EB differentiated cells to DNA/RNA FISH using an *Xist* RNA probe in combination with an X chromosome specific Bac probe (day 3) or an X chromosome paint probe (day 7). Since the ΔXTX and $\Delta Xist$ cell lines had a tendency to become XO, (reported to occur for many inbred lines) cells with two X chromosomes were selected prior to examination for an *Xist* signal. Interestingly, ~38% of the cells at day 3 of differentiation and ~87% of the cells at day 7 of differentiation showed an *Xist* RNA cloud, similar to the percentages obtained with the $\Delta Xist$ cell lines. Both at day 7 and, more pronounced at day 3, the percentages of cells which initiated XCI were lower for the ΔXTX and $\Delta Xist$ lines than for the wild type control. We attribute this difference to the fact that in both the ΔXTX and $\Delta Xist$ cells only one X chromosome has a probability to initiate XCI while wild type female cells have two X chromosomes with a probability to initiate XCI.

To test our findings *in vivo*, we injected the $XX_{\Delta XTX}$ ES cells into blastocysts and generated chimeras. In the second litter of the female founder, two out of nine embryos contained an $X_{\Delta XTX}$ chromosome (Figure 6I and J). This was verified by Southern blotting (data not shown). PCR analysis with *Sry* specific primers indicated that one ΔXTX embryo was male and one female (figure 6K). The $XX_{\Delta XTX}$ and $X_{\Delta XTX}Y$ embryos did not show any structural abnormalities or growth retardation (Figure 6I). MEFs were derived from all embryos and subjected to DNA/RNA FISH (*Xist* probe and two BAC probes). We observed *Xist* RNA clouds in 99% of the $XX_{\Delta XTX}$ MEFs and 98% of the wild type MEFs, confirming our finding with the $XX_{\Delta XTX}$ ES cell lines (Figure 6L).

These data demonstrate that female diploid cells show XCI despite the ΔXTX -deletion, and confirmed that the probability to initiate XCI is determined independently by each X chromosome. Since XO and XY ES cells do not initiate XCI, these results also indicate the presence of an, as yet unidentified, X-encoded trans-acting factor located outside the deleted region that is required for XCI.

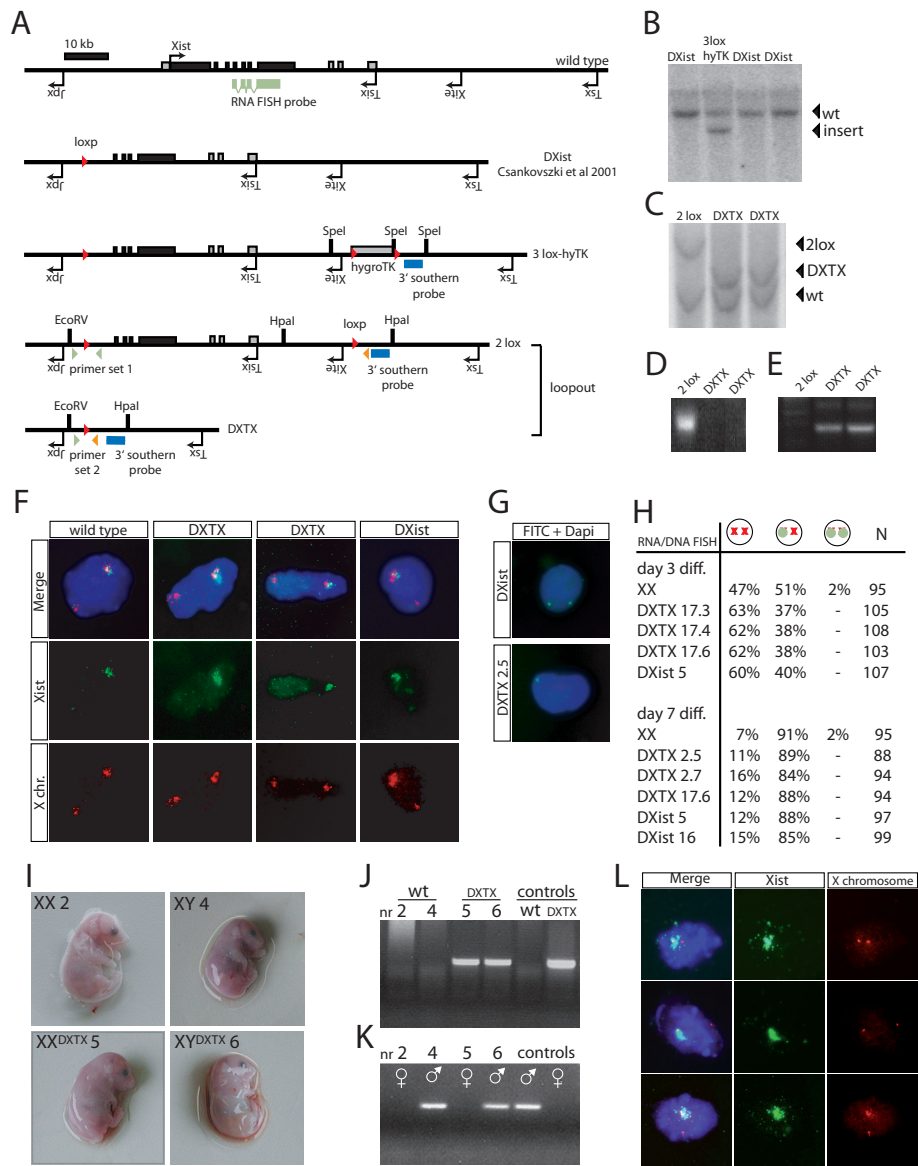


Figure 6. Analysis of XCI in XTX deletion cell lines

(A) Schematic representation of the generation of the XTX deletion ES cell lines.

(B) Southern blot analysis with a 3' external probe on SpeI digested DNA of different targeted clones.

(C) Southern analysis with DNA of different clones after transient Cre expression. DNA was digested with HpaI and EcoRV, and the 3' external probe was used for hybridization.

(D,E) Correct loopout was confirmed with PCR analysis using primer set 1 amplifying the original Δ Xist deletion (D) and primer set 2 amplifying the correct loopout (Δ XTX, E).

(F) RNA/DNA FISH analysis with an *Xist* probe (FITC) and X-chromosome paint (Cy3, DNA stained with Dapi) on 7 day differentiated wild type (XX) and mutant Δ XTX and Δ Xist cells.

Truncation of *Tsix* leads to earlier onset of XCI

What factors determine the probability for an X chromosome to inactivate? Studies with *Xist* promoter driven transgenes show a clear difference in expression between differentiating male and female ES cells, indicating the presence of a sex-linked transcription factor driving *Xist* expression [25]. In addition, more abundant *Xist* expression has been correlated with a weaker Xce allele in mice [26], suggesting that the *Xist* expression level could be a positive parameter correlating with XCI-probability. An additional parameter is *Tsix*, known as a negative regulator of *Xist*. Previous studies have shown that introduction of a stop cassette in *Tsix* prematurely abrogates *Tsix* transcription and results in almost exclusive inactivation of the mutated X chromosome [12]. Conversely, if *Tsix* expression persists upon differentiation, the wild type allele is always selected for inactivation [12]. These observations suggest that *Tsix* expression reduces the probability by inhibiting *Xist* expression. Therefore, abolishing *Tsix* expression greatly increases the probability of that allele to initiate XCI, and implies that XCI initiation should occur faster on the *Tsix*-stop allele compared to the wild type allele.

To test this hypothesis we analyzed *Xist* cloud formation by RNA FISH in the heterozygous *Tsix*-stop female ES cell line [12] at different time points of differentiation. Indeed, analysis of XCI in wild type and *Tsix*-stop cells showed that the *Tsix*-stop cells initiate XCI much faster compared to wild type cells (Figure 7A-C). Also, the number of cells with two *Xist* clouds is significantly reduced compared to wild type cells at all time points measured (Figure 7C). Because XCI in *Tsix*-stop cells is skewed towards inactivation of the mutated allele, we conclude that initiation of XCI is initiated faster on the mutated allele than the wild type allele. The reduced number of cells with two Xi-s is most likely due to the fact that the mutated X chromosome generates a probability to initiate XCI well before the wild type allele does, and as a consequence only in a few cells will both X chromosomes have a probability to initiate XCI. Our results showing accelerated initiation of XCI in *Tsix* stop cells, is consistent with the finding that *Xist* promoter methylation is detected much earlier in cells with a heterozygous Δ CpG *Tsix* deletion compared to wild type cells, indicating that the XCI process is accelerated on the mutant X chromosome [25].

(G) *Xist* RNA FISH analysis (FITC, DNA in DAPI) on Δ *Xist* and Δ TX 2.5 cells showing pinpoint signals in undifferentiated ES cells.

(H) Quantification of cells with no, one or two *Xist* clouds at day 3 and day 7 of differentiation using wild type, Δ TX cells and Δ *Xist* cells, determined by RNA/DNA FISH.

(I) Wild type and Δ TX mutant female and male littermates.

(J) PCR analysis of the mice shown in (I) with primer set 2 amplifying the Δ TX loopout.

(K) PCR analysis of the mice shown in (I) with a primer set amplifying the *Sry* gene.

(L) *Xist* RNA/DNA FISH analysis (FITC) and X chromosome specific BAC probes (Rhodamine red, DNA is DAPI stained, blue) on MEFs isolated from the Δ TX mutant female. The panels show three representative cells.

Discussion

We find that in the course of the XCI process a significant proportion of cells do not comply with the 1Xa/diploid genome rule and have less or more than the expected number of Xi-s.

This finding suggests that XCI is a stochastic process with an independent probability for each X chromosome to initiate XCI and that this probability is directly proportional to the X:ploidy ratio. These results also suggest the presence of an X-encoded probability-promoting factor, which is located outside the region we deleted in our female Δ TX lines.

Comparing different tetraploid studies

Our findings that 10 day differentiated XXXX tetraploid ES cells preferably inactivate two X chromosomes, are in agreement with Webb et al. 1992. Similar to our findings in differentiating ES cells, Webb et al. reported a significant number of cells with zero, one or three Xi-s in 10-day-old tetraploid XXXX embryos, indicating that cells with an aberrant Xi number are also present *in vivo* (Webb, 1992). A different study analyzing 9 to 12 day differentiated tetraploid XXXX lines, generated by fusion of EC cells with lymphocytes, showed variable results [27]. We attribute the different findings presented in this study to the method used to detect Xi-s; i.e. BrdU incorporation in metaphase spreads, a technique that does not allow detection of cells that stop dividing. Also, ES cell x somatic cell fusion lines have been reported to be karyotypically unstable [28] in contrast to our ES x ES cell fusion lines, that retain a stable karyotype for more than 20 passages.

Each X chromosome has a probability to initiate XCI

Different models have been proposed explaining the XCI counting and choice process. One model explains XCI counting and choice through the presence of a single autosomally encoded blocking factor, which prevents inactivation of one X chromosome per diploid genome. XCI counting and choice could also be explained through transient spatial cross communication between the different X chromosomes, or pre-determined Xic's prior to the start of XCI [8,17,18]. These deterministic models predict a tightly regulated XCI counting and choice process and do not explain the presence of XXXX cells with three or four Xi-s. Aberrant numbers of Xi-s in XXXY and XXXX ES cells could be an artifact introduced by tetraploidization or an instable karyotype. However, our tetraploid cells maintain a stable karyotype and the expected number of X chromosomes throughout differentiation. Hence, our finding that XCI is properly regulated in XYY tetraploid cells argues against this possibility. Instead, the distribution of cells with different numbers of Xi-s can be explained by

assuming a stochastic model, in which each X chromosome has a certain probability to be inactivated.

A stochastic model predicts the presence of diploid female cells with two Xi-s. We did observe 2 Xi-s in some differentiating ES and ICM cells and others also reported the presence of diploid cells with two Xi-s [13]. Nonetheless, the number of cells with two Xi-s is lower than would be expected based on a 27% probability we calculated for each X chromosome in the tetraploid XXXX line (same X:ploidy ratio as a diploid cell). Although the differences could be due to potentially different cell volumes, cell division or differentiation characteristics of diploid and tetraploid cells, this discrepancy is most likely based on the fact that there is a strong selection against cells with all X chromosomes inactivated.

Examination of cell division kinetics by BrdU incorporation analysis indicates that cells with one or more Xa per diploid genome keep dividing. Nonetheless, cells with more than one Xa per diploid genome decrease in time, suggesting that these cells keep initiating XCI, or are eliminated due to aberrant dosage compensation, although the latter may only play a role at later stages during differentiation. Cells with less than one Xa per diploid genome stop dividing. Therefore, continued proliferation of the other cells within the population will result in a relative decrease of cells with less than one Xa per diploid genome. Currently, we do not know whether these cells remain in the population, are actively selected against or disassemble their *Xist* cloud(s) and rejoin the pool of dividing cells.

In vivo evidence supporting cell loss as a consequence of the XCI process comes from studies that show a significant size difference between female and male early implantation diploid embryos before hormonal cues start to influence growth [29]. Interestingly, female mouse XO embryos did not differ in size compared to XY male embryos. The size difference between male and normal female embryos is most pronounced around the time of XCI and decreases later during development. Thus, similar to our *in vitro* findings with differentiating tetraploid ES, gender specific size differences could very well be related to the loss of XiXi and XaXa cells during development.

Evidence against a single blocking factor

If the probability to initiate XCI is an independent property of the deleted *Xist-Tsix-Xite* region, and dependent on trans-acting factors located elsewhere in the genome, deletion of this region in female cells should have no effect on the probability of the wild type allele to initiate XCI. Our results with the Δ TX ES cell lines and mice confirm this hypothesis and show that the deleted area is not required for the counting process in female cells. We find initiation of XCI as expected for a single

Figure 7. Analysis of the *Tsix* stop mutation, and a stochastic model for XCI counting and choice

(A,B) *Xist* RNA FISH analysis on day 1 EB differentiated wild type ES cells (A) and cells heterozygous for the *Tsix*-stop insertion (B). Triangles: *Xist* clouds, stars: *Tsix* pinpoints.

(C) Quantification of cells with an *Xist* cloud (line graph), and cells with two *Xist* clouds (bar graph) at different time points of EB differentiation for wild type and heterozygous *Tsix*-stop ES cells. Shown is the average and standard deviation of three independent experiments.

(D) Before differentiation *Tsix* transcription represses *Xist* expression, and the level of XCI-activator is insufficient to overcome *Tsix* repression. Upon differentiation, the XCI-activator level rises and in female cells reaches a level sufficient to overcome *Tsix* repression with a certain probability. After *Tsix* is silenced, *Xist* accumulates and silences the XCI-activator gene *in cis*, preventing inactivation of the second X chromosome.

(E) Schematic representation of D: after start of differentiation the XCI-activator level will rise and, in female cells (red lines), exceed the level required to generate a chance to initiate XCI. After XCI is initiated, cells have either two Xa-s, one Xa and one Xi or two Xi-s. Cells with two Xi-s stop dividing and disappear from the population (dashed lines). In cells with a Xa and a Xi the XCI-activator level drops below the level required to generate a probability. Cells with two Xa-s continue with XCI (faint red lines).

(F) In XXXX ES cells the XCI-activator concentration increases during differentiation generating a probability to initiate XCI for each X chromosome. After the choice is made there are five different outcomes. Cells with less than 2 Xa-s stop dividing and disappear from the population (dashed lines), cells with two Xi-s and two Xa-s stop the XCI process, and cells with no or one Xi continue the XCI process (faint red lines). Note that in cells with one Xi the probability will drop.

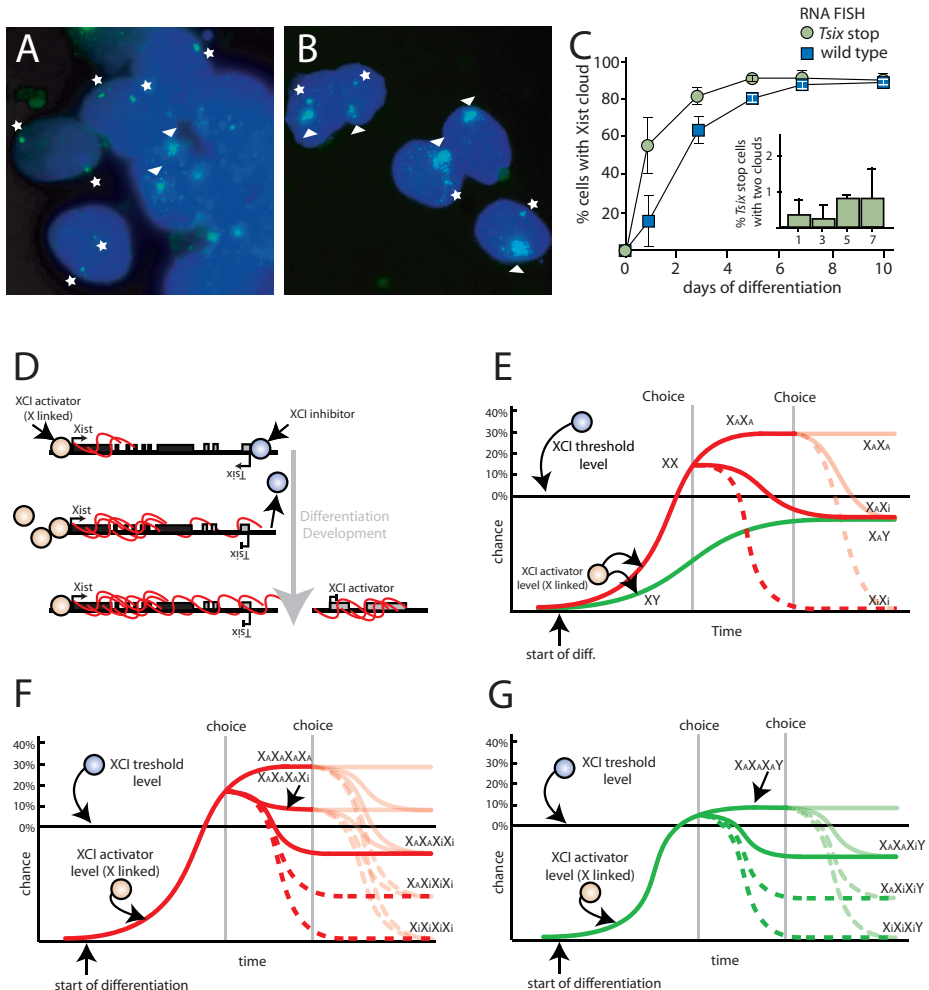
(G) For XXXY cells there are four possible outcomes, and the probability to initiate XCI is lower when compared to the XXXX line because of a lower level of the XCI-activator. Cells with two or three Xi-s stop dividing and disappear from the population (dashed lines). Cells with one Xi stop the XCI process, and cells that have not initiated XCI will continue the inactivation process (faint green lines).

allele in Δ XTX cells, indicating that our results are not the consequence of initiation in a few cells followed by a selection process.

These and other findings indicate that a single blocking factor may not be present at all, because of the following arguments. XCI is initiated in male ES cells with a 65kb deletion, a 20 kb bipartite deletion and a smaller 1.2 kb DXPas34 deletion, all located 3' of *Xist* [9,10,30], placing the putative blocking factor binding site inside this region. Nevertheless, we find robust initiation of XCI despite the deletion of this entire region. This does not exclude the possibility that the blocking factor binding site is located outside the deleted region. However, if this were true an increased number *Xist* double clouds would be expected in female cells heterozygous for the 65kb deletion or the *Tsix* stop insertion, because in both cell lines half of the wild type X chromosomes are unprotected from XCI. Remained presence of a blocking factor binding site on the mutated allele would therefore have resulted in an increased number of cells with two Xi-s. Neither we nor others have found this [9]. We therefore conclude that our findings preclude a blocking factor model.

Evidence for an X-encoded factor involved in promoting XCI

Our findings that XX _{Δ XTX} cells initiate XCI in contrast to XY cells, provides evidence for the presence of an unidentified X-linked gene encoding a trans-acting factor that is involved in promoting initiation of XCI (XCI-activator). Analysis of the XCI initiation



frequency at day 3 of differentiation shows that the XXXX ES cells initiate XCI much faster than XXXY ES cells. In addition, the calculated probability to initiate XCI is much lower for XXXY cells than the XXXX cells. Both observations indicate the presence of an X-encoded probability-determining factor that is located outside our *XTX*-deletion but resides in the genetically defined *Xic*. The presence of a XCI-activator is supported by studies with *Xist* promoter driven transgenes that show a clear difference in expression between differentiating male and female ES cells, also indicating the presence of a sex-linked transcription factor [25].

Interestingly, a previous study, which analyzed XCI in a male cell line with a 450kb transgene, encompassing *Xist* and flanking regions, showed initiation of XCI on the single X chromosome, indicating that the transgene may harbor the gene

encoding this XCI-activator [31]. A different study showed that introduction of a BAC sequence located 5' to *Xist*, not including *Xist* itself, into ES cells also results in initiation of XCI on the single X chromosome in male cells, and on both X chromosomes in female cells [32]. This result was attributed to ectopic pairing between the transgene and the Xic. We think that this study indicates that the sequence encoding the XCI-activator may be located within the transgene. The reported transient pairing could be the consequence of the differentiation process, and related to changes in the expression of genes located within the Xic, resulting in transient changes in the nuclear positioning of these genes.

A stochastic model for XCI counting and choice

This study indicates that XCI is a stochastic process, in which each X chromosome has a probability to be inactivated. The outcome of the XCI process is the resultant of; 1) an equal probability for each individual X chromosome to be inactivated (in the same genetic background), 2) the probability to initiate XCI is directly proportional to the X:ploidy ratio, 3) selection in favor of cells retaining one Xa per diploid genome.

What factors determine the probability for an X chromosome to be inactivated? Cell line studies indicate that the *Xist*, *Tsix*, and *Xite* genes play a key role in determining the probability of an X chromosome to initiate XCI. Although the molecular factors involved in the regulation of these genes remain elusive so far, studies with *Xist* promoter driven transgenes indicate the presence of a sex-linked transcription factor, which is supported by our observations [25]. *Tsix* is transcribed in both male and female cells before the onset of XCI indicating the presence of a, most likely autosomal, factor that drives *Tsix* transcription in both male and female cells [33]. These observations suggest that the probability to initiate XCI is the resultant of the balance between an X-encoded *Xist* activator (XCI-activator), that itself is inactivated by XCI, and a *Tsix* activator (XCI-inhibitor). Upon differentiation, the concentration of the XCI-activator rises (Figure 7D and E). In contrast, the XCI-inhibitor concentration remains stable or may even decrease in time, providing a stable threshold level throughout early differentiation or development, which has to be overcome to generate a probability to initiate XCI. In male cells the maximum XCI-activator concentration is not sufficient to overcome the XCI threshold level. In female cells the concentration of the XCI-activator will be twice as high and sufficient to induce *Xist* mediated silencing of *Tsix* with a certain probability in a particular time frame, e.g. one cell division. Because both X chromosomes generate a certain probability, a proportion of the differentiating cells will inactivate two X chromosomes. After XCI has been initiated, the X-encoded XCI-activator gene will be silenced *in cis*. This results in a drop in the XCI-activator level to a level equal to that

found in male cells, preventing inactivation of the second X chromosome. Cells that have not initiated XCI will start another round of inactivation. *Xist* expression on the future Xi persists because less XCI-activator is required as a result of a lack of *Tsix* inhibition *in cis*. In addition, chromatin modifications or *cis* interactions may fix the *Xist* active state on the future Xi.

For tetraploid cells this model becomes more complicated because of the increased number of possibilities (Figure 7F and G). XXXY tetraploid ES cell lines will have less XCI-activator when compared to the XXXX lines. This explains the decreased probability that was calculated for the XXXY line (8%) compared to the XXXX line (27%).

Important prerequisites for this model are the rapid down-regulation of the XCI-activator level after the initiation of XCI, and *Xist* mediated silencing of *Tsix*. Indeed, studies with cell lines with an inducible *Xist* cDNA transgene showed that inactivation of flanking genes occurs within several hours after *Xist* up-regulation [34]. To date, it is unclear whether *Tsix* is silenced by *Xist*, or whether *Xist* up-regulation is due to autonomous silencing of *Tsix* by developmental cues. Constitutive or inducible expression of *Tsix* shows that persistent expression of *Tsix* results in preferential inactivation of the (other) wild type X chromosome. Conversely, elevated transcription through *Xist*, as a consequence of an integration of a selection cassette upstream of the *Xist* promoter, results in preferential inactivation of the mutated X chromosome [35]. Although we cannot exclude a model in which the probability is solely dependent on autonomous down-regulation of *Tsix*, these findings indicate the presence of a transcriptional balance between *Xist* and *Tsix*, in which both genes have mutual inhibiting properties.

Interpretation of the stochastic model

A stochastic model for XCI predicts that SNPs, mutations or deletions of binding sites for the XCI-activator or -inhibitor will change the probability to inactivate the respective X chromosome and will result in skewed XCI. According to this model, a truncation of *Tsix* or deletions that lead to severe down-regulation of *Tsix* expression, will result in a reduced level of XCI-activator required for initiation of XCI, and would explain ectopic XCI observed in mutant male cells [9]. Similarly, *Xist* transgenes lacking *Tsix* repression will require less XCI-activator, which may lead to ectopic XCI in male cells [36]. In addition, a homozygous mutation of the *Tsix* major promoter that abolishes *Tsix* expression in female cells will lead to increased probabilities for both X chromosomes explaining the high frequency of differentiating cells with two Xi-s [13].

A stochastic model would also explain the sex-ratio distortion found for

Tsix double mutant offspring as a consequence of expression differences of the XCI-activator between male and female cells [14]. These observations indicate that *Tsix* may not be required for proper XCI to occur, as proposed for humans. As long as the probability to initiate XCI on an X chromosome remains low. This could be accomplished by down-regulation of the XCI-activator activity or *Xist* promoter activity. Although the factors driving the XCI process remain as yet elusive, the Δ XTX deletion described here locates the X-encoded XCI-activator gene outside the deleted region but within the region delineated by the Searle's translocation and the HD3 truncation, which originally defined the *Xic* [37,38]. Future identification of the XCI-activator and -inhibitor will be crucial for our understanding of the XCI process.

Methods

Generation of tetraploid ES cell lines

M. cast / 129/Sv F1 female (F1 2-1) and male (F1 2-3) ES cell lines and a male C57Bl6 / 129/Sv (V6.5) ES cells were targeted with neomycin and puromycin resistance cassettes. PEG 1500 (Roche Cat. No. 783 641) fusion was performed according to manufacturers instructions. Tetraploid ES cell lines were grown on male MEFs, under continuous double selection and have not been frozen before analysis.

DNA and RNA FISH

Pre-plated ES cells were transferred to non gelatinized bacterial dishes to start EB differentiation, in IMDM + Glutamax (Gibco), 15% FCS, Asc. Acid 50 μ g/ μ l, NEAA, PenStrep (PS), Monothioglycerol (97%) 37,8 μ l/l. One day prior to fixation, EBs were trypsinized and transferred to dishes with gelatin coated cover slips. BrdU (20 μ M) was added 16 hours (less than one cell division) prior to harvesting.

For RNA FISH experiments on differentiating ICM cells 3.5dpc blastocysts were flushed out of the uterus, and allowed to attach for two days in DMEM, 15% FCS, NEAA, PS, β -mercapthoeth. 8 μ l/l. Expanded ICMs were micro dissected with a mouth pipette and plated on gelatinized slides. ICM cells were allowed to attach and proliferate for two more days before fixation.

DNA and RNA FISH were performed as described [11], *Xist* RNA and chr. 6, 7 and Y specific probes have been described [11,39]. Criteria for scoring the *Xist* clouds: first in Dapi a non-overlaid intact nucleus was selected, then in FITC, the number of clouds was counted. Every *Xist* cloud that was counted was clearly distinguishable from neighboring clouds. If not specifically indicated more than 100 cells were counted per cell line per time point. For combined DNA/RNA FISH, slides were pretreated for 4 min with 0.2% pepsin in 10mM HCl at 37°C, post fixed for 5 minutes in 4% PFA/PBS, washed twice with PBS and dehydrated prior to denaturation. Probes for

hybridization were *Xist*, a Cy3 labeled X paint probe (Cambio), or a combination of two biotin labeled BACs (CT7-155J2 and CT7-474E4). Slides were washed at 42°C in 2xSSC and 3 washes of 2xSSC / 50% formamide. Detection was as described [11]. For DNA/RNA FISH diploid cells with two and tetraploid cells with four X chromosomes were selected in the red channel, then *Xist* clouds were counted in the FITC channel.

Karyotyping

Cells were treated with colcemid for 1h, fixed and hybridized with an X paint probe (Cambio). Criteria for scoring painted X chromosomes: first in Dapi a metaphase spread was selected, next in the red channel the number of X chromosomes was counted.

Generation of the Δ XTX ES cell line

An 8.2 kb XhoI-ClaI fragment from BAC 299K20 was subcloned into pBluescript KS, followed by the insertion of a PGK-DTA cassette into the ClaI site. Next, a floxed hygro-TK cassette was cloned into an EcoRV site. The resulting p*Xite*-DTA-hygroTK was targeted to a heterozygous Δ *Xist* 1lox ES cell line [11]. After transient Cre expression, positive clones were identified by southern analysis (SpeI digest) with a 3' external probe, a 565 bp PCR product (AAGCTTGGGTCCTCCTCTGT and CCACTCAGACATCCCCAGAT). Cre mediated excision was confirmed by PCR analysis using primer set 1 (A, TTTCTGGTCTTTGAGGGCAC x B, CACTGGCAAGGTGAATAGCA) detecting the original Δ *Xist* 1lox allele and primer set 2 (A x C, GGACATTTGTCTGGCAGT) detecting the Δ XTX allele.

Acknowledgements

We thank R. Jaenisch, J.A. Grootegeod, W. Baarends and Elaine Dzierzak for discussions and critical review of the manuscript, R. Jaenisch for *Tsix*-stop cells, M. Wijgerde, B de Hoon and T. de Wit for technical assistance and J. IJzermans, R.G. Boers, and B de Hoon for helpful discussions. This work was supported by HFSP CDA and NWO-VIDI grants to J.G., a NWO-AGIKO grant to K.M and a grant from the Dutch government (BSIK programme 03038, SCDD).

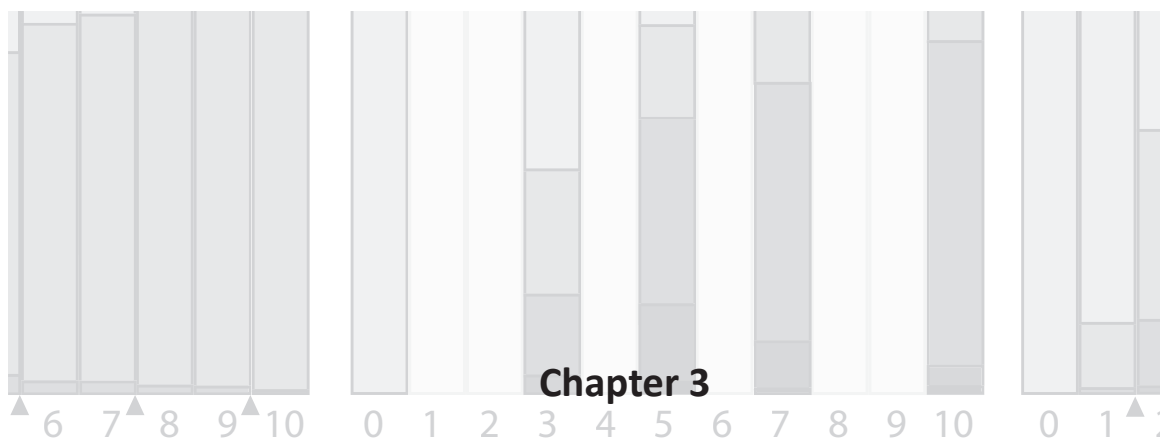
References

1. Lyon MF (1961) Gene action in the X-chromosome of the mouse (*Mus musculus* L.). *Nature* 190: 372-373.
2. Marahrens Y, Panning B, Dausman J, Strauss W, Jaenisch R (1997) *Xist*-deficient mice are defective in dosage compensation but not spermatogenesis. *Genes Dev* 11: 156-166.
3. Ogawa Y, Lee JT (2003) *Xite*, X-inactivation intergenic transcription elements that regulate the probability of choice. *Mol Cell* 11: 731-743.
4. Penny GD, Kay GF, Sheardown SA, Rastan S, Brockdorff N (1996) Requirement for *Xist* in X chromosome inactivation. *Nature* 379: 131-137.
5. Lee JT, Lu N (1999) Targeted mutagenesis of *Tsix* leads to nonrandom X inactivation. *Cell* 99: 47-57.
6. Brockdorff N, Ashworth A, Kay GF, McCabe VM, Norris DP, et al. (1992) The product of the mouse *Xist* gene is a 15 kb inactive X-specific transcript containing no conserved ORF and located in the nucleus. *Cell* 71: 515-526.
7. Brown CJ, Hendrich BD, Rupert JL, Lafreniere RG, Xing Y, et al. (1992) The human XIST gene: analysis of a 17 kb inactive X-specific RNA that contains conserved repeats and is highly localized within the nucleus. *Cell* 71: 527-542.
8. Rastan S (1983) Non-random X-chromosome inactivation in mouse X-autosome translocation embryos--location of the inactivation centre. *J Embryol Exp Morphol* 78: 1-22.
9. Clerc P, Avner P (1998) Role of the region 3' to *Xist* exon 6 in the counting process of X-chromosome inactivation. *Nat Genet* 19: 249-253.
10. Morey C, Navarro P, Debrand E, Avner P, Rougeulle C, et al. (2004) The region 3' to *Xist* mediates X chromosome counting and H3 Lys-4 dimethylation within the *Xist* gene. *Embo J* 23: 594-604.
11. Gribnau J, Luikenhuis S, Hochedlinger K, Monkhorst K, Jaenisch R (2005) X chromosome choice occurs independently of asynchronous replication timing. *J Cell Biol* 168: 365-373.
12. Luikenhuis S, Wutz A, Jaenisch R (2001) Antisense transcription through the *Xist* locus mediates *Tsix* function in embryonic stem cells. *Mol Cell Biol* 21: 8512-8520.
13. Lee JT (2005) Regulation of X-chromosome counting by *Tsix* and *Xite* sequences. *Science* 309: 768-771.
14. Lee JT (2002) Homozygous *Tsix* mutant mice reveal a sex-ratio distortion and revert to random X-inactivation. *Nat Genet* 32: 195-200.
15. Mlynarczyk-Evans S, Royce-Tolland M, Alexander MK, Andersen AA, Kalantry S, et al. (2006) X chromosomes alternate between two states prior to random

X-inactivation. PLoS Biol 4: e159.

16. Marahrens Y (1999) X-inactivation by chromosomal pairing events. *Genes Dev* 13: 2624-2632.
17. Bacher CP, Guggiari M, Brors B, Augui S, Clerc P, et al. (2006) Transient colocalization of X-inactivation centres accompanies the initiation of X inactivation. *Nat Cell Biol* 8: 293-299.
18. Xu N, Tsai CL, Lee JT (2006) Transient homologous chromosome pairing marks the onset of X inactivation. *Science* 311: 1149-1152.
19. Webb S, de Vries TJ, Kaufman MH (1992) The differential staining pattern of the X chromosome in the embryonic and extraembryonic tissues of postimplantation homozygous tetraploid mouse embryos. *Genet Res* 59: 205-214.
20. Till JE, McCulloch EA, Siminovitch L (1964) A Stochastic Model of Stem Cell Proliferation, Based on the Growth of Spleen Colony-Forming Cells. *Proc Natl Acad Sci U S A* 51: 29-36.
21. Cohn M, Langman RE (1990) The protection: the unit of humoral immunity selected by evolution. *Immunol Rev* 115: 11-147.
22. Shykind BM (2005) Regulation of odorant receptors: one allele at a time. *Hum Mol Genet* 14 Spec No 1: R33-39.
23. Wernet MF, Mazzoni EO, Celik A, Duncan DM, Duncan I, et al. (2006) Stochastic spineless expression creates the retinal mosaic for colour vision. *Nature* 440: 174-180.
24. Csankovszki G, Panning B, Bates B, Pehrson JR, Jaenisch R (1999) Conditional deletion of *Xist* disrupts histone macroH2A localization but not maintenance of X inactivation. *Nat Genet* 22: 323-324.
25. Sun BK, Deaton AM, Lee JT (2006) A transient heterochromatic state in *Xist* preempts X inactivation choice without RNA stabilization. *Mol Cell* 21: 617-628.
26. Brockdorff N, Ashworth A, Kay GF, Cooper P, Smith S, et al. (1991) Conservation of position and exclusive expression of mouse *Xist* from the inactive X chromosome. *Nature* 351: 329-331.
27. Takagi N (1993) Variable X chromosome inactivation patterns in near-tetraploid murine EC x somatic cell hybrid cells differentiated in vitro. *Genetica* 88: 107-117.
28. Matveeva NM, Pristiyazhnyuk IE, Temirova SA, Menzorov AG, Vasilkova A, et al. (2005) Unequal segregation of parental chromosomes in embryonic stem cell hybrids. *Mol Reprod Dev* 71: 305-314.
29. Burgoyne PS, Thornhill AR, Boudrean SK, Darling SM, Bishop CE, et al. (1995) The

- genetic basis of XX-XY differences present before gonadal sex differentiation in the mouse. *Philos Trans R Soc Lond B Biol Sci* 350: 253-260 discussion 260-251.
30. Vigneau S, Augui S, Navarro P, Avner P, Clerc P (2006) An essential role for the DXPas34 tandem repeat and *Tsix* transcription in the counting process of X chromosome inactivation. *Proc Natl Acad Sci U S A* 103: 7390-7395.
 31. Lee JT, Strauss WM, Dausman JA, Jaenisch R (1996) A 450 kb transgene displays properties of the mammalian X-inactivation center. *Cell* 86: 83-94.
 32. Augui S, Filion GJ, Huart S, Nora E, Guggiari M, et al. (2007) Sensing X chromosome pairs before X inactivation via a novel X-pairing region of the Xic. *Science* 318: 1632-1636.
 33. Lee JT, Davidow LS, Warshawsky D (1999) *Tsix*, a gene antisense to *Xist* at the X-inactivation centre. *Nat Genet* 21: 400-404.
 34. Wutz A, Jaenisch R (2000) A shift from reversible to irreversible X inactivation is triggered during ES cell differentiation. *Mol Cell* 5: 695-705.
 35. Nesterova TB, Johnston CM, Appanah R, Newall AE, Godwin J, et al. (2003) Skewing X chromosome choice by modulating sense transcription across the *Xist* locus. *Genes Dev* 17: 2177-2190.
 36. Herzing LB, Romer JT, Horn JM, Ashworth A (1997) *Xist* has properties of the X-chromosome inactivation centre. *Nature* 386: 272-275.
 37. Lyon MF, Searle AG, Ford CE, Ohno S (1964) A Mouse Translocation Suppressing Sex-Linked Variegation. *Cytogenetics* 15: 306-323.
 38. Rastan S, Robertson EJ (1985) X-chromosome deletions in embryo-derived (EK) cell lines associated with lack of X-chromosome inactivation. *J Embryol Exp Morphol* 90: 379-388.
 39. Geijsen N, Horoschak M, Kim K, Gribnau J, Eggan K, et al. (2004) Derivation of embryonic germ cells and male gametes from embryonic stem cells. *Nature* 427: 148-154.



The probability to initiate X chromosome inactivation is determined by the X to autosomal ratio and X chromosome specific allelic properties

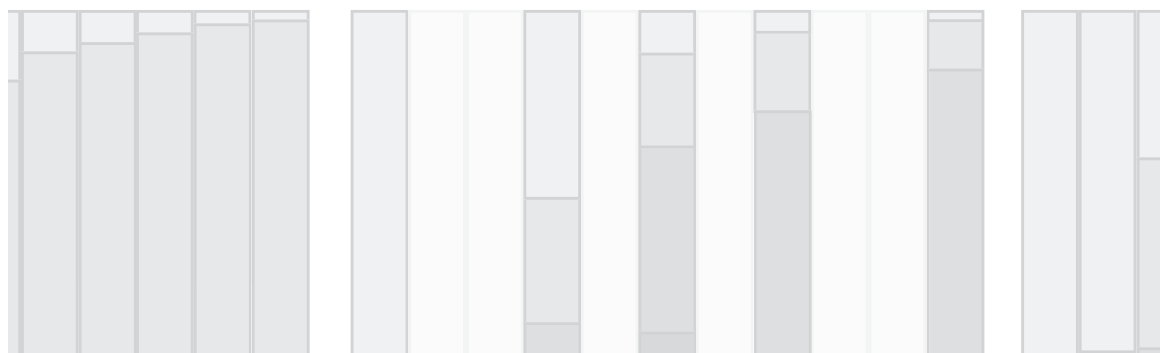
sim.

XXXXX/4n exp.



sim.

XXXXX/4n exp.
 Accepted by PLoS ONE



Abstract

Background:

In female mammalian cells, random X chromosome inactivation (XCI) equalizes the dosage of X-encoded gene products to that in male cells. XCI is a stochastic process, in which each X chromosome has an independent probability to be inactivated. To obtain more insight in the factors setting up this probability, we studied the role of the X to autosome (X:A) ratio in initiation of XCI, and have used the experimental data in a computer simulation model to study the cellular population dynamics of XCI.

Methodology/Principal Findings:

To obtain more insight in the role of the X:A ratio in initiation of XCI, we generated triploid mouse ES cells by fusion of haploid round spermatids with diploid female and male ES cells. These fusion experiments resulted in only XXY triploid ES cells. XYY and XXX ES lines were absent, suggesting cell death related either to insufficient X-chromosomal gene dosage (XYY) or to inheritance of an epigenetically modified X chromosome (XXX). Analysis of active (Xa) and inactive (Xi) X chromosomes in the obtained triploid XXY lines indicated that the initiation frequency of XCI is low, resulting in a mixed population of XaXiY and XaXaY cells, in which the XaXiY cells have a small proliferative advantage. This result, and findings on XCI in diploid and tetraploid ES cell lines with different X:A ratios, provides evidence that the X:A ratio determines the probability for a given X chromosome to be inactivated. Furthermore, we found that the kinetics of the XCI process can be simulated using a given probability, proportional to the X:A ratio, for an X chromosome to be inactivated. These simulation studies re-emphasize our hypothesis that the probability is effectuated by the concentration of an X-encoded activator of XCI, and X chromosome specific allelic properties determining the threshold for this activator.

Conclusions:

The present findings reveal that the probability for an X chromosome to be inactivated is proportional to the X:A ratio. This finding supports the presence of an X-encoded activator of the XCI process.

Introduction

In placental mammals, dosage compensation of X-encoded gene products is achieved by inactivation of either of the two X chromosomes in female cells [1]. Random X chromosome inactivation (XCI) is initiated early during female embryonic development, and results in a transcriptionally inactive X chromosome (Xi). The inactive state of the Xi is clonally propagated through many cell divisions. At the onset of XCI the X-linked non-coding *Xist* gene is transcriptionally up-regulated on the future Xi, and *Xist* RNA coats the Xi in *cis* [2,3,4,5]. *Xist* RNA is required for XCI and most

likely attracts chromatin modifying enzymes involved in the silencing process [6,7]. The *Tsix* and *Xite* genes play a crucial role in the early stages of XCI by suppression of *Xist* transcription and *Xist* RNA accumulation. Both *Tsix* and *Xite* also are non-coding genes that overlap with *Xist*, but are transcribed in anti-sense direction [8,9].

The first phase of XCI comprises a counting process, followed by initiation of XCI when more than one X chromosome is present per diploid nucleus. We have recently shown that initiation of XCI is directed by a stochastic mechanism, in which all X chromosomes in a nucleus have an independent probability to initiate XCI within a certain time-span [10]. We proposed that this probability is proportional to the X to autosome ratio (X:A), and most likely depends on at least two factors that act through *Xist* and *Tsix*: an X-encoded XCI-activator that stimulates *Xist* expression, and itself is transcriptionally inactivated by the XCI process, and an autosomally encoded XCI-inhibitor that suppresses *Xist* by activating *Tsix*. Although the action of *Tsix* is still not understood, *Tsix* transcription and chromatin modifications in the *Xist* promoter (possibly mediated by *Tsix*) provide a threshold that has to be overcome by the XCI-activator, allowing accumulation of sufficient *Xist* molecules to silence *Tsix* and spread in *cis*. Early in mouse development or upon differentiation of embryonic stem (ES) cells, the XCI-activator concentration in a cell will increase, and in female cells this will drive the initiation of XCI with a specific probability. This probability is the consequence of stochastic transcriptional activation of both *Xist* and *Tsix*. In male cells, the XCI-activator concentration will be too low; therefore, these cells induce XCI only sporadically [10].

Several findings support the presence of an X-linked XCI-activator. Tetraploid XXXX ES cells initiate XCI significantly faster than XXXY cells [10]. In addition, female ES cells with a heterozygous deletion including *Xist*, *Tsix* and *Xite*, still show initiation of XCI on the wild type X chromosome, indicating a novel *trans* acting activator, encoded by a gene located outside the deleted area [10]. Also, studies in differentiating ES cell lines with stably integrated *Xist* promoter transgenes show significantly more expression of a linked reporter in female cells compared to male cells [11]. The genomic location of the XCI-activator is unknown so far. However, previous studies which analyzed XCI in male cell lines with YAC transgenes ranging in size from 320 to 460 kb, encompassing *Xist* and flanking regions, revealed initiation of XCI on the single X chromosome [12,13]. In addition, a smaller BAC sequence covering a region upstream of *Xist* also induces ectopic XCI in transgenic male and female cells [14]. These studies indicate that the sequence encoding the XCI-activator is likely to be located within the sequence covered by these transgenes.

In diploid and tetraploid cells, one X chromosome will remain active per diploid genome. However, in triploid cells this ratio of one active X chromosome per

diploid autosomal set cannot be achieved. Therefore, triploid cells provide a unique situation for studying the mechanism of XCI counting and choice and gene dosage related cell selection. Several studies have been conducted with human and mouse XXY and XXX triploid embryos and embryo-derived cell lines, to try to determine the pattern of X inactivation. In these experiments cultured differentiated cells were examined which had completed the XCI process [15], and indicated that the majority of cell lines derived from human live born XXX triploids predominantly show two active X chromosomes [16,17,18]. In contrast, analysis of 10-day-old XXY and XXX mouse triploid embryos showed that most cells had one active X chromosome [19]. Unfortunately, both studies did not discriminate between primary choice in XCI and cell selection processes.

To explore the mechanism determining the probability of an X chromosome to be inactivated, we have generated XXY triploid mouse ES cells. Analysis of XCI in these cells allowed us to determine the influence of the X:A ratio on the initiation of XCI, and to discriminate between XCI initiation and cell selection. In addition, we have used stochastic and mathematical simulation studies to follow the kinetics of XCI in a population of developing or differentiating cells.

Results

Generation of triploid ES cells

Our previous studies with tetraploid XXXX, XXXY and XXYY mouse ES cell lines have indicated that the probability for an X chromosome to be inactivated is directly related to the X:A ratio [10]. To further explore this finding we aimed to generate triploid ES cell lines with XYY and XXY karyotypes, having an X:A ratio of 1:3 and 2:3, respectively, for which XCI has not been studied before. To generate triploid ES cell lines we decided to fuse puromycin resistant female and male ES cells with round spermatids or spermatozoa containing a *neomycin resistance (neo)* gene targeted to either the autosomal *Ube2b* gene or the X-chromosomal *Ube2a* gene. Both *Ube2a* and *Ube2b* encode ubiquitin-conjugating enzymes involved in DNA replicative damage bypass [20]. The encoded proteins have at least partially overlapping functions, and two functional alleles of either *Ube2a* or *Ube2b* per cell are sufficient to generate viable diploid mice. Also, spermatogenesis is not dysregulated in *Ube2a* knockout and *Ube2b* heterozygous mutant mice [21,22]. Therefore, it was expected that loss-of-function of one targeted *Ube2a* or *Ube2b* allele, in the *Ube2b*^{+/-} and *Ube2a*^{+/-} mice, respectively, will not have an effect on the viability of hybrid fusion products. In the present study, the targeted mutant alleles serve the function of selection for fused cells.

All PEG mediated fusion experiments were conducted twice. Fusion of the

iodide to determine the DNA content, indicated that all our cell lines were triploid (Figure 1C). The small 2n population we attribute to contamination of the triploid cells with diploid male feeders that we used to grow the ES cells on. Karyotyping also indicated that, in all cell lines, the majority of cells had 60 chromosomes, which are stably maintained through many passages (Figure 1D, and data not shown). Interestingly, X and Y chromosome paint analysis showed that all cell lines had an XXY 3n karyotype (N=18) although the haploid round spermatids that were used for fusion can be expected to contain either an X chromosome or a Y chromosome in a 50/50 ratio (Figure 1E and 1F).

These results suggest that XYY cells are absent due to an insufficient dosage of X-encoded genes. In addition, the lack of XXX 3n karyotypes suggests that introduction of an X chromosome through a round spermatid leads to a non-viable triploid ES cell. The absence of triploid XXX ES cell lines can not be explained by a dosage problem, but might be due to the presence of an epigenetically modified X chromosome present in spermatids. During spermatogenesis, the largely unpaired X and Y chromosomes are transcriptionally inactivated, forming the XY body or sex body in a process called meiotic sex chromosome inactivation (MSCI) [23]. Chromatin modifications present on the XY body may be partly maintained in post-meiotic round spermatids. Such modifications, particularly relevant for the X chromosome with a large gene content, may explain lethality of the triploid XXX ES cells.

To test whether the spermatid derived X was reactivated after cell fusion, we fused round spermatids of males containing an X-linked *GFP* transgene [24] with male and female ES cells. Analysis of diploid ES cells containing the X-linked *GFP* transgene shows robust GFP expression, indicating that the transgene is properly expressed in ES cells. In contrast, after fusion of *GFP* round spermatids with ES cells, we did not see reactivation of the transgene (data not shown). Selection for reactivation of the transgene by applying puromycin selection, at days 0, 3 and 5 after fusion, did not result in clones resistant to both selection reagents. Therefore, we conclude that ES cells are incapable of reactivating the X from spermatids. This is in contrast to ES fusions with female somatic cells, which lead to reactivation of the Xi [25].

X chromosome inactivation in triploid XXY ES cells

To study XCI in the obtained XXY triploid ES cells, we differentiated 9 of these cell lines into embryoid bodies (EB). Cells were fixed and subjected to RNA-FISH after 3, 5, 7, and 10 days of differentiation, using an *Xist* specific probe to stain the *Xist* coated Xi's. After a three-day differentiation period, we mainly found cells with zero or one Xi, indicating that the triploid XXY cells are capable to initiate XCI (Figure 2A). At this timepoint only ~2.5% of cells had one Xi (XaXiY) and we sporadically (<0.1%) found

cells with two Xi's (XiXiY). During the differentiation process, the relative number of cells with one Xi increased, to ~40% at day 10 of differentiation (Figure 2B).

To exclude the possibility that our triploid XXY ES cells lost or gained X chromosomes over the differentiation process, we performed DNA-FISH with an X chromosome specific BAC probe on cells differentiated for seven days. To obtain a reliable measurement, at least 100 nuclei were scored for every cell line. We found that over 93% of the XXY cells still contained two X chromosomes, and only 3% of the cells were found to have three X chromosomes, suggesting that the karyotype of these triploid XXY ES cells is stable throughout differentiation (Figure 2C).

We further examined whether the increase in time of the percentage of XiXaY cells (Figure 2B) might be caused by cell selection. We therefore added BrdU 24 hours prior to cell fixation of day 7 differentiated ES cells, and performed immuno/RNA FISH, detecting BrdU positive cells and *Xist* RNA. Comparison of BrdU positive

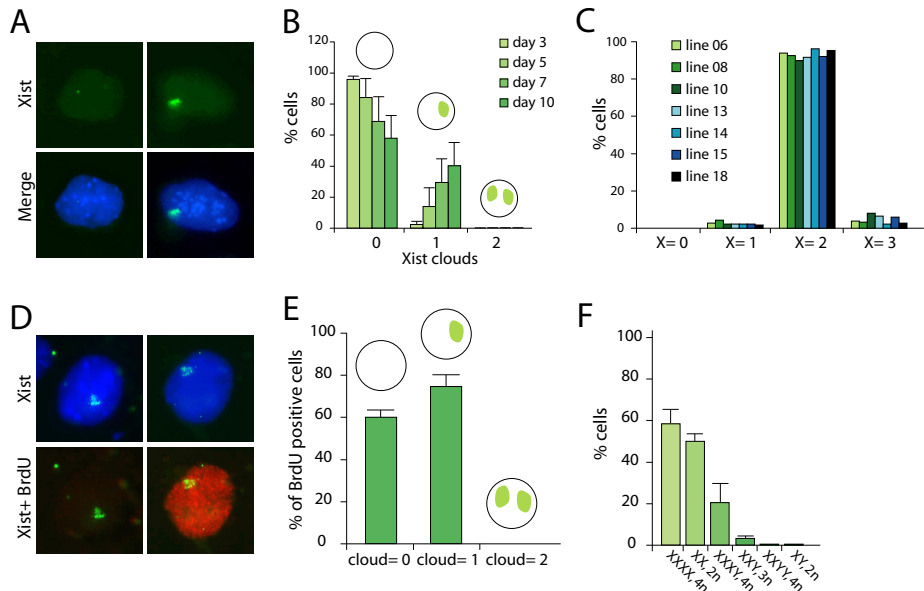


Figure 2. Analysis of XCI in differentiating triploid XXY ES cells

A) RNA FISH analysis with an *Xist* probe (FITC, DNA in blue) on day 3 differentiated triploid ES cells, shows cells with no (left panels), one (right panels) *Xist* cloud.

B) The distribution of cells with different numbers of *Xist* clouds throughout differentiation.

C) DNA FISH analysis on day 7 differentiated triploid ES cells. Shown is the relative number of cells with 0, 1, 2 and 3 X chromosomes.

D) Combined *Xist* RNA-BrdU detection (*Xist* in FITC, BrdU in Rhodamine red, DNA in DAPI blue), indicating the presence of cells with negative and positive BrdU staining (from left to right).

E) Quantification of the *Xist* RNA-BrdU detection, shown are the relative number of BrdU positive cells with 0, 1 and 2 *Xist* clouds.

F) The relative number of cells that have initiated XCI (at least one Xi), per cell line at day 3 of differentiation.

cells with one or no *Xist* cloud(s) shows that there are significantly more cells with one cloud, indicating that XiXaY cells indeed have a small proliferative advantage ($p < 0.001$; Figure 2D and 2E).

Previously, we have proposed that the probability for an X chromosome to be inactivated is proportional to the X:A ratio [10]. To further explore this finding we compared the percentage of cells that had initiated XCI at day 3 of differentiation, for our XXY triploid ES cell lines (with an X:A ratio of 0.67) and cells with different X:A ratios (4n XXXX cells with X:A=1; 4n XXXY cells with X:A=0.75; 4n XXYY cells with X:A=0.5; 2n XX cells with X:A=1; and 2n XY cells with X:A=0.5). ES cell lines were differentiated through EB differentiation and subjected to RNA FISH to detect *Xist* RNA. For each line with a different X:A ratio or a different ploidy number, we performed three independent differentiation experiments.

The results (Figure 2F) confirm our previous findings [10] that, at day 3 of differentiation, XXXX cells have initiated XCI in significantly more cells (58%) than XXXY cells (20%). Furthermore, tetraploid XXYY and diploid XY cells initiated XCI in less than 0.3% of the cells, whereas diploid XX ES cells initiated XCI in 50% of the cells (Figure 2F). At day 3, triploid XXY cells had initiated XCI in 3-4% of the cells (Figure 2F). This percentage falls between that found for XXXY and XXYY cells. From these results we conclude that the probability to initiate XCI depends on the X:A ratio, and that this relationship appears not to be linear (Figure 2F).

Parameters required for computer simulated XCI

To better understand the kinetics of XCI in a developing female embryo or a differentiating population of female ES cells we decided to simulate the XCI process. There are four important parameters required to simulate XCI, based on a stochastic model for XCI: 1) the probability for an X to initiate XCI, 2) the time window required for one choice round, 3) the rate of cell division, and 4) cell selection.

As indicated by our findings, the probability for an X to initiate XCI is proportional to the X:A ratio, and XCI is most likely triggered by a threshold nuclear concentration of an X-encoded XCI-activator. Although the nuclear concentration of XCI-activator will be the same for both X chromosomes present in a female cell, specific allelic properties of the individual X chromosomes can result in different probabilities. Previous studies with female ES cell lines harboring deletions of either *Xist*, *Tsix* or *Xite* have indicated that this probability positively correlates with *Xist* transcription rate and negatively with transcription rate of *Tsix* and *Xite* [6,7,8,9,26]. Therefore, transcription initiated by the *Tsix* and *Xite* promoters provides a threshold for *Xist* to accumulate in *cis*. Also, *Xist* promoter related modifications could restrict the action of the XCI-activator and may therefore be involved in setting up the threshold. Only

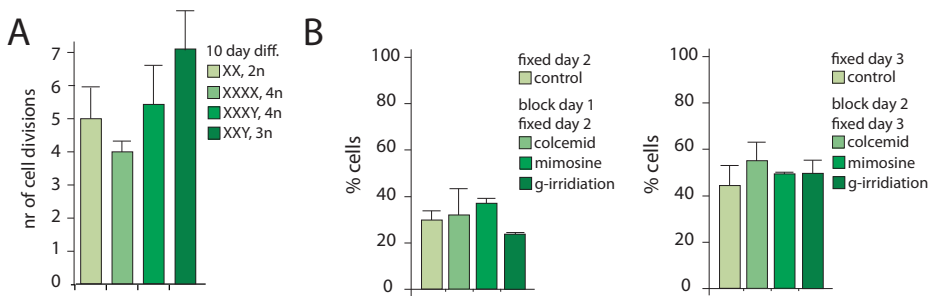


Figure 3. Initiation of XCI independent of cell division

A) Determination of the number of cell divisions during a 10 day EB differentiation period. Shown are the average and standard deviation of two separate experiments with two different ES lines per X:A ratio or ploidy number.

B) Analysis of initiation of XCI after a cell cycle block. Diploid female ES cells were EB differentiated for one day (left graph) or two days (right graph), and treated with colcemid or mimosine, or cells were lethally γ -irradiated, and allowed to differentiate for one more day before fixation. Control samples were allowed to differentiate for two or three days. The percentage of cells that initiated XCI was determined by *Xist* RNA FISH, followed by the quantification of the number of cells with *Xist* clouds.

when sufficient XCI-activator is present in the nucleus enough *Xist* transcription is initiated to overcome *Tsix* mediated repression, thereby effectuating a probability to initiate XCI. *Xist* transcription initiation is a stochastic process itself, and depending on the nuclear XCI-activator concentration, bursts of *Xist* transcription will generate a continuum of small probabilities to initiate XCI in time. This probability will drop after inactivation of an X chromosome with the decline in the XCI-activator concentration that depends on the nuclear half life of the XCI-activator. In our simulations we have used a time window with a specified probability, which represents the integrated probability within that time window.

To test whether XCI is dependent on cell division, we first analyzed the number of cell divisions during a 10 day period of embryoid body (EB) differentiation, for ES cells with different X:A ratios. To determine the increase in cell number we differentiated 10^5 cells, and isolated DNA before and after differentiation. OD measurements of two independent differentiation experiments indicated that the different ES lines divided between 4 and 7 times in the 10 day differentiation period (Figure 3A). Next, female diploid ES cells were EB differentiated for one or two days, and then subjected to γ -irradiation-, mimosine- or colcemid-mediated cell cycle arrests for one day. Initiation of XCI in treated and untreated cells was compared by counting the number of cells with or without an Xi, using RNA FISH with an *Xist* probe. We found no significant increase or decrease in the number of cells with an Xi after cell cycle arrest, although the cells that had been γ -irradiated at day 1 showed a slight decrease in cells that initiated XCI (Figure 3B). This result suggests that cell division is not required, or perhaps plays a minor role in the initiation of XCI. Nevertheless, cell

division characteristics are important in the XCI process, because previous studies have shown that cells that inactivate too many X chromosomes stop dividing or slow down the cell division rate, which allows the cycling population of cells to outgrow the cells that inactivated too many X chromosomes [10,27].

Cell selection also plays an important role in the XCI process, as male cells that inactivate their single X chromosome will die. Studies with inducible *Xist* cDNA transgenes integrated on the single X chromosome in male cells showed that *Xist* mediated silencing manifests within 24 hours, and that cell death becomes imminent within three days of *Xist* induction [27]. Also, diploid female cells inactivating two X chromosomes or incapable of initiating XCI are prone to die [6,28].

Computer simulated XCI

To comprehend the kinetics of XCI, we have applied a stochastic simulation model to determine the populations of cells with a different number of X_a 's and X_i 's. In this approach, the distribution of different cell populations is derived using a simulation program with an implemented randomizer to assign the X_i 's, based on a stochastic principle, thereby mimicking the choice process. With a small starting population of cells, as present in the female mouse embryo around the time XCI is induced, a stochastic principle may result in different outcomes of the choice process, which is different from mathematically calculated cell populations. However, an increased starting population of cells, or several repetitive experiments in a stochastic simulation model will result in an outcome similar to a mathematical approach. The stochastic simulation of the XCI process was performed in a three-dimensional matrix, in which each Z stack represents one choice round (Figure 4A). For our simulations we used a fixed or changing probability per choice round per X chromosome, and specific cell cycle characteristics depending on the X:A ratio.

We started by simulating the XCI process in XX diploid female ES cells through a 10 day differentiation period, using a fixed probability in time to run the simulations, and compared the resulting distributions with experimental data obtained with differentiating XX female ES cells. We used a cell division rate for cells with an X:A ratio ≥ 0.5 of once every two days, based on our cell division analysis (described above). In addition, the simulation included that cells with all X chromosomes inactivated stop dividing, which is based on previous studies [29]. To be able to compare the simulations with available experimental data, we have set the time window to 1 day, representing the integrated probability for cells choosing the X to be inactivated over 1 day. In the calculations we have excluded the option that, in X_aX_i cells that just have inactivated an X chromosome, the active second X chromosome may still have a probability to be inactivated. We performed the simulations with 100 cells, which

mimics the number of cells present in the female mouse embryo around the time XCI is initiated. A number of 5 independent stochastic simulations generated the data for statistical analysis of the average and standard deviation. The graphs in the figures only show the average value for each time point. Comparison of the simulations, using an increasing range of fixed probabilities from 5% to 40% for both X-chromosomes, with previously obtained experimental results for differentiated XX female ES cells indicate that a fixed probability between 10% and 20% fits our experimental data best (Figure 4A; Supplementary Table 1A and 1B) [10]. To validate the simulation results we also compared these with data obtained using a mathematical approach where fixed probabilities were used to calculate the different XaXa, XaXi and XiXi populations, which showed similar population dynamics (Supplementary Data and Supplementary Figure 1). The fluctuation in the percentage of XiXi cells in time is the consequence of applying two choice rounds (1 per day) within one round of one cell division (once every two days for XaXa and XaXi cells). Because cell division is synchronized in the simulations, XiXi cells are diluted out after every cell division.

From previous experimental data it appears that the probability to initiate XCI is lower in the beginning than later during the XCI process, and we proposed that the probability is dependent on the concentration of XCI-activator in the nucleus [10]. The XCI-activator is produced at a rate ($v_{a.synthesis}$) that is proportional to the number of active X chromosomes. The half-life of XCI-activator is considered constant, and this leads to the following differential equation for the concentration of the XCI-activator:

$$[1] \quad \frac{d[\text{XCI} - \text{activator}]}{dt} = v_{a.synthesis}(t) - k_d \cdot [\text{XCI} - \text{activator}]$$

The concentration of the XCI-activator will change in time according to the above differential equation with:

$$[2] \quad v_{a.synthesis}(t) = k_s \cdot [m_{active}(t)]$$

Here, k_s is the rate constant for synthesis (in μMolar per second per active promoter), and m_{active} is the number of active X chromosomes per haploid genome, which can be substituted by the X:A ratio. Before XCI, at the start of the simulation, all X chromosomes are active, and the above equation integrates as:

$$[3] \quad [\text{XCI} - \text{activator}](m,t) = \frac{m \cdot k_s}{k_d} \cdot (1 - e^{-k_d \cdot t}) = \frac{m \cdot k_s}{k_d} \cdot (1 - (1/2)^{t/t_{1/2}})$$

where:

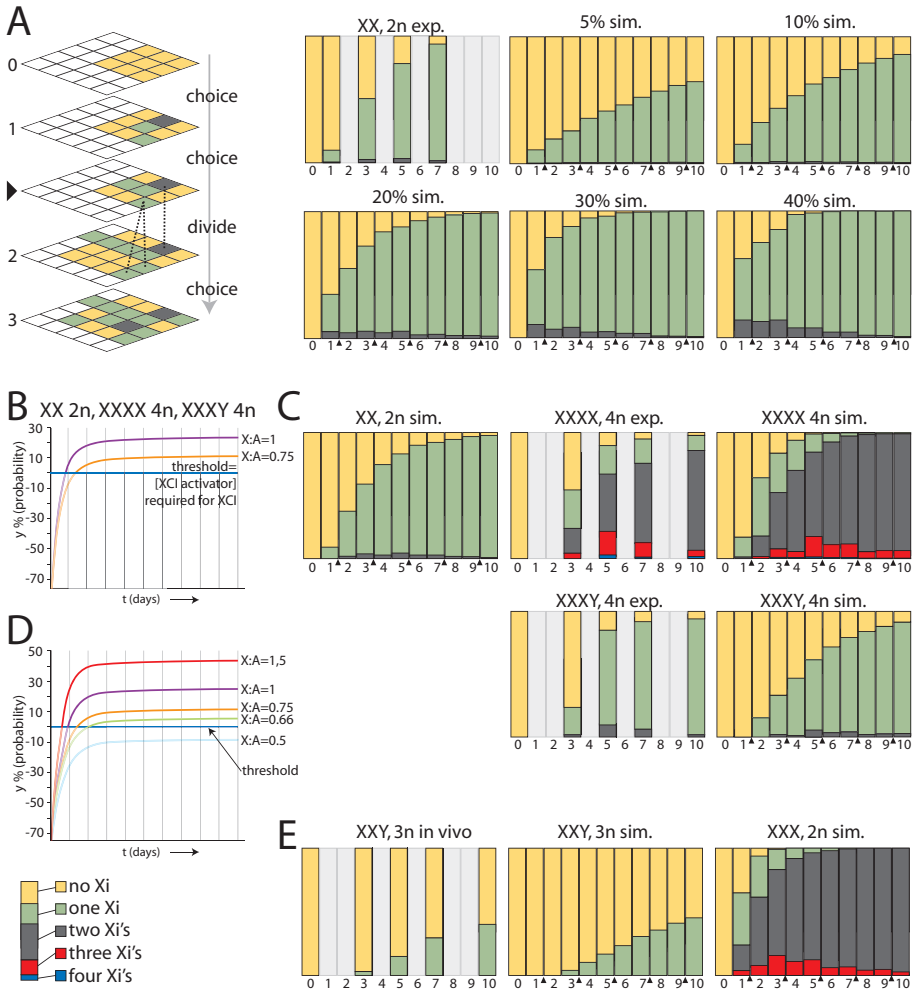


Figure 4. Computer simulation of XCI

(A) Left upper panel shows a schematic representation of the stochastic simulation which is executed in a three dimensional matrix. Cells (boxes) go through consecutive choice rounds (numbers) interrupted by cell divisions (triangle). The three different cell types are represented by $XaXa$ = yellow, $XiXa$ = green, $XiXi$ = gray boxes. The dashed lines indicate the origin of progeny of one $XiXa$ and one $XiXi$ cell after cell division (not all lines are shown, and note that the $XiXi$ cells do not divide). The right panels show the experimental data from differentiated 2n female XX ES cells (exp.), and the stochastic simulation of XCI with a 5%, 10%, 20%, 30%, and 40% fixed probability per X chromosome (sim.). The different bar-graphs show the relative distribution of the three different cell types ($XaXa$ = yellow, $XiXa$ = green, $XiXi$ = gray). Numbers below the bar graphs indicate days of differentiation (1-10), and cell division is indicated with a triangle. For time points represented by light gray bars no data is available.

(B) Probability curves representing the increase of the probability y in time based on equation [6], with $m=1$, for XX 2n and XXXX 4n cells (purple), and $m=0.75$ for XXXY 4n cells (orange). The probability at a given time point is the integrated probability over a time frame of one day. A negative value for y results in a probability of 0, and is represented by a faint line.

(C) Upper left panel shows simulation of XCI in XX diploid cells based on probabilities determined using

$$[4] \quad t_{1/2} = \frac{k_d}{\ln(2)} = 1.44 \cdot k_d$$

We expect that the probability for initiation of XCI is proportional to the nuclear concentration of y . Here, y represents molecules or chromosome modifications that effectuate *Xist* promoter activation. The function of y most likely involves enzymatic activity that depends on the concentration of XCI-activator through a Michaelis-Menten relationship, with V_{ys} and K_{Ma} as maximum rate and Michaelis constant, respectively. Degradation or removal of y will be mediated by another enzymatic process, which depends on the concentration of y through a Michaelis-Menten relationship, with V_{yd} and K_{My} as maximum rate and Michaelis constants, respectively. We anticipate that K_{My} is very small, so that the loss of y will occur at a constant rate. Also, we expect that the degradation of y represents a first order process, with a rate constant k_{dy} :

$$[5] \quad \frac{dy}{dt} = \frac{[\text{XCI} - \text{activator}](t) \cdot V_{ys}}{K_{Ma} + [\text{XCI} - \text{activator}](t)} - \frac{y \cdot V_{yd}}{K_{My} + y} - k_{dy} \cdot y$$

These molecular processes will reach a quasi steady state. By equation of dy/dt to zero, and assuming that K_{My} is much smaller than any relevant concentration of y , the concentration of y is given by:

$$[6] \quad y = \left(\frac{[\text{XCI} - \text{activator}](t)}{K_{Ma} + [\text{XCI} - \text{activator}](t)} \cdot \frac{V_{ys}}{k_{dy}} - \frac{V_{yd}}{k_{dy}} \right)$$

or y will be zero if this yields a negative number. At the threshold level, y will be zero, resulting in:

different probabilities in time indicated in the curve, shown in (B). Upper middle panel shows the experimental percentages of 4n XXXX cells with a different number of Xi's throughout EB differentiation. The upper right panel shows the simulation of XCI using the same parameters as used for the XX diploid simulation (XaXaXaXa = yellow, XaXaXaXi = green, XaXaXiXi = grey, XaXiXiXi = red, XiXiXiXi, blue). Bottom left panel shows the experimentally determined percentages of 4n XXXY cells with a different number of Xi's throughout EB differentiation. Bottom right panel shows the XCI simulation of 4n XXXY cells using the different probabilities in time indicated in the curve presented in (B) (XaXaXaY = yellow, XaXaXiY = green, XaXiXiY = grey, XiXiXiY = red).

(D) Curves representing the probability y in time using equation [6] for cells with a different X:A ratio, ranging from 0,5 to 1,5.

(F) Left panel shows the experimentally determined percentages of 3n XXY cells with a different number of Xi's throughout EB differentiation. Middle panel shows the XCI simulation of 3n XXY cells using different probabilities indicated in the curve presented in (D) (XaXaY = yellow, XaXiY = green, XiXiY = grey). Right panel shows the simulation of XCI in XXX 2n cells (XaXaXa = yellow, XaXaXi = green, XiXiXi = grey, XiXiXi, red).

$$[7] \quad [\text{XCI} - \text{activator}](t) = K_{Ma} \cdot \frac{V_{yd}}{V_{ys} - V_{yd}}$$

Above the threshold level its value will increase with an increase in [XCI-activator] towards a maximum. We assume the probability of initiation of XCI to be proportional to y . By plotting y in time we generated a probability curve, which in the simulations represents the integrated probability over a time frame of 1 day. The values for y at different days from 0-10 were imported in the simulation program to assign the different Xi's with a specific probability per choice round. After XCI has started on one or more X chromosomes, the concentration of the XCI-activator will drop, according to the half-life of the XCI-activator protein (Supplementary Data). For cells that started XCI in one choice round the probability will drop according to the m value reached after that choice round.

We started with training our stochastic simulation, to establish the final values for variables to be applied throughout the stochastic simulations reported here. In this training, the outcome of the simulation, using graded preset values for variables, was compared with experimental data sets that were obtained by differentiation of diploid XX ($m=1$) and tetraploid XXXX ($m=1$) and XXXY ($m=0.75$) cells (Monkhorst et al., 2009). This approach allowed us to obtain the final values for the variables, and we also could determine the K_{Ma} value, which represents the XCI-activator concentration at which half the binding sites are filled, and is a measure for saturation of the XCI-activator. We obtained the best results with a K_{Ma} of 3.3 μM , equal to the maximum XCI-activator concentration in diploid XX and tetraploid XXXX cells, and values for ks , kd , kdy , V_{ys} and V_{yd} of 2 μM , 0.6 μM , 1.5 μM , 3 μM and 1.15 μM respectively. Probability curves for $m=1$ (2n XX and 4n XXXX) and $m=0.75$ (4n XXXY) were derived (Supplementary Table 2A, B and C, and Figure 4B), which resulted in simulated populations with different Xa's and Xi's in time that matched our experimental data with diploid XX and tetraploid XXXX, XXXY cells (Figure 4C, and Supplementary Table 3A and B). In a different approach, we used the same probabilities in time for diploid female XX cells in a mathematical model, and obtained distributions of different cell populations that supported our findings with the stochastic simulations (Supplementary Data, and Supplementary Figure 1).

To validate the findings, we introduced two different m values of 0.67 found in XXY triploid cells, and 0.5 found in diploid XY and tetraploid XXYY cells, keeping all other variables constant. The probability curves obtained with these m values resulted in a negative probability (is equal to 0) for diploid XY and tetraploid XXYY cells, as expected (Figure 4D). For XXY cells with a $m=0.67$ we obtained a positive value for y , predicting initiation of XCI, albeit at an even lower level than found in

XXXY tetraploid cells (Figure 4D). Using the probabilities derived with $m=0.67$ we obtained simulated distributions that match well with our experimental data (Figure 4E, and Supplementary Table 4). Raising m to 1.5, as found in females with an 47,XXX aneuploid karyotype, increases the probability to a maximum of 44% (Supplementary Table 2C and Figure 4D). Simulations using this probability curve result in a majority of cells that inactivate two X chromosomes (Figure 4E, and Supplementary Table 4), as reported for 47,XXX human individuals. Interestingly, simulation of XXX diploid (aneuploid) cells only resulted in a 29% cell loss. This percentage is well below the 50% cell loss obtained for human individuals and viable mice with X:autosome translocations [30,31], and does explain why mice and humans with one or more additional X chromosomes are viable. Taken together, the results show that the XCI process can be simulated using a probability curve representing the effective XCI-activator concentration in combination with a threshold level required to initiate XCI.

Allele specific activation levels for the XCI-activator

A stochastic model implies that different X chromosomes within one nucleus can have different probabilities to be inactivated, because X chromosome specific thresholds are determined independently. In inbred mice, the X chromosomes are genetically identical and XCI will therefore result in two evenly distributed populations of XiXa cells with one of the parental X chromosomes inactivated. However, in several F1 hybrid mice XCI has been reported to be skewed towards one of the parental alleles. For mouse, skewing of XCI has been attributed to differences in the X controlling element (Xce), a region overlapping and extending 3' of *Xist* [32,33]. In cells where two X chromosomes are present with different Xce alleles, a strong Xce is associated with a lower probability to initiate XCI compared to the X chromosome harboring the weaker Xce. These reported differences in probabilities could be explained as allele specific thresholds for the XCI-activator. A more sensitive allele (weak Xce) for the XCI-activator will result in a higher probability for XCI at a certain XCI-activator concentration than a less sensitive allele (strong Xce). As a consequence, one XCI-activator concentration can result in different probabilities for different alleles in the same nucleus. *Mus musculus castaneus* (Cast/Ei) mice harbor a strong Xce in contrast to *Mus musculus* 129/SV (129/Sv) mice, which harbor a weak Xce, and in somatic tissues of Cast/Ei-129/Sv F1 female mice and differentiated F1 female ES cells, the 129/Sv X chromosome is inactivated in ~70% of the cells (Figure 5H). Allele specific sequence differences in *Xist*, *Tsix*, and *Xite* will lead to different values for V_{ys} and/or V_{yd} .

As indicated above, y represents molecules or chromatin modifications (as targets

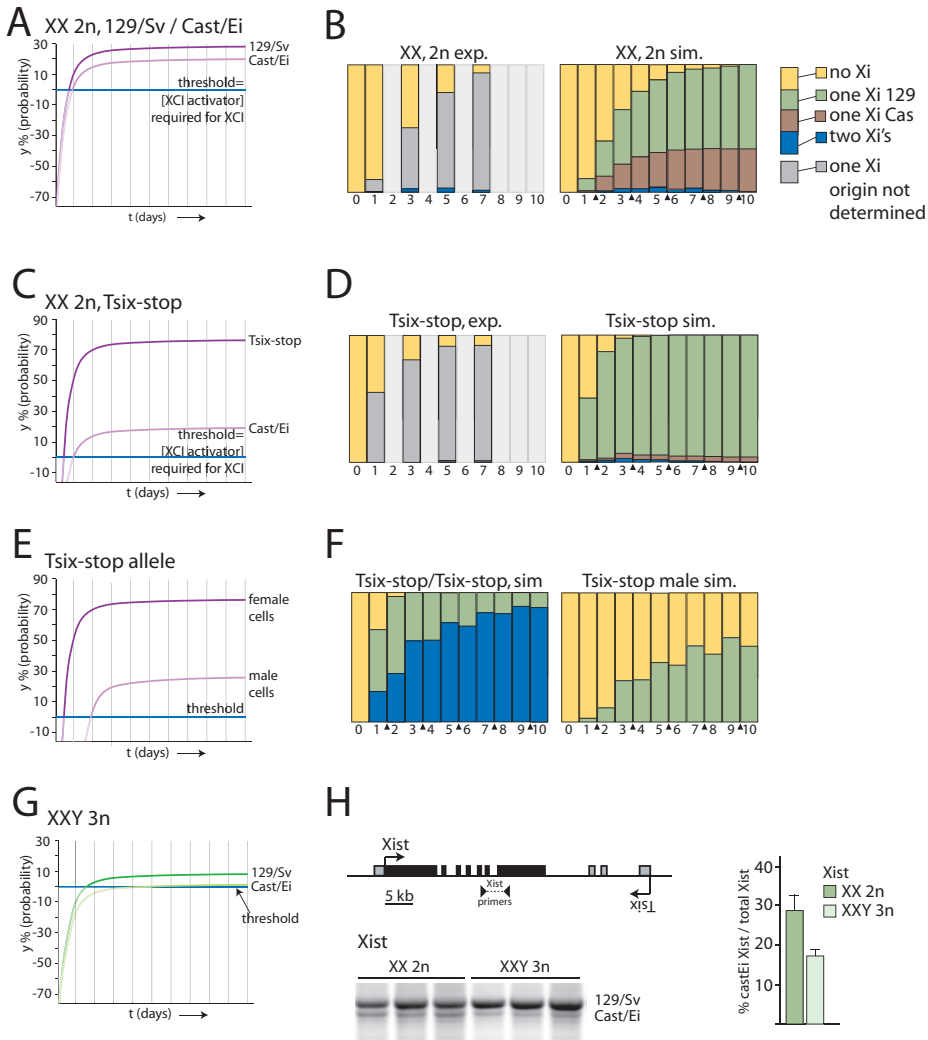


Figure 5. Implementing allele specific thresholds

A, B) XCI skewing can be simulated by attributing different probabilities to the two X chromosomes in female XX cells. To simulate the 30%:70% skewing of XCI observed in Cast/Ei – 129/Sv F1 mice and differentiating F1 ES cells different allele specific probabilities were applied. The experimentally obtained XCI data with differentiating XX Cast/Ei – 129/Sv F1 ES cells does not discriminate between inactivation of the Cast/Ei or 129/Sv X chromosome.

C) Almost complete skewing of XCI towards the *Tsix-stop* containing 129/Sv X chromosome was simulated using allele specific probabilities for the Cast/Ei and mutated 129/Sv X chromosomes.

D) Left panel shows the experimentally obtained XCI data with 2n XX heterozygous *Tsix-stop* female cells. In this experiment no discrimination was made between inactivation of the Cast/Ei and 129/Sv X chromosomes. The right panel shows simulated XCI experiments using the probability y presented in (C).

E) Predicted probabilities in time for a *Tsix-stop* X chromosome in male and female ES cells.

F) Left panel shows simulation experiments with homozygous female *Tsix-stop* cells. Right panel shows

for XCI-activator), for which V_{ys} and V_{yd} reflect the composition and breakdown, respectively, of the complex involved in *Xist* transcriptional activation and/or *Xist* RNA mediated silencing. The values for V_{ys} and V_{yd} will depend on allelic properties of different X chromosomes, such as SNPs in the Xce region associated with allelic threshold levels to initiate XCI. We have investigated both options, using different allele specific values for V_{ys} or V_{yd} . By training the stochastic simulation program, we found allele specific V_{ys} values for the 129/Sv X and Cast/Ei X alleles of 3.19 and 2.87, respectively, or V_{yd} values for the 129/Sv X and Cast/Ei X alleles of 1.05 and 1.20, respectively (Supplementary Table 2D and E). Keeping all other variables constant, these obtained values resulted in probability curves that, in stochastic simulations of XCI, generated a relative distribution of 129/Sv : Cast/Ei of 70% : 30% (Figure 5A and 5B, and Supplementary Table 5).

Completely skewed XCI has been reported in female mice and ES cells, in which *Tsix* transcription is abrogated by deletion of *Tsix* regulatory elements or a block of *Tsix* transcription through insertion of poly-adenylation sequences. These mice and ES cells show almost completely skewed XCI towards inactivation of the *Tsix* mutant X chromosome. We have recently shown that XCI starts earlier in differentiating *Tsix* mutant ES cells compared to wild type female cells, and that by day one of differentiation already 50% of the mutant cells have initiated XCI, compared to ~10% of the wild type cells. In the stochastic simulation, a raise in the probability for the 129/Sv X chromosome harboring the *Tsix* stop by increasing V_y to 4.60 μ M, results in an outcome that matched the experimental findings (Figure 5C and 5D, and Supplementary Table 2F and 5A). This simulation also shows that in this case only few cells inactivate both X chromosomes, as we previously reported [10], because early during differentiation the mutant X chromosome is subject to a high probability to undergo XCI compared to the wild type X, meaning that the XCI-activator level will drop well before the second X might become a target. Using the same parameters in a simulation of homozygous female *Tsix*-stop cells we found a very high number of cells inactivating both X chromosomes (Figure 5F and Supplementary Table 5B), as was reported for differentiating female ES cells with a homozygous mutation of *Tsix* [28]. Interestingly, in wild type male cells with $m=0.5$ we still find that y can eventually, over a period of time, reach a value above zero, suggesting that the single X in these male cells will still have a probability to undergo initiation of XCI upon

initiation of XCI occurring in simulation experiments with *Tsix*-stop male cells.

G) Predicted probability curves for Cast/Ei and 129/Sv X chromosomes in 3n XXY ES cells.

H) Schematic presentation of the *Xist* locus and the localization of the PCR primers used to determine skewing of *Xist* expression. RT PCR was performed with cDNA of 7 day differentiated 2n XX cells and 3n XXY cells, with *Xist* primers spanning intron 6, amplifying a length polymorphism present in exon 7. The average percentage, and standard deviation, of *Xist* emanating from the Cast/Ei X chromosomes relative to the total amount of *Xist* is shown in the right graph.

differentiation or development. Indeed this has been reported in differentiating male ES cells with this *Tsix*-stop mutation [34,35].

Although the thresholds for both Cast/Ei and 129/Sv X chromosomes are similar in F1 2-1 diploid XX cells and the triploid XXY cells that we generated for this study, the putative X-encoded XCI-activator concentration in the nucleus will be different. In the 3n XXY cells, the XCI-activator concentration will be lower than in 2n XX cells, related to the larger volume of the nucleus of triploid cells as compared to diploid cells. Hence, the allele specific threshold for the strong Xce of the Cast/Ei X chromosome in 3n XXY cells may be too high to generate a probability to start XCI (Figure 5G). To test whether this is true, we differentiated 2n XX and 3n XXY lines for 7 days (in triplo), and performed RT-PCR analysis with an *Xist* specific primer set. As predicted, we found that skewing of XCI is enhanced towards the weak Xce of the 129/Sv X chromosome in the 3n XXY cell lines (Figure 5H). We conclude that the stochastic simulation studies support our hypothesis that the probability for an X chromosome to undergo initiation of XCI is effectuated by an X-encoded activator of XCI, above a nuclear threshold level. This level is dependent on the number of X chromosomes per nucleus as well as the nuclear volume related to ploidy, and differential thresholds for specific Xce alleles.

Discussion

We have analyzed XCI in differentiating triploid mouse ES cells, and found that XXY cells with an X:A ratio of 0.67 initiate XCI less frequently compared to cells with a higher X:A ratio. Cells that do initiate XCI (XaXiY) proliferate slightly faster than XaXaY cells, and slowly accumulate in time. Simulation studies of XCI, based on a stochastic principle, indicate that XCI counting and choice can be mimicked when using a probability for an X chromosome to be inactivated, in which the probability is dependent on a nuclear XCI-activator concentration acting at differential threshold levels for X chromosomes with specific Xce alleles.

Triploid ES cells and the need for speed

In this study, we have generated triploid mouse ES cells by PEG mediated fusion of diploid ES cells with haploid round spermatids. Interestingly, we could only generate triploid ES cells with a XXY karyotype, in which the Y chromosome was donated by the round spermatid. The fact that we could not generate an ES cell line with the same XXY karyotype by fusion of a male ES cell with a round spermatid donating an X chromosome indicates that the presence of a spermatid derived X chromosome results in a triploid cell that is not viable. This difference could be the consequence of epigenetic interference with transcription of the X chromosome from spermatids,

which hampered the viability of our triploid cells. However, such an effect has never been reported in mice [36]. Epigenetic modification of the X in spermatids might be a consequence of meiotic sex chromosome inactivation (MSCI) [23], that is overcome in normal sperm development and fertilization, but cannot be reversed by the ES cell. Indeed, fusion experiments with round spermatids harboring an X-linked *GFP* transgene indicate that the spermatidal X chromosome is not reactivated by the ES cell. In contrast, fusion of ES cells with somatic XaXi diploid cells results in proper reactivation of the inactive X chromosome [25]. Therefore, the apparent absence of spermatidal X reactivation in our triploid XXY and XXX ES cells indicates the presence of epigenetic differences laid down on an Xi during the MSCI and the XCI processes. The Y chromosome is also subject to MSCI, but fusion of XX diploid ES cells with a round spermatid containing a Y chromosome does result in viable 3n ES cell lines. This shows that the spermatidal autosomes do not affect the viability. The Y chromosome has little gene content, compared to the large X chromosome, such that possible epigenetic modification of the Y chromosomes by MSCI may not impact on the outcome of the fusion process.

The absence of triploid XYY ES cells can be attributed to these cells having an X:A ratio of 0.33, which is probably lower than required for normal viability and growth for ES cells. Lethality due to an elevated level of Y chromosome transcripts is not likely, in view of the viability of 47,XYX aneuploid male individuals. Although XYY triploid embryos have been observed to occur in mouse and human, the observed frequencies are much lower than expected [37,38]. Interestingly, for differentiating mouse triploid XXY ES cells we find many cells with a single Xa, indicating that an X chromosome under-dosage problem, of one active X per triploid genome, plays a role in particular in undifferentiated ES cells or during early embryonic development. Moreover, after 10 days of EB differentiation of these XXY triploid ES cells, we found an increase in the relative number of XaXiY cells, making up 41% of the total cell population. This indicates that XaXiY is the inactivation pattern that results in a cell with the preferred dosage of X-linked genes. This observation is supported by previous *in vivo* experiments, examining XCI in mouse XXY and XXX triploid 10 dpc (days *post coitum*) embryos, which showed that 83% of the cells were XaXiY, and 92% of the cells were XaXiXi, respectively [19]. Therefore, we conclude that mouse triploid cells preferably keep only one of their X chromosomes active.

Our previous studies have indicated that the probability to inactivate an X chromosome is proportional to the X:A ratio [10]. Based on this observation, we proposed the presence of an X-linked gene encoding an XCI-activator, which itself is transcriptionally inactivated during the XCI process. During differentiation or development, the nuclear concentration of this XCI-activator will increase and reach

a threshold level required to generate a probability to initiate XCI. In cells with a relatively high X:A ratio, the XCI-activator concentration will reach the threshold level at an earlier time point and will plateau at a higher level, and therefore generate a higher probability, compared to cells with a lower X:A. This model assumes that the nuclear volume is directly proportional to the ploidy, which in mice is indeed the case [39,40]. We found that triploid XXY ES cells, and tetraploid XXXY and XXXX ES cells showed a significant difference in the number of cells that initiated XCI after three days of differentiation, supporting the presence of an XCI-activator. Moreover, tetraploid XXXX cells have initiated XCI after three days of differentiation more effectively than diploid XX cells, despite a similar XCI-activator concentration (number of X chromosomes per nuclear volume). We attribute this difference to the different number of X chromosomes, that each have a probability to initiate XCI. This is supported by our simulations, that also show a faster increase of tetraploid XXXX cells with one or more Xi's than the rate of appearance of diploid XX cells with an Xi.

The present observation that after three days of ES cell differentiation 3-4% of XXY triploid ES cells have started XCI provides additional evidence for the hypothesis that the X:A ratio indeed determines the probability to initiate XCI. Our studies also show that the XCI initiation rate for the differentiating XXY triploid ES cells is too low to allow all cells to inactivate one X chromosome within the time span where XCI can be initiated. These cells cannot meet the need for speed.

Cellular population dynamics of XCI

The present simulation studies of XCI indicate that the XCI counting and initiation process can be simulated by inclusion of relatively few variable parameters. First, there is a probability to initiate XCI for any individual X chromosome. Second, specific Xce alleles respond to different nuclear threshold levels of an XCI-activator. This is all that is required to explain the initiation of XCI. The simulations only tested whether a stochastic model for XCI could explain the available and new experimental data. Other models explaining the initiation phase of XCI, including the blocking factor, symmetry breaking, and transvection models, hypothesize that XCI is directed by a mutual exclusive choice process [41]. Unfortunately, this situation could not be simulated in our program. Nevertheless, the simulations based on a stochastic model make predictions, some of which we have thoroughly tested and other predictions that await further analysis.

In the computer simulations, we have used ten XCI choice rounds over a 10 day differentiation period. However, *in vivo* the number of choice rounds may be less than ten, resulting in more cells with too many Xa's, which would be selected against. This is supported by observations made in female embryos that show a significant

number of cells with two Xa's after completion of the X inactivation process [19,42]. Our simulations also predict less cells with too many Xi's than we detected *in vivo*, especially for the 4n XXXX and XXXY cells. This can be explained, if initiation of XCI on the right number of X chromosomes does not result in an immediate drop of the XCI-activator level below the threshold, so that XCI can still be initiated on additional chromosomes until turnover of the XCI-activator has resulted in a drop below the threshold level. We have not incorporated this possibility in our simulation program.

With regard to embryo development, it is interesting that simulations with 2n XX ES cells indicate that the cell number in female diploid XX embryos will be significantly reduced by about 12% when compared to male diploid XY embryos (Supplementary Table 4, blue box). This is in the range of reported size differences between female and male embryos around the time XCI has been completed, and before hormonal cues start to influence growth of the embryo [43]. Therefore, this reported *in vivo* size difference could be explained by female specific cell loss as a by-product of the X inactivation process. Furthermore, for female homozygous *Tsix*-stop cells, our simulation showed that almost all the cells are lost during the XCI process. In male ES cells the reduction in expected cell number is 88%. This may explain the reported sex-ratio distortion in homozygous Δ CpG *Tsix* knockout mice [44]. However, the high loss of cells in our simulations of male and female embryos with a homo/hemizygous *Tsix*-stop mutation indicates that these mice will most likely not be viable. Interestingly, viable mice, albeit at a lower mendelian ratio, have been reported with a homo/hemizygous Δ CpG *Tsix* knockout allele suggesting that the probability to initiate XCI for this allele is lower than for the *Tsix*-stop allele used in our simulations [44]. This indicates that the Δ CpG *Tsix* allele is a partial knockout of *Tsix*, which is supported by *in vivo* studies showing that a heterozygous *Tsix*-stop allele results in a non-viable phenotype, in contrast to the heterozygous Δ CpG *Tsix* mice that are viable and breed [44,45]. Also, two other mutations of *Tsix* result in activation of *Xist* in male cells upon ES cell differentiation, in contrast to male cells with a Δ CpG *Tsix* mutation that do not show initiation of XCI [34,35].

The XCI-activator has not been identified yet. However, several lines of evidence indicate that it acts through *Xist*, and could be a protein or RNA involved in activation and/or stabilization of *Xist* [10]. Studies with different *Tsix* mutant cell lines suggest that, in mice, *Tsix* plays a crucial role in determining the XCI-activator level required for generating a probability to initiate XCI by suppression of *Xist*. In addition, chromatin modifications of the *Xist* promoter may also play a role in determining the threshold, which might be even more relevant in human were the presence and function of *Tsix* are still speculative. Identification and characterization

of the XCI-activator, and factors involved in setting up the threshold, will be of crucial importance for a better understanding of the initiation phase of XCI.

Materials and Methods

Culture and differentiation of ES cells

ES cells were cultured in DMEM supplemented with 15% heat inactivated foetal calf serum, 100 U ml⁻¹ penicillin, 100 mg ml⁻¹ streptomycin, non-essential amino acids, 1000 U/ml leukaemia inhibitory factor (LIF) and 0,1 mM β -mercaptoethanol. ES cells were grown on a layer of male mouse embryonic fibroblast (MEF) feeder cells. To induce differentiation into EBs, ES cells were pre-plated for 60 minutes and non-adherent ES cells were transferred to non-gelatinized bacterial culture dishes without feeder cells in differentiation medium, IMDM Glutamax, 15% heat inactivated foetal calf serum, 50 μ g/ml ascorbic acid, 100 U ml⁻¹ penicillin, 100 mg ml⁻¹ streptomycin, 37.8 μ l/l monothioglycerol.

Mice and staput isolation of round spermatids

All animals were treated in accordance with guidelines of the Erasmus MC, Rotterdam, the Netherlands. Testes from two *Ube2a* homozygous mutant mice and two *Ube2b* heterozygous mutant mice were excised and decapsulated to remove the tunica albuginea. Decapsulated testes were pooled in 20 ml PBS (140 mM NaCl, 3 mM KCl, 1.5 mM KH₂PO₄, 8 mM NaH₂PO₄) / 1.1 mM Ca²⁺/ 0.5 mM Mg²⁺/ 12 mM lactate (Sigma-Aldrich) of 34°C, containing 10mg hyaluronidase (from ovine testes, Roche-Diagnostics), 20mg trypsin (from bovine pancreas, Roche-Diagnostics) and 20 mg collagenase A (Roche-Diagnostics). Testes were shaken for 20 minutes at 90 rpm with 10 mm amplitude to release seminiferous tubuli from interstitial cells. Tubuli were collected by centrifugation for 3 minutes at 2000 rpm and resuspended in 34°C PBS/ 12 mM lactate. After shaking 10 minutes at 120 rpm with 10 mm amplitude to release germinal cells from the tubuli, tubuli remnants were removed. Germinal cells were collected by centrifugation and resuspended in 34°C PBS/ 1.1 mM Ca²⁺/ 0.5 mM Mg²⁺/ 12 mM lactate. The cell suspension was filtrated using a 60 μ m filtration cloth. Germinal cells were collected by centrifugation and resuspended in 50 ml PBS/ 1.1 mM Ca²⁺/ 0.5 mM Mg²⁺/ 12 mM lactate/ 0.5% w/v BSA. Cells were separated by sedimentation velocity at unit gravity in a 1-4% w/v BSA gradient at room temperature. First 20 ml PBS/ 1,1 mM Ca²⁺/ 0.5 mM Mg²⁺/ 12 mM lactate was bottom-loaded in a chamber, followed by 50 ml cell suspension. A BSA gradient was created by loading a total of 500 ml of 1%, 2% and 4% w/v BSA in PBS. Cells were allowed to sediment for 2 hours. The chamber was emptied in 8 ml fractions using a fraction collector, and fractions containing peak amounts of cells were identified

using a 340 nm UV light source. Fractions containing round spermatids were pooled, collected by centrifugation and resuspended in PBS/ 1.1 mM Ca^{2+} / 0.5 mM Mg^{2+} / 12 mM lactate. Purity of round spermatid preparations derived by this procedure were shown to be >90%, as determined by microscopic analysis of an aliquot of purified cells fixed in Bouins' fixative on glass slides [46].

Fusion experiments

Mus musculus castaneus/ 129/Sv F1 (F1-2 1) female and C57Bl6/ 129/Sv (V6.5) male ES cell-lines were separated from MEF feeder cells by trypsinizing and preplating for 45 minutes on uncoated culture dishes. PEG1500 fusion was performed according to the manufacturer's instructions (Invitrogen). Briefly, $4 \cdot 10^6$ cells were combined with $4 \cdot 10^6$ round spermatids in DMEM. After centrifugation cells were resuspended in 300 μl 50% v/v PEG1500 and incubated for 2 minutes at 37°C under continuous stirring. The mixture was gradually diluted with serum containing medium and plated on drug-resistant MEF feeder cells. After 24 hours medium was replaced with medium containing 0.3 $\mu\text{g}/\text{ml}$ neomycin and 2 $\mu\text{g}/\text{ml}$ puromycin. After nine days, individual ES cell colonies were picked, trypsinized and plated on individual culture dishes in neomycin and puromycin containing medium.

Cell cycle block

ES cells were EB differentiated for one or two days and then blocked in the cell cycle by adding 0.75 mM mimosine, 12 $\mu\text{l}/\text{ml}$ colcemid (KaryoMax, Gibco) or 2100centiGray γ -irradiation. Cells were fixed one day after applying the cell cycle block.

Karyotyping

ES cells were blocked in metaphase by incubation in medium containing 0.12 $\mu\text{g}/\text{ml}$ colcemid for 1 hour. Cells were trypsinized and resuspended in 5 ml 0.075 M KCl at 37°C, collected and resuspended in 0.0625M KCl/ 12.5% methanol/ 4.17% acetic acid. Cells were fixed by washing three times in 75% methanol/ 25% acetic acid and stored in 200 μl at 4°C. The fixed cell suspension was spotted on ethanol cleaned slides and air dried. For determining the total number of chromosomes slides were mounted with 20 μl Dapi vectashield.

To determine the number of X chromosomes, slides were denatured by a three minute incubation at 80°C in 100 μl 50% formamide/ 2x SSC/ 10 mM phosphate buffer. Subsequently slides were dehydrated, and hybridised overnight at 37°C with a Cy3 labelled X-paint probe (Cambio). After hybridisation, slides were washed once with 2xSSC at 45°C, three times with 2xSSC/ 50% formamide at 45°C and two times with PBS. Slides were dehydrated through ethanol steps (70%, 90%

and 100%) air-dried and mounted with 20 μ l dapi vectashield. For determining the number of Y chromosomes, Y-chromosome paint (Cambio) was applied, following the same protocol as for the X chromosome paint.

RNA FISH analysis

One day prior to fixation, non-adherent EBs were trypsinized and differentiated ES cells were grown on gelatin-coated cover slips. Cells were rinsed once with PBS and permeabilized by successive incubation in cytoskeletal buffer (100 mM NaCl, 300 mM sucrose, 3 μ M $MgCl_2$, 10 mM PIPES pH 6.8 in H_2O) for 30 seconds, cytoskeletal buffer containing detergent (0.5% triton X-100, 100 mM NaCl, 300 mM sucrose, 3 μ M $MgCl_2$, 10 mM PIPES pH 6.8 in H_2O) for 2 minutes and cytoskeletal buffer for 30 seconds. Cells were fixed in 4% paraformaldehyde/PBS for 10 minutes, rinsed three times with 70% ethanol and stored in 70% ethanol at 4°C.

The *Xist* probe was a digoxigenin labelled 5.5 kb cDNA sequence [10]. To suppress repetitive sequences 25 μ g/ml mouse Cot1 DNA was added and probe mixture was incubated at 95°C for 5 minutes and at 37°C for 45 minutes. After overnight hybridisation at 37°C, slides were washed in 2xSSC at 37°C for 5 minutes, and three times in 50% formamide/ 2xSSC at 37°C for 10 minutes. Probe detection was performed at room temperature. Detection was with a sheep anti-digoxigenin antibody (Roche diagnostics), followed by a FITC labelled rabbit anti-sheep antibody (Jackson labs) and a FITC labelled goat anti-rabbit antibody (Jackson labs), each for 30 minutes, in 100 mM Tris pH 7.5/ saline/ Tween, BSA. After detection cover slips were dehydrated and mounted on a slide in Vectashield and DAPI to counter stain DNA. To determine the number of inactive X chromosomes in a cell, a non-overlapped intact nucleus was selected, and the number of *Xist* clouds were scored.

BrdU analysis

For BrdU analysis, differentiated ES cells of trypsinized non-adherent EBs were grown on gelatin-coated cover slips in the presence of 20 μ M BrdU, and fixed as described in the RNA FISH section. Cover slips were dehydrated, air-dried and denatured in 70% formamid/ 2x SSC/ 50 mM phosphate for 3 minutes at 85°C. Coverslips were washed in ice cold 70% ethanol and through 70%, 90% and 100% ethanol washes and air dried after which the *Xist* probe was applied. Detection of *Xist* RNA was as described in the previous section, detection of BrdU was performed with a mouse monoclonal BrdU antibody (DAKO), followed by a rhodamin labelled donkey anti-mouse antibody (Jackson labs), 30 minutes incubation each.

To determine the number of BrdU labelled cells for the XaXaY and XaXiY cell populations, first a microscope field was selected, containing one or more intact

nuclei with an *Xist* cloud. Within this field, the number of cells containing an *Xist* cloud with negative, intermediate and highly positive BrdU staining was determined. Subsequently this was also done for all cells without an *Xist* cloud in the same microscopic field.

DNA FISH analysis

For DNA FISH, cells were fixed as for RNA FISH, and pretreated for 4 min with 0.5% pepsin in 10mM HCl at 37°C, post fixed for 5 minutes in 4% paraformaldehyde/PBS, washed twice with PBS, and dehydrated prior to denaturation. Denaturation of target sequences was as described in the BrdU analysis section. Cover slips were incubated with a combination of two biotin-labelled BACs (CT7-155J2 and CT7-474E4) at 37°C overnight. BACs were detected using mouse anti-biotin (Roche diagnostics) and donkey anti-mouse antibodies (Jackson labs) as described for RNA FISH. To determine the number of X chromosomes, non-overlapping nuclei were selected and the number of signals per nucleus was determined.

Genotyping and RT PCR analysis

For genotyping the mutant *Ube2b* allele was amplified with primers CTTTACGGTATCGCCGCTCCCGAT, TTGAAATCCCGCATGAGC, and CGGAGGGAGACGTCATTG. For RT-PCR RNA was isolated with Trizol reagent, treated with RNase free DNase and reverse transcribed (all Invitrogen). *Xist* RNA was amplified with primers ACTGGGTCTTCAGCGTGA, and GGGAATAGGTAAGACACACTG spanning intron 6, which amplify a length polymorphism in exon 7 (129/Sv fragment is 888 bp, Cast/Ei fragment is 845 bp).

Stochastic simulations

Stochastic simulations were performed in a SQL based program (the source code can be found in the supplementary data), using 10 Z-stacks, and 100 starting cells. The program allows the use of different probabilities in time, a different number of X chromosomes per cell, and a different rate of cell division depending on the number of *Xi*'s.

Acknowledgements

We would like to thank all department members for helpful discussions. This work was supported by HFSP CDA and NWO-VIDI grants to J.G., a NWO-AGIKO grant to K.M. and a grant from the Dutch government (BSIK programme 03038, SCDD).

All Supplementary Figures and Tables are available at request with J. Gribnau.

References

1. Lyon MF (1961) Gene action in the X-chromosome of the mouse (*Mus musculus* L.). *Nature* 190: 372-373.
2. Brown CJ, Hendrich BD, Rupert JL, Lafreniere RG, Xing Y, et al. (1992) The human *Xist* gene: analysis of a 17 kb inactive X-specific RNA that contains conserved repeats and is highly localized within the nucleus. *Cell* 71: 527-542.
3. Borsani G, Tonlorenzi R, Simmler MC, Dandolo L, Arnaud D, et al. (1991) Characterization of a murine gene expressed from the inactive X chromosome. *Nature* 351: 325-329.
4. Brockdorff N, Ashworth A, Kay GF, McCabe VM, Norris DP, et al. (1992) The product of the mouse *Xist* gene is a 15 kb inactive X-specific transcript containing no conserved ORF and located in the nucleus. *Cell* 71: 515-526.
5. Brown CJ, Ballabio A, Rupert JL, Lafreniere RG, Grompe M, et al. (1991) A gene from the region of the human X inactivation centre is expressed exclusively from the inactive X chromosome. *Nature* 349: 38-44.
6. Marahrens Y, Panning B, Dausman J, Strauss W, Jaenisch R (1997) *Xist*-deficient mice are defective in dosage compensation but not spermatogenesis. *Genes Dev* 11: 156-166.
7. Penny GD, Kay GF, Sheardown SA, Rastan S, Brockdorff N (1996) Requirement for *Xist* in X chromosome inactivation. *Nature* 379: 131-137.
8. Ogawa Y, Lee JT (2003) *Xite*, X-inactivation intergenic transcription elements that regulate the probability of choice. *Mol Cell* 11: 731-743.
9. Lee JT, Lu N (1999) Targeted mutagenesis of *Tsix* leads to nonrandom X inactivation. *Cell* 99: 47-57.
10. Monkhorst K, Jonkers I, Rentmeester E, Grosveld F, Gribnau J (2008) X inactivation counting and choice is a stochastic process: evidence for involvement of an X-linked activator. *Cell* 132: 410-421.
11. Sun BK, Deaton AM, Lee JT (2006) A transient heterochromatic state in *Xist* preempts X inactivation choice without RNA stabilization. *Mol Cell* 21: 617-628.
12. Lee JT, Strauss WM, Dausman JA, Jaenisch R (1996) A 450 kb transgene displays properties of the mammalian X-inactivation center. *Cell* 86: 83-94.
13. Heard E, Mongelard F, Arnaud D, Avner P (1999) *Xist* yeast artificial chromosome transgenes function as X-inactivation centers only in multicopy arrays and not as single copies. *Mol Cell Biol* 19: 3156-3166.
14. Augui S, Filion GJ, Huart S, Nora E, Guggiari M, et al. (2007) Sensing X chromosome pairs before X inactivation via a novel X-pairing region of the *Xic*. *Science* 318: 1632-1636.

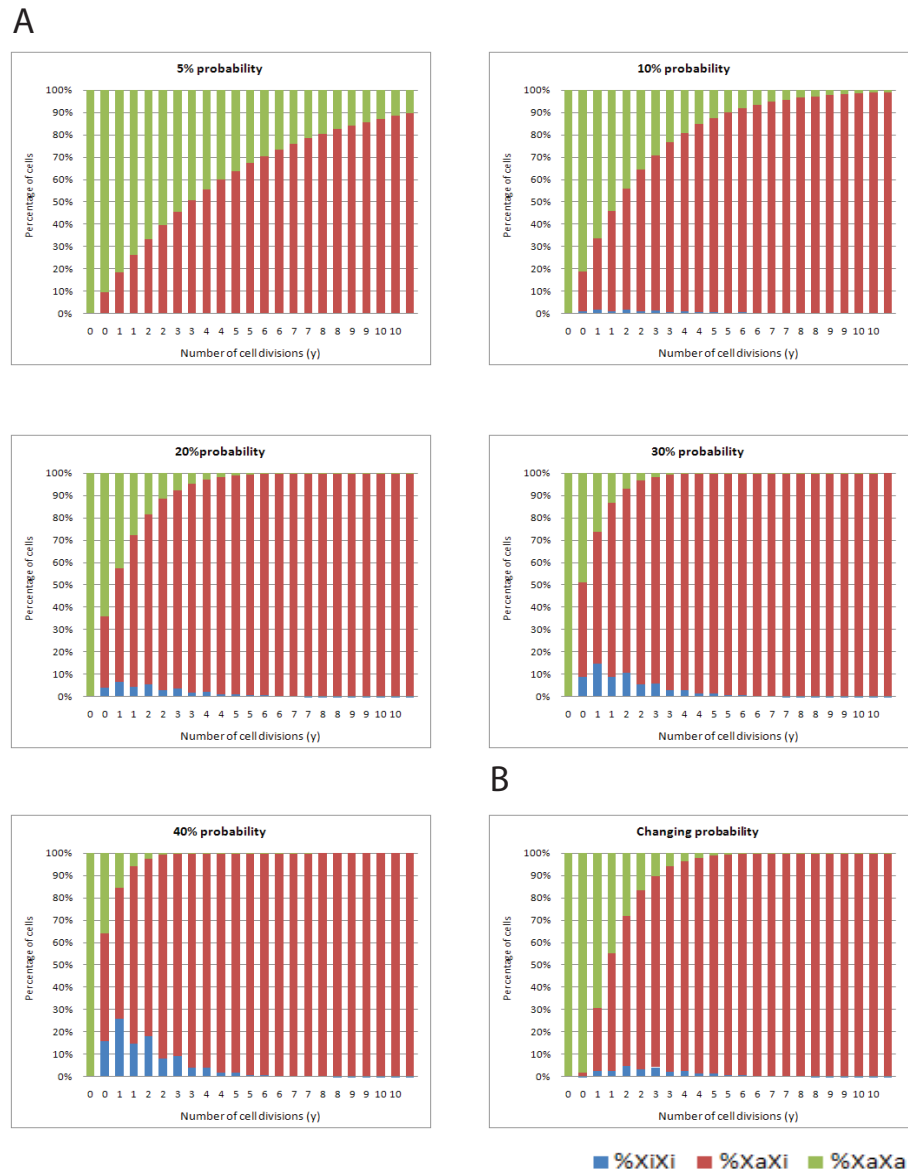
15. Gartler SM, Varadarajan KR, Luo P, Norwood TH, Canfield TK, et al. (2006) Abnormal X: autosome ratio, but normal X chromosome inactivation in human triploid cultures. *BMC Genet* 7: 41.
16. Hendriksson P, Hakansson L, Sandahl B (1974) A live-born triploid infant. *Acta Paediatr Scand*: 447-449.
17. Leisti J, Raivo KO, Rapola J, Saksela E, Aula P (1970) Triploidy (69, XXY) in a newborn infant: a new syndrome in man? *Scand J Clin Lab Invest* 25: 60.
18. Willard HF, Breg WR (1977) Two highly synchronous, early-replicating X chromosomes in fibroblasts from a live-born 69, XXY triploid infant. *Am J Hum Genet* 29.
19. Speirs S, Cross JM, Kaufman MH (1990) The pattern of X-chromosome inactivation in the embryonic and extra-embryonic tissues of post-implantation digynic triploid LT/Sv strain mouse embryos. *Genet Res* 56: 107-114.
20. Ulrich HD (2005) The RAD6 pathway: control of DNA damage bypass and mutagenesis by ubiquitin and SUMO. *Chembiochem* 6: 1735-1743.
21. Roest HP, Baarends WM, de Wit J, van Klaveren JW, Wassenaar E, et al. (2004) The ubiquitin-conjugating DNA repair enzyme HR6A is a maternal factor essential for early embryonic development in mice. *Mol Cell Biol* 24: 5485-5495.
22. Roest HP, van Klaveren J, de Wit J, van Gurp CG, Koken MH, et al. (1996) Inactivation of the HR6B ubiquitin-conjugating DNA repair enzyme in mice causes male sterility associated with chromatin modification. *Cell* 86: 799-810.
23. Turner JM (2007) Meiotic sex chromosome inactivation. *Development* 134: 1823-1831.
24. Hadjantonakis AK, Cox LL, Tam PP, Nagy A (2001) An X-linked GFP transgene reveals unexpected paternal X-chromosome activity in trophoblastic giant cells of the mouse placenta. *Genesis* 29: 133-140.
25. Takagi N, Yoshida MA, Sugawara O, Sasaki M (1983) Reversal of X-inactivation in female mouse somatic cells hybridized with murine teratocarcinoma stem cells in vitro. *Cell* 34: 1053-1062.
26. Nesterova TB, Johnston CM, Appanah R, Newall AE, Godwin J, et al. (2003) Skewing X chromosome choice by modulating sense transcription across the *Xist* locus. *Genes Dev* 17: 2177-2190.
27. Wutz A, Rasmussen TP, Jaenisch R (2002) Chromosomal silencing and localization are mediated by different domains of *Xist* RNA. *Nat Genet* 30: 167-174.
28. Lee JT (2005) Regulation of X-chromosome counting by *Tsix* and *Xite* sequences. *Science* 309: 768-771.
29. Wutz A, Jaenisch R (2000) A shift from reversible to irreversible X inactivation is

- triggered during ES cell differentiation. *Mol Cell* 5: 695-705.
30. Du Sart D, Kalitsis P, Schmidt M (1992) Noninactivation of a portion of Xq28 in a balanced X-autosome translocation. *Am J Med Genet* 42: 156-160.
 31. McMahon A, Monk M (1983) X-chromosome activity in female mouse embryos heterozygous for Pgk-1 and Searle's translocation, T(X; 16) 16H. *Genet Res* 41: 69-83.
 32. Chadwick LH, Pertz LM, Broman KW, Bartolomei MS, Willard HF (2006) Genetic control of X chromosome inactivation in mice: definition of the Xce candidate interval. *Genetics* 173: 2103-2110.
 33. Cattanach BM, Isaacson JH (1967) Controlling elements in the mouse X chromosome. *Genetics* 57: 331-346.
 34. Vigneau S, Augui S, Navarro P, Avner P, Clerc P (2006) An essential role for the DXPas34 tandem repeat and *Tsix* transcription in the counting process of X chromosome inactivation. *Proc Natl Acad Sci U S A* 103: 7390-7395.
 35. Luikenhuis S, Wutz A, Jaenisch R (2001) Antisense transcription through the *Xist* locus mediates *Tsix* function in embryonic stem cells. *Mol Cell Biol* 21: 8512-8520.
 36. Kaufman MH, Speirs S, Lee KK (1989) The sex-chromosome constitution and early postimplantation development of diandric triploid mouse embryos. *Cytogenet Cell Genet* 50: 98-101.
 37. Uchida IA, Freeman VC (1985) Triploidy and chromosomes. *Am J Obstet Gynecol* 151: 65-69.
 38. Iliopoulos D, Vassiliou G, Sekerli E, Sidiropoulou V, Tsiga A, et al. (2005) Long survival in a 69,XXX triploid infant in Greece. *Genet Mol Res* 4: 755-759.
 39. Henery CC, Kaufman MH (1992) Relationship between cell size and nuclear volume in nucleated red blood cells of developmentally matched diploid and tetraploid mouse embryos. *J Exp Zool* 261: 472-478.
 40. Henery CC, Kaufman MH (1993) Cellular and nuclear volume of primitive red blood cells in digynic and diandric triploid and control diploid mouse embryos. *Eur J Morphol* 31: 237-249.
 41. Wutz A, Gribnau J (2007) X inactivation Xplained. *Curr Opin Genet Dev* 17: 387-393.
 42. Webb S, de Vries TJ, Kaufman MH (1992) The differential staining pattern of the X chromosome in the embryonic and extraembryonic tissues of postimplantation homozygous tetraploid mouse embryos. *Genet Res* 59: 205-214.
 43. Burgoyne PS, Thornhill AR, Boudrean SK, Darling SM, Bishop CE, et al. (1995) The genetic basis of XX-XY differences present before gonadal sex differentiation

in the mouse. *Philos Trans R Soc Lond B Biol Sci* 350: 253-260 discussion 260-251.

44. Lee JT (2002) Homozygous *Tsix* mutant mice reveal a sex-ratio distortion and revert to random X-inactivation. *Nat Genet* 32: 195-200.
45. Sado T, Wang Z, Sasaki H, Li E (2001) Regulation of imprinted X-chromosome inactivation in mice by *Tsix*. *Development* 128: 1275-1286.
46. Baarends WM, Wassenaar E, Hoogerbrugge JW, van Cappellen G, Roest HP, et al. (2003) Loss of HR6B ubiquitin-conjugating activity results in damaged synaptonemal complex structure and increased crossing-over frequency during the male meiotic prophase. *Mol Cell Biol* 23: 1151-1162.

Supplementary Figure 1



Supplementary Figure 1

A) The panels show the mathematical computation the XaXa, XaXi and XiXi populations with a 5%, 10%, 20%, 30%, and 40% fixed probability per X chromosome. The different bar-graphs show the relative distribution of the three different cell types (XaXa = green, XiXi = blue).

B) This panel shows the mathematical computation the XaXa, XaXi and XiXi populations with a changing probability for $m=1$ presented in figure 4B.

Chapter 4

RNF12 is an X-encoded activator of X chromosome inactivation

Iris Jonkers[#], Tahsin Stefan Barakat[#], Eskeatnaf Mulugeta Achame, Kim Monkhorst, Eveline Rentmeester, Frank Grosveld, J. Anton Grootegoed and Joost Gribnau

[#] These authors contributed equally

~~Submitted to Science~~

○ RNF12

■ *Rnf12*

Abstract

In somatic cells of female placental mammals, one X chromosome is inactivated to minimize sex-related dosage differences of X-encoded genes. X chromosome inactivation (XCI) is a stochastic process, in which each X has an independent probability to initiate XCI [1]. This probability is determined by the nuclear concentration of an X-linked XCI-activator [1]. Here, we identify RNF12 as an activator. Additional copies of *Rnf12/RNF12* result in initiation of XCI in male mouse ES cells, and in initiation of XCI on both X chromosomes in a substantial percentage of female ES cells. This activity depends on an intact open reading frame, providing evidence that RNF12 protein is required for XCI. *Rnf12* transcription is subject to XCI, supporting a role for RNF12 in the XCI counting process.

Results and Discussion

In the mouse embryo proper, XCI is random with respect to the parental origin of the inactivated X chromosome [2], and is initiated around 5 days post coitum in the mouse embryo, or upon ES cell differentiation *in vitro*. Initiation of XCI is marked by transcriptional up-regulation of the X-encoded *Xist* gene on the future inactive X chromosome (Xi). *Xist* is a non-coding spliced and poly-adenylated RNA, which spreads over the Xi while attracting protein complexes required for the silencing process [3,4,5]. *Tsix* and *Xite* gene sequences overlap with *Xist*, but are transcribed in anti-sense direction, and play an important role in suppression of *Xist* transcription during the XCI process [6,7].

XCI starts with counting of the number of X chromosomes and selection of the future active X (Xa) and Xi. This process is stochastic, and the independent probability for any X chromosome to be inactivated increases with an increased X to autosome ratio, suggesting involvement of an X-encoded activator in counting and the XCI process [1]. In female cells, but not in male cells, the concentration of the XCI-activator is sufficient to initiate XCI with a certain probability per time frame. Inactivation of both X chromosomes in female cells is prevented by *cis* inactivation of the gene encoding the XCI-activator and the stochastic nature of the XCI process. Our previous finding that female cells with a heterozygous deletion of a region including *Xist*, *Tsix*, and *Xite* still initiate XCI upon differentiation [1], also supports the involvement of an additional factor in counting and XCI.

Studies with mouse cell lines harboring truncated and translocated X chromosomes have indicated that the gene encoding this XCI-activator is most likely located within a region of 10 megabases (Mb) surrounding the *Xist* locus [8,9,10,11]. To identify the XCI-activator, we generated transgenic male and female ES cell lines with stably integrated BAC transgenes covering this 10 Mb region. Our working

hypothesis predicts that initiation of XCI upon differentiation in male ES cells on the single X, or initiation of XCI on both X chromosomes in a substantial percentage of female ES cells, indicates the presence of additional copies of the gene encoding the XCI-activator.

Previous studies with autosomally integrated mouse or human *Xist/Xist* transgenes in mouse ES cells indicated that autosomal integration of these transgenes results in activation of the endogenous *Xist* gene [12,13]. This suggests that these transgenes include sequences encoding the XCI-activator. We therefore started our screen with a BAC covering mouse *Xist*, excluding the transcription start sites of *Tsix* and *Xite*. BAC RP24-180B23 was stably transfected into male ES cells. Clones were expanded under neomycin selection and differentiated for 3 days before analysis. Besides wild type ES cells, we also made use of a male ES cell line 1.3 which contains 16 copies of a ms2 repeat integrated in exon 7 of *Xist* (Figure 1A). This tag does not interfere with XCI, and allows discrimination between endogenous *Xist*-ms2 and transgenic *Xist* [14]. BAC integration and copy number were determined by DNA-FISH and qPCR. The percentage of cells with accumulated *Xist* covering the Xi (*Xist* cloud) was determined by RNA-FISH using an *Xist* cDNA probe. In most cell lines with an autosomal integration of the transgene we found a significant percentage (>5%) of male cells with single *Xist* clouds (Figure 1B, Supplementary Table 1A), confirming previous findings [13]. The pinpoint signal represents basal *Tsix/Xist* transcription. RNA-FISH using *Xist* (FITC) and ms2 (rhodamine red) probes performed on five different transgenic 1.3 ES cell lines which were differentiated for 3 days revealed no ms2 positive clouds (Figure 1C), indicating that the endogenous *Xist* gene was never up-regulated leading to conversion of the pinpoint signal to a cloud, excluding this region as a candidate region harboring the XCI-activator. Male ES cells transgenic for a BAC sequence CTD2183M22 covering human *Xist* (Figure 2C) did not show significant induction of murine *Xist* in male cells (Figure 1D, and Supplementary Table 1A), also excluding this region from playing a role in activation of XCI.

We continued our search for the XCI-activator gene by generating transgenic male ES lines with BACs covering *Tsix* including a region 100kb centromeric to *Tsix* (RP23-447O10), and BACs covering a region 300 kb telomeric to *Xist* (CT7-474E4, RP24-224E13, and RP23-100E1). RNA FISH analysis only revealed pinpoint *Tsix/Xist* signals at day 3 of differentiation, indicating the absence of XCI initiation on the wild type X chromosome (Figure 1E, 1F, and Supplementary Table 1B). BACs CT7-474E4 and RP23-224E13 include the *Xpr* region, which recently was implicated in pairing and counting of X chromosomes at the onset of XCI [15]. Surprisingly, we did not observe XCI in transgenic male cells harboring at least one additional copy of these transgenes, nor did we observe an increased percentage of female cells with two Xi's

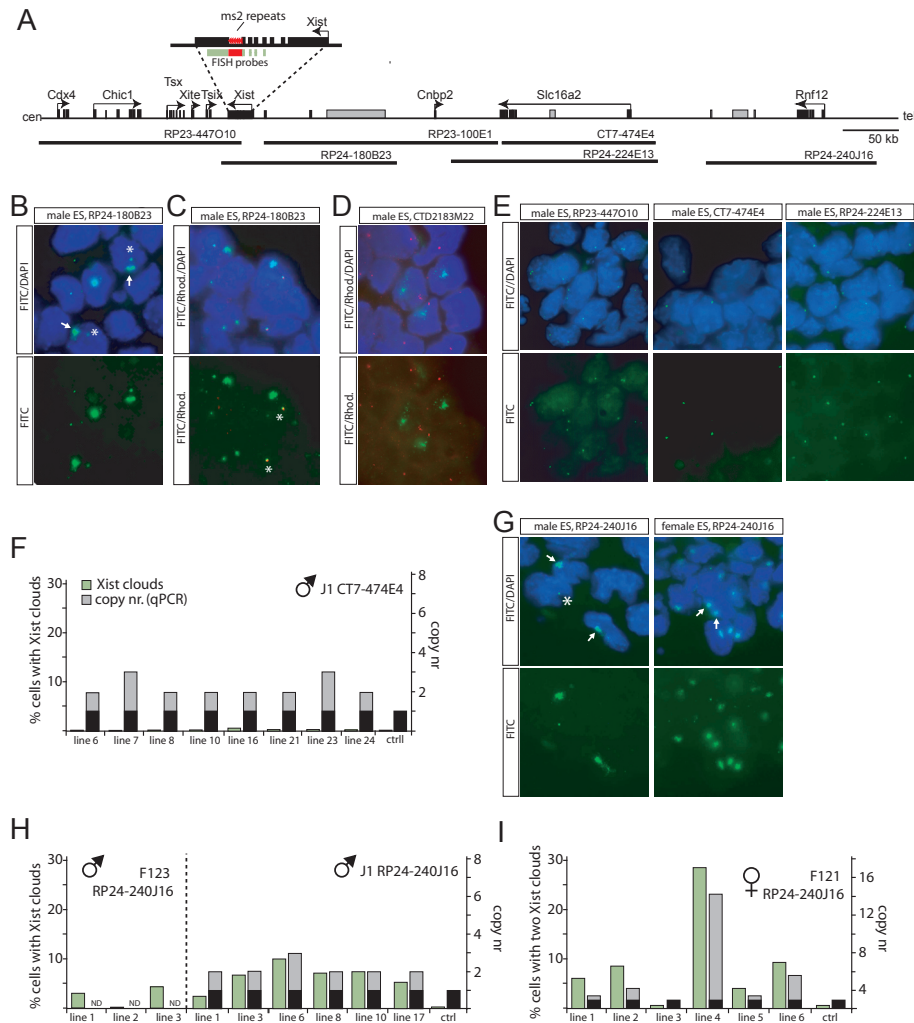


Figure 1. BAC contig covering the X inactivation center

A) Map showing part of the mouse X chromosome, the location of the BAC sequences used in this study, and the position of ms2 repeats within *Xist*. RNA-FISH probes are indicated in green and red, and non-annotated genes in grey.

B) RNA-FISH with an *Xist* probe (FITC) on day 3 differentiated male ES cells with an integration of BAC RP24-180B23, showing cells with *Xist* clouds (arrows), and pinpoint signals (star). DNA is stained with DAPI.

C) RNA-FISH with *Xist* (FITC) and ms2 (rhodamine red) probes on day 3 differentiated 1.3 male ES cells with an integration of BAC RP24-180B23, showing that *Xist* clouds are associated with autosomes, and ms2 positive *Tsix/Xist* pinpoint signals (star). DNA is stained with DAPI.

D) RNA-FISH detecting mouse *Xist* (rhodamine red) and human *Xist* (FITC) on day 3 differentiated male cells transgenic for human CTD2183M22 (Figure 2C) shows that human *Xist* (clouds) does not induce XCI on the endogenous mouse X chromosome (*Xist* pinpoints). DNA is stained with DAPI.

E) Similar to B), but with BACs RP23-447O10, CT7-474E4, and RP24-224E13. Only pinpoint signals, no clouds are seen.

F) Percentage of CT7-474E4 transgenic cells with *Xist* clouds (green), and BAC copy number as determined

(Supplementary Table 1C), excluding the *Xpr* region from playing a role in activation of XCI.

We next analyzed transgenic cells with an integration of BAC RP24-240J16, which covers an area from 410 kb to 570 kb telomeric to *Xist* (Figure 1A). We established transgenic male ES cell lines using three different ES cell lines (F1 2-3, J1, and 1.3), and confirmed the BAC integration (Figure 1H, and Supplementary Figure 1A, B). Interestingly, RNA-FISH analysis of day 3 differentiated BAC transgenic ES cell lines showed several lines with a significant number (>5%) of cells with *Xist* clouds, which we never observed with control male cell lines ($\leq 1\%$; Figure 1G, 1H, and Supplementary Figure 1A). DNA/RNA-FISH analysis detecting both the X chromosome and *Xist* RNA confirmed that these male ES cells initiated XCI on the single X chromosome (Figure 2A). In transgenic female cell lines we also obtained an increased percentage of cells with two *Xist* clouds, which positively correlated with the BAC copy number (Figure 1G, 1I). RNA-FISH analysis on two different day 3 differentiated RP24-240J16 transgenic female lines, heterozygous for the ms2 tag, showed that female cells with two *Xist* clouds only had one ms2 positive cloud (Figure 2B). Because aneuploidy would have resulted in a significant proportion of cells with two ms2 positive or negative clouds, this finding confirms that the transgenic female cells contained two X chromosomes. Our results therefore suggest that BAC RP24-240J16 harbors a gene encoding an XCI-activator. RP24-240J16 transgenic cells did not initiate XCI on all X chromosomes, which could be attributed to the fact that additional copies of this BAC will only lead to an increased probability to initiate XCI, and death of cells that initiated XCI on all X chromosomes. In addition, expression of the transgenes may be variegated, or more than one different X-encoded XCI-activator is involved in initiation of the XCI process.

To test whether the XCI-activator is conserved between mouse and human, we generated transgenic mouse ES cells with human BAC CTD2530-H13 (Figure 2C), which covers an area that is homologous to the region covered by mouse RP24-240J16 (Figure 1A). Upon differentiation of these CTD2530-H13 transgenic cells, XCI is induced in a significant proportion of the male cells, and on both X chromosomes in an increased percentage of the female cells, indicating that indeed the XCI-activator is functionally conserved between mouse and human (Figure 2D, 2E, 2F). We fine-mapped the area required for induction of XCI in male cells using mouse

by qPCR (additional BAC copies in grey, endogenous copies in black, $n > 100$ per cell line).

G) Similar to B), but with BAC RP24-240J16, showing male cells with *Xist* clouds (arrows) or pinpoint signals (star), and female cells with two *Xist* clouds (arrows).

H, I) Percentage of male cells with single *Xist* clouds (H) and female cells with two *Xist* clouds (I), and copy number of the region covered by the BACs determined by qPCR (additional BAC copies in grey, endogenous copies in black, $n > 100$ per cell line).

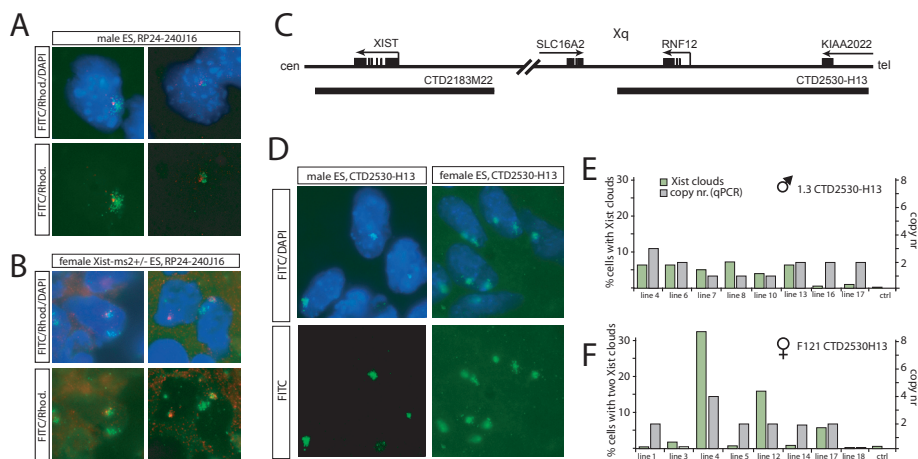


Figure 2. The XCI-activator is conserved between mouse and human

A) RNA/DNA FISH detecting *Xist* (FITC) and an X chromosome specific probe (rhodamine red), on day 3 differentiated 1.3 male ES cells, showing *Xist* accumulation (cloud) on the single X chromosome. DNA is stained with DAPI.

B) RNA-FISH detecting *Xist* (FITC) and ms2 (rhodamine red) on day 3 differentiated female ES cells heterozygous for the *Xist*-ms2 tag, showing cells with two *Xist* clouds, one marked by ms2. Cells with two *Xist* clouds only showed one *Xist* and one *Xist*-ms2 cloud (Line 8 n=46, line 9 n=55).

C) Map of part of the human X chromosome and location of the BACs used for the analysis.

D) RNA-FISH detecting *Xist* (FITC) on day 3 differentiated CTD2530-H13 transgenic male (left panels) and female (right panels) ES cells shows initiation of XCI in male cells and initiation of XCI on both X chromosomes in female cells (*Xist* clouds).

E, F) Quantification of RNA-FISH presented in D), for BAC transgenic male (E) and female (F) cell lines, and copy number of the region covered by the BACs determined by qPCR (grey, n>100 per cell line).

BAC sequences covering part of BAC RP24-240J16 (Figure 3A). With this strategy we reduced the minimal region required for ectopic XCI to 10 kb (Figure 3A, 3B, and Supplementary Table 2). Expression analysis using total RNA of day 3 differentiated female ES cells hybridized to a tiling array covering BAC RP24-240J16 indicated that *Rnf12* is the only transcribed sequence and that the 10 kb region overlaps with the promoter and exons 1 and 2 of *Rnf12* (Figure 3C). In addition, alignment of BACs RP24-240J16 and CTD2530-H13 revealed a high sequence homology in the 10 kb area and the rest of *Rnf12*, suggesting that mouse *Rnf12* and human *RNF12* both encode a conserved XCI-activator.

Attempts to over-express *Rnf12* cDNA resulted in extensive cell death. Also, the RP24-240J16 ES cell lines did not survive freeze-thawing. To establish the role of *RNF12* in XCI, we inserted a neomycin/kanamycin resistance cassette in two orientations into exon 5 of *Rnf12*, disrupting most of the open reading frame, but leaving the 10 kb minimal region required for ectopic XCI intact. This allowed us to test whether the induction of XCI is evoked by either *Rnf12*-encoded protein or

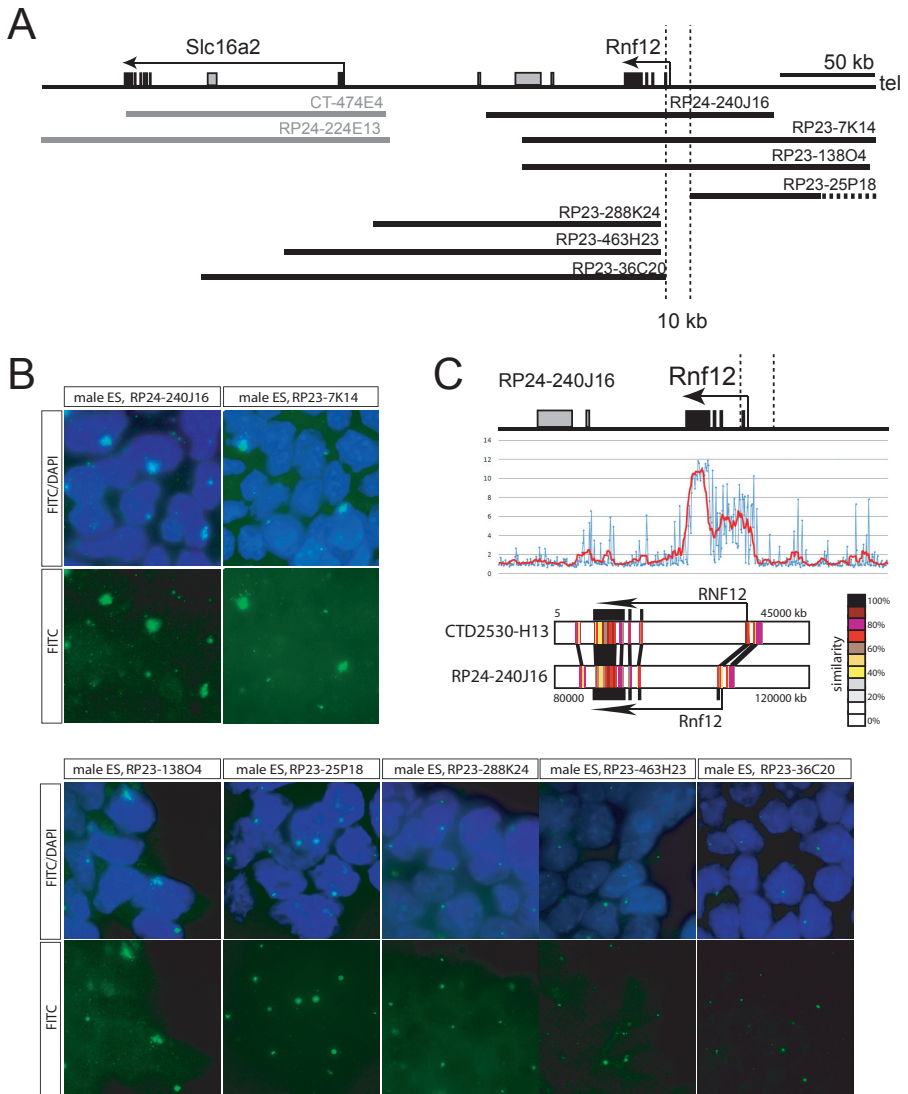


Figure 3. Fine-mapping the area required for XCI counting

A) Position of BAC Contigs used for the fine-mapping. BAC RP23-25P18, covering part of BAC RP24-240J16, was truncated (the part shown as a solid line was shown to be present using PCR analysis).

B) RNA-FISH detecting *Xist* (FITC) on day 3 differentiated male ES cells with different BAC transgenes, showing that the 10 kb region depicted in A) is required for initiation of XCI in male cells. DNA is stained with DAPI.

C) Tiling array expression analysis with total RNA of day 3 differentiated female ES cells (top panel, moving average in red, raw data in blue), and alignment of mouse (RP24-240J16) and human (CTD2530-H13) BAC sequences (bottom panel), shown is the region surrounding the *Rnf12* / *RNF12* gene.

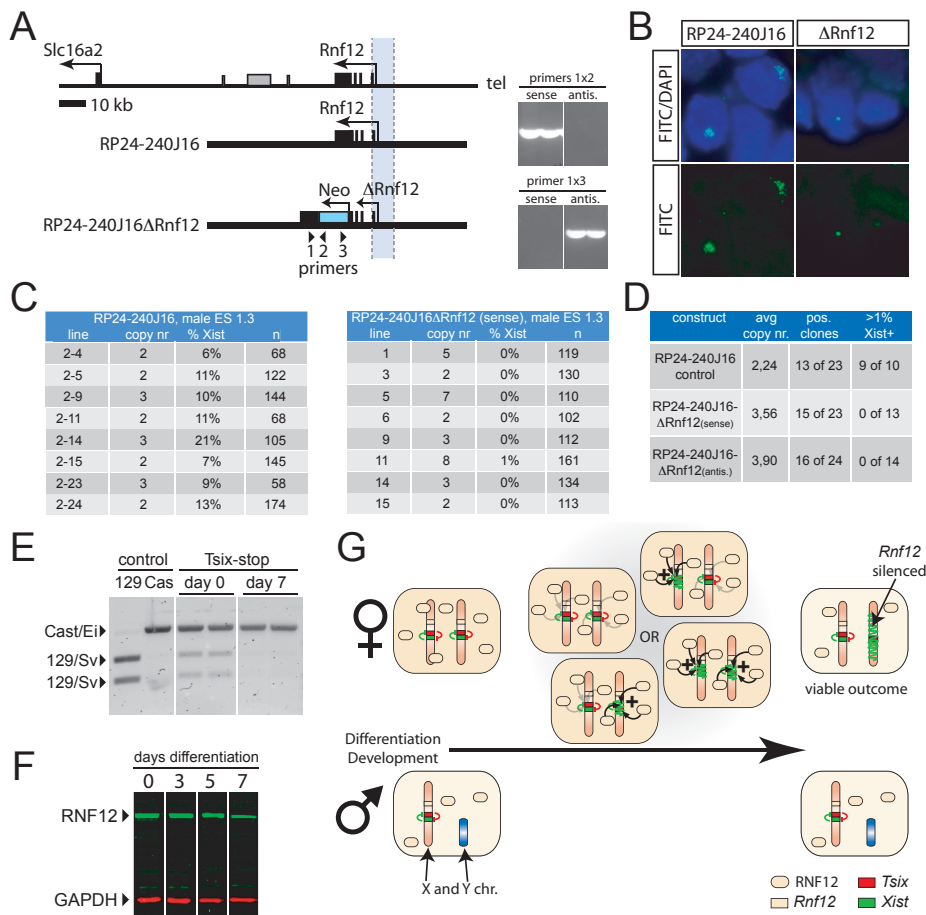


Figure 4. RNF12 is an XCI-activator

A) A map of part of the X chromosome covered by BAC RP24-240J16, and the modified BAC RP24-240J16ΔRnf12 with a neomycin resistance cassette inserted in two orientations (only sense orientation is shown). Right panels show confirmation of homologous recombination by PCR using different primer combinations as indicated.

B) RNA-FISH detecting *Xist* (FITC) on day 3 differentiated BAC RP24-240J16 (left panels) and RP24-240J16ΔRnf12 (right panels). Transgenic male ES cells show initiation of XCI (clouds) in RP24-240J16 male cells only.

C, D) Copy number determination and quantification of the percentage of cells that initiated XCI in 8 different RP24-240J16 and RP24-240J16ΔRnf12 (sense) lines (C). Right table (D) shows a summary of the results obtained with all RP24-240J16 and RP24-240J16ΔRnf12 cell lines. Not all positive clones with BAC integrations could be analyzed.

E) RT-PCR expression analysis of *Rnf12* with RNA isolated from undifferentiated and day 7 differentiated 129/Sv Cast/Ei *Tsix*-stop ES cells using a *NheI* cleavage of the PCR product at an RFLP present in the 129/Sv allele. The left two lanes show control 129/Sv and Cast/Ei samples.

F) Western blot analysis detecting RNF12 (green) and GAPDH (red) in undifferentiated and day 3, 5, and 7 differentiated female ES cells.

G) A model for XCI. Before XCI is initiated, the nuclear RNF12 concentration is twice as high in female

by a DNA element within the 10 kb region (Figure 4A). Analysis of different day 3 differentiated male ES cell lines transgenic for BAC RP24-240J16 Δ Rnf12 (sense and antisense) containing the mutated *Rnf12* gene, revealed no significant induction of XCI ($\leq 1\%$), in contrast to control transgenic male ES lines which showed induction of XCI ($>5\%$) in most cell lines (Figure 4B, 4C, 4D, and Supplementary Table 3A). This result was confirmed with transgenic 30 Δ 1 female ES cells, where only integration of the unmodified BAC RP24-240J16 resulted in an increased percentage of cells with two Xi's (Supplementary Table 3B), indicating that *Rnf12* encodes an XCI-activator.

Rnf12 is ubiquitously expressed in embryos around the onset of XCI [16] and encodes a 67 kD E3 ubiquitin ligase with one known target, LDB1, that is involved in the regulation of LIM-homeodomain transcription factors [17]. Hence, it is likely that RNF12 has functions also outside the context of XCI.

In three reported girls carrying a ring X chromosome, which is associated with short stature and developmental delay, there is lack of expression of *Xist* from the ring X chromosome [18,19]. Despite the presence of *Xist*, these ring chromosomes are not inactivated, and it appears that the ring X chromosomes in these cases also lack *RNF12*. This implies that the 46,X,r(X) cells in these girls carry only one functional *RNF12* gene, and reinforces a dose-dependent role of RNF12 in XCI. Allele specific RT-PCR analysis with RNA of undifferentiated and day 7 differentiated heterozygous *Tsix* mutant ES cells, which exclusively inactivate the mutant 129/Sv X [20], showed that *Rnf12* expression is subject to XCI (Figure 4E). X-linkage of the gene encoding XCI-activator guarantees a role in counting, as the XCI-activator concentration will be twice as high in female compared to male cells. In addition, stochastic initiation of XCI and XCI mediated silencing of *Rnf12* in *cis* prohibits the inactivation machinery from silencing all X chromosomes.

Whether RNF12 is the only XCI-activator regulating initiation of XCI remains to be determined. Protein expression analysis of differentiating female ES cells indicated that RNF12 expression is not up-regulated around the time XCI is initiated (Figure 4F). This would imply that an additional factor, acting as target or modifier of RNF12 action and not necessarily X-encoded, is up-regulated upon differentiation. Potentiation of RNF12 action by this unknown factor in female cells would result in activation of *Xist* transcription with a certain probability (Figure 4G). The conservation

compared to male ES cells. Upon differentiation of the ES cells, the concentration of an unknown target or modifier of RNF12 increases, which potentiates the action of RNF12. This leads to up-regulation of *Xist* transcription, resulting in a probability to initiate XCI, to silence *Tsix* and to accumulate along the X. Spreading of *Xist* RNA leads to silencing of *Rnf12* transcription in *cis*, resulting in a drop of the nuclear RNF12 concentration, prohibiting inactivation of the second X. In male cells, the RNF12 concentration does not reach the threshold required to start this sequence of events.

of RNF12 activity between mouse and human, and the absence of an established role for *Tsix* in human X inactivation, suggests that RNF12 acts through activation of *Xist* / *Xist* transcription. This is supported by studies with *Xist* promoter transgenes which showed higher expression in female cells compared to male cells [21]. Identification and characterization of the direct target or modifier of RNF12 will be the next step, to further elucidate the XCI process.

Methods

Modification of BACs

BACs were acquired from BACPAC (C57/B6 libraries) or Resgen (129/Sv library), and a kanamycin/neomycin resistance cassette was introduced by *in vitro* lox recombination (NEB). This cassette was generated by introduction of a lox sequence and SclI site BglII-NotI into pEGFP-N1 (Clontech). RP24-240J16ΔRnf12 was generated by homologous recombination in bacteria [22]. The targeting cassette was PCR amplified using primers (GCCTTCGAACATCTCTGAGC, GAGCCGGACTAATCCAAACA), cloned into pCR-BluntII-TOPO (Invitrogen), and linearized with NheI to introduce a kanamycin/neomycin cassette AflII-EcoO109I excised from EGFP-N1. Homologous recombination was confirmed by PCR with primers 1, GGCAGAGAGCCACTTTCATC, 2, CTGGCACTCTGTGATACCC, 3, TTCCACAGCTGGTTCTTTCC, and gel electrophoresis. BACs were SclI linearized and electroporated into ES cells.

Cell lines

Transgenic ES cell lines were generated using wild type male J1 (129/Sv), F1 2-3 (129/Sv-Cast/Ei) ES lines or a wild type female line F1 2-1 (129/Sv-Cast/Ei). For determination of the origin of *Xist* a male line 1.3 and female line 30Δ1 were used, which both contain one *Xist* allele with 16 ms2 repeats integrated in exon 7[14]. ES cells were grown and differentiated as described[1].

RNA and RNA/DNA FISH

RNA-FISH and RNA/DNA FISH were performed as described [1,14,23]. For detection of the region surrounding *Xist* a cocktail of biotin labeled BAC sequences was used (CT7-474E4, CT7-45N16, CT7-155J2 and CT7-211B4).

Expression analysis

For *Rnf12* RT-PCR analysis, RNA was reverse transcribed (Invitrogen Superscript III) and amplified with primers TAAAGAGGGTCCACCACCAC and GGCAGAGAGCCACTTTCATC. PCR products were purified and digested with NheI, which digests the 129/Sv but not the Cast/Ei PCR product. RNF12 was detected with a rabbit anti RNF12 antibody

(Abcam), GAPDH was detected with a mouse anti GAPDH antibody (Chemicon). For expression analysis of the region covered by RP24-240J16 total RNA was isolated from two day 3 differentiated wild type female ES lines, labeled and hybridized to Niblegene tiling arrays, covering the X chromosome with 30 bp intervals, excluding repetitive and non annotated sequences.

BAC copy number determination

BAC copy number was determined with real time PCR using primers; GTTCTTACCACCAATTGAAAACG, CAAAACAGACTCCAAATTCATCC, for RP24-180B23, ACCATGACCAAAGCAACTCC, CTCCTCCAGTACCATGTCTGC, for RP23-447O10 CCGCTGAAGATAGCTCTTGG, GCCACAACCAAACAGAATCC for RP24-224E13 and CT7-474E4, ATCTCACCGTACCCATGAGC, CCTCTGGTACGACCTCTTGC, for RP23-100E1, AGCCCCGATGAAAATAGAGG, GGCATTCTGGATAATCTTTGG for RP24-240J16, RP23-7K14, RP23-138O4, RP23-288K24, RP23-463H23 and RP23-36C20, AGTCATTGGCTGGTCACTCC, ATCAACCCAGACACCAAACC, for RP23-25P18, GATAGCAGGTCAGGCAGAGG, ACGCAAAGCTCCTAACAAGC, for CTD-2183M22, CTCATTTTGAGCCCTTCTGC, ACCACATTTGCCTCAGATCC, for CTD-2530H13 and GCACCCATATCCGCATCCAC, GCATTTCTCCCGCCTTTG, for Zfp-42 as an autosomal normalization control.

Acknowledgements

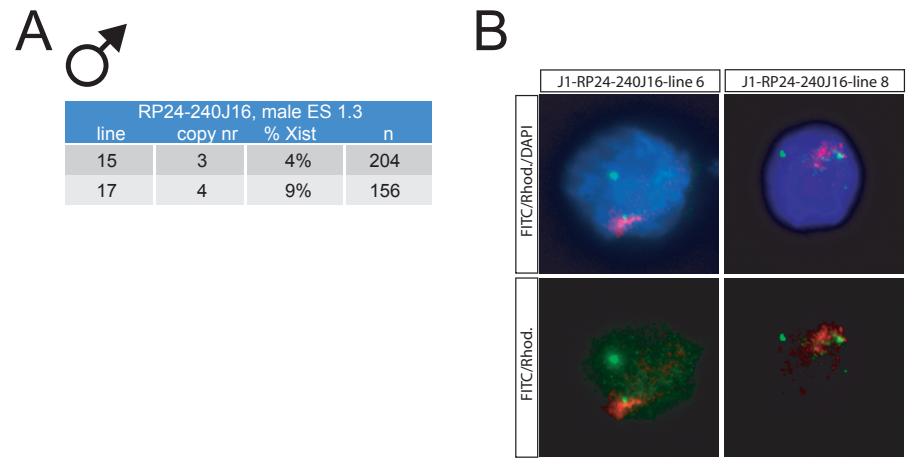
We would like to thank Nilhan Gunhanlar, Akiko Inagaki, Bas de Hoon, Annegien Kenter and Maureen Eijpe for their help with some of the experiments. We also thank all department members for helpful discussions. This work was supported by HFSP CDA, NWO-VIDI and TOP grants to J.G., and a grant from the Dutch government (BSIK programme 03038, SCDD).

References

1. Monkhorst K, Jonkers I, Rentmeester E, Grosveld F, Gribnau J (2008) X inactivation counting and choice is a stochastic process: evidence for involvement of an X-linked activator. *Cell* 132: 410-421.
2. Wutz A, Gribnau J (2007) X inactivation Xplained. *Curr Opin Genet Dev* 17: 387-393.
3. Brown CJ, Hendrich BD, Rupert JL, Lafreniere RG, Xing Y, et al. (1992) The human *Xist* gene: analysis of a 17 kb inactive X-specific RNA that contains conserved repeats and is highly localized within the nucleus. *Cell* 71: 527-542.
4. Zhao J, Sun BK, Erwin JA, Song JJ, Lee JT (2008) Polycomb proteins targeted by a short repeat RNA to the mouse X chromosome. *Science* 322: 750-756.
5. Brockdorff N, Ashworth A, Kay GF, McCabe VM, Norris DP, et al. (1992) The product of the mouse *Xist* gene is a 15 kb inactive X-specific transcript containing no conserved ORF and located in the nucleus. *Cell* 71: 515-526.
6. Lee JT, Lu N (1999) Targeted mutagenesis of *Tsix* leads to nonrandom X inactivation. *Cell* 99: 47-57.
7. Ogawa Y, Lee JT (2003) *Xite*, X-inactivation intergenic transcription elements that regulate the probability of choice. *Mol Cell* 11: 731-743.
8. Lyon MF, Searle AG, Ford CE, Ohno S (1964) A Mouse Translocation Suppressing Sex-Linked Variegation. *Cytogenetics* 15: 306-323.
9. Rastan S, Robertson EJ (1985) X-chromosome deletions in embryo-derived (EK) cell lines associated with lack of X-chromosome inactivation. *J Embryol Exp Morphol* 90: 379-388.
10. Lafreniere RG, Brown CJ, Rider S, Chelly J, Taillon-Miller P, et al. (1993) 2.6 Mb YAC contig of the human X inactivation center region in Xq13: physical linkage of the RPS4X, PHKA1, *Xist* and DXS128E genes. *Hum Mol Genet* 2: 1105-1115.
11. Rastan S (1983) Non-random X-chromosome inactivation in mouse X-autosome translocation embryos--location of the inactivation centre. *J Embryol Exp Morphol* 78: 1-22.
12. Migeon BR, Winter H, Kazi E, Chowdhury AK, Hughes A, et al. (2001) Low-copy-number human transgene is recognized as an X inactivation center in mouse ES cells, but fails to induce cis-inactivation in chimeric mice. *Genomics* 71: 156-162.
13. Herzing LB, Romer JT, Horn JM, Ashworth A (1997) *Xist* has properties of the X-chromosome inactivation centre. *Nature* 386: 272-275.
14. Jonkers I, Monkhorst K, Rentmeester E, Grootegoed JA, Grosveld F, et al. (2008) *Xist* RNA is confined to the nuclear territory of the silenced X chromosome throughout the cell cycle. *Mol Cell Biol* 28: 5583-5594.

15. Augui S, Filion GJ, Huart S, Nora E, Guggiari M, et al. (2007) Sensing X chromosome pairs before X inactivation via a novel X-pairing region of the Xic. *Science* 318: 1632-1636.
16. Bach I, Rodriguez-Esteban C, Carriere C, Bhushan A, Krones A, et al. (1999) RLIM inhibits functional activity of LIM homeodomain transcription factors via recruitment of the histone deacetylase complex. *Nat Genet* 22: 394-399.
17. Ostendorff HP, Peirano RI, Peters MA, Schluter A, Bossenz M, et al. (2002) Ubiquitination-dependent cofactor exchange on LIM homeodomain transcription factors. *Nature* 416: 99-103.
18. Jani MM, Torchia BS, Pai GS, Migeon BR (1995) Molecular characterization of tiny ring X chromosomes from females with functional X chromosome disomy and lack of cis X inactivation. *Genomics* 27: 182-188.
19. Tomkins DJ, McDonald HL, Farrell SA, Brown CJ (2002) Lack of expression of *Xist* from a small ring X chromosome containing the *Xist* locus in a girl with short stature, facial dysmorphism and developmental delay. *Eur J Hum Genet* 10: 44-51.
20. Luikenhuis S, Wutz A, Jaenisch R (2001) Antisense transcription through the *Xist* locus mediates *Tsix* function in embryonic stem cells. *Mol Cell Biol* 21: 8512-8520.
21. Sun BK, Deaton AM, Lee JT (2006) A transient heterochromatic state in *Xist* preempts X inactivation choice without RNA stabilization. *Mol Cell* 21: 617-628.
22. Lee EC, Yu D, Martinez de Velasco J, Tessarollo L, Swing DA, et al. (2001) A highly efficient *Escherichia coli*-based chromosome engineering system adapted for recombinogenic targeting and subcloning of BAC DNA. *Genomics* 73: 56-65.
23. Plath K, Fang J, Mlynarczyk-Evans SK, Cao R, Worringer KA, et al. (2003) Role of histone H3 lysine 27 methylation in X inactivation. *Science* 300: 131-135.

Supplementary Data



Supplementary Figure 1. XCI in RP24-240J16 transgenic male ES cell lines
A) Copy number determination and quantification of the percentage of cells that initiated XCI at day 3 of differentiation in 1.3 male ES cell lines transgenic for RP24-240J16.
B) DNA FISH analysis with a RP24-240J16 BAC probe (FITC) and an X chromosome paint probe (Cy3), showing the autosomal integration of the BAC in J1 transgenic lines 6 and 8. DNA is stained with DAPI.

A ♂

RP24-180B23, male ES 1.3				
line	copy nr	% Xist autosomal	% Xist mouse	n
1	+	8%	0%	90
3	+	10%	0%	455
18	+	3%	0%	77
21	+	12%	0%	112
25	+	16%	0%	272

CTD2183M22, male ES 1.3				
line	copy nr	% XIST autosomal	% Xist mouse	n
1	2	0%	0%	125
3	2	0%	1%	101
5	2	40%	0%	192
6	2	14%	0%	116
7	3	0%	2%	124
8	1	38%	0%	240
9	1	31%	0%	189

CTD2183M22, male ES 1.3				
line	copy nr	% XIST autosomal	% Xist mouse	n
10	1	0%	0%	118
11	4	60%	0%	224
14	1	0%	0%	122
15	1	49%	0%	212
16	2	0%	0%	140

B ♂

RP23-447O10, male ES J1			
line	copy nr	% Xist	n
10	2	0%	73
14	5	0%	46

RP23-100E1, male ES J1			
line	copy nr	% Xist	n
2	2	0%	>100
3	2	0%	>100
4	2	0%	>100
14	3	0%	112
15	3	0%	143

CT7-474E4, male ES 1.3			
line	copy nr	% Xist	n
2	2	0%	>100
3	2	0%	>100
11	2	0%	94
13	4	0%	85

RP24-244E13, male ES J1			
line	copy nr	% Xist	n
4	3	0%	>100
7	2	0%	>100
14	2	0%	>100
15	2	0%	>100

C ♀

RP23-100E1, female ES F1 2-1			
line	copy nr	% 2xXist	n
5	3	0%	110
8	12	0%	61
10	2	1%	177

CT7-474E4, female ES F1 2-1			
line	copy nr	% 2xXist	n
2	+	1%	117
3	+	2%	70
4	+	0%	90
5	+	1%	72
6	+	1%	133

RP24-244E13, female ES F1 2-1			
line	copy nr	% 2xXist	n
1	+	2%	49
2	+	4%	49
3	+	2%	43
4	+	0%	40
13	+	0%	38
14	+	0%	40

Supplementary Table 1. XCI in BAC transgenic male and female ES cell lines

- A)** Copy number determination and quantification of the percentage of cells that show accumulated *Xist* and/or *Xist* at day 3 of differentiation in male ES cell lines transgenic for RP24-180B23 and CTD2183M22. (+), Integration confirmed by DNA FISH only.
- B)** Copy number determination and quantification of the percentage of cells that initiated XCI at day 3 of differentiation in male ES cell lines transgenic for RP23-447O10, RP23-100E1, CT7-474E4, and RP24-224E13.
- C)** Copy number determination and quantification of the percentage of cells that initiated XCI on two X chromosomes at day 3 of differentiation in female ES cell lines transgenic for RP23-447O10, CT7-474E4, and RP24-224E13. (+), Integration confirmed by DNA FISH only.



RP23-7K14, male ES J1			
line	copy nr	% Xist	n
17	2	9%	142
18	2	2%	205

RP23-138O4, male ES J1			
line	copy nr	% Xist	n
6	5	5%	377
9	2	5%	320
13	4	6%	228

RP23-25P18, male ES J1			
line	copy nr	% Xist	n
1	2	0%	>100
2	2	0%	>100
3	2	0%	>100
4	2	0%	>100
10	2	0%	>100
13	8	0%	>100
16	12	0%	>100
23	5	0%	>100

RP23-288K24, male ES J1			
line	copy nr	% Xist	n
2	3	0%	140
3	3	0%	106
5	3	0%	102
13	15	0%	122
16	1	0%	109

RP23-463H23, male ES J1			
line	copy nr	% Xist	n
2	2	0%	140
3	3	0%	106
5	2	0%	102
13	15	0%	122
16	2	0%	109

RP23-36C20, male ES J1			
line	copy nr	% Xist	n
1	6	0%	133
2	3	0%	111
3	3	0%	92
15	3	0%	75

Supplementary Table 2. XCI in BAC transgenic male ES cell lines covering part of BAC RP24-240J16
Copy number determination and quantification of the percentage of cells that initiated XCI at day 3 of differentiation in J1 male transgenic RP23-7K14, RP23-138O4, RP23-25P18, RP23-288K24, RP23-463H23 and RP23-36C20 ES cell lines.

A

RP24-240J16, male ES 1.3			
line	copy nr	% Xist	n
2-16	2	0%	105
2-21	2	9%	58

RP24-240J16ΔRnf12(sense), male ES 1.3			
line	copy nr	% Xist	n
16	2	0%	121
19	2	0%	116
20	13	0%	150
21	2	0%	136
23	4	1%	156
24	3	0%	162

RP24-240J16ΔRnf12(antis.), male ES 1.3			
line	copy nr	% Xist	n
1	2	0%	101
5	3	0%	121
6	4	0%	114
9	6	0%	136
11	3	0%	133
12	6	1%	113
13	2	0%	114
14	2	0%	107
15	2	0%	108
16	5	0%	108
17	2	0%	147
19	5	1%	139
22	3	1%	105

B

RP24-240J16, ♀ ES 30Δ1			
line	copy nr	% 2xXist	n
2-2	3	2%	232
2-3	3	8%	79
2-5	3	4%	117
2-6	5	7%	105

RP24-240J16ΔRnf12(sense), ♀ ES 30Δ1			
line	copy nr	% 2xXist	n
1	3	0%	63
3	3	0%	127
6	3	0%	134

RP24-240J16ΔRnf12(antis.), ♀ ES 30Δ1			
line	copy nr	% 2xXist	n
1	5	1%	134
3	3	0%	114
7	6	0%	121

Supplementary Table 3. XCI in BAC transgenic RP24-240J16 and RP24-240J16ΔRnf12 male ES cell lines

A) Copy number determination and quantification of the percentage of cells that initiated XCI at day 3 of differentiation in 1.3 male transgenic RP24-240J16, RP24-240J16ΔRnf12(sense), and RP24-240J16ΔRnf12(anti sense) ES cell lines.

B) Copy number determination and quantification of the percentage of cells that initiated XCI at day 3 of differentiation in 30Δ1 female transgenic RP24-240J16, RP24-240J16ΔRnf12(sense), and RP24-240J16ΔRnf12(anti sense) ES cell lines.



it



5'

Chapter 5



***Xist* RNA is confined to the nuclear territory of the silenced X chromosome throughout the cell cycle**



it



Xist

Iris Jonkers, Kim Monkhorst, Eveline Rentmeester, J. Anton Grootegoed, Frank Grosveld and Joost Gribnau

transcription locus



it



5'



Published in Mol Cell Biol. 2008 Sep;28(18):5583-94.

Abstract

In mammalian female cells one X chromosome is inactivated, to prevent a dose difference in expression of X-encoded proteins between males and females. *Xist* RNA, required for X chromosome inactivation (XCI), is transcribed from the future inactivated X chromosome (Xi) where it spreads in *cis*, to initiate silencing. We have analyzed *Xist* RNA transcription and localization throughout the cell cycle. It was found that *Xist* transcription is constant and that the mature RNA remains attached to the Xi, throughout mitosis. Diploid and tetraploid cell lines with an MS2-tagged *Xist* gene were used to investigate spreading of *Xist*. Most XXXX_{MS2} tetraploid mouse ES cells inactivate the X_{MS2} chromosome and one other X chromosome. Analysis of cells with two Xi's indicates that *Xist* RNA is retained by the Xi of its origin, and does not spread in *trans*. Also in XX_{MS2} diploid mouse ES cells with an autosomal *Xist* transgene, there is no *trans* exchange of *Xist* RNA from the Xi to the autosome. We propose that *Xist* RNA does not dissociate from the Xi of its origin, which precludes a model of diffusion-mediated *trans* spreading of *Xist* RNA.

Introduction

During embryonic development of female mammals, one of the two X chromosomes is silenced in all somatic cell lineages. X chromosome inactivation (XCI) is a mechanism to compensate for the difference in gene expression from sex chromosomes between males and females. In mice, XCI is initiated at 5.5 dpc, after which the proliferating cells clonally propagate the inactivated X (Xi) through many cell cycles. A single locus on the X chromosome, the X chromosome inactivation centre (XIC), is essential for XCI and is home to the *Xist* gene, one of the main regulators in the process. *Xist* does not encode a protein, but is transcribed into a functional RNA that is sufficient for, and necessary to silencing. *Xist* RNA spreads in *cis* over the X chromosome upon the onset of X inactivation. This RNA contains eight different repeat domains, most of which play a redundant role in the localization of the *Xist* RNA on the Xi, although the exact mechanism of its association with the Xi is not known. One repeat domain of *Xist* RNA, the A-repeat transcribed from exon1, is required exclusively for X chromosome silencing. Deletion studies show that loss of this repeat does not interfere with localization of the *Xist* RNA, but completely abolishes the silencing process [1].

After establishment of XCI, the silenced state of the Xi is fixed by DNA methylation and many chromatin modifications, including tri-methylation of H3K27 (H3K27me3), ubiquitylation of H2A, hypoacetylation of histones, and accumulation of macroH2A. The Xi also starts DNA replication in late S phase and its silenced state is propagated after every cell cycle. This phase of XCI is referred to as the maintenance phase [2,3,4].

Despite many studies on the function of *Xist* RNA, it is still not clear how *Xist* RNA is restricted to the Xi. Thus far, no proteins involved in recruitment of *Xist* RNA to DNA have been identified. It has been hypothesized that *Xist* RNA is targeted to the Xi through LINE1 repeats, which are more abundant on the X chromosome than on autosomes [5,6,7]. This would be in agreement with the observation that *Xist* RNA spreading into an autosomal region that has a low density of LINE1 repeats, in cases of X-autosomal translocations, is hampered [8,9]. For silencing of the Xi, sufficient amounts of *Xist* RNA have to be bound to the Xi only, and after initiation of XCI the *Xist* RNA cloud is remarkably stable. Interestingly, when the nucleus of a cell with completed X inactivation is depleted of DNA and chromatin by DNaseI treatment and salt extraction, *Xist* RNA still remains in place, suggesting that *Xist* RNA localization is facilitated by the nuclear matrix [10]. This hypothesis is underlined by the observations that the Xi co-localizes with the well-known nuclear scaffold component SAF-A and that deletion of the RNA binding domain of SAF-A abolishes this co-localization [11,12]. It is unclear, however, whether loss of RNA binding activity of SAF-A also results in loss of *Xist* RNA from the Xi. Furthermore, Zhang et al. [13] have shown that, during S phase of the cell cycle, the nuclear position of the Xi shifts from perinuclear to perinucleolar, indicating that Xi interacts with structural components of the nucleus, potentially in the form of interaction with a nuclear matrix and through the action of *Xist* RNA. Although *Xist* RNA is confined to the Xi which is stably propagated to daughter cells, several reports have indicated that *Xist* RNA dissociates from the Xi around telophase of mitosis. The *Xist* cloud, as visualized by fluorescent in situ hybridisation (FISH), persists into metaphase of mitosis [9] but is eventually lost from the Xi at telophase, after which it can be seen as distinct spots floating in the nucleoplasm [9,14,15]. This would indicate that *Xist* RNA is absent during some time from the Xi and diffuses through the cell. We aimed to reinvestigate these dynamic aspects of *Xist* RNA, using new methods. Transcription and localization of *Xist* were monitored throughout the cell cycle, in differentiated mouse ES cells. Using diploid and tetraploid female ES cells with a modified *Xist* gene encoding tagged *Xist* RNA, and cells carrying an autosomal *Xist* transgene, we obtained evidence that *Xist* RNA does not dissociate from its site of origin, where it is confined to the nuclear territory of the silenced X chromosome throughout the cell cycle.

Materials and Methods

Generation of the F1 2-1 MS2 cell line

The MS2 lox-neo-lox targeting vector was created by insertion of a lox-neo-lox resistance cassette into the unique HindIII site in *Xist* exon7 of pBgIII5k [16], of which *Xist* exons 3-6 were removed with a PstI/ClaI digest. Sixteen MS2 repeats, which were

generated by duplication of two tandem repeats of 8 MS2 hairpin sequences [17], were inserted in sense orientation in the unique BamHI site present in the polylinker of the neo resistance cassette. For targeting we used the polymorphic *Mus musculus*/*Mus castaneus* F1 2-1 ES cell line [18] and the resistance cassette was removed by transient Cre-expression.

Cell culture

ES cells were differentiated into embryoid bodies with EB medium (Iscoves's modified Dulbecco's medium (IMDM)-glutamax supplemented with 15% v/v fetal calf serum, 1% v/v penicillin/streptomycin, 1% v/v non-essential amino acids, 0.5 mg/ml ascorbic acid, and 0.038 µl/ml monothioglycerol) on non-gelatinised bacterial dishes. For FISH analysis, the differentiated cells were trypsinised and plated onto gelatinised glass cover slips one day before fixation. For 5-bromo-2'-deoxyuridine (BrdU) incorporation, the cells were grown overnight in the presence of 10 µM BrdU (Sigma).

Generation of tetraploid ES cells

10⁶ cells of an F1 2-1 cell line with a randomly integrated puromycin resistance gene and 10⁶ cells of the F1 2-1 MS2 cell line containing a randomly integrated neomycin resistance gene were mixed and washed twice with serum-free Dulbecco's modified Eagle's medium (DMEM). We used polyethylene glycol 1500 (PEG1500, Roche) as a cell fusion agent. Cells were fused as described by the manufacturer. After fusion, the cells were seeded in ES medium with 1 µg/ml puromycin and 250 µg/ml G418, and selected for approximately 10 days until clones could be picked. Clones were tested for tetraploidy by measuring the DNA content with FACS analysis and by karyotyping.

Generation of cell lines ectopically expressing *Xist* RNA

A kanamycin/neomycin resistance cassette was integrated in BAC RP24-180B23, which contains the *Xist* gene and not *Tsix*, by lox recombination. Female 30Δ1 XX_{MS2} ES cells were transfected with the BAC that was linearized with *Sce*-I, followed by selection with neomycin. The autosomal integration site of the BAC was verified with DNA-FISH and the copy number was estimated by performing Q-PCR with primers for *Xist* and *Zfp42* on genomic DNA of the clones.

Karyotyping

Cells were grown in ES medium and blocked in metaphase by addition of 12 µl/ml Karyomax (Gibco) 1 hr before harvesting. The cells were trypsinised, resuspended

in 0.075 M KCl at 37 °C, centrifuged and fixed in 5 volumes of 0.075 M KCl and 1 volume of fixative (methanol/acetic acid 3:1). After centrifuging the cells, the pellet was washed three times in fixative, and stored. The cells were spotted onto slides, air-dried, stained with DAPI and analysed.

Cell cycle synchronisation

F12-1 cells were synchronised with mimosine according to Krude et al. [19], with slight modifications. Cells were differentiated as described above, trypsinised at day 3 of differentiation, and plated onto gelatin-coated plates for the RNA and FACS samples and on gelatin-coated coverslips for the RNA-FISH samples. Cells were blocked for ~16 hrs with 1 mM mimosine, and released in EB medium after washing twice with PBS. Every two hours, samples were taken for FACS analysis, RNA isolation and RNA-FISH over a period of 16 hrs. We analysed day 4 differentiated ES cells, because ES cells become insensitive to mimosine later during EB differentiation.

FACS analysis

Synchronised cells were trypsinised, washed once with PBS, and fixed for two hours in 100 µl PBS and 900 µl 70% EtOH at 4 °C. After fixation, the cells were washed with PBS and incubated 3 hrs in detection buffer (0.1% Triton X-100; 20 mg/L propidium iodide; 0.2 g/L RNase). The DNA content was measured on a FACScan (Becton Dickinson).

Allele-specific and quantitative PCR

RNA was isolated with Trizol (Invitrogen), and 2 µg RNA was DNase treated and reverse-transcribed with Superscript III (Invitrogen).

Allele-specific RT-PCR was performed with primers spanning a length polymorphism identifying the 129 and *M. castaneus* Xist RNA (forward 5'-ACTGGGTCTTCAGCGTGA-3', reverse 5'-GCAACAACGAATTAGACAACAC-3').

Quantitative PCR was performed with primers detecting Xist mRNA spanning an exon-exon junction (forward 5'-TACTTCAAGATGCACTGCTACCC-3', reverse 5'-CTTTGGGGAAGGGTAATTTGG-3'), Xist primary RNA spanning an intron-exon junction (forward 5'-GTTCTTACCACCAATTGAAAACG-3', reverse 5'-CAAAACAGACTCCAAATTCATCC), and primers detecting beta-actin mRNA as amplification control (forward 5'-ACTATTGGCAACGAGCGGTTC-3', reverse 5'-AGAGGTCTTTACGGATGTCAACG).

The copy number of the B23 BAC was determined with Q-PCR on gDNA of the targeted cell lines compared to WT gDNA of a diploid XX cell line with the Xist primary RNA primerset and control primerset over the autosomal Zpf42 gene

(forward 5'- GCACCCATATCCGCATCCAC- 3', reverse 5'-GCATTCTTCCCGGCCTTTG-3').

DNA and RNA-FISH

Coverslips with cells obtained during cell synchronisation were fixed 10' with 4% PFA/PBS and washed with 70% EtOH. Cells were made permeable by washing twice with PBS and by 5' treatment with 25 µg/ml ProteinaseK/PBS at room temperature (RT) or 4' with 0.2% pepsin at 37°C. Postfixation was performed for 5' with 4% PFA/PBS. The coverslips were washed twice with PBS and dehydrated by sequential addition of 70%, 90% and 100% EtOH. Nick-translated DNA probes were dissolved in a hybridisation mixture containing 50% formamide, 2x SSC, 50 mM phosphate buffer, pH 7.0, 10% dextran sulfate, and 100 ng/µl mouse Cot DNA to a final concentration of 1 ng/µl. The probe mix was denatured for 5 min, pre-hybridised for 45 min at 37 °C, and then applied to the slide. Slides were incubated over night in a humid chamber at 37°C.

After hybridisation, coverslips were washed once in 2x SSC and three times in 50% formamide/2x SSC, both at 37 °C, and twice in TST (0.1 M Tris, 0.15 M NaCl, and 0.05% Tween 20) at RT. Then the coverslips were incubated for 30 minutes in blocking buffer (2 mg/ml BSA in 0.1 M Tris and 0.15 M NaCl) in a humidified chamber at RT. Detection was done with subsequent incubation steps of anti-digoxigenin (Boehringer), anti-sheep (FITC; Jackson ImmunoResearch Laboratories) and anti-rabbit (FITC; Jackson ImmunoResearch Laboratories), or anti-biotin (Roche), anti-mouse (rhodamine red; Jackson ImmunoResearch Laboratories) and anti-donkey (rhodamine red; Jackson ImmunoResearch Laboratories) antibodies in blocking buffer for 30 minutes at RT. Slides were washed twice between each detection step with TST. After the last detection step, the coverslips were washed twice with TST and once with TS (0.1 M Tris, 0.15 M NaCl) and dehydrated after which they were mounted on slides with Vectashield (Vector Laboratories), and stored at 4°C.

Coverslips with cells differentiated normally as described above were washed twice with PBS and then treated for 30 seconds with cytoskeletal buffer (100 mM NaCl; 300 mM sucrose; 3mM MgCl₂; 10 mM PIPES, pH 6.8), 2 minutes with cytoskeletal buffer with detergent (100 mM NaCl; 300 mM sucrose; 3mM MgCl₂; 10 mM PIPES, pH 6.8; 0.5% TritonX-100) and 30 seconds with cytoskeletal buffer. The cells were fixed for 10 minutes in 4% PFA/PBS and stored in 70% EtOH. Hybridisation and detection were performed as described above.

Coverslips with BrdU-labelled cells were either pretreated and fixed with cytoskeletal buffer and detergent, as described above. Then, the cells were dehydrated by sequential EtOH steps. To make the BrdU accessible for the anti-BrdU antibody (Abcam) the cells were denatured. For this, 100 µl denaturing buffer

was added (70% formamide; 2x SSC; 10 mM phosphate buffer, pH7) and cells were incubated on a hotplate for 3 minutes at 85 °C, followed by 5' incubation in ice-cold 70% ethanol. Cells were again dehydrated and hybridised over night and detection was done as described above. The anti-BrdU (Abcam) and anti-rat (AMCA; Jackson ImmunoResearch Laboratories) antibodies were used for detection.

To determine the integration site of the RP24-180B23 BAC, DNA-FISH was performed. Cells were treated with Karyomax (Gibco) and fixed with methanol/acetic acid as described for karyotyping. Permeabilization was done by treating the cells 4' with 0.5% pepsin at 37°C. After dehydration of the cells, they were denatured as described for 3' at 85°C, followed by 5' incubation in ice-cold 70% ethanol. Cells were again dehydrated, and hybridisation and detection were done with the anti-biotin (Roche) and goat-anti-mouse (FITC; Jackson ImmunoResearch Laboratories).

Five different probes were used for the various experiments. *Xist* mRNA was detected with the 5.5 kb cDNA *Xist* probe which is previously described by Gribnau et al. [20]. The probe was labelled with DIG by nick translation (Roche). The probe used to identify the MS2-tagged *Xist* RNA is a 0.5 kb BamHI-HindIII fragment of pBluescript8xMS2 consisting 8 times the MS2-repeats and was labelled with biotin by nick translation (Roche). The probe to detect the primary transcript of *Xist* RNA was a combination of 6 PCR products from the primer sets intron1P1 (forward 5'-GTACGCCAAGGGTAGCAAGA-3', reverse 5'-CGTACAAAAGGCCAAATGCAA-3'), intron1P2 (forward 5'-TTGCATTGCTTTTGTGACG-3', reverse 5'-GCCTCCAGATGGTTTTGTGT-3'), intron1P3 (forward 5'-TTAGGAGGTGCCATCACACA, reverse 5'-GGTTCAGTGGACTGGGAGAG-3'), intron3 (forward 5'-GGGGCAAGTCAATAAAGCAC-3', reverse 5'-GAGGGGCTTGAGAGTGAAC-3'), intron5 (forward 5'-AGCTATTACGAGTACACTGTTGC-3', reverse 5'-CAAAGAACAAAAGAAGCTGTATGAA-3') and intron6 (forward 5'-GGATTTCATTTGCTGGAAG-3', reverse 5'-GGACACACCCGTCAACTCTT-3'). The PCR products were labelled with biotin by nick translation (Roche).

The RP24-180B23 BAC was labelled as a whole with biotin by nick translation (Roche). The X chromosome was detected with X chromosome paint directly labelled with Cy3 (Cambio).

Counting and imaging of cells

In the cell-synchronisation experiment, only cells with a single *Xist* RNA cloud were counted. We assumed that these cells had established XCI, whereas cells still containing a pinpoint *Tsix/Xist* signal together with a cloud had not yet completed XCI. At least 100 cells were counted at each time point for at least 2 separate experiments.

The tetraploid XXXX_{MS2} cells were counted similarly. Per separate experiment,

the number of *Xist* clouds in tetraploid XXXX_{MS2} cells was counted in at least 100 cells per cell line.

The analysis of the fluorescent intensity of the *Xist* RNA and MS2 repeats RNA-FISH signal was measured with the ImageJ programme.

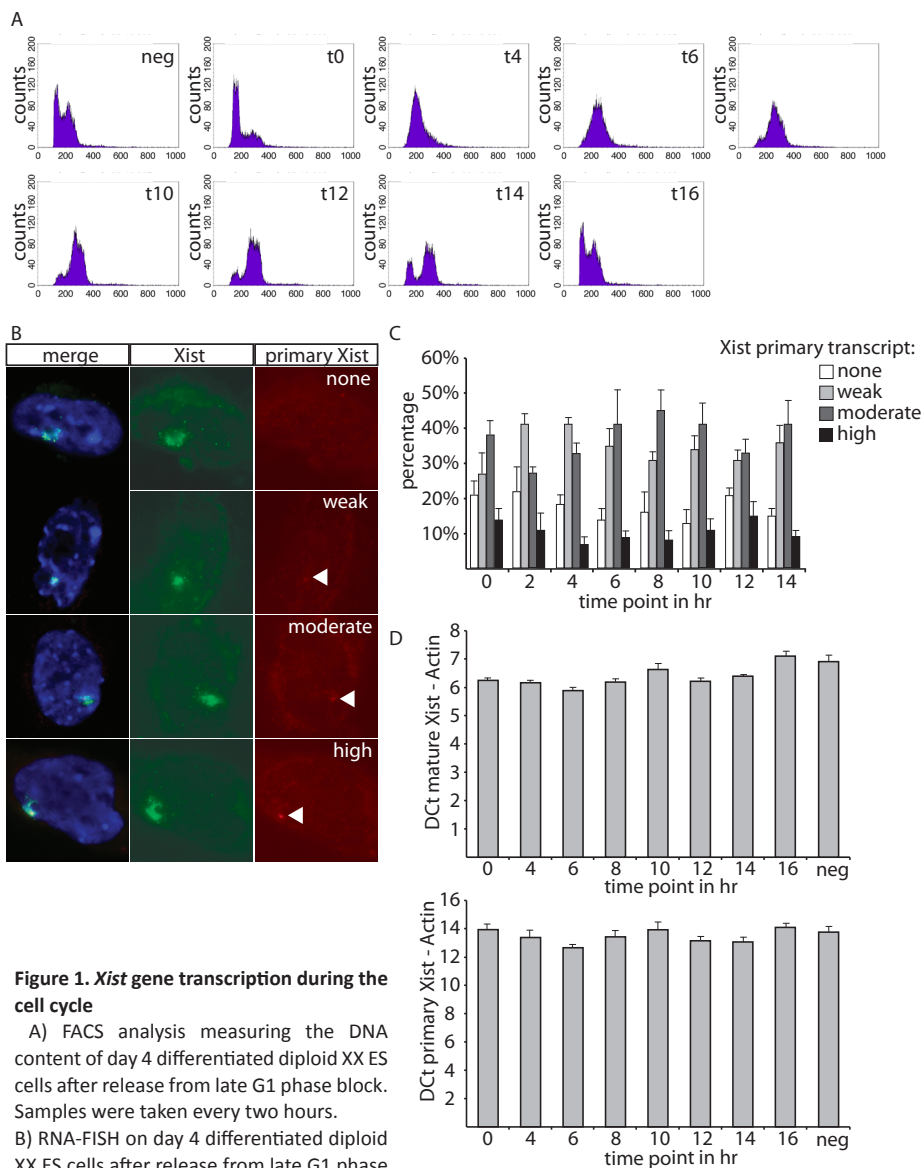
Results

Xist RNA expression throughout the cell cycle

One crucial question in understanding how *Xist* RNA is restricted to the Xi during progression through the cell cycle, is whether the Xi of the daughter cells is re-coated by *Xist* RNA still present in the nucleoplasm or by newly synthesized *Xist* RNA, after loss of *Xist* RNA during mitosis. For the latter, one would expect that the *Xist* transcription rate is increased in G1 to compensate for the loss of *Xist* RNA during each mitotic cell cycle. Moreover, DNA replication itself will reduce the concentration of *Xist* RNA per Xi during the mid to late S phase. Therefore, we studied if the transcription of *Xist* is regulated during the cell cycle, by analysis of the ratio primary/mature *Xist* transcripts. The expression profile of *Xist* was analysed, using F1 2-1 ES cells after 3 days of EB differentiation, that were synchronised in the cell cycle by treatment with mimosine for 16 hours, which blocks the cells in the G1/S transition. The cells were released from the block at day 4 of EB differentiation [19]. Samples for FACS analysis, RNA-FISH and quantitative PCR were taken every two hours for the period of approximately one cell cycle.

FACS analysis, determining the DNA content, indicated that the vast majority of the cells was synchronised in G1 and went through the cell cycle simultaneously (Fig 1A). RNA-FISH was performed with intronic and exonic *Xist* probes to visualise primary and mature transcripts. The intensity of the intronic FISH signal was taken as a measure of *Xist* expression in cells and was classified as no signal, weak, moderate, or high (Fig 1B). Only cells with an *Xist* cloud and without *Xist*/*Tsix* pinpoints were counted, because these cells have finished the XCI initiation phase and have established an inactive X [21]. Cells from four separate experiments showed no significant difference in the abundance of *Xist* primary transcripts between the different time points of the cell cycle (Fig 1C).

This was confirmed by quantitative PCR, in which the amount of primary *Xist* RNA and spliced *Xist* RNA was compared to β -actin mRNA at sequential time points after release from the cell cycle block (Fig 1D). At all time points, there was no significant change in the ratio of primary to mature *Xist* RNA amounts. We therefore conclude that the *Xist* transcription rate is stable during the cell cycle.



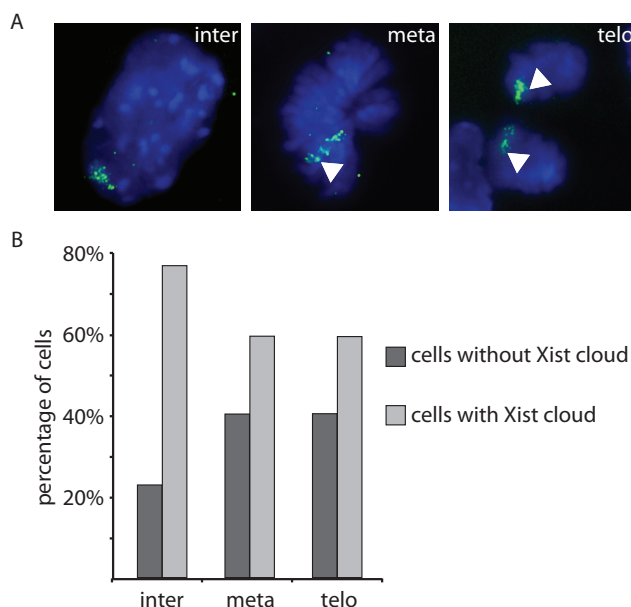


Figure 2. *Xist* clouds in 4 day differentiated F1 2-1 cells throughout the cell cycle

A) *Xist* cloud in green in an interphase and metaphase cell, followed by two clouds at telophase.

B) Percentage of F1 2-1 cells that have *Xist* cloud(s) in interphase, metaphase, or telophase cells.

***Xist* RNA associates with the Xi throughout mitosis**

From our finding that *Xist* transcription is not up-regulated at specific time points during the cell cycle, and the reported loss of *Xist* during mitosis [9,14,15], one would expect that *Xist* RNA clouds will be absent in early G1 phase of the cell cycle. This prompted us to analyze *Xist* RNA clouds in female Mefs, which were expanded *in vitro*. After *Xist* RNA FISH we detected only a very small number, less than 2% of the cells (5 out of 292 cells), without *Xist* cloud, and no cells with small pinpoint signals indicative for *Xist* accumulation just after mitosis (data not shown). These results indicate that *Xist* may not dissociate from the Xi during mitosis. Previously reported dissociation of *Xist* [9,14,15] might be the result of pre-treatment of the cells prior to RNA FISH. We therefore fixed 4 day differentiated female F1 2-1 cells in 4% paraformaldehyde in the absence of detergent or acetic acid. In this experiment, *Xist* RNA-FISH confirmed the presence of *Xist* clouds at telophase of mitosis (Fig 2A). The percentage of cells with an *Xist* cloud is decreased at metaphase and telophase, but ~60% of the cells still contained a specific *Xist* RNA signal (Fig 2B). We attribute the smaller number of *Xist* clouds to the pepsin treatment used to permeabilize the cells. Based on these results, we conclude that *Xist* most likely does not dissociate from the Xi at any phase during progression through the mitotic cell cycle.

Generation of a cell line expressing tagged *Xist* RNA

The finding that *Xist* does not dissociate from the Xi at any phase of the cell cycle would make redundant a diffusion mediated reassembly of *Xist* to the Xi after completion of mitosis. Nonetheless, it is unclear if diffusion has any role in the establishment of the *Xist* cloud.

To test whether newly synthesized *Xist* spreading along the X chromosome is diffusion mediated, or if *Xist* is retained within its own chromosomal territory, we have generated tetraploid XXXX cell lines with one X chromosome harbouring a modified *Xist* gene which is transcribed into a marked *Xist* RNA, allowing us to determine the origin of the *Xist* molecules. We started by creating a diploid XX ES line with a marked *Xist* gene, which was later used to generate tetraploid ES cells. The *Xist* gene

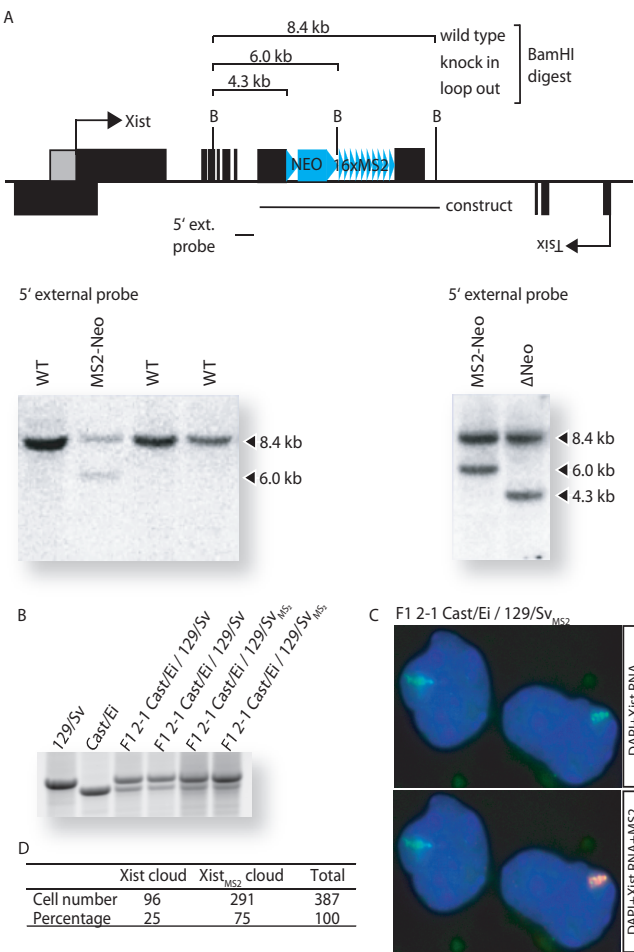


Figure 3. Construction of ES cells expressing *Xist*_{MS2} RNA

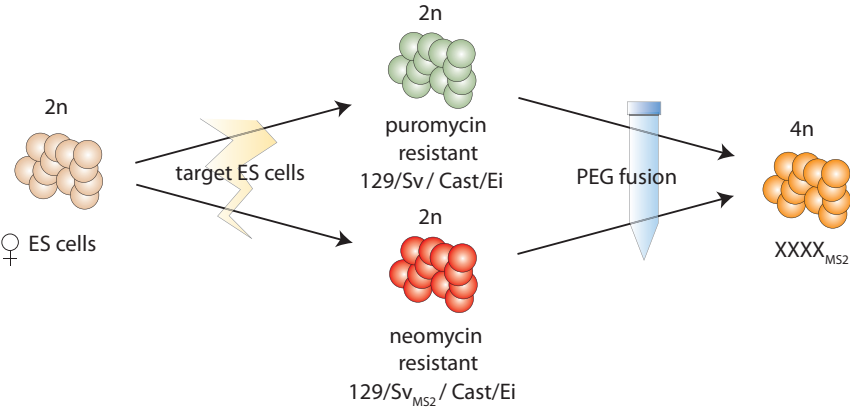
A) A construct containing 16 repeats of the MS2 sequence next to a neomycin selection marker enclosed by lox sites was integrated into exon7 of the *Xist* gene. Positive clones were selected by Southern hybridization with the 5' external probe for a BamHI digest. Loop out of the neomycin resistance cassette was detected by Southern hybridization with the same digest and probe.

B) Allele-specific RT-PCR on *Xist* RNA isolated from 7 day differentiated ES cells using a length polymorphism to distinguish whether *Xist* RNA originated from the *X*_{Cast/Ei} or the *X*_{129/Sv} allele.

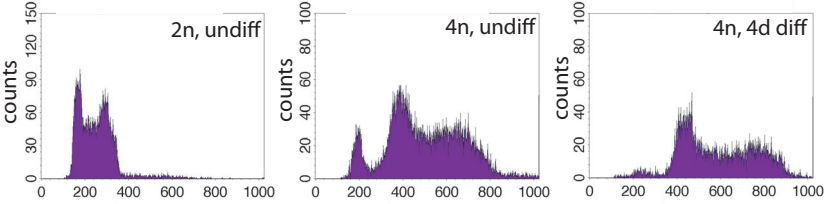
C) RNA-FISH on 10 day differentiated XX_{MS2} cells. *Xist* RNA is in green (FITC), MS2-repeats are in red (rhodamin) and DNA is stained with DAPI.

D) Quantification of the number of cells containing either an *Xist* cloud or an *Xist*_{MS2} cloud after 10 days of differentiation was determined.

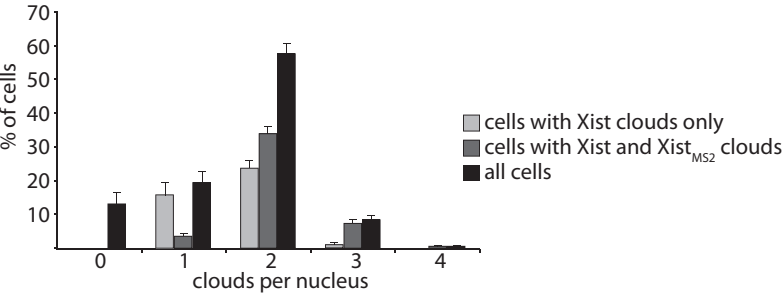
A



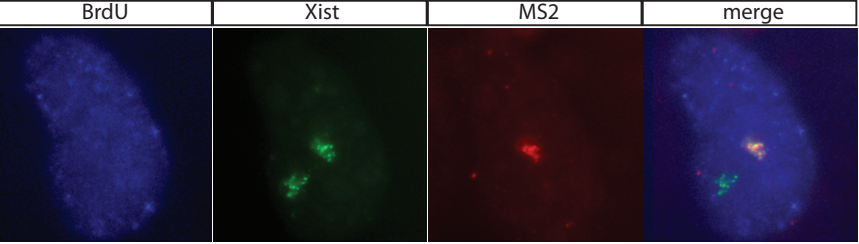
B



C



D



was labeled on one allele, by the integration of MS2 repeats in the gene. The phage specific MS2 sequence was chosen [22], because this sequence is nonfunctional in mammalian cells and therefore not likely to interfere with XCI. Sixteen tandem MS2

Figure 4. Tetraploid XXXX_{MS2} ES cells

- A) Schematic overview of the formation of tetraploid XXXX_{MS2} ES cells.
 B) FACS analysis of the DNA content of undifferentiated diploid XX ES cells (2n, undiff), undifferentiated tetraploid XXXX_{MS2} ES cells (4n, undiff), and day 4 differentiated tetraploid XXXX_{MS2} ES cells (4n, 4d diff). The 2n peak in undiff 4n cells represents male feeders.
 C) RNA-FISH with *Xist* and MS2-repeat probes was performed on day 10 differentiated tetraploid XXXX_{MS2} ES cells. The percentage of cells with a certain number of *Xist* clouds was counted and depicted in black bars. The percentage of cells containing wild type *Xist* RNA clouds only are depicted in the light grey bars and the cells containing no, one, or more wild type *Xist* RNA clouds together with an *Xist*_{MS2} RNA cloud are depicted in the dark grey bars.
 D) *Xist* clouds in tetraploid XXXX_{MS2} ES cells contain either *Xist* or *Xist*_{MS2}. RNA-FISH on day 7 differentiated tetraploid XXXX_{MS2} ES cells after overnight incorporation of BrdU. The panels show incorporation of BrdU (blue with cascade blue), *Xist* RNA (green with FITC) and *Xist*_{MS2} RNA (rhodamin red).

repeats were inserted into exon7 of the *Xist* gene on the 129/Sv allele of an F1 2-1 *Mus musculus* / *Mus castaneus* (129/Sv / Cast/Ei) ES cell line. After verification of the right insertion, the neomycin resistance cassette was excised with transient Cre-recombinase expression (Fig 3A).

XCI was analyzed in the mutated XX_{MS2} cell line by differentiation of the cells into embryoid bodies (EBs). No increased cell death of the XX_{MS2} cell line was observed after EB differentiation (data not shown), indicating that XCI was functional. RNA-FISH with *Xist* and MS2 probes on XX_{MS2} cells that were differentiated for 10 days showed that these cells either had an *Xist* or an *Xist*_{MS2} cloud (Fig 3C).

We tested whether insertion of the MS2-repeat had any effect on XCI by measuring the ratio of tagged and WT Xi's. The X_{Cast/Ei} allele and X_{129/Sv} allele of the F1 2-1 cell line are not equally inactivated, because both X chromosomes harbour different X chromosome controlling elements (Xce). Since the X_{Cast/Ei} allele in the F1 2-1 cell line contains a strong Xce^c and the targeted X_{129/Sv} allele a weak Xce^a, the X_{129/Sv} allele is inactivated in 70% of the cells [23]. Allele-specific RT-PCR on *Xist* using a length polymorphism to distinguish the X_{Cast/Ei} and the X_{129/Sv} alleles indicated that skewing of XCI was not affected by insertion of the repeats (Fig. 3B). Determination of the number and origin of Xi's in day 10 differentiated cells confirmed skewing towards the X_{129/SvMS2} allele (Fig 3D).

XCI in tetraploid XXXX_{MS2} cells

To study the dynamics of the intra-nuclear localization of *Xist* RNA throughout the cell cycle, a tetraploid XXXX_{MS2} cell line was generated. These cells preferentially inactivate two X chromosomes instead of one [24], so *Xist* RNA is transcribed from two different Xi's. The MS2-tagged allele allows distinction of the origin of *Xist* RNA in an *Xist* cloud.

To obtain the tetraploid cell line, a neomycin resistance cassette was randomly integrated into the XX_{MS2} cell line and fused with an XX ES cell line containing

a puromycin resistance cassette. After PEG1500 mediated fusion, XXXX_{MS2} tetraploid ES cells were selected with puromycin and neomycin double selection (Fig 4A). The DNA content of the double resistant XXXX_{MS2} tetraploid cell lines was verified by FACS analysis before and after differentiation, and this analysis indicated that our cell lines were 4n and stable throughout differentiation (Fig 4B). This was confirmed by karyotyping, in which we counted the number of chromosomes in metaphase spreads (data not shown). To test if the tetraploid XXXX_{MS2} cell lines initiated XCI normally, we differentiated the cells for 7 days and determined the number of *Xist* and *Xist*_{MS2} clouds. We found that almost 60% of the cells had two *Xist* clouds at day 7, which is in agreement with previous data for tetraploid ES cells without MS2 repeats [24]. The fact that not all cells have a XaXaXiXi pattern can be attributed to stochastic XCI and loss of X chromosomes [24]. There is, however, no indication that the total number of X chromosomes within one nucleus has any effect on binding and spreading of *Xist* RNA during mitosis or interphase.

***Xist* spreading is not diffusion mediated**

Examination of *Xist* and *Xist*_{MS2} clouds of the XXXX_{MS2} tetraploid cell lines in cells with clearly distinguishable Xi's, by RNA-FISH using *Xist* and MS2 specific probes, indicated that *Xist* clouds from wild type Xi's never contain *Xist*_{MS2} RNA from the targeted Xi (Fig 5A). After labelling of our cells with BrdU 24 hours prior to fixation, we found that the same holds true for XaXaXiXi_{MS2} cells that went through mitosis, as determined by immuno-RNA-FISH detecting *Xist*, MS2, and BrdU (Fig 4D). This suggests that *Xist* RNA is directly retained to the Xi from which it is transcribed, and does not diffuse through the nucleus to bind to other Xi's. Thus, *Xist* RNA is present on an Xi not because it is the only entity in the cell capable of binding *Xist* RNA, due to epigenetic modifications of the Xi chromatin, but because it does not dissociate from the Xi.

In some cells, *Xist* clouds were located close together and could only be distinguished as two separate clouds because one was tagged with MS2 repeats (Fig 5B, C). This was the case in 8% of the cells that had two or more clouds of which one *Xist* cloud was MS2-tagged (Fig 5D). To see if this result may point to a targeted and functional association between the two clouds, as opposed to random non-functional association, we performed a simplified mathematical calculation based on literature derived data showing that the probability of two Xi's being in close proximity to each other is also 8% (Supplementary data I). Therefore, our results are feasible and seem to reflect a random positioning of the Xi's in the periphery of the nucleus.

Intriguingly, in about half the cells that had clouds located in close proximity, the *Xist*_{MS2} RNA cloud of the targeted Xi seemed to overlap the *Xist* cloud of the wild type Xi, as can be judged by merging the *Xist* signal and the MS2 signal from

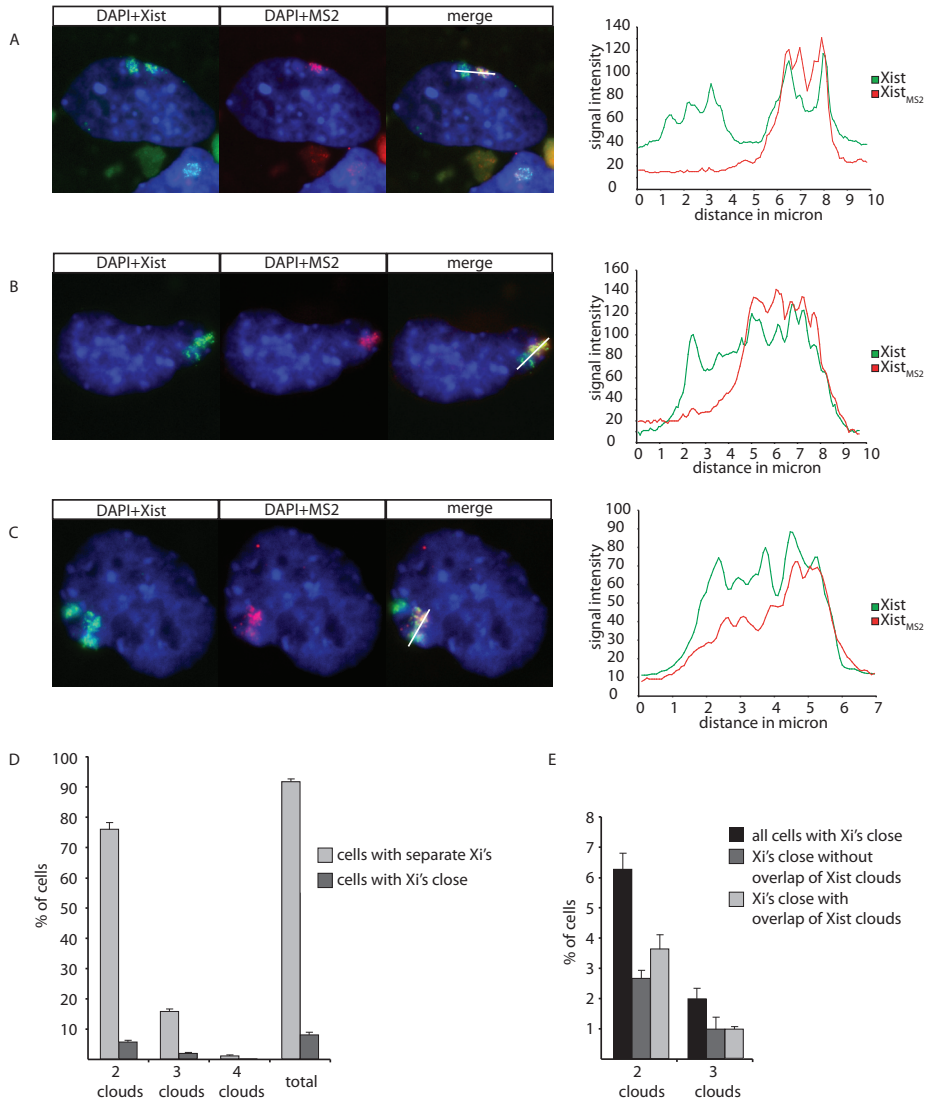


Figure 5. *Xist* and *Xist*_{MS2} clouds in close proximity

A, B, C) The left panels show RNA-FISH on day 7 differentiated tetraploid XXXX_{MS2} ES cells showing DNA (blue with DAPI), *Xist* RNA (green with FITC) and *Xist*_{MS2} RNA (rhodamin red). The right panels show the intensity of the *Xist* and *Xist*_{MS2} signals, measured along the indicated white line across both *Xist* clouds.

A) a cell with two separate *Xist* clouds;

B) a cell with two *Xist* clouds in close proximity to each other but without overlap;

C) a cell with three *Xist* clouds, two of which are adjacent to each other and have overlapping *Xist* clouds;

D) Percentage of cells that have separate *Xist* clouds (in light grey bars) or *Xist* clouds in close proximity to each other (in dark grey bars);

E) Percentage of the cells with *Xist* clouds in close proximity to each other that have non-overlapping or overlapping *Xist* clouds.

RNA-FISH experiments (Fig 5C, 5E). This result might suggest that *Xist* RNA is able to spread in *trans* when nuclear territories of two Xi's are in close proximity to each other. However, two Xi's and their respective *Xist* clouds may share the same nuclear territory without any inter-chromosomal exchange of *Xist* RNA. Indeed, no cells were found with two MS2-labeled *Xist* clouds, and only cells with two Xi's in close proximity to each other show overlap of *Xist* clouds, which supports the hypothesis that *Xist* RNA does not leave the Xi of its origin.

Ectopic *Xist* expression on autosomes

From the above, we conclude that *Xist* RNA is directly bound to the Xi from which it is transcribed. To study whether this retention of *Xist* to the X chromosome requires specific X-chromosomal *Xist* binding sites which are not abundant on autosomes, we generated transgenic XX_{MS2} ES cells with an autosomal BAC transgene containing the *Xist* gene, but not *Tsix*. These cell lines allow us to compare *Xist* retention on an X chromosome and an autosome within the same cell. A kanamycin/neomycin resistance cassette was integrated in the *Xist* containing BAC by lox recombination, and female XX_{MS2} ES cells were transfected followed by selection with neomycin. The autosomal integration site of the BAC was verified with DNA-FISH (Fig S1A) and the copy number was estimated by performing Q-PCR with primers for *Xist* and the autosomal *Zfp42* gene as a normalization control for diploidy on genomic DNA of the clones (Fig S1B). High copy transgenic cell lines (30Δ1 4, 8, 9 and 10) were differentiated for 4 days and subjected to RNA-FISH with *Xist* and MS2 specific probes which allow discrimination between the transgene (*Xist* only) and endogenous *Xist* (*Xist* only for *Xist* originating from the Cast/Ei chromosome, and *Xist* and MS2 positive for *Xist* originating from the129/SV chromosome). The number of *Xist* clouds in cells was counted for each cell line, in which an extra cloud would most likely result from the autosome with the transgenic *Xist* gene. All cell lines showed a significant percentage of cells with double clouds from ~50% (30Δ1 9) up to ~80% (30Δ1 8) (Fig S1C). As expected, we found that most cells of line 30Δ1 8 had inactivated the X_{MS2} chromosome and an autosome (Fig 6A, 6B). The wild type and transgenic *Xist* clouds are indistinguishable in nearly all interphase cells. In metaphase cells the autosomal *Xist* cloud is of different size than wild type *Xist* clouds, and seems to cover the entire chromosome in most cases, showing that the *Xist* clouds are of either endogenous or ectopic origin (Fig S1D, S1E, 6E). Cells with two $Xist_{MS2}$ clouds are never observed. Similar to the present findings with tetraploid $XXXX_{MS2}$ cells, we find a small but significant proportion of the *Xist* clouds in close proximity of each other. Again, approximately 50% of the clouds seemed to overlap, whereas the rest did not (Fig S2A, S2B).

Next, we analyzed binding of the transgenic *Xist* RNA to its autosome in

mitosis of day 4 differentiated 30Δ1 8 ES cells. Similar to the observed localization of endogenous *Xist* to the Xi, we found that the transgenic *Xist* RNA is present on the autosome throughout mitosis, including telophase (Fig 6C). At telophase, we found less autosomal *Xist* clouds relative to *Xist* clouds on the Xi. This difference is less pronounced in interphase or metaphase cells (Fig 6D). Increased loss of autosomally located *Xist* at telophase could represent a real loss of *Xist* during mitosis, but more likely is a consequence of removal of less stringently bound RNA in the RNA-FISH procedure (Fig 6D). Since *Xist* RNA is less tightly bound to the Xi at telophase, small

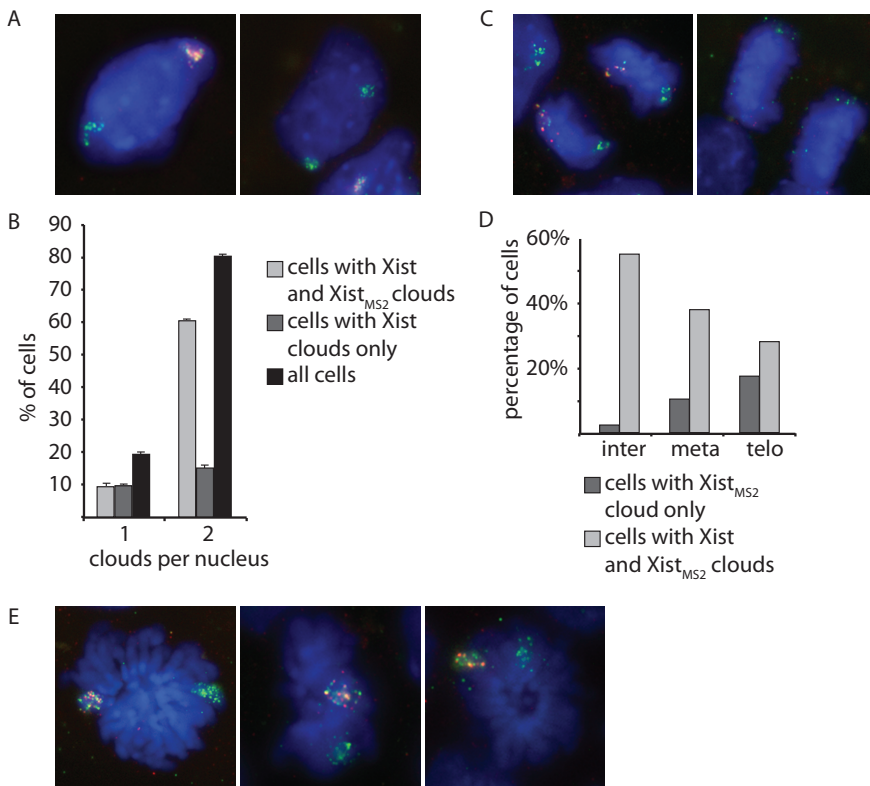


Figure 6. Transgenic *Xist* RNA expression in 30Δ1 8 cell line

A) Interphase cells with either *Xist*_{MS2} (in red) and autosomal *Xist* (green) clouds (left panel), or endogenous *Xist* and autosomal *Xist* clouds (both in green) (right panel).

B) Percentage of cells with one cloud of either *Xist* or *Xist*_{MS2}, two clouds of either *Xist*_{MS2} or autosomal *Xist*, or two clouds of either endogenous *Xist* or autosomal *Xist*.

C) Cells in telophase with *Xist*_{MS2} (red) or autosomal *Xist* (green) still attached (left panel), or with *Xist* RNA detached and floating in the nucleoplasm (right panel).

D) Percentage of cells with *Xist*_{MS2} cloud only, or both *Xist*_{MS2} and autosomal *Xist* clouds, at interphase, metaphase, or telophase.

E) Three metaphase cells showing *Xist*_{MS2} (in red) and autosomal *Xist* (green) clouds.

changes in affinity of *Xist* to the autosome compared to the Xi are likely to present itself at this stage of the cell cycle. Therefore, this finding indicates that the Xi specific chromatin state or DNA sequence do increase the binding affinity of *Xist* to the chromosome, but are not a necessity.

Taken together, *Xist* RNA expressed from an autosome can form a cloud, that is tightly bound, over the entire chromosome. This cloud is almost indistinguishable in appearance from a wild type *Xist* cloud. Only during telophase the transgenic *Xist* RNA is more prone to detach from the autosome, compared to detachment of endogenous *Xist* RNA from the X chromosome, indicating that an autosome is capable of binding *Xist* RNA, but with slightly lower affinity than the X chromosome.

Discussion

In this study, the behaviour of *Xist* RNA on the Xi was investigated during different phases of the mitotic cell cycle, in mouse ES cells that have established XCI. We found that *Xist* is retained at the Xi at all phases during mitosis, and that *Xist* transcription is constant throughout the cell cycle. For XXXX_{MS2} tetraploid cells and *Xist* transgenic XX_{MS2} cells, where one of the X chromosomes transcribes a tagged *Xist*_{MS2} RNA, it was found that *Xist*_{MS2} RNA is associated with only one *Xist* cloud, indicating that *Xist* RNA is retained by the Xi of its origin. In other words, *Xist* RNA does not leave the territory of the Xi.

***Xist* RNA is present on the Xi throughout mitosis**

Previous reports have indicated that during mitotic telophase of mouse ES cells, *Xist* RNA dissociates from the Xi [14,15] and can be detected as punctate spots floating around in the nucleoplasm. In contrast, we observed mitotic cells in telophase with *Xist* clouds present on the Xi or autosomes. We attribute this difference to the variation in procedures used to fix cells prior to RNA-FISH analysis. In previous studies [14,15] cells were pretreated with a hypotonic solution and fixed with a combination of formaldehyde and acetic acid. The *Xist* interaction with the Xi may be weakened by the chromatin compaction during mitosis, and the absence of a nuclear membrane may have facilitated loss of the *Xist* cloud during the fixation procedure. In the present study the cells were fixed with paraformaldehyde without any pretreatment, which most likely allowed *Xist* to stay attached to the Xi. Nevertheless, also in our analysis we find a decrease in the number of *Xist* clouds upon progression through mitosis, which we attribute to weakened interactions of *Xist* with either DNA or chromatin. The finding that *Xist* is more readily lost from an autosome than from Xi, in the experiments with transgenic female ES cells, suggests that this interaction is DNA mediated, since DNA sequence is the most apparent difference between

the observed autosomal *versus* X-chromosomal spreading of *Xist* RNA, at least at telophase. Nonetheless, we can not exclude a role for histone modifications, present specifically at the X chromosome prior to and after XCI, in the more efficient spreading of *Xist* RNA over the Xi [25].

***Xist* RNA retention at the Xi**

The present analysis of tetraploid XXXX ES cells and cells with autosomal *Xist* transgenes indicates that *Xist* RNA is retained at its own Xi or at its autosomal origin, and spreads only in *cis*, also when more than one Xi is present in the same nucleus. This result suggests that endogenous *Xist* RNA is restricted to the nuclear territory of its own Xi, rather than binding the Xi in *cis* or *trans* as a result of free diffusion and recognition of specific epigenetic modifications on the Xi. However, in about half of the cases when two Xi's are located close together, we found an overlap between the *Xist* clouds. A plausible explanation for this is that *Xist* RNA may spread in *trans* when the nuclear territories of two Xi's are in very close proximity to each other and stay together continuously. Indeed, separate *Xist* clouds containing *Xist*_{MS2} RNA were not found. Still, we find it more likely that the chromosome territories of Xi's sometimes intermingle but without any *trans* exchange of *Xist* RNA. Intermingling of chromosome territories has previously been described as a common feature of chromosomes in interphase cells [26].

Taken together, there is consensus that *Xist* RNA can spread in *cis* on the Xi or autosomal regions. However, as discussed above, we find that *Xist* RNA does not migrate to an adjacent Xi. In addition, *Xist* RNA does not spread to autosomal regions in *trans*, not even when there is very close proximity with the Xi. How can this be explained?

A possible model for this conundrum is that *Xist* RNA remains on the Xi in *cis* because of the high local concentration of binding sites, possibly LINE1 repeats, other DNA sequences specific for the X chromosome or specific X-chromosomal chromatin marks that are present before and after initiation of XCI [25]. The *Xist* binding sites may fold towards the *Xist* gene, binding the *Xist* RNA while it is transcribed to prevent diffusion to the (future) active X. Utilization of LINE1 repeats by the inactivation machinery is supported by studies with X:autosomal translocations, which showed that *Xist* RNA is capable of spreading in *cis* into the autosomal region, but less efficiently [8,9,27,28,29]. The efficiency with which *Xist* RNA spreads into the autosomal region seems to be correlated with the density of LINE1 repeats [6], which are good candidates for binding *Xist* RNA, because they are 1) enriched twice as much on the X chromosome as on autosomes; 2) less abundant in the pseudoautosomal region of the X chromosome and near X-linked genes that escape XCI; and 3) increased in

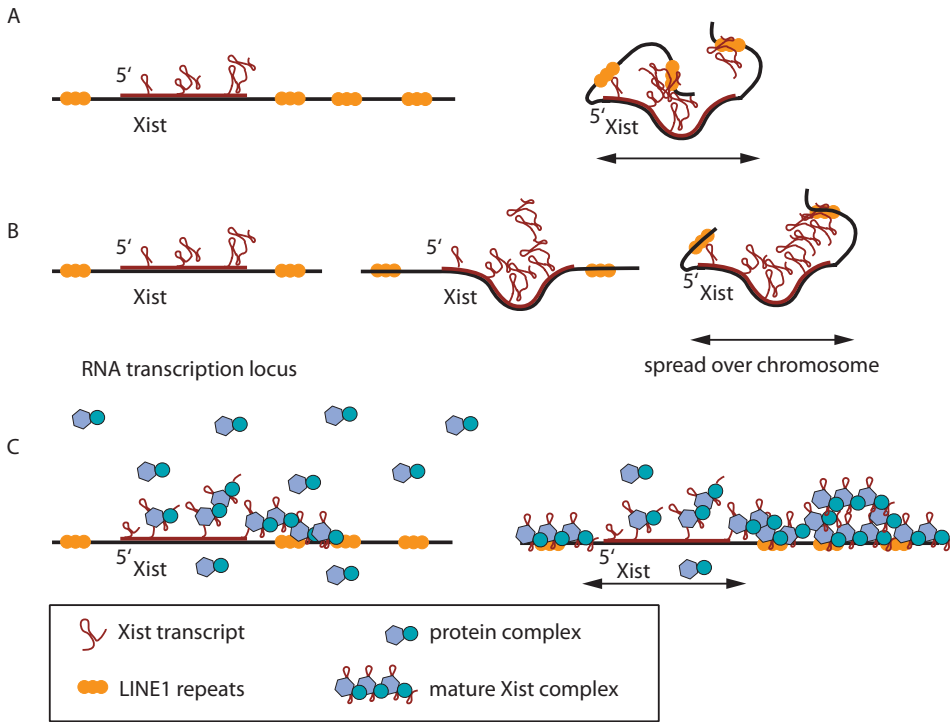


Figure 7. Schematic models for *Xist* RNA spreading in *Mus musculus*

A) *Xist*-to-DNA; *Xist* RNA binds the DNA sequence directly, and the DNA folds to capture *Xist*.

B) *Xist*-to-*Xist*; *Xist* RNA binds to itself, creating *Xist* RNA clouds that are tethered to the Xi by a DNA sequence.

C) *Xist*-to-protein-to-DNA; a protein, present in excess, captures *Xist* RNA during transcription and binds it to DNA.

abundance around the XIC [5,7]. However, for *Xist* transgenes inserted at autosomal positions, we and others have shown that *Xist* RNA spreads in *cis* [28,29], showing that even though DNA binding sites might play a role, they are not the only factor in binding the *Xist* to DNA.

In a different model, *Xist* RNA is self-interacting, forming a web of RNA molecules that remain located on the Xi and interact either with LINE1 repeats, other specific DNA sequences or chromatin marks. *Xist*-to-*Xist* interactions could already form during transcription of *Xist* on the template, because roughly 8 *Xist* molecules are simultaneously transcribed from the gene at any time during the cell cycle, thereby preventing diffusion of *Xist* away from the Xi (Supplementary data II).

Finally, lack of *trans* spreading of *Xist* RNA could also depend on the amount of *Xist* RNA transcribed, which might be limited in relation to the abundance of a putative protein that ties *Xist* RNA to the Xi, acting in synergy with the *Xist* binding sites. In this model, similar to *Drosophila* where association of Rox1 and Rox2 RNAs with

the hyper-activated X in male cells requires the MSL complex [30,31,32], a putative mammalian protein involved in binding the few hundred copies of *Xist* RNA to the X chromosome would be present in excess. Such a protein would quickly immobilise *Xist* RNA, allowing spreading across an X chromosome in *cis*, but not in *trans*. The reports that *Xist* remains present on the Xi after removal of DNA from the nucleus [10] and that *Xist* is more loosely bound to the Xi in mitosis, when a nuclear matrix is no longer present, support the hypothesis that protein-RNA interactions are involved in *Xist* localization to the Xi. If the amount of *Xist* RNA per nucleus is quite low, some 300 transcripts per nucleus, it is feasible that the highest affinity *Xist* binding sites on the X chromosome will not be saturated. This may result in preferential association of *Xist* RNA with the binding sites of the X chromosome, usually excluding autosomal regions in X:autosomal translocations in which the autosomal region is not enriched in these or comparable *Xist* binding sites. However, when *Xist* is expressed at a higher level, as is the case for most autosomal *Xist* transgenes, *Xist* RNA will be forced to spread in *cis* onto the autosomal region with *Xist* binding sites with less affinity, because the putative *Xist* binding protein will prevent *Xist* from going elsewhere.

Acknowledgements

The authors would like to thank Ken Kosik for kindly providing the MS2 repeat sequence, Thasin Stefan Barakat for technical assistance. This work was supported by HFSP-CDA, and NWO-VIDI grants.

References

1. Wutz A, Rasmussen TP, Jaenisch R (2002) Chromosomal silencing and localization are mediated by different domains of Xist RNA. *Nat Genet* 30: 167-174.
2. Plath K, Mlynarczyk-Evans S, Nusinow DA, Panning B (2002) Xist RNA and the mechanism of X chromosome inactivation. *Annu Rev Genet* 36: 233-278.
3. Heard E (2004) Recent advances in X-chromosome inactivation. *Curr Opin Cell Biol* 16: 247-255.
4. Xiao C, Sharp JA, Kawahara M, Davalos AR, Difilippantonio MJ, et al. (2007) The XIST noncoding RNA functions independently of BRCA1 in X inactivation. *Cell* 128: 977-989.
5. Bailey JA, Carrel L, Chakravarti A, Eichler EE (2000) Molecular evidence for a relationship between LINE-1 elements and X chromosome inactivation: the Lyon repeat hypothesis. *Proc Natl Acad Sci U S A* 97: 6634-6639.
6. Lyon MF (1998) X-chromosome inactivation: a repeat hypothesis. *Cytogenet Cell Genet* 80: 133-137.
7. Ross MT, Grafham DV, Coffey AJ, Scherer S, McLay K, et al. (2005) The DNA sequence of the human X chromosome. *Nature* 434: 325-337.
8. Popova BC, Tada T, Takagi N, Brockdorff N, Nesterova TB (2006) Attenuated spread of X-inactivation in an X;autosome translocation. *Proc Natl Acad Sci U S A* 103: 7706-7711.
9. Duthie SM, Nesterova TB, Formstone EJ, Keohane AM, Turner BM, et al. (1999) Xist RNA exhibits a banded localization on the inactive X chromosome and is excluded from autosomal material in cis. *Hum Mol Genet* 8: 195-204.
10. Clemson CM, McNeil JA, Willard HF, Lawrence JB (1996) XIST RNA paints the inactive X chromosome at interphase: evidence for a novel RNA involved in nuclear/chromosome structure. *J Cell Biol* 132: 259-275.
11. Fackelmayer FO (2005) A stable proteinaceous structure in the territory of inactive X chromosomes. *J Biol Chem* 280: 1720-1723.
12. Helbig R, Fackelmayer FO (2003) Scaffold attachment factor A (SAF-A) is concentrated in inactive X chromosome territories through its RGG domain. *Chromosoma* 112: 173-182.
13. Zhang LF, Huynh KD, Lee JT (2007) Perinucleolar targeting of the inactive X during S phase: evidence for a role in the maintenance of silencing. *Cell* 129: 693-706.
14. Hall LL, Lawrence JB (2003) The cell biology of a novel chromosomal RNA: chromosome painting by XIST/Xist RNA initiates a remodeling cascade. *Semin Cell Dev Biol* 14: 369-378.
15. Smith KP, Byron M, Clemson CM, Lawrence JB (2004) Ubiquitinated proteins

- including uH2A on the human and mouse inactive X chromosome: enrichment in gene rich bands. *Chromosoma* 113: 324-335.
16. Luikenhuis S, Wutz A, Jaenisch R (2001) Antisense transcription through the *Xist* locus mediates *Tsix* function in embryonic stem cells. *Mol Cell Biol* 21: 8512-8520.
 17. Rook MS, Lu M, Kosik KS (2000) CaMKIIalpha 3' untranslated region-directed mRNA translocation in living neurons: visualization by GFP linkage. *J Neurosci* 20: 6385-6393.
 18. Panning B, Dausman J, Jaenisch R (1997) X chromosome inactivation is mediated by *Xist* RNA stabilization. *Cell* 90: 907-916.
 19. Krude T (1999) Mimosine arrests proliferating human cells before onset of DNA replication in a dose-dependent manner. *Exp Cell Res* 247: 148-159.
 20. Gribnau J, Luikenhuis S, Hochedlinger K, Monkhorst K, Jaenisch R (2005) X chromosome choice occurs independently of asynchronous replication timing. *J Cell Biol* 168: 365-373.
 21. Lee JT, Davidow LS, Warshawsky D (1999) *Tsix*, a gene antisense to *Xist* at the X-inactivation centre. *Nat Genet* 21: 400-404.
 22. Peabody DS (1993) The RNA binding site of bacteriophage MS2 coat protein. *Embo J* 12: 595-600.
 23. Cattanaach BM, Rasberry C (1994) Identification of the *Mus castaneus* *Xce* allele. *Mouse Genome* 92: 2.
 24. Monkhorst K, Jonkers I, Rentmeester E, Grosveld F, Gribnau J (2008) X inactivation counting and choice is a stochastic process: evidence for involvement of an X-linked activator. *Cell* 132: 410-421.
 25. O'Neill LP, Randall TE, Lavender J, Spotswood HT, Lee JT, et al. (2003) X-linked genes in female embryonic stem cells carry an epigenetic mark prior to the onset of X inactivation. *Hum Mol Genet* 12: 1783-1790.
 26. Branco MR, Pombo A (2006) Intermingling of chromosome territories in interphase suggests role in translocations and transcription-dependent associations. *PLoS Biol* 4: e138.
 27. Keohane AM, Barlow AL, Waters J, Bourn D, Turner BM (1999) H4 acetylation, *XIST* RNA and replication timing are coincident and define X-autosome boundaries in two abnormal X chromosomes. *Hum Mol Genet* 8: 377-383.
 28. Herzing LB, Romer JT, Horn JM, Ashworth A (1997) *Xist* has properties of the X-chromosome inactivation centre. *Nature* 386: 272-275.
 29. Lee JT, Strauss WM, Dausman JA, Jaenisch R (1996) A 450 kb transgene displays properties of the mammalian X-inactivation center. *Cell* 86: 83-94.
 30. Kelley RL, Meller VH, Gordadze PR, Roman G, Davis RL, et al. (1999) Epigenetic

spreading of the *Drosophila* dosage compensation complex from roX RNA genes into flanking chromatin. *Cell* 98: 513-522.

31. Oh H, Park Y, Kuroda MI (2003) Local spreading of MSL complexes from roX genes on the *Drosophila* X chromosome. *Genes Dev* 17: 1334-1339.
32. Park Y, Kelley RL, Oh H, Kuroda MI, Meller VH (2002) Extent of chromatin spreading determined by roX RNA recruitment of MSL proteins. *Science* 298: 1620-1623.

Supplementary Data and Figures

I. Calculation of the probability of two Xi's to be in close proximity

In order to calculate the chance that two Xi's are found in close proximity in the nucleus we made the following assumptions based on previous results. It is known that the Xi's are preferably localised at the periphery of the nucleus [1,2]. Furthermore, there is no correlation between the positions of two Xi's when they are together in a nucleus [1]. Also, although the Xi is rounder and smoother than the active X, they have approximately the same volume [3]. Therefore, we assumed that the Xi's in the tetraploid XXXX_{MS2} cell line are spherical entities that are randomly distributed in the periphery of the nucleus.

Next, we started by calculating the volume of a diploid cell according to the following formula: $V = 4\pi r^3 / 3$

in which $r = 5 \mu\text{m}$ resulting in a volume of $523 \mu\text{m}^3$. Tetraploid nuclei have twice this volume, $1046 \mu\text{m}^3$, resulting in an r of $6.3 \mu\text{m}$. The volume of an X chromosome is roughly $(167 \text{ megabases} / 5.2 \text{ gigabases}) \times 523 = 168 \mu\text{m}^3$, which results in an r of $1.6 \mu\text{m}$. The chance of finding an Xi in close proximity to another X chromosome will be equal to the volume of a torus surrounding one Xi divided by the total volume of the tetraploid cell. The volume of a torus can be calculated according to the following formula: $V = 2\pi^2 Rr^2$.

in which the radius was taken equal to the distance to the center (because the Xi is located in the periphery of the nucleus). So $R=r=1.6 \mu\text{m}$, resulting in a volume for the torus of $81 \mu\text{m}^3$ in a volume of $1046 \mu\text{m}^3$ of a tetraploid nucleus, indicating that the chance that two inactive X chromosomes will be found in close proximity is roughly 8% ($81 \mu\text{m}^3 / 1046 \mu\text{m}^3$).

II. Calculation of the in *Xist* RNA in time

To calculate the initiation time of *Xist* used the following formula to iterate to 300 *Xist* transcripts that have been reported by [4] to be present in a cell:

$$X_t = X_{t-1} \cdot \frac{1}{2^{t/t_{1/2}}} + i_t, \text{ in which}$$

t is time interval

X_{t-1} is the number of transcripts at $t-1$

X_t is the number of transcripts after t

$t_{1/2}$ is the half life of *Xist*

i_t is the number of transcripts initiated in t

For our iteration we used steps of 60 minutes ($t=60$), a half life of 6 hours ($t_{1/2}=360$) and found that *Xist* has to be initiated once every 78 seconds to maintain 300 *Xist*

molecules in the nucleus. The transcription velocity is 1500 bp per minute, and it takes 15.3 minutes to finish an *Xist* transcript (the size of *Xist* is 23 kb). Therefore $15.3 \text{ minutes} / 78 \text{ seconds} = \sim 12$ *Xist* transcripts are present on the transcribed template.

1. Belmont AS, Bignone F, Ts'o PO (1986) The relative intranuclear positions of Barr bodies in XXX non-transformed human fibroblasts. *Exp Cell Res* 165: 165-179.
2. Bourgeois CA, Laquerriere F, Hemon D, Hubert J, Bouteille M (1985) New data on the in-situ position of the inactive X chromosome in the interphase nucleus of human fibroblasts. *Hum Genet* 69: 122-129.
3. Eils R, Dietzel S, Bertin E, Schrock E, Speicher MR, et al. (1996) Three-dimensional reconstruction of painted human interphase chromosomes: active and inactive X chromosome territories have similar volumes but differ in shape and surface structure. *J Cell Biol* 135: 1427-1440.
4. Sun BK, Deaton AM, Lee JT (2006) A transient heterochromatic state in *Xist* preempts X inactivation choice without RNA stabilization. *Mol Cell* 21: 617-628.

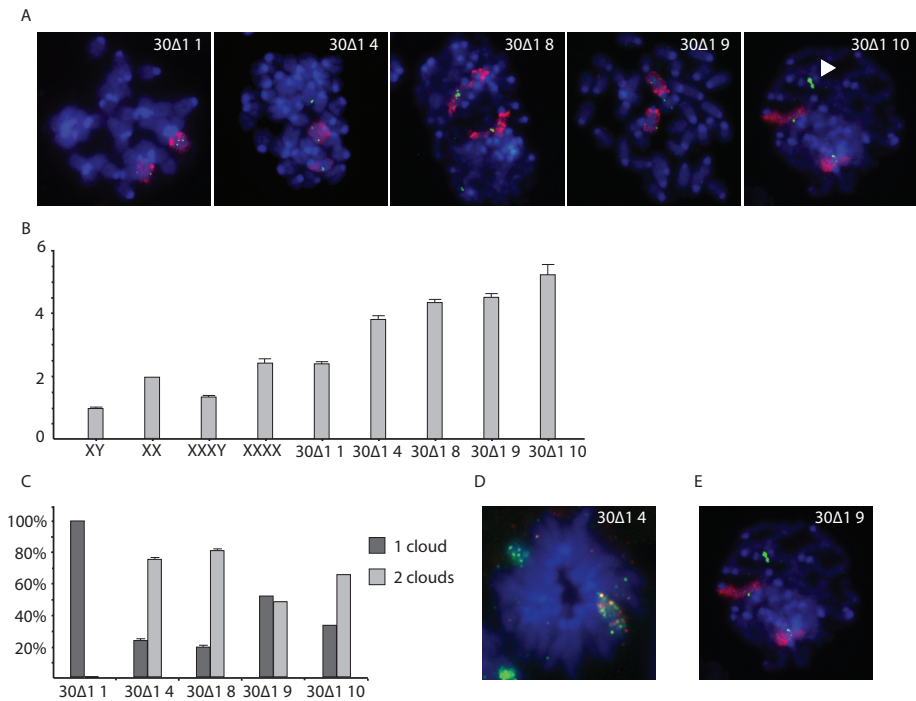


Figure S1. Overview of $X_{\text{Cast/EI129/Sv}}$ cell lines with a BAC containing the *Xist* gene which was randomly integrated.

A) DNA-FISH on the XX_{MS2} BAC cell lines. The BAC sequence is detected in green (FITC) and the X chromosome in red (Cy3). Autosomal integration sites are indicated with a white arrowhead.

B) Q-PCR with an *Xist* and the autosomal *Zfp42* gene primerset. The wild type XX F1 2-1 cell line was taken as two, so that 30Δ1 1 does not contain an extra *Xist* copy, 30Δ1 4, 30Δ1 8, 30Δ1 9 have 2 extra *Xist* copies and 30Δ1 10 has 3 extra *Xist* copies.

C) Percentage of cells of the XX_{MS2} BAC cell lines containing one or two *Xist* clouds.

D) RNA-FISH of a 30Δ1 4 cell in metaphase, *Xist* in green, MS2 in red.

E) RNA-FISH of a 30Δ1 9 cell in metaphase, *Xist* in green, MS2 in red.

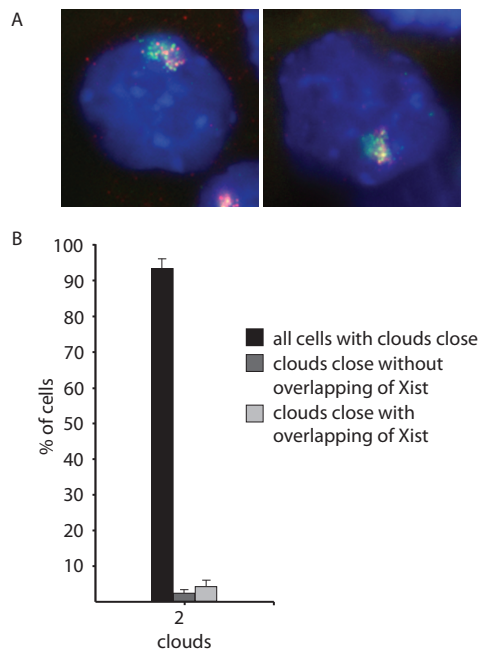


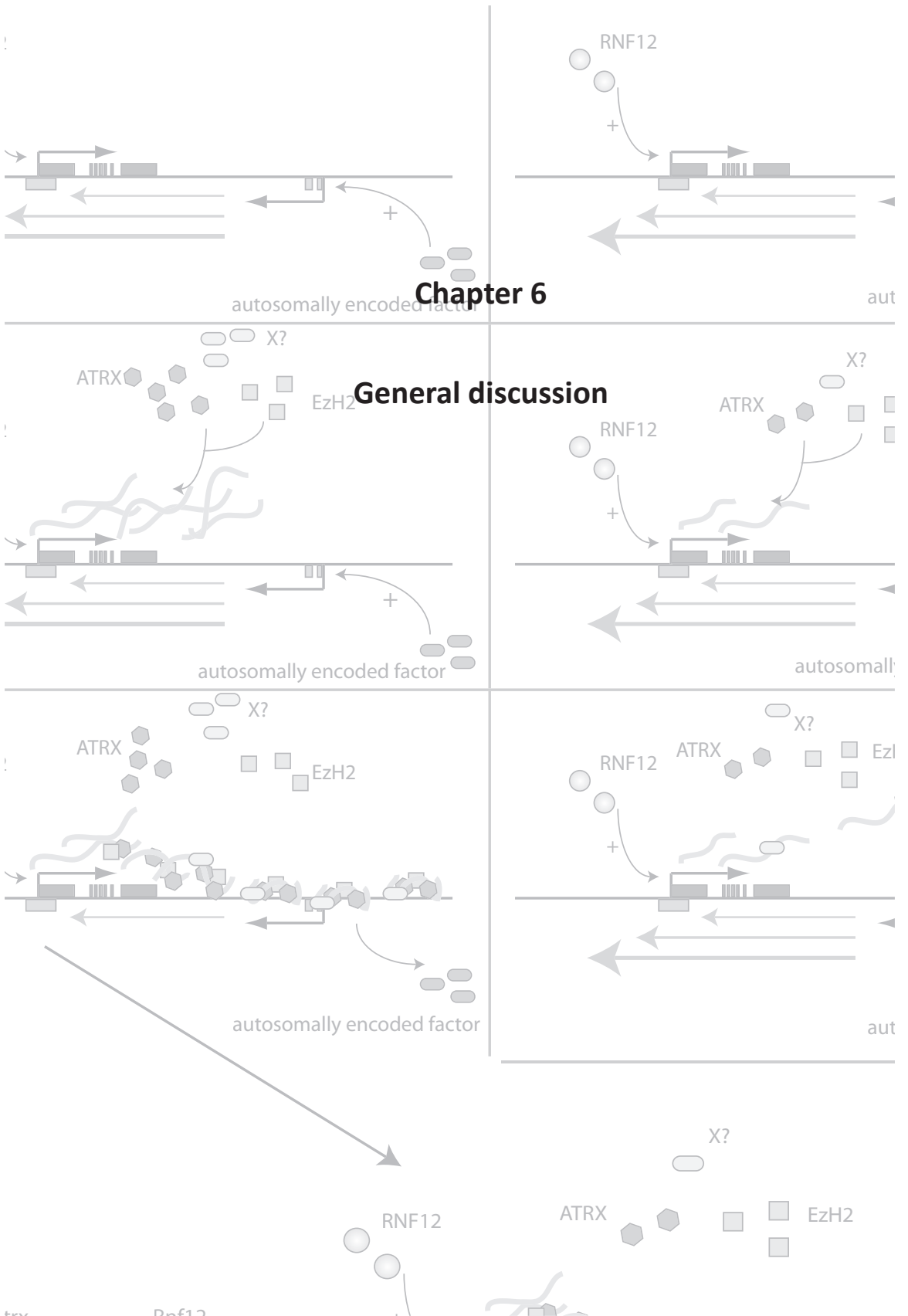
Figure S2. Cells with *Xist* clouds close together in cell line 30Δ1 8.

A) $Xist_{MS2}$ and autosomal *Xist* clouds in close proximity in interphase cells. *Xist* is labeled in green (FITC) and MS2 in red (rhodamin). The left panel shows a cell with overlapping clouds, the right panel a cell with non-overlapping clouds.

B) Percentage of cells with $Xist_{MS2}$ and autosomal *Xist* clouds separate, in close proximity without overlapping *Xist* or close together with overlapping *Xist*.

Chapter 6

General discussion



6. General discussion

6.1 A new model for initiation of XCI

A number of models regarding the XCI counting and choice process have been postulated over the years, some of which are put forward in the Introduction (Chapter 1). However, none of these models manage to explain all the experimental evidence coming from numerous deletion and overexpression studies, and a comprehensive model encompassing all experimental data is dearly needed.

In Chapter 2, we propose a stochastic model for XCI, based on outcomes of XCI that could not be explained by a deterministic model (Chapter 2). We observed that a low but consistent number of XX ES cells display two Xi's after 3 days of differentiation. All previous models depend on the assumption that the choice process is mutually exclusive, which does not fit with inactivation of both X chromosomes. To explore this finding further, we generated XXXX tetraploid ES cells to increase the number of the XCI outcomes after 3 days of differentiation. Intriguingly, all potential outcomes were observed, from no inactivated X chromosomes to all X chromosomes inactivated in a single XXXX tetraploid cell, making a deterministic model highly unlikely. Therefore, we propose a stochastic model, in which each X chromosome has a probability to become inactivated during the onset of XCI. This probability is determined by the X:autosome ratio, which ensures the ability of a cell to “count” the number of X chromosomes. How can a cell sense the X:autosome ratio? For this, an X-linked XCI-factor is needed, which acts in a dose-dependent manner to activate XCI. Because the dose of an X-linked factor will be twice as high in female XX ES cells as in male XY ES cells, the cells will have a measure of the number of X chromosomes compared to the nuclear volume, which is related to the number of autosomes. We think the X-linked factor is an activator of XCI, because a reporter gene under control of the *Xist* promoter is more highly expressed in female as in male ES cells [1]. Also, we propose the presence of an XCI repressor, most likely encoded by an autosome, providing a constant repression (threshold) of XCI in both male and female cells, which can only be overcome by a sufficient level of XCI-activator in female cells (Fig. 1A). Upon inactivation of one of the two X chromosomes, the *de novo* synthesis of the X-encoded XCI-activator will also be repressed, resulting in a drop in the concentration to the level of XCI-activator in male cells, and a block of XCI on the second X chromosome. The presence of an X-encoded XCI-activator therefore provides an intrinsic negative feedback loop that prevents most female XX cells from inactivating both X chromosomes (Fig. 1A).

At a molecular level, the X-linked XCI-activator will drive the expression of *Xist* directly or indirectly, whereas the autosomal XCI repressor will regulate *Tsix* (Fig.

1B). Upon differentiation, the XCI-activator is upregulated or activated in female cells, which results in increasingly frequent initiation of *Xist* transcription. In male cells, an increase in *Xist* transcription may also occur, but this will not be enough to overcome *Tsix* repression (it is unknown how *Tsix* represses *Xist* transcription in *cis* at the molecular level, which has been discussed in the Introduction). *Xist* RNA will spread on the X chromosome, and once it has reached the *Tsix* promoter *Tsix* will be repressed, resulting in further upregulation of *Xist* and ultimately, in the silencing of the gene encoding the X-linked XCI-activator. Once the XCI-activator is silenced on one allele, *Xist* transcription will be downregulated while *Tsix* transcription remains constant, and the cell will stop initiation of XCI on other X chromosomes, providing a break on further XCI. So, the interplay of *Xist* and *Tsix* transcription on a single allele, regulated by an X-linked activator and an autosomal repressor respectively, will determine the probability of an X chromosome to be inactivated (Fig. 1B).

The interplay of *Xist* and *Tsix* expression can be different on each individual X chromosome, so that the probability of each X chromosome to be inactivated is an intrinsic allelic property. For instance, a SNP or mutation in the *Xist* promoter can alter the binding affinity of a transcription factor for that site, which may change the expression rate of *Xist* and subsequently the probability of the X chromosome to be inactivated. A SNP or point mutation in the sequence regulating *Tsix* expression may change the probability in a similar way. Therefore, SNPs in sequences that regulate *Xist* and *Tsix* transcription, or even a mutation in the RNA itself, may appear as a particular X-controlling-element (Xce). Indeed, a SNP in the *Xist* promoter was found when sequences of an Xce^a allele were compared to sequences of an Xce^c X chromosome (Fig. 1C, 1D and 1E, and data not shown). Furthermore, following the definition of the stochastic model, an X chromosome with a *Tsix* deletion could be defined as an X chromosome with an extremely weak Xce (Fig 1F and 1G).

The validity of the stochastic model was tested further by quantifying the extent of XCI and the speed at which XCI is initiated in cell lines with a variety of X:autosome ratios.

So, if the X:autosome ratio is 1.0 as in female cells, XCI will initiate, whereas it will not in male cells, which have an X:autosome ratio of 0.5 (Fig 1H). As expected, XXXX tetraploid cells initiate XCI just as fast or even faster as XX diploid cells, because they also have an X:autosome ratio of 1.0. Based on the stochastic model, however, cells with a ratio between 1.0 and 0.5 might still initiate XCI, but at a slower rate, because the concentration of the X-linked XCI-activator will be lower and it will take longer for XCI-activator to build up and overcome the autosomal threshold. To test this, initiation of XCI in XXXY tetraploid ES cells (X:autosome ratio of 0.75), and XXY triploid cells (X:autosome ratio of 0.66) was measured by counting the number of Xi's at different

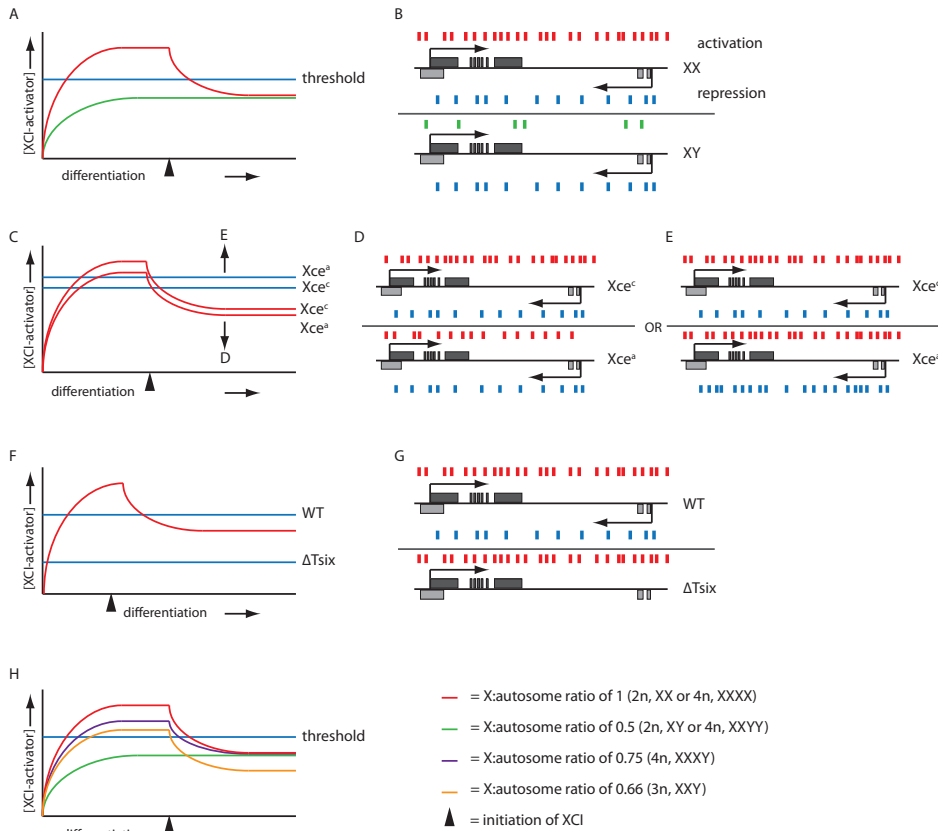


Figure 1. Schematic overview of the stochastic model

A. Schematic graph of accumulation of XCI-activator (on the Y-axis) during differentiation (on the X-axis), and initiation of XCI (arrowhead). The level of XCI-activator in female cells is represented by the red line, and the level of XCI-activator in male cells by a green line. The blue line represents the autosomally encoded repression, which is the same in female and male cells. The combination of the XCI-activator level and the autosomally encoded repressor determine the probability of an X chromosome to inactivate. Thus, in female cells the level of XCI-activator overcomes the autosomally encoded repression, resulting in a high probability to initiate XCI, while in male cells the level XCI-activator does not overcome the autosomally encoded repression, and therefore a very low probability to inactivate an X chromosome.

B. Rate of transcription of *Xist* and *Tsix* at the XIC, with *Xist* in dark grey and *Tsix* in light grey. In red, green or blue blocks, transcription activity is represented as bursts of polymerase activity over the gene. In red, *Xist* transcription in female cells; in green, *Xist* transcription in male cells; in blue, *Tsix* transcription.

C. Graph of the probabilities of X chromosomes with either an *Xce*^a or *Xce*^c. The strength of the *Xce* of each X chromosome can be determined by the expression of *Xist* (in red, top line represents *Xce*^a *Xist* expression level, bottom line represents *Xce*^a *Xist* expression level) or by the repression of *Tsix* (in blue, top line represents *Xce*^c *Tsix* repression level, bottom line represents *Xce*^c *Tsix* repression level).

D. Representation of *Xist* (red) and *Tsix* (blue) expression at the molecular level for an *Xce*^a or *Xce*^c X chromosome, when *Xist* expression is variable and determines skewing.

E. Representation of *Xist* (red) and *Tsix* (blue) expression at the molecular level for an *Xce*^a or *Xce*^c X chromosome, when *Tsix* expression is variable and determines skewing.

F. Graph of the probabilities of a wild type X chromosome (top blue line) and an X chromosome with a *Tsix* deletion (bottom blue line). The red line represents accumulation of the XCI-activator and subsequent

timepoints during differentiation. As expected, XCI was initiated, but at a slower rate as in cells with an X:autosome ratio of 1.0, resulting in a single Xi in XXXY tetraploid cells and thus one active X chromosome per diploid genome (Chapters 2 and 3). Also, XCI was initiated to some extent in XXY triploid cells, even though the optimal ratio of one active X per diploid genome cannot be achieved. The initiation speed in XXY triploid cells was very slow, and XCI is incomplete, leading to the inactivation of a single X chromosome in ~40% of the cells and no inactivation in ~60% of the cells after 10 days of differentiation (Chapter 3). These experiments confirm that the X:autosome ratio in cells is the most critical factor to ensure counting and initiation of XCI.

6.2 The stochastic model versus other models

Previous models, such as the blocking factor model and transvection model, can only partly explain established experimental data and experimental observations put forward in this thesis. The stochastic model proposed in this provides more reasonable explanations for observations and experimental outcomes of others and our own, as will be argued in the following paragraphs.

6.2.1 The blocking factor and symmetry breaking models

The blocking factor model states that a single factor or nuclear entity protects a single X chromosome per diploid genome from being inactivated, so that XCI is initiated in XX females but not in XY males (see also paragraph 1.4.4.1 and Fig. 6 of the Introduction). The most important argument that can be made against the blocking factor model is that differentiation of female XX ES cells or development of embryos with a heterozygous *Xist* deletion results in primary non-random XCI, which means that all cells correctly inactivate the wild type X chromosome [2]. The blocking factor model predicts, however, that the blocking factor would protect the wild type X chromosome just as well as the *Xist* deleted X chromosome, so that half the cells would be unable to initiate XCI on either X chromosome, resulting in cell death of half the cell population. In contrast, the stochastic model predicts that the probability of the *Xist* deleted X chromosome to become inactivated drops to zero, so that only the wild type X chromosome becomes inactivated, leading to the observed primary non-random XCI.

Xist expression.

G. Representation of the expression of *Xist* and *Tsix* at the molecular level in a female *Tsix* deleted cell line. *Xist* expression is in red and *Tsix* expression is in blue.

H. Probability of an X chromosome to inactivate based on XCI-activator concentration and subsequent *Xist* expression, which is determined on the X:autosome ratio. In red, an X:autosome ratio of 1; in purple, an X:autosome ratio of 0.75; in orange, an X:autosome ratio of 0.66; and in green, an X:autosome ratio of 0.5.

The observation that some diploid male and female ES cells and tetraploid XXXX, XXXY, and XYY ES cells inactivate all their X chromosomes is also an argument against the blocking factor model. These cells apparently did not have sufficient blocking factor activity to protect one X chromosome from being inactivated, although their autosomal genomic background should encode for enough blocking factor to prevent one X chromosome per diploid genome from initiating XCI. Again, a stochastic model provides a reasonable explanation for cells that inactivate all X chromosomes, because each X chromosome has an independent chance of initiating XCI. If all X chromosomes will take that chance to initiate XCI simultaneously, the cell will not have any active X chromosomes left, resulting in cell death. In Chapters 2 and 3 the chance of each X chromosome to initiate XCI was predicted in a model, and from that the number of cells that inactivate all X chromosomes could be quantified. The percentage of cells that are estimated to die because all X chromosomes are inactivated is remarkably similar to the experimentally obtained percentage of tetraploid XXXX ES cells found to inactivate all X chromosomes after differentiation was started. Furthermore, Burgoyne et al. [3] observed that female mouse embryos of 7.5 dpc are significantly smaller than their male counterparts. Intriguingly, the weight difference between female and male mouse embryos is within the same range as would be estimated based on the assumed percentage of female cells that die due to incorrect inactivation of both X chromosomes in a female cell population. Thus, a stochastic model not only explains the occurrence of cells with less than one active X chromosome per diploid genome, but also predicts the percentage of cells that will have a certain outcome of XCI.

Also, the phenotype of female cells with a heterozygous *Tsix* deletion poses a problem for the blocking factor model. Reduction or loss of *Tsix* transcription in female XX ES cells leads to primary non-random XCI of the targeted allele [4,5,6]. This can be expected based on the blocking factor model by assuming that the blocking factor binds in the *Tsix* region. Loss of *Tsix* would therefore prevent the blocking factor from protecting the targeted X chromosome, and thus the wild type X chromosome is always bound by the blocking factor and will never be inactivated. However, in Chapter 3 it was observed that a female cell line with a heterozygous *Tsix* deletion not only inactivates the wild type X chromosome in all cells, but also that the initiation speed of XCI is enhanced. While the blocking factor model is unable to explain this, the stochastic model provides a reasonable explanation. It predicts that both X chromosomes will upregulate *Xist* equally, but that the overall *Xist* expression will be much higher on the targeted X chromosome, because *Tsix* expression is gone (Fig 1F and 1G). This will lead to an increased probability of the targeted allele to be inactivated, and thus to primary non-random XCI. Moreover, the initiation of

XCI will be faster, because the threshold to start XCI will be lowered greatly and is overcome rapidly by the X-linked XCI-activator (Fig 1F and 1G). In Chapters 2 and 3 both predictions of the stochastic model regarding cells with a heterozygous *Tsix* deletion were tested and shown to be correct.

Moreover, a few observations regarding differences in XCI initiation between male and female cells and embryos can be made that indicate that a single blocking factor is not sufficient to explain the regulation of XCI counting and choice completely. Male and female embryos homozygous for a deletion decreasing *Tsix* transcription (XΔCpG/ XΔCpG and XΔCpG/Y) are born less frequently as their heterozygous or wild type littermates [7]. This is expected based on the blocking factor model, because no X chromosome is protected from XCI as the blocking factor cannot bind the targeted X chromosomes in males and females anymore. However, more male than female offspring is born with the homozygous ΔCpG, while the severity of the ΔCpG should be equal for male and female cells, based on the blocking factor model. Also, male ES cells without *Tsix* transcription do not initiate XCI on the targeted X chromosome in all cells, while the same targeted X chromosome is inactivated in all female cells [6]. Finally, a luciferase reporter gene under control of the *Xist* promoter is activated more efficiently in female than in male cells [1]. These results all implicate that female cells and embryos are more efficient at initiation of XCI than male cells and embryos. This cannot be explained by the blocking factor model, whereas a stochastic model can. The blocking factor model, postulates that unprotected X chromosomes are inactivated by default, which implicates that XCI is a passive process that is initiated regardless of the genomic background of a cell. The stochastic model predicts a higher concentration of X-linked XCI-activator in female cells, resulting in higher *Xist* transcription and a higher probability of an X chromosome to initiate XCI in a female cell.

Finally, the blocking factor model postulates that a counting element within the XIC enables cells to count the number of X chromosomes in a cell and to decide how many X chromosomes should be inactivated. By definition, the XIC encompasses all factors necessary for XCI, which were thought to be *Xist*, *Tsix* and *Xite*. Therefore, deletion of *Xist*, *Tsix* and *Xite* in a female diploid cell on one X chromosome should trick the cell into counting of only one X chromosome and no XCI should take place. In Chapter 2 it was demonstrated that female cells and embryos heterozygous for the deletion of *Xist*, *Tsix* and *Xite* correctly execute XCI on the wild type X chromosome. This result provides further evidence that each X chromosome has an independent probability to initiate XCI, which is in favor of the stochastic model. Furthermore, it indicates that an additional factor involved in counting is located elsewhere on the X chromosome.

The symmetry breaking model is very similar to the blocking factor model, but hypothesizes that an autosomally encoded and dose dependent protein preferably forms a blocking aggregate of proteins on a single X chromosome per diploid background [8,9] (see also paragraph 1.4.4.2 and Fig. 6 of the Introduction). The symmetry breaking model circumvents the problem of a single blocking factor regulating XCI, which would make the XCI process slow and prone to errors. However, many of the arguments made against the blocking factor model can also be used against the symmetry breaking model. For instance, the blocking factor model and symmetry breaking model predict the same phenotype when considering a female cell line or embryo with a heterozygous *Xist*, *Tsix* or *Xist-Tsix-Xite* deletion, which have been shown to be incorrect in this thesis and by others [2,6](previous paragraph).

However, another argument can be made against the symmetry breaking model based on the experiments with XXY triploid cell lines described in Chapter 3 of this thesis. The symmetry breaking model postulates that the concentration of blocking factor encoded by an autosome in a diploid cell ensures the protection of one X chromosome in that cell. Subsequently, if more than one X chromosome is present in the cell, it will be inactivated by default. The concentration of autosomally encoded factors in the XXY triploid cells is the same as in diploid cells, because the volume of the nucleus is related to the DNA content, so that the increased volume eliminates the extra autosomal dose of a third blocking factor gene. Therefore, enough blocking factor should be at hand to protect one of two X chromosomes, which would result in a homogeneous XaXiY cell population after XCI has completed. However, the experimental data clearly show that in many cells both X chromosomes are active and fail to undergo XCI, which provides a strong argument against the symmetry breaking model.

6.2.2 The blocking factor model complemented with the competence factor

As mentioned, the blocking factor model cannot explain why primary non-random XCI takes place in female cells with a heterozygous *Xist* deletion. Therefore, a competence factor (CF) was introduced as an XCI initiation factor. The CF activates XCI on the X chromosomes that are not protected by the transiently binding blocking factor, and the CF and blocking factor bind an X chromosome in a mutually exclusive fashion. Now, XCI is not initiated in a female cell with a heterozygous *Xist* deletion until the blocking factor binds the targeted X chromosome and the CF binds the wild type X chromosome, resulting in primary non-random XCI. The CF is postulated to be X-encoded and present in an extremely low concentration or as a nuclear entity, like the autosomally encoded blocking factor. The CF is thought to be titrated away by the blocking factor when only one copy of the X-encoded CF is present, as in

male ES cells, while in female cells one dose of untitrated CF would still be present after titration of the autosomal blocking factor, resulting in XCI initiation on one X chromosome [5,10] (see also paragraph 1.4.4.1 and Fig. 6 of the introduction).

Interestingly, this model is able to explain the XCI profile of the XXY triploid cells presented in Chapter 3. It is to be expected that in these triploid cells the optimal ratio of CF and blocking factor cannot be achieved, which results in XCI initiation in a subset of cells only. However, the observation that XCI is initiated in a percentage of male ES cells that have a *Tsix* or *DXPas34* deletion cannot be explained by the blocking factor model complemented with the CF [6,11]. The CF is thought to be titrated away by the blocking factor when only one copy of the X-encoded CF is present as in male ES cells. Therefore, no CF to initiate XCI on the single *Tsix* deleted X chromosome should be present, resulting in absence of XCI initiation in male cells. The stochastic model does provide a logical explanation for initiation of XCI in male ES cells that have a *Tsix* or *DXPas34* deletion [4,6,11]. The threshold put in place by the autosomal repressor on the single *Tsix*-deleted X chromosome in male cells will be lowered, increasing the probability of that X chromosome to be inactivated. Therefore, upregulation of *Xist* will lead to initiation of XCI, even in male cells.

Decrease of *Tsix* transcription on both X chromosomes, resulting from the Δ CpG on both alleles, leads to increased cell death, because both X chromosomes are inactivated in a substantial proportion of the cell population, while random XCI still takes place [7]. These results are contradictory to the blocking factor model and symmetry breaking model, which would predict that both Δ CpG X chromosomes in all cells would be inactivated because of the inability of the autosomal blocking factor(s) to bind an X chromosome and protect it from XCI. Even if the CF is taken into account, the phenotype of the female ES cells with homozygous Δ CpG cannot be explained, because the single remaining dose of CF that has not been titrated away by the blocking factor, should still be able to bind and initiate XCI on a single unprotected X chromosome, subsequently resulting in inactivation of one of two X chromosomes and correct XCI. In contrast, the stochastic model postulates that both X chromosomes will have a greatly enhanced probability to become inactivated, resulting in many cells with two Xi's, and subsequent cell death. Moreover, the random nature of XCI will not be affected, as observed in the experimental data.

6.2.4 The alternate states and transvection models

The alternate states model postulates that X chromosomes adopt a transient chromatin state that is mutually exclusive in female cells before XCI is initiated. Upon differentiation of the cells, the chromatin states of the X chromosomes is 'locked in' and the X chromosome with the chromatin state that is most prone for XCI will be

inactivated [12] (see paragraph 1.4.4.3 and Fig. 6 of the introduction). Reduction of *Tsix* transcription on an X chromosome will enhance the chance that the targeted X chromosome adopts an XCI-prone chromatin state before XCI commences so that the targeted X chromosome is always inactivated, thereby ensuring primary non-random XCI in female cells. However, in male cells with a *Tsix* deleted allele inactivation of the single X chromosome is not always observed [6,11], indicating that the *Tsix* deleted X chromosome is treated differently in male and female cells, which is an observation that the alternate states model cannot account for. Another experimental result that conflicts with the alternate states model, is the XCI pattern observed in triploid XXY cells. Two X chromosomes that should be able to adopt transient mutually exclusive chromatin states are present in these cells, which should result in inactivation of one of the two X chromosomes. The results presented in Chapter 3 show however that many cells do not undergo XCI. Taken together, the alternate states model is unlikely to fully represent the XCI process.

The transvection model hypothesizes that prior to XCI both X chromosomes in female cells have similar chromatin states, but come in close proximity, after which one of the X chromosomes is chosen to be inactivated. In male cells the X chromosome is unable to colocalize with another X chromosome and therefore cannot initiate XCI, which provides a counting mechanism independent of the genomic background [13,14,15] (see paragraph 1.4.4.4 and Fig. 6 of the Introduction). The *Tsix* gene and an X chromosomal region approximately 350 kb upstream of *Xist* called the Xpr region are thought to come together during initiation of XCI, and CTCF is postulated to be the autosomally encoded mediator of colocalization [14,16,17]. The colocalization of the Xpr region provides a counting mechanism, and colocalization subsequently activates *Xist* on one of the X chromosomes to activate XCI. The colocalization of *Tsix* provides a feedback loop that inhibits *Xist* activation of the other X chromosome. XCI can still take place in the female heterozygous XIC deletion cell line (Chapter 2), because the Xpr region that ensures counting is located outside the deleted region. Also, integration of extra copies of the Xpr region in a male cell line induces XCI on the X chromosome.

A few observations made previously conflict with the transvection model. First, male cells with a *Tsix* deletion should not inactivate the single X chromosome, because the Xpr region, which is thought to be the counting element, is present in only one copy. Furthermore, triploid XXY ES cells have two X chromosomes and the same concentration of CTCF or any other autosomal factor as in diploid XX ES cells, so X chromosome pairing and subsequent XCI should take place as in diploid XX ES cells. However, the results presented in Chapter 3 show that XCI is initiated in less than 50% of triploid XXY ES cells. Finally, if pairing is a prerequisite for XCI, than differentiated

diploid XX cells and differentiated tetraploid XXXX cells with all X chromosomes inactivated should never be observed. Nevertheless, a small but significant fraction of cells does inactivate all its X chromosomes, as demonstrated in Chapter 2.

Molecularly, the transvection model raises a few questions too. First of all, the close proximity that is mentioned in the studies on transvection is approximately a micron, which is a considerable distance in a nucleus with a 15 micron diameter [13,15]. Furthermore, the percentage of cells that show close proximity between the two X chromosomes is less than 20% at any given time point during the initiation of XCI [13,15]. This is a low percentage considering that nearly all cells undergo XCI in a few days after the start of differentiation. It implicates that the interaction of the X chromosomes that is needed to initiate XCI is either very transient, or that it is not a functional, but random and sporadic colocalization of two identical loci that are active simultaneously. Finally, the molecular mechanism that enables a cell to count the number of X chromosomes present in a cell by interacting with each other is hard to envision. What factor(s) would be able to distinguish the presence of two X chromosomes within close proximity of each other and then decide to only initiate XCI on one of the two X chromosomes present and subsequently repress XCI on the other?

The ultimate proof that the transvection model is not required for, or merely a consequence of random XCI initiation, would be the identification of an X-linked gene encoding a *trans*-acting protein factor functioning as an XCI-activator, which would indicate that X chromosome pairing is not the cause, but merely a consequence of XCI initiation.

6.3 The XCI-activator

6.3.1 Is *Xist* the XCI-activator?

The stochastic model proposes that a dose-dependent *trans*-acting factor, most likely a protein but possibly an RNA molecule, that is encoded by an X-linked gene activates XCI. In female cells, the dose of the XCI-activator is high enough to increase the probability of the X chromosomes to initiate XCI, which will result in a chance for each X chromosome to become inactivated within a time frame. A few reports have postulated that this activator is *Xist* itself. Transgenic cell lines with multi-copy *Xist* cDNA cosmid integrations or multi-copy integrations of YACs of 450 to 550 kb containing *Xist*, *Tsix* and *Xite*, were reported to not only initiate XCI on the autosome on which the constructs were integrated, but also on the endogenous X chromosome [18,19,20,21,22]. However, we found that transgenic male cell lines with one or multiple BACs containing the complete *Xist* gene integrated onto an

autosome (which allowed us to trace the endogenous *Xist*) only displayed ectopic *Xist* expression (Chapter 4). Furthermore, a heterozygous deletion of *Xist* or the *Xist-Tsix-Xite* region in female cells does not affect XCI initiation, showing that *Xist* alone is not the dose-dependent XCI-activator [2](Chapter 2).

Endogenous *Xist* expression in the male cell lines with the *Xist* cosmid transgenes was confirmed by RT-PCR on the exonic non-spliced sequence, which however does not exclude the possibility that the male cell lines were unstable, resulting in aneuploidy and possible XCI of superfluous X chromosomes. Nevertheless, the ploidy and number of X chromosomes of transgenic male cell lines containing the YACs were confirmed, which implicates that the YACs of 450 to 550 kb not only encode *Xist*, *Tsix* and *Xite*, but also the XCI-activator. Indeed, the Xpr region defined by Augui et al. [16] to be the pairing region needed for counting and initiation of XCI, could also be a candidate region for the location of the XCI-activator, and seems to border the region mapped to the YAC described by Lee et al. [19]. The Xpr region does not appear to map to the YAC described by Heard et al. [21]. Moreover, endogenous XCI activation in the transgenic male cell lines described by Lee et al. is much more extensive as in the transgenic male cell lines of Heard et al., which implies that the YAC used by Heard et al. does not contain the complete XCI activating region. Nevertheless, even the YAC used by Lee et al. integrated into transgenic male cell lines could only induce endogenous XCI if they were integrated in multi-copy repeats, indicating that other sequences outside the YAC region might be important for XCI initiation. Also, mapping of a YAC without sequencing as performed by Heard et al. [20] and Lee et al. [19] is not very precise, and deletions, duplications and integrations of additional DNA sequences in the YAC may have occurred without being detected.

6.3.2 RNF12, an XCI-regulator

As described in Chapter 4 of this thesis, we tried to determine the location of the XCI-activator on the X chromosome by integrating BAC sequences into male ES cell lines. Initiation of XCI on the single male X chromosome would indicate that the dose-dependent *trans*-acting XCI-activator is located on the BAC integrated in the male cell line. The borders of the region where the XCI-activator might be located were defined by the unbalanced Searle's translocation cell line and the HD3 truncation cell line [23,24], which leave a substantial candidate region of 10 Mb. Examining the Xpr region, which also met the criteria of the location of the XCI-activator, surprisingly showed that this region did not induce XCI on the male X chromosome. In contrast, a BAC mapped to a region approximately 475 Mb upstream of *Xist* did. Fine mapping, together with transcription analysis of the region, indicated that *Rnf12* encoded the XCI-activator (Chapter 4). To exclude that the region containing *Rnf12* functioned as

a pairing region necessary to induce XCI, as postulated by the transvection model, we disrupted the *Rnf12* gene in the BAC by integrating a Neomycin resistance cassette, without interfering with the putative pairing region. As expected, BACs with a disrupted *Rnf12* ORF could not induce XCI in transgenic male ES cells, proving that the gene product of *Rnf12* is an XCI-activator instead of the *Rnf12* genomic DNA sequence.

Moreover, the human BAC region homologous to the mouse region containing *Rnf12* also induced XCI when it was integrated into male mouse ES cells, indicating that the function of *Rnf12* is conserved between mouse and human. Interestingly, some females with a tiny ring X chromosome (46, X, (r)X) instead of a complete X chromosome do not initiate XCI. Breakpoint analysis shows that some of these ring X chromosomes still contain *XIST*, but seem to have lost *RNF12*, indicating that *RNF12* is needed to initiate XCI [25,26]. Some 46, X, (r)X females that include *XIST* but do not initiate XCI however, do contain *RNF12*, suggesting either that ring X chromosome analysis is not conclusive due to the mosaic nature of the females, or that another XCI-activator located further upstream of *RNF12* is lost [25].

The finding that *Rnf12* is an XCI-activator is supported by the recently obtained female ES cell line targeted with the *Rnf12* disrupted BAC sequence, which yielded a heterozygous *Rnf12* knockout ES cell line. Although XCI was not completely abolished, a 20 to 30% decrease in XCI initiation in female cells was observed (data not shown).

Rnf12 is expressed ubiquitously in the early embryo at 7 dpc and encodes an E3 ubiquitin ligase called RNF12 or RLIM, which binds LIM domain transcription factors and LDB1 [27,28,29]. RNF12 contains a RING-H2 zinc-finger domain, which is common for ubiquitin ligases and needed for ubiquitination, and a basic domain that mediates interaction with LDB1 [29]. RNF12 ubiquitinates and targets LDB1 and other LIM domain transcription factors (TFs) to the proteasome in a dose dependent way, so that a high concentration of RNF12 causes increased degradation of LDB1 and other LIM domain TFs [29,30]. It was postulated that RNF12, LIM domain TFs and LDB1 (and LDB1 interacting proteins [31]) together convey a tissue and developmental specific regulatory system that is dependent on the concentration of the individual components [32,33].

How RNF12 activates XCI is unknown. Until now, RNF12 has mostly been described as a transcriptional repressor. Not only does it target TFs towards proteasomal degradation, but it also interacts with SIN3A, a histone deacetylase [27]. It is unlikely that RNF12 regulates XCI through LDB1, the most described interaction partner of RNF12, because LDB1 does not seem to be functional in XCI. The heterozygous LDB1 knockout embryos do not have a phenotype, and homozygous

knockout embryos die at E9.5-10 due to severe embryonic patterning defects [34]. Neither the heterozygous or homozygous LDB1 knockout phenotype are what would be expected if LDB1 would play a dose dependent role in XCI, because the heterozygous knockout should give rise to offspring in non-mendelian ratios, while the homozygous knockout should result in earlier embryonic lethality. Nevertheless, other factors than LDB1 and LIM domain TFs might interact with RNF12 to regulate the XCI process. RNF12 might ubiquitinate an *Xist* repressor or a *Tsix* activator and target it for proteasomal degradation. Furthermore, RNF12 action or incorporation of RNF12 might facilitate the formation of a silencing complex that associates with *Xist* RNA. For example, RING1, a PRC1 component that has a RING-H2 zinc-finger domain similar to that of RNF12, acts in the XCI process in such a way. At present, not enough information is at hand to provide a complete molecular model on RNF12 function in XCI. First, more interaction partners of RNF12 that might have a potential role in XCI need to be found.

6.3.3 Other XCI regulators?

Although RNF12 clearly plays a role in regulation of XCI, it is not likely that it is the only dose dependent factor important in XCI. As described above, it is difficult to envision that RNF12 is a direct transcriptional activator or repressor, but probably functions through other factors. These factors may also act dose dependently and could be equally important for the regulation of XCI. Furthermore, transgenic male *Rnf12* ES cells do not initiate XCI in all cells after differentiation, even when multiple copies of *Rnf12* are integrated. If *Rnf12* was the only XCI-activator, one extra copy of *Rnf12* should have been enough to initiate XCI in all male ES cells. Also, female ES cells heterozygous for *Rnf12* are still able to initiate XCI to some extent (data not shown). Another indication that more dose dependent XCI regulators exist, is that female ES cells seem to respond more to extra copies of *Rnf12* than male ES cells, i.e. extra copies of *Rnf12/RNF12* induce XCI more efficiently in female ES cells than in male ES cells (Chapter 4, Fig. 1H and 1I, and Fig. 2E and 2F). Thus, female ES cells appear to have a cellular background that is more prone for XCI as male ES cells, which can be achieved by other X-linked XCI regulators. Moreover, a few ring X chromosome found in human 46, X, (r)X females, contain *RNF12* and *XIST* but do not initiate XCI, indicating that perhaps another gene located telomeric of *XIST* and *RNF12* might be important for XCI in humans [25]. Finally, none of the YACs that were used to obtain transgenic male cell lines that initiated endogenous XCI contain *Rnf12* [19,20,21]. As mentioned, mapping of large genomic DNA sequences without sequencing may be imprecise and deletions, duplications and integrations may have taken place without being observed. Nevertheless, other XCI-activators that have not been detected by

our analysis might be located in the YACs.

If RNF12 would be the only XCI-activator, *Rnf12* expression or RNF12 stability should be increased upon differentiation in female ES cells to initiate XCI. Furthermore, XCI would stop when one X chromosome, and therefore one copy of *Rnf12*, is transcriptionally silenced in female cells, which would reduce the *Rnf12* mRNA concentration to the level in male cells. This assumption was tested by qPCR analysis on *Rnf12* mRNA in various male and female ES cell lines (data not shown). Preliminary data suggest that the transcription of *Rnf12* is downregulated in male and female cells upon differentiation. After 10 days of differentiation, the *Rnf12* mRNA level is maximally 2.5 times lower when compared to the level in undifferentiated male and female ES cells. However, none of the male and female cell lines displayed an increase in *Rnf12* mRNA, indicating that other changes during differentiation help activating XCI in female ES cells. Detection of a two-fold decrease in *Rnf12* expression in female cells during differentiation, or a two-fold difference in *Rnf12* levels between male and female cells appears to be difficult, in particular because the differences in

Gene	Location (in kb)	(putative) function
Xist	100,666-100,679 rev	essential for XCI, coats and silences Xi in cis
Tsix	100,627-100,680 for	negative regulator of Xist transcription
Rnf12	101,153-101,177 rev	E3 ubiquitin ligase, induces XCI
Atrx	102,993-103,125 rev	SWI/SNF related, role in DNA methylation, colocalizes to Xi
Suv39H1	7,638-7,652 rev	H3K9 methyltransferase
Jarid1C	148,668-148,709 for	H3K4 demethylase, escapes XCI, interacts with CTCF
Brcc3	72,662-72,699 for	component BRCA1/BRCA2 complex, potential colocalization Xi
Mecp2	71,272-71,331 rev	methyl-CpG-binding protein, maintenance CpG-methylation
SuhW3	45,895-45,948 rev	Zinc-finger containing, DNA-binding transcription factor
Smarca1	45,163-45,246 rev	SWI-SNF related, matrix associating protein, regulated by actin
Phf16	20,003-20,097 for	PHD Zinc-finger containing transcription factor
Fhl1	53,985-54,047 for	LIM-domain transcription factor
Zfp185	70,233-70,277 for	LIM-domain transcription factor, actin-binding

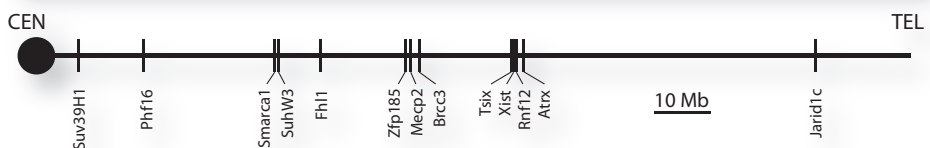


Table 1 Putative XCI-regulatory genes

Overview of putative X-linked XCI-regulators, including their position and established function.

Figure 2. Putative XCI-regulatory genes

Location of putative XCI-regulatory genes from table 1 on the X chromosome.

mRNA levels between the various cell lines are probably larger than the differences between male and female cell lines.

6.4 Spreading of *Xist*

In this thesis, it has been shown that *Xist* RNA does not leave the nuclear territory of the X chromosome but is locally confined (Chapter 5). This was demonstrated by examining tetraploid XXXX mouse ES cells that preferentially inactivate two out of four X chromosomes after differentiation, and contain an X chromosome with an *Xist* gene that was homologously targeted with ms2 repeats. These ms2 repeats allowed us to determine the origin of *Xist* transcripts after XCI had completed. It was found that *Xist* originating from one Xi was not found at the other Xi, thus indicating that the *Xist* RNAs were immediately restricted at the X chromosome from which they were transcribed (Chapter 5).

How is it possible that an *Xist* RNA molecule does not diffuse into the nucleus, but stays in one location? *Xist* itself is a large molecule of 17 kb, but probably folds into a smaller tertiary structure, so that it should be able to diffuse through the nucleus relatively freely. Therefore, it appears that *Xist* RNA is restricted to the X chromosome during or just after transcription. Localization of *Xist* could be mediated by (1) DNA-RNA interactions, (2) RNA-RNA interactions, or (3) protein-RNA-DNA interactions. Mediation of *Xist* binding by DNA-RNA interactions suggests that the X chromosome would have to fold around the *Xist* locus to 'catch' all transcribed RNA before it can diffuse. However, the *Xist* locus is located at the outer rim of the X chromosomal territory, so folding of the X chromosome around the *Xist* gene is unlikely [35,36]. RNA-RNA interactions might also prohibit *Xist* RNA from floating into the nucleus. *Xist* RNA molecules could bind each other while being transcribed and form a lattice of RNA molecules over the Xi that excludes RNA polIII and attracts histone and DNA modifying protein complexes. Such a lattice of RNA molecules would not be very specific, however, and would not enable some genes to escape XCI, like *Xist* itself and others [37]. Also, autosomes close to the Xi might get covered with the '*Xist* web', resulting in inappropriate autosomal silencing. Therefore, a sequence specific interaction with X chromosomal DNA seems likely. This leaves the postulation that proteins bind *Xist* RNA while it is transcribed and that the subsequent protein-RNA complex is targeted to the X chromosome in a sequence specific manner. Proteins that might interact directly with *Xist* RNA are Ezh2, a component of PRC2 [38], CBX7, a polycomb protein of the PRC1 complex containing a putative RNA binding chromodomain [39,40], SAF-A, a nuclear scaffold component containing a putative RNA binding domain [41,42], and ATRX, a protein that co-localizes with the Xi and contains a putative RNA/DNA helicase domain [43].

To explain how spreading of *Xist* RNA in *cis* might take place in eutherians, spreading of the dosage compensation complex (MSL complex) over the male X chromosome in *Drosophila melanogaster* may be taken as an example. The dosage compensation process in *Drosophila* is mediated by the MSL complex, which consists of the proteins MSL1, MSL2, MSL3, MLE and MOF together with X-linked ncRNAs *roX1* and *roX2*. MSL2 and *roX1* and *roX2* are male specific, so that MSL complex only binds the single male X chromosome, which results in a twofold upregulation of X chromosomal genes in *Drosophila* males. Interestingly, spreading of the MSL complex seems to be controlled by the balance between expression of the *roX* genes and the abundance of MSL protein components. Overexpression of MSL protein complex components enhances local spreading, while spreading over longer distances is perturbed [44]. Also, when expression of *roX* ncRNA becomes limiting, spreading of the MSL complex is localized around the *roX* (trans)gene and spreading in *trans* is inhibited, as experimentally demonstrated by lowering expression of autosomal *roX* transgenes [45] or expression of an autosomal *roX* transgene in a *roX1* and *roX2* deleted background [46]. Thus, the concentration of MSL complex proteins and *roX* ncRNA determines the local spreading of MSL complex. Furthermore, the MSL complex binds the MSL recognition elements (MRE), which is a sequence that is not specific to and only slightly enriched on the X chromosome. The high affinity of X-linked MRE sites for the MSL complex seems to be mediated by their location on the X chromosome, which is mostly in the nucleosome poor 3' region of actively transcribed genes [47]. So, the expression of the X-linked *roX* genes and MSL complex components, in combination with DNA binding elements that have a higher affinity on the X chromosome than on autosomes, ensures spreading of MSL complex over the X chromosome in *cis*.

When the observations made in *Drosophila* regarding spreading of the MSL complex are conveyed to spreading of *Xist* RNA, a similar process can be envisioned. An abundantly present protein complex encompassing one or several of the putative *Xist* associating proteins might facilitate localization of the *Xist* RNA. Furthermore, the well titrated levels of *Xist* RNA expression could also ensure that *Xist* RNA only spreads locally over the X chromosome, and does not diffuse onto an autosome. Finally, X-chromosomal binding sites, that might be enriched or positioned in such a way that their binding affinity is enhanced on the X chromosome, could also facilitate preferential binding of *Xist* RNA to the X chromosome.

This hypothesis for *Xist* spreading is supported by several observations. For instance, *Xist* RNA expressed from the endogenous *Xist* gene of an X;autosome translocation chromosome readily spreads over the X chromosomal part, but displays attenuated spread into the autosomal part of the translocated chromosome

[48,49,50], which is an indication that the affinity of *Xist* RNA for X chromosomal DNA binding sites is much higher than for autosomal DNA binding sites under endogenous expression levels of *Xist*. Furthermore, *Xist* RNA does not spread over the X chromosome evenly, but seems to prefer gene rich regions that are located at the periphery of the Xi [35,36,51,52,53,54], indicating that putative *Xist* binding sites are specifically enriched or have a higher affinity for *Xist* RNA in the gene rich regions of the X chromosome, like the MRE sites on the *Drosophila* X chromosome. Nevertheless, the putative *Xist* binding sites are not likely to be exclusive to the X chromosome. Overexpression of *Xist* transgenes on an autosome in male and female cells can also result in spreading over the autosome (this thesis) and subsequent silencing in *cis* [18,55], as has been found in *Drosophila* when a *roX1* transgene was overexpressed from an autosome in a *roX* deleted background [46].

Thus, the putative *Xist* binding sites located on the X chromosome should have a higher affinity for *Xist* than *Xist* binding sites on an autosome or around X-linked genes escaping XCI. However, the high affinity of the X chromosome for *Xist* RNA does not have to be related to the relative abundance or exclusiveness of X-chromosomal *Xist* binding sites. MRE sites in *Drosophila* are only mildly enriched on the X chromosome, and their X-specific binding affinity by the MSL complex is mostly based on their 3' positioning at active genes [47]. Also, the two DNA motifs of the recruitment-element-on-X (*rex*) sequences that bind the dosage compensation complex of *C.elegans* to the X chromosome are not enriched on the X chromosome, but have a high affinity when both motifs are clustered locally [56]. LINE1 repeats have previously been hypothesized as potential *Xist* binding sites [57]. The most important observation in favor of the LINE1 repeat hypothesis is that the repeats are enriched twofold on the X chromosome [58,59,60], although as mentioned, MRE sites in *Drosophila* and *rex* sequences in *C. elegans* show that abundance does not determine the affinity of binding sites [47,56]. Furthermore, enrichment of LINE1 repeats does not seem to correlate with gene rich regions of the X chromosome, even though *Xist* RNA seems to preferentially bind to those regions [36,51], which weakens the argument of abundance in favor of LINE1 repeats. Also, computational studies of LINE1 repeat sequences around genes escaping XCI have not been conclusive [61,62,63,64]. Therefore, LINE1 repeats may facilitate preferential *Xist* binding to the X chromosome, but evidence supporting this hypothesis is incomplete at best.

Overall, a balance between the concentration of a functional ncRNA, the concentration of protein complex components and DNA binding sites with varying affinity may regulate spreading of the dosage compensation machinery over the X chromosome. However, of these three components important for spreading, only the

ncRNA, being *Xist*, is known in mammals, whereas the other components still need to be unraveled. Also, the model should be tested further by changing the concentration of the individual components that might be important for *Xist* spreading in *cis*.

6.5 The comprehensive model for XCI

In this thesis, both initiation of XCI and spreading of *Xist* over the X chromosome in *cis* have been postulated to be dependent on the concentration of factors involved in XCI in the nucleus. The concentration of the XCI-activator determines whether XCI is initiated, based on the stochastic model. The XCI-activator was predicted to be X-linked, which ensures that only cells with two or more X chromosomes per diploid genome initiate XCI. Subsequently, the X-linked gene *Rnf12* was found to initiate XCI when extra copies of the gene were integrated in male cells. However, how RNF12 regulates the XCI process is unknown. Furthermore, RNF12 is not likely to be the only X-linked XCI-activator, as discussed in paragraph 6.3.3.

The balance between the concentration of *Xist* RNA and the concentration of factors that bind and localize *Xist* to *Xist* binding sites could determine spreading of *Xist* RNA over the X chromosome. The putative proteins that facilitate *Xist* spreading are not exclusive to female cells. This is concluded from the fact that spreading of *Xist* not only takes place in female cells, but also in male cells (Chapter 4, Fig. 1B and 1C). Nevertheless, a more optimal concentration of *Xist* associating proteins in female cells could make female cells more prone for initiation of XCI. An X chromosome is destined to become inactivated when it overcomes the repression of *Tsix* transcription in *cis*. *Xist* RNA and the *Xist* associating proteins could achieve this by silencing of *Tsix* transcription. Therefore, if local spreading of *Xist* is more optimal in female cells than in male cells, than female cells are more likely to silence *Tsix* and initiate XCI in *cis*. As described above, in *Drosophila*, spreading in *cis* of the MSL complex is localized around the *roX* genes when individual MSL complex components are overexpressed, so enhanced local spreading of *Xist* RNA in female cells could be mediated by a higher concentration of one of the protein factors that associate with *Xist* RNA, which can be achieved by an X chromosome-encoded *Xist* associating factor.

If loss of one copy of the X-linked *Xist* associating factor is enough to prevent or impair XCI in female cells, than the same deletion studies used to determine the localization of the X-linked XCI-activator can be applied to localize the gene encoding the dose dependent *Xist* association factor. Combination of data obtained with the Searle's translocation embryos and HD3 truncation embryos, defines a region that is approximately 10 Mb long, that should encode the crucial dose dependent XCI factors. *Rnf12* is located within this region, and interestingly so is *Atrx*, which makes ATRX an immediate candidate for a dose dependent *Xist* associating factor.

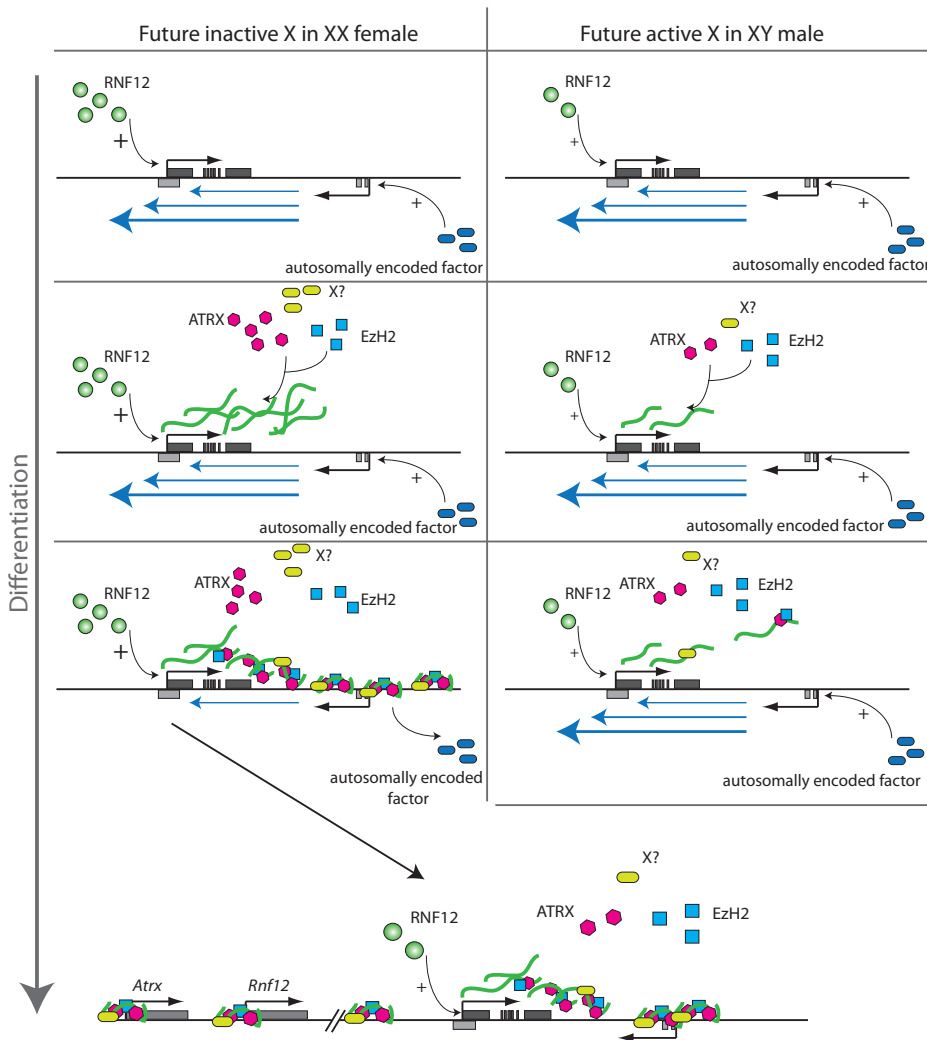


Figure 3. A comprehensive model for XCI

Overview of the comprehensive XCI model. The grey left arrow represents the progression of differentiation in time. The top panel row represents early dose-dependent upregulation of *Xist* by RNF12 and constant *Tsix* repression by an autosomally encoded factor in female (left) and male cells (right). X-encoded *Xist* associating factors (ATRX and X? in the figure) in female cells are twice as abundant in female cells (left) as in male cells (right)(second panel row). In female cells (left), *Xist* is associated to the X chromosome by dose-dependent (ATRX and X?) and/or autosomally encoded (EzH2) *Xist* associating factors whereas in males (right), *Xist* and *Xist* associating factors cannot form a complex efficiently. *Xist* and the *Xist* associating complex turn of *Tsix* transcription. Ultimately, *Xist* and *Xist* associating complex inhibit X-linked gene expression in *cis* (bottom).

ATRX is a protein of the SWI/SNF chromatin remodeling family that causes X-linked mental retardation and α -thalassemia in humans when it is mutated [65]. ATRX directly or indirectly regulates the methylation status of repeat sequences such as CpG islands and rDNA repeats [66], and thus can indirectly regulate gene expression. It also appears to directly interact with the SET domain of EzH2 in human cells [67,68]. Recently, ATRX was found to accumulate on the Xi after 8 days of differentiation in approximately 50% of female ES cells [43]. Deletion of *Atrx* in male ES cells results in a proliferative defect and deletion of *Atrx* in male embryos causes embryonic lethality at 9.5 dpc due to a defect in trophoblast giant cell proliferation [69]. Furthermore, heterozygous female embryos that inherit the null allele maternally are able to reactivate the wild type paternal X chromosome after imprinted XCI has taken place, which rescues more than 50% of the embryos [69]. This indicates that *Atrx* has a function in maintaining the silenced state of the paternal X chromosome after imprinted inactivation. In female embryos with a maternally inherited *Tsix* deleted X chromosome, reactivation of the maternal X chromosome does not take place, which results in embryonic lethality [70,71]. Inactivation of the paternal X chromosome with the wild type *Atrx* should also lead to embryonic lethality, because the extraembryonic tissue would lack functional ATRX. Nevertheless, in these embryos the inactivated X can be reactivated, indicating that the silencing and maintenance of the inactive Xp is impaired due to the mutation of the *Atrx* gene on the active Xm. The role of ATRX in XCI might be recognition or binding of X-linked binding sites or genes, because ATRX regulates genes that have been translocated from the pseudoautosomal region to autosomes in mice [72].

Nevertheless, ATRX could be one of many X-linked factors that interact with *Xist* in a dose dependent way, but result in a mild phenotype when deleted, or only show a phenotype when they are deleted in combination with other factors that have a function in XCI. Therefore, extra copies of *Atrx* in male cells in combination with integration of extra copies of *Rnf12* might still initiate XCI only partially upon differentiation. Other X-linked factors that could have a function in XCI are shown in Table 1 and Fig. 2.

Could RNF12 also be an *Xist* associating factor? RNF12 could facilitate formation, or be part of, an *Xist* associating complex, that spreads and silences *Tsix* in *cis* in female cells only. This would be similar to the action of RING1A and B of the PRC1 complex, which are also E3 ubiquitin ligases, and have a function in gene silencing on the Xi [73]. However, *Xist* expression is higher in female cells compared to male cells when *Tsix* is not present [1], which indicates that expression of *Xist* is dependent on the X:autosome ratio in a cell and must therefore be regulated by an X-linked gene. Presently, RNF12 is the most likely candidate, but functional studies of

Rnf12/RNF12 will have to determine what the exact role is in XCI regulation.

Ultimately, expression of *Xist*, regulated by one or multiple X-linked XCI-activators, together with spreading and silencing of *Xist* RNA in *cis* by an *Xist* associating complex that contains one or multiple X-linked components, could ensure that XCI is a process that is tightly regulated by the X:autosome ratio in cells and embryos (Fig. 3). In cells with an X:autosome ratio of 1.0, as in female cells, RNF12 may directly or indirectly regulate *Xist* expression, while ATRX, probably together with other autosomal or X-linked factors, may associate with *Xist* and facilitate spreading of *Xist* RNA over the X chromosome. Cells with an X:autosome ratio equal to or below 0.5, as in male cells, are expected not to have a sufficient dose of RNF12 to upregulate *Xist* expression to overcome *Tsix* repression. Furthermore, a relatively low level of ATRX may reduce the concentration of *Xist* associating complex, which would impair spreading towards *Tsix*, followed by subsequent silencing, in male cells. Together, dose dependent upregulation and spreading of *Xist* would reinforce that the XCI process is regulated by the X:autosome ratio, as proposed by the stochastic model.

References

1. Sun BK, Deaton AM, Lee JT (2006) A transient heterochromatic state in Xist preempts X inactivation choice without RNA stabilization. *Mol Cell* 21: 617-628.
2. Marahrens Y, Loring J, Jaenisch R (1998) Role of the Xist gene in X chromosome choosing. *Cell* 92: 657-664.
3. Burgoyne PS, Thornhill AR, Boudrean SK, Darling SM, Bishop CE, et al. (1995) The genetic basis of XX-XY differences present before gonadal sex differentiation in the mouse. *Philos Trans R Soc Lond B Biol Sci* 350: 253-260 discussion 260-251.
4. Clerc P, Avner P (1998) Role of the region 3' to Xist exon 6 in the counting process of X-chromosome inactivation. *Nat Genet* 19: 249-253.
5. Lee JT, Lu N (1999) Targeted mutagenesis of Tsix leads to nonrandom X inactivation. *Cell* 99: 47-57.
6. Luikenhuis S, Wutz A, Jaenisch R (2001) Antisense transcription through the Xist locus mediates Tsix function in embryonic stem cells. *Mol Cell Biol* 21: 8512-8520.
7. Lee JT (2002) Homozygous Tsix mutant mice reveal a sex-ratio distortion and revert to random X-inactivation. *Nat Genet* 32: 195-200.
8. Nicodemi M, Prisco A (2007) Self-assembly and DNA binding of the blocking factor in x chromosome inactivation. *PLoS Comput Biol* 3: e210.
9. Nicodemi M, Prisco A (2007) Symmetry-breaking model for X-chromosome inactivation. *Phys Rev Lett* 98: 108104.
10. Lee JT (2005) Regulation of X-chromosome counting by Tsix and Xite sequences. *Science* 309: 768-771.
11. Vigneau S, Augui S, Navarro P, Avner P, Clerc P (2006) An essential role for the DXPas34 tandem repeat and Tsix transcription in the counting process of X chromosome inactivation. *Proc Natl Acad Sci U S A* 103: 7390-7395.
12. Mlynarczyk-Evans S, Royce-Tolland M, Alexander MK, Andersen AA, Kalantry S, et al. (2006) X chromosomes alternate between two states prior to random X-inactivation. *PLoS Biol* 4: e159.
13. Bacher CP, Guggiari M, Brors B, Augui S, Clerc P, et al. (2006) Transient colocalization of X-inactivation centres accompanies the initiation of X inactivation. *Nat Cell Biol* 8: 293-299.
14. Xu N, Donohoe ME, Silva SS, Lee JT (2007) Evidence that homologous X-chromosome pairing requires transcription and Ctcf protein. *Nat Genet* 39: 1390-1396.
15. Xu N, Tsai CL, Lee JT (2006) Transient homologous chromosome pairing marks the

- onset of X inactivation. *Science* 311: 1149-1152.
16. Augui S, Filion GJ, Huart S, Nora E, Guggiari M, et al. (2007) Sensing X chromosome pairs before X inactivation via a novel X-pairing region of the Xic. *Science* 318: 1632-1636.
 17. Scialdone A, Nicodemi M (2008) Mechanics and dynamics of X-chromosome pairing at X inactivation. *PLoS Comput Biol* 4: e1000244.
 18. Herzing LB, Romer JT, Horn JM, Ashworth A (1997) Xist has properties of the X-chromosome inactivation centre. *Nature* 386: 272-275.
 19. Lee JT, Strauss WM, Dausman JA, Jaenisch R (1996) A 450 kb transgene displays properties of the mammalian X-inactivation center. *Cell* 86: 83-94.
 20. Heard E, Kress C, Mongelard F, Courtier B, Rougeulle C, et al. (1996) Transgenic mice carrying an Xist-containing YAC. *Hum Mol Genet* 5: 441-450.
 21. Heard E, Mongelard F, Arnaud D, Avner P (1999) Xist yeast artificial chromosome transgenes function as X-inactivation centers only in multicopy arrays and not as single copies. *Mol Cell Biol* 19: 3156-3166.
 22. Migeon BR, Kazi E, Haisley-Royster C, Hu J, Reeves R, et al. (1999) Human X inactivation center induces random X chromosome inactivation in male transgenic mice. *Genomics* 59: 113-121.
 23. Rastan S (1983) Non-random X-chromosome inactivation in mouse X-autosome translocation embryos--location of the inactivation centre. *J Embryol Exp Morphol* 78: 1-22.
 24. Rastan S, Robertson EJ (1985) X-chromosome deletions in embryo-derived (EK) cell lines associated with lack of X-chromosome inactivation. *J Embryol Exp Morphol* 90: 379-388.
 25. Jani MM, Torchia BS, Pai GS, Migeon BR (1995) Molecular characterization of tiny ring X chromosomes from females with functional X chromosome disomy and lack of cis X inactivation. *Genomics* 27: 182-188.
 26. Tomkins DJ, McDonald HL, Farrell SA, Brown CJ (2002) Lack of expression of XIST from a small ring X chromosome containing the XIST locus in a girl with short stature, facial dysmorphism and developmental delay. *Eur J Hum Genet* 10: 44-51.
 27. Bach I, Rodriguez-Esteban C, Carriere C, Bhushan A, Krones A, et al. (1999) RLIM inhibits functional activity of LIM homeodomain transcription factors via recruitment of the histone deacetylase complex. *Nat Genet* 22: 394-399.
 28. Ostendorff HP, Bossenz M, Mincheva A, Copeland NG, Gilbert DJ, et al. (2000) Functional characterization of the gene encoding RLIM, the corepressor of LIM homeodomain factors. *Genomics* 69: 120-130.
 29. Ostendorff HP, Peirano RI, Peters MA, Schluter A, Bossenz M, et al. (2002)

- Ubiquitination-dependent cofactor exchange on LIM homeodomain transcription factors. *Nature* 416: 99-103.
30. Hiratani I, Yamamoto N, Mochizuki T, Ohmori SY, Taira M (2003) Selective degradation of excess Ldb1 by Rnf12/RLIM confers proper Ldb1 expression levels and Xlim-1/Ldb1 stoichiometry in *Xenopus* organizer functions. *Development* 130: 4161-4175.
 31. Xu Z, Meng X, Cai Y, Liang H, Nagarajan L, et al. (2007) Single-stranded DNA-binding proteins regulate the abundance of LIM domain and LIM domain-binding proteins. *Genes Dev* 21: 942-955.
 32. Matthews JM, Visvader JE (2003) LIM-domain-binding protein 1: a multifunctional cofactor that interacts with diverse proteins. *EMBO Rep* 4: 1132-1137.
 33. Retaux S, Bachy I (2002) A short history of LIM domains (1993-2002): from protein interaction to degradation. *Mol Neurobiol* 26: 269-281.
 34. Mukhopadhyay M, Teufel A, Yamashita T, Agulnick AD, Chen L, et al. (2003) Functional ablation of the mouse Ldb1 gene results in severe patterning defects during gastrulation. *Development* 130: 495-505.
 35. Chaumeil J, Le Baccon P, Wutz A, Heard E (2006) A novel role for Xist RNA in the formation of a repressive nuclear compartment into which genes are recruited when silenced. *Genes Dev* 20: 2223-2237.
 36. Clemson CM, Hall LL, Byron M, McNeil J, Lawrence JB (2006) The X chromosome is organized into a gene-rich outer rim and an internal core containing silenced nongenic sequences. *Proc Natl Acad Sci U S A* 103: 7688-7693.
 37. Disteche CM (1999) Escapees on the X chromosome. *Proc Natl Acad Sci U S A* 96: 14180-14182.
 38. Zhao J, Sun BK, Erwin JA, Song JJ, Lee JT (2008) Polycomb proteins targeted by a short repeat RNA to the mouse X chromosome. *Science* 322: 750-756.
 39. Gil J, Bernard D, Peters G (2005) Role of polycomb group proteins in stem cell self-renewal and cancer. *DNA Cell Biol* 24: 117-125.
 40. Bernstein E, Duncan EM, Masui O, Gil J, Heard E, et al. (2006) Mouse polycomb proteins bind differentially to methylated histone H3 and RNA and are enriched in facultative heterochromatin. *Mol Cell Biol* 26: 2560-2569.
 41. Fackelmayer FO (2005) A stable proteinaceous structure in the territory of inactive X chromosomes. *J Biol Chem* 280: 1720-1723.
 42. Helbig R, Fackelmayer FO (2003) Scaffold attachment factor A (SAF-A) is concentrated in inactive X chromosome territories through its RGG domain. *Chromosoma* 112: 173-182.
 43. Baumann C, De La Fuente R (2008) ATRX marks the inactive X chromosome (Xi) in somatic cells and during imprinted X chromosome inactivation in

- trophoblast stem cells. *Chromosoma*.
44. Oh H, Park Y, Kuroda MI (2003) Local spreading of MSL complexes from roX genes on the *Drosophila* X chromosome. *Genes Dev* 17: 1334-1339.
 45. Kelley RL, Lee OK, Shim YK (2008) Transcription rate of noncoding roX1 RNA controls local spreading of the *Drosophila* MSL chromatin remodeling complex. *Mech Dev* 125: 1009-1019.
 46. Park Y, Kelley RL, Oh H, Kuroda MI, Meller VH (2002) Extent of chromatin spreading determined by roX RNA recruitment of MSL proteins. *Science* 298: 1620-1623.
 47. Alekseyenko AA, Peng S, Larschan E, Gorchakov AA, Lee OK, et al. (2008) A sequence motif within chromatin entry sites directs MSL establishment on the *Drosophila* X chromosome. *Cell* 134: 599-609.
 48. Keohane AM, Barlow AL, Waters J, Bourn D, Turner BM (1999) H4 acetylation, XIST RNA and replication timing are coincident and define x;autosome boundaries in two abnormal X chromosomes. *Hum Mol Genet* 8: 377-383.
 49. Duthie SM, Nesterova TB, Formstone EJ, Keohane AM, Turner BM, et al. (1999) Xist RNA exhibits a banded localization on the inactive X chromosome and is excluded from autosomal material in cis. *Hum Mol Genet* 8: 195-204.
 50. Popova BC, Tada T, Takagi N, Brockdorff N, Nesterova TB (2006) Attenuated spread of X-inactivation in an X;autosome translocation. *Proc Natl Acad Sci U S A* 103: 7706-7711.
 51. Smith KP, Byron M, Clemson CM, Lawrence JB (2004) Ubiquitinated proteins including uH2A on the human and mouse inactive X chromosome: enrichment in gene rich bands. *Chromosoma* 113: 324-335.
 52. Chadwick BP (2007) Variation in Xi chromatin organization and correlation of the H3K27me3 chromatin territories to transcribed sequences by microarray analysis. *Chromosoma* 116: 147-157.
 53. Chadwick BP, Willard HF (2004) Multiple spatially distinct types of facultative heterochromatin on the human inactive X chromosome. *Proc Natl Acad Sci U S A* 101: 17450-17455.
 54. Gilbert SL, Pehrson JR, Sharp PA (2000) XIST RNA associates with specific regions of the inactive X chromatin. *J Biol Chem* 275: 36491-36494.
 55. Lee JT, Jaenisch R (1997) Long-range cis effects of ectopic X-inactivation centres on a mouse autosome. *Nature* 386: 275-279.
 56. McDonel P, Jans J, Peterson BK, Meyer BJ (2006) Clustered DNA motifs mark X chromosomes for repression by a dosage compensation complex. *Nature* 444: 614-618.
 57. Lyon MF (1998) X-chromosome inactivation: a repeat hypothesis. *Cytogenet Cell*

Genet 80: 133-137.

58. Bailey JA, Carrel L, Chakravarti A, Eichler EE (2000) Molecular evidence for a relationship between LINE-1 elements and X chromosome inactivation: the Lyon repeat hypothesis. *Proc Natl Acad Sci U S A* 97: 6634-6639.
59. Boyle AL, Ballard SG, Ward DC (1990) Differential distribution of long and short interspersed element sequences in the mouse genome: chromosome karyotyping by fluorescence in situ hybridization. *Proc Natl Acad Sci U S A* 87: 7757-7761.
60. Ross MT, Grafham DV, Coffey AJ, Scherer S, McLay K, et al. (2005) The DNA sequence of the human X chromosome. *Nature* 434: 325-337.
61. Carrel L, Park C, Tyekucheva S, Dunn J, Chiaromonte F, et al. (2006) Genomic environment predicts expression patterns on the human inactive X chromosome. *PLoS Genet* 2: e151.
62. Chureau C, Prissette M, Bourdet A, Barbe V, Cattolico L, et al. (2002) Comparative sequence analysis of the X-inactivation center region in mouse, human, and bovine. *Genome Res* 12: 894-908.
63. Ke X, Collins A (2003) CpG islands in human X-inactivation. *Ann Hum Genet* 67: 242-249.
64. Wang Z, Willard HF, Mukherjee S, Furey TS (2006) Evidence of influence of genomic DNA sequence on human X chromosome inactivation. *PLoS Comput Biol* 2: e113.
65. Gibbons RJ, Picketts DJ, Villard L, Higgs DR (1995) Mutations in a putative global transcriptional regulator cause X-linked mental retardation with alpha-thalassemia (ATR-X syndrome). *Cell* 80: 837-845.
66. Gibbons RJ, McDowell TL, Raman S, O'Rourke DM, Garrick D, et al. (2000) Mutations in ATRX, encoding a SWI/SNF-like protein, cause diverse changes in the pattern of DNA methylation. *Nat Genet* 24: 368-371.
67. Cardoso C, Timsit S, Villard L, Khrestchatisky M, Fontes M, et al. (1998) Specific interaction between the XNP/ATR-X gene product and the SET domain of the human EZH2 protein. *Hum Mol Genet* 7: 679-684.
68. Kourmouli N, Sun YM, van der Sar S, Singh PB, Brown JP (2005) Epigenetic regulation of mammalian pericentric heterochromatin in vivo by HP1. *Biochem Biophys Res Commun* 337: 901-907.
69. Garrick D, Sharpe JA, Arkell R, Dobbie L, Smith AJ, et al. (2006) Loss of Atrx affects trophoblast development and the pattern of X-inactivation in extraembryonic tissues. *PLoS Genet* 2: e58.
70. Sado T, Wang Z, Sasaki H, Li E (2001) Regulation of imprinted X-chromosome inactivation in mice by Tsix. *Development* 128: 1275-1286.

71. Lee JT (2000) Disruption of imprinted X inactivation by parent-of-origin effects at Tsix. *Cell* 103: 17-27.
72. Levy MA, Fernandes AD, Tremblay DC, Seah C, Berube NG (2008) The SWI/SNF protein ATRX co-regulates pseudoautosomal genes that have translocated to autosomes in the mouse genome. *BMC Genomics* 9: 468.
73. de Napoles M, Mermoud JE, Wakao R, Tang YA, Endoh M, et al. (2004) Polycomb group proteins Ring1A/B link ubiquitylation of histone H2A to heritable gene silencing and X inactivation. *Dev Cell* 7: 663-676.

Summary

Samenvatting

Summary

All mammals employ genetic means to determine their sex, and have sex chromosomes of very different composition between males and females. In addition to the 20 pairs of autosomes, each male mouse cell has an X and a Y chromosome, while female mouse cells have two X chromosomes. Most molecular processes in an organism are dependent on the dose of the components involved, and as a consequence differences in X-chromosomal gene dosage between males and females would be lethal. Therefore, one of the X chromosomes is inactivated early during female development. This process is called X chromosome inactivation (XCI) and the current understanding of XCI is described in the Introduction of this thesis.

XCI is dependent on the X-linked *Xist* gene, which encodes an untranslated but functional RNA. Upon initiation of XCI in female cells, *Xist* is upregulated and eventually *Xist* RNA spreads over one of the two X chromosomes in *cis*. *Xist* RNA attracts many factors that together ensure that the X chromosome is silenced and remains silent through many cell divisions. *Tsix* is a gene that, like *Xist*, also does not encode a protein, and is transcribed in the antisense direction of *Xist*, overlapping *Xist* completely. Thereby, it functions as a *cis* repressor of *Xist* expression.

A satisfactory model that describes all aspects of the initiation of XCI, including the regulation of *Xist* and *Tsix* expression, has not been formulated yet. In Chapter 2, we describe a model for XCI based on the stochastic expression of *Xist* and *Tsix*. In this model, *Xist* expression is dependent on the number of X chromosomes in a cell, while *Tsix* expression is determined by the number of autosomes, which results in initiation of XCI in female cells only. Therefore, an X-linked XCI-activator most likely drives *Xist* expression. The female *Xist-Tsix-Xite* mouse knockout cell line described in this Chapter 2, still exhibits XCI, which suggests the presence of a novel X-linked gene involved in induction of *Xist* upon XCI initiation. Transcription initiation of *Xist* and *Tsix* is stochastic, resulting in a probability for *Xist* to inactivate *Tsix* and subsequent silencing in *cis*. After initiation of XCI on one X chromosome, one copy of the X-linked XCI-activator is silenced, which decreases the level of the XCI-activator and the probability of the other X chromosome to be inactivated. This results in inactivation of one of two X chromosomes in most female cells, but also in inactivation of both X chromosomes in a small but significant proportion of female cells. Analysis of XCI initiation in diploid and tetraploid cell lines underscores the validity of the stochastic model for XCI initiation.

In Chapter 3, initiation of XCI is also examined in triploid XXY mouse ES cells, which provides more evidence indicating that the X:autosome ratio determines the probability to initiate XCI, which supports the stochastic model for XCI initiation.

Furthermore, mathematical and computer simulations, based on a stochastic model, are employed to predict the outcome of XCI in male and female cells, in cells with an aberrant ploidy, and in cells with a variable probability for each X chromosome to inactivate.

One of the most important predictions of the stochastic model is the presence of an X-linked XCI-activator. In Chapter 4, *Rnf12* is identified as an X-linked XCI-activator gene. Integration of extra copies of this gene in male ES cells results in induction of XCI on the single X chromosome. Nevertheless, other factors might be involved, as indicated by the fact that RNF12 is already expressed before the onset of XCI, and that it is not a straightforward transcription factor, but an E3 ubiquitin ligase.

In Chapter 5, experiments on the spreading of *Xist* RNA over the X chromosome in *cis* are described. *Xist* RNA does not seem to spread over the X chromosome via diffusion, but is confined to the X chromosomal territory during or immediately after transcription of *Xist*. This can be achieved by trapping the *Xist* RNA with *Xist* associating factors. We postulate that spreading of *Xist* is dependent on the concentration of *Xist* RNA and *Xist* associating factors, combined with the presence of X-chromosomal binding sites for the *Xist*-protein complex.

Ultimately, the models for initiation of XCI and spreading of *Xist* RNA are combined in the Discussion and a comprehensive model for XCI is introduced. X-linked factors, like RNF12, are important for *Xist* upregulation upon initiation of XCI, and putative X-linked *Xist* associating factors are essential for in *cis* silencing of *Tsix*. Together, these X-linked factors ensure dose-dependent activation of XCI, based on the X:autosome ratio.

Samenvatting

Bijna alle zoogdieren gebruiken genetische determinanten om hun seks te bepalen en hebben seks chromosomen waarvan de samenstelling verschilt tussen vrouwen en mannen. Naast de 20 paar autosomen, bevatten mannelijke muizen cellen een X en een Y chromosoom, terwijl vrouwelijke muizen cellen twee X chromosomen hebben. De concentratie van componenten die van belang zijn in een moleculair proces van een organisme is zeer belangrijk, waardoor verschillen in de dosering van X chromosomale genen tussen mannen en vrouwen lethaal kan zijn. Daarom wordt vroeg tijdens de ontwikkeling van een vrouwelijk embryo een van de twee X chromosomen uitgezet. Dit proces heet X chromosoom inactivatie (XCI) en onze hedendaagse kennis van XCI wordt beschreven in de Introductie van deze thesis.

XCI is afhankelijk van het X gelinkte gen *Xist*, wat een ongetransleerd maar functioneel RNA codeert. Tijdens de initiatie van XCI wordt *Xist* opgereguleerd en uiteindelijk spreidt *Xist* over een van de twee X chromosoom in *cis*. *Xist* RNA trekt allerlei factoren aan die ervoor zorgen dat het X chromosoom wordt uitgezet en ook uitblijft in de vele celdelingen die daarna volgen. *Tsix* is een gen dat niet codeert voor een eiwit en het wordt overgeschreven in de tegenovergestelde richting van *Xist*, waarbij *Tsix* het hele *Xist* gen overlapt. Hierdoor heeft het een remmende werking voor *Xist* expressie in *cis*.

Een bevredigend model dat alle facetten van de initiatie van XCI beschrijft, inclusief de regulatie van *Xist* en *Tsix* expressie, is nog niet geformuleerd. In Hoofdstuk 2 beschrijven we een model voor XCI dat is gebaseerd op de stochastische expressie van *Xist* en *Tsix*. *Xist* expressie is afhankelijk van het aantal X chromosomen in een cel, terwijl *Tsix* expressie afhankelijk is van de hoeveelheid autosomen, zodat alleen vrouwelijke cellen XCI initiëren. Daarom is er waarschijnlijk een X gelinkte XCI-activator die *Xist* expressie aanstuurt. De vrouwelijke *Xist-Tsix-Xite* knockout muizen cel lijnen die zijn beschreven in dit Hoofdstuk, zijn nog steeds in staat XCI te initiëren, wat suggereert dat een vooralsnog onbekende factor van belang is voor de initiatie van XCI. Transcriptie initiatie van *Xist* en *Tsix* is stochastisch, wat ervoor zorgt dat *Xist* een kans heeft om *Tsix* uit te zetten en vervolgens het X chromosoom te inactiveren in *cis*. Na initiatie van XCI op een X chromosoom wordt de X gelinkte XCI-activator uitgezet en daalt de kans van de overgebleven X om te worden geïnactiveerd samen met de concentratie van de XCI-activator. Dit resulteert in de inactivatie van een van de twee X chromosomen in de meeste vrouwelijke cellen, maar ook in inactivatie van beide X chromosomen in een klein maar significant deel van de cellen. Analyse van XCI initiatie in diploïde en tetraploïde cellen bevestigt de beschrijvende waarde van het stochastische model voor XCI initiatie.

In Hoofdstuk 3 wordt de initiatie van XCI ook bepaald in triploïde XXY muizen cellen, wat wederom bevestigd dat de X:autosoom ratio de initiatie van XCI bepaald, en waardoor het stochastische model voor initiatie van XCI wordt onderschreven. Bovendien worden mathematische en computer modellen, die gebaseerd zijn op het stochastische model, toegepast om de uitkomst van XCI te voorspellen in mannelijke en vrouwelijke cellen, in cellen met een afwijkende hoeveelheid seks chromosomen en in cellen met een variabele kans per X chromosoom om te inactiveren.

Een van de belangrijkste voorspellingen die het stochastische model maakt is dat er een X gelinkte XCI-activator bestaat. In Hoofdstuk 4 wordt *Rnf12* geïdentificeerd als potentiële XCI-activator. Extra kopieën van het *Rnf12* gen veroorzaken inductie van XCI in mannelijke stam cellen, resulterend in inactivatie van het enige X chromosoom in de cel. Andere factoren kunnen echter ook een rol spelen, zoals wordt gesuggereerd door het feit dat RNF12 al voor de initiatie van XCI tot expressie komt en doordat het niet een voor de hand liggende transcriptie factor is, maar een E3 ubiquitin ligase.

In Hoofdstuk 5 komt de spreiding van *Xist* over het X chromosoom in *cis* ter sprake. *Xist* RNA lijkt zich niet te verspreiden over het X chromosoom door middel van diffusie, maar wordt tijdens of direct na transcriptie van het *Xist* gen vastgehouden in de X chromosomale omgeving. Dit is mogelijk door *Xist* te vangen met *Xist* associërende factoren. We postuleren dat de spreiding van *Xist* afhankelijk is van de concentratie van *Xist* RNA en *Xist* associërende factoren, gecombineerd met de aanwezigheid van X chromosomale bindingselementen voor het *Xist*-eiwit complex.

Uiteindelijk worden de modellen voor het initiëren van XCI en het verspreiden van *Xist* RNA gecombineerd in de Discussie, en wordt een compleet model voor XCI geïntroduceerd. X gelinkte factoren zoals RNF12 zijn belangrijk voor het opreguleren van *Xist* tijdens de initiatie van XCI, terwijl X gelinkte *Xist* associërende factoren essentieel zijn voor het stilleggen van *Tsix* in *cis*. Samen zorgen deze X gelinkte factoren voor een concentratie afhankelijke activering van XCI gebaseerd op de X:autosoom ratio.

Curriculum Vitae

Personal details

Name: Iris Hélène Jonkers
Birth date: 28-5-1979
Birthplace: Eindhoven, The Netherlands

Education

1997 – 2004 BSc and MSc degree Bioprosesstechnology
Wageningen University, Wageningen, The Netherlands

1990 – 1997 VWO, Gymnasium β
*Stedelijke Scholen Gemeenschap Middelburg,
Middelburg, The Netherlands*

Scientific background

From 2009 Postdoctoral fellow
*Department of Molecular Biology and Genetics, Cornell
University, USA*

2004-2009 PhD research
*Department of Reproduction and Development,
ErasmusMC, Rotterdam, The Netherlands*

2003 Internship
*Department of Chemistry and Biomolecular Sciences,
Macquarie University, Sydney, Australia*

2003 MSc research project
*Laboratory of Virology, Wageningen University,
Wageningen, The Netherlands*

2002-2003 MSc research project
*Fungal Genomics, Wageningen University, Wageningen,
The Netherlands*

Publication list

Published in refereed journals:

1. **Monkhorst, K., I. Jonkers, E. Rentmeester, F. Grosveld, and J. Gribnau.** 2008. X inactivation counting and choice is a stochastic process: evidence for involvement of an X-linked activator. *Cell*; **132**:410-21.
2. **Jonkers, I., Monkhorst, K., Rentmeester, E., Grootegoed, J.A., Grosveld, F., Gribnau, J.** 2008. *Xist* RNA is confined to the nuclear territory of the silenced X chromosome throughout the cell cycle. *Mol. Cell. Biol.*; **28(18)**:5583-94.
3. **Heath H, Ribeiro de Almeida C, Sleutels F, Dingjan G, van de Nobelen S, Jonkers I, Ling KW, Gribnau J, Renkawitz R, Grosveld F, Hendriks RW, Galjart N.** 2008. CTCF regulates cell cycle progression of alphabeta T cells in the thymus. *EMBO J.*; **27(21)**:2839-50.
4. **Monkhorst, K., de Hoon, B., Jonkers, I., Mulugeta Achame E., Monkhorst, W., Hoogerbrugge, J., E., Rentmeester, E., Westerhoff, H., Grosveld, F., Grootegoed, J.A., and Gribnau, J.** 2009. The probability to initiate X chromosome inactivation is determined by the X to autosomal ratio and X chromosome specific allelic properties. Accepted by PLoS One.



PhD Portfolio Summary

Name PhD student: Iris Hélène Jonkers PhD period: 13-04-2004 until 13-05-2009 Promotor(s): F. Grosveld en J.A. Grootegoed Supervisor: J. Gribnau Erasmus MC Department: Department of Reproduction and Development Research School: MGC graduate school		
1. PhD training	Year	Workload (hours)
General academic skills		
Laboratory animal science	2005	108
Scientific communication course Marburg	2005	24
Biomedical English Writing and Communication	2007	84
Research skills		
Save laboratory techniques	2004	8
Working in the C-lab	2004	24
In-depth courses (e.g. Research school, Medical Training)		
In vivo imaging; From cell to organism	2004	32
Experimental approach to Molecular and Cell Biology	2005	168
From Development to Disease	2005	32
Molecular Medicine	2005	32
Analysis of microarray gene expression data	2008	32
Presentations		
Winterschool Klein Walsertal	2005 - 2008	128
International conferences		
- Conference on 'Chromatin and Transcription'; FASEB summer research conference; Snowmass Village, Colorado, USA (poster contribution)	2005	32
- Conference on 'X chromosome inactivation'; Paris, France (poster contribution)	2006	32
- 16th International chromosome conference; Amsterdam, The Netherlands	2007	32
- Conference on 'Transcriptional regulation during cell growth, differentiation and development'; FASEB summer research conference Snowmass Village, Colorado, USA (poster contribution)	2008	32
Seminars and workshops		
MGC Promovendi Workshop	2004 - 2005	64
Third Dutch chromatin community meeting	2005	16
SCDD BSIK conference	2009	8

Dankwoord

Het zit erop! Ik mag mezelf Doctor noemen en ik kan een boekje in de kast zetten waar ik heel trots op ben. Vijf jaar heb ik met veel plezier bij het ErasmusMC gewerkt, en die periode zal ik niet snel vergeten. En dat komt natuurlijk vooral door alle mensen die ik hier heb ontmoet, waarmee ik heb samengewerkt en ongelooflijk veel fantastische ervaringen heb opgedaan!

Allereerst wil ik Joost bedanken. Wat een enorm geluk dat ik jou als begeleider heb getroffen. Het is een hele leerzame en interessante ervaring geweest om met jou een lab op te zetten en te zwoegen voor de eerste resultaten. Dat ging in het begin niet altijd even soepel, maar een groot deel van jou kracht zit in het feit dat je mislukkingen opzij kan zetten en altijd een stortvloed van nieuwe ideeën hebt om uit te voeren. Ik ben dan ook enorm blij dat dat uiteindelijk heeft geresulteerd in hele mooie artikelen en een groeiende groep X-perts. Dank je wel voor je niet aflatende ideeën, interesse, geduld, goede humeur en humor.

Natuurlijk hebben mijn promotors Frank en Anton ook een grote rol vervuld in de totstandkoming van dit proefschrift. Frank, je hebt vooral in de eerste jaren een belangrijke rol gespeeld in het vormgeven van mijn promotie onderzoek. Nu nog steeds ben je iemand waar ik altijd advies aan kan vragen en ik wil je daar dan ook hartelijk voor bedanken. Anton, ik ben je steeds meer gaan waarderen. De gedetailleerde manier waarop je aandacht hebt besteed aan mijn projecten, artikelen, en promotie onderzoek is heel waardevol geweest voor me en ik stel het enorm op prijs. Samen zijn jullie echt het ideale promotor koppel!

Verder wil ik de kleine commissie, bestaande uit Dies, Ben en Niels heel hartelijk bedanken voor het zorgvuldig lezen van m'n proefschrift. De opbouwende kritiek wordt zeer gewaardeerd.

Eveline, als Joost de hersenen zijn, dan ben jij het kloppende hart van ons clubje. Je bent de stille kracht die het lab draaiende houdt en voor al de goede zorgen wil ik je heel erg bedanken. Verder ben je natuurlijk een schat van een meid en ik heb altijd enorm veel plezier met je. Ik mis je nu al (je bent namelijk de Kilimanjaro aan het beklimmen terwijl ik dit schrijf)!

Kim, Stefan, and Eskeww, your scientific influence and advice is much appreciated. Of course, I want to thank the students in the lab as well: Annegien, Nilhan, Hakima, Bas and Ruben, it was great to work with you! You are the reason labs should have as many students as possible. You were hilarious and helpful.

A special thanks goes to the office members Sam, Akiko, and Eskeww. There

is never a dull moment when you are there. Lab 910 was already a great place to work at before you came, but you brought life, laughter and personality to the office! Like with all good friends, I sometimes want to stick you behind wall paper, but I can never stay irritated and I really hope that we will always remain friends. Thank you for all the great times.

To all other (former) people in the lab, Willy, Peng, Eveliene, Esther, Marja, Jos, Albert, Leen and Mark, I want to say thank you very much for your interest, advice, and fun! Peng, a special thanks to you for all the computer wisdom from the “Chinese connection”.

Samenwerkingen zijn super, zeker als ze met lab 1030 zijn. Niels, Helen en Suzanne super bedankt voor de leuke en soepel lopende samenwerkingen, hopelijk worden de resultaten snel gepubliceerd. Frankie Keys, onze samenwerking reikt zo ver als Lowlands, en is nog lang niet klaar! Ik vond het echt heel tof om samen over proeven na te denken, experimenten te optimaliseren (tot in den treuren) en enorme bomen op te zetten over vrijwel alles. Picknick tafels hebben een hele nieuwe betekenis voor me.....

Verder wil ik de cell culture buddies niet overslaan: Maureen, Jeffrey, Petra, en Erik en Daniel (de “Splitsers”) heel erg bedankt voor de tips en de hilariteit. Celkweek zuigt, maar niet als jullie erbij zijn.

There are a lot more colleagues and friends that I haven’t mentioned here, but there are just too many! I always thought the working atmosphere inside and outside the building (read: in a bar or restaurant) was amazing and I thank you all very much for it. Cheers! I can only wish that I will have as many fun colleagues in the future.

Last but not least, I would like to thank Sanja, Akiko (again) and Daan for providing a PhD-support-system for me. You are amazing! Daan, good luck in Lausanne, I know you will do great over there and I can’t wait to set up our first collaboration. Our paths will cross eventually, they always do. Sanja, although you won’t be able to come to my defense, you will be in my mind, and that will be a great comfort. I wish you and Nir a great future in Isreal. Akiko, you are unique, in the best possible way, and you really have to do a postdoc in New York!! I will be waiting.

Natuurlijk wil ik ook alle “andere” vrienden uit Wageningen en Rotterdam bedanken voor de afleiding en ontspanning. Zonder jullie zou het maar een saaie bedoeling zijn, en ook al ga ik naar de Verenigde Staten, ik hoop dat jullie zo nu en dan de oceaan over zullen steken (met het vliegtuig, de mail, skype of telefoon). Tegen Jasperien wil ik zeggen, het spreekwoord ‘gedeelde smart is halve smart’ is bewezen, lijkt me.

Franz, dank je voor de afleiding en de introductie tot de Rotterdamse cultuur, beter laat dan nooit.

Uiteindelijk zijn de belangrijkste mensen in dit dankwoord mijn ouders, Frans en Hélène. Jullie hebben me opgevoed met het idee dat ik een intelligente en zelfstandige meid zou worden, die doet wat ze belangrijk en leuk vindt. Dat is gelukt (denk ik). Ik weet dat jullie trots op me zijn en me onvoorwaardelijk steunen in mijn besluit om in de VS te gaan werken, ook al vinden jullie het ook heel jammer om me te zien vertrekken. Wees niet getreurd, ik verdwijn niet van de aardbodem! Dank jullie wel voor alles, ik ben er ongelooflijk trots op jullie dochter te zijn.

Heel veel liefs,
Iris